2024

Ecosystem-Scale Patterns in the Diversity, Seasonal Dynamics and Physiology of Antagonistic Diatom-Bacteria Interactions in the Western English Channel

Branscombe, Laura

UNIVERSITY OF PLYMOUTH

ECOSYSTEM-SCALE PATTERNS IN THE DIVERSITY, SEASONAL DYNAMICS AND PHYSIOLOGY OF ANTAGONISTIC DIATOM-BACTERIA INTERACTIONS IN THE WESTERN ENGLISH CHANNEL

by

Laura Branscombe

A thesis submitted to the University of Plymouth

in partial fulfilment for the degree of

DOCTOR OF PHILOSOPHY

School of Biological and Marine Sciences

August 2023

Table of Contents

Acknowledgements

I would first of all like to thank my supervisory team, particularly Dr Katherine Helliwell for creating such an incredibly supportive environment throughout my PhD journey. You not only created an engaging and exciting research space for me, but your endless support, enthusiasm and words of encouragement have helped me grow in confidence as both a scientist and a person. I could not have asked for a better PhD experience nor a better mentor.

To Professor Michael Cunliffe, thank you for your continued support and advice throughout my PhD, and for welcoming me into your research group during Katherine's maternity leave. Your academic insights and feedback have helped shaped this thesis. To Professor Willie Wilson, although I never managed to fit viruses into this thesis, I have greatly valued your enthusiasm and support, particularly during the development of the early work of this thesis.

I would also like to say a huge thank you to the Cell and Molec team at the MBA for all of the technical support and expertise, for creating such a warm and supportive lab environment, and for never complaining when you had to listen to me ramble on about plaque assays at lab meetings time and time again. A special thanks to Yasmin for never tiring of hearing me complain, and to the MBA swimmers for regularly dragging me out of the office to make the most of being able to go for lunch time dips.

I also owe a special thanks to Dr Colin Munn, without whom I would likely never have embarked on this journey, and who has provided invaluable guidance and encouragement throughout my entire academic career, even when I didn't believe in myself.

Cordelia, we've known each other from a distance since we were both fresh-faced undergrads just starting out at Plymouth University. I am so grateful that this PhD finally brought us both together as I could not have asked for a better office mate to spend the last four years with. Thank you so much for all the support, academic, lab and otherwise, and thank you for dragging me kicking and screaming into the world of coding. Most of this thesis would not have been possible without your help and patience. But most of all, thank you for all of the laughs, the tears, for being an ever-sympathetic ear, and for always being an amazing role model. I hope our career paths cross again soon.

A huge thank you to my Mum and Dad who have listened enthusiastically to my (often non-sensical) ramblings over the last four years. All of your support and words of encouragement have meant the world to me, and I really wouldn't be where I am today without you both.

And lastly, to Adam, this PhD would not have been possible without you. Your unwavering patience and support over the past nine years has carried me through some of my greatest challenges, and for that I will be forever grateful. I cannot thank you enough for sticking by my side throughout this period, patiently waiting for us to be able to start our lives together. You have not only supported my academic journey, even when it meant trekking across countries to see each

other for just a weekend at a time, but you have also enriched my personal growth. Thank you for always being my personal cheerleader and for always making sure that, if nothing else, I've always had cake to see me through the stress.

Author's Declaration

At no time during the registration for the degree of Doctor of Philosophy has the author been registered for any other University award without prior agreement of the Doctoral College Quality Sub-Committee.

Work submitted for this research degree at the University of Plymouth has not formed part of any other degree either at the University of Plymouth or at another establishment.

This study was financed with the aid of a studentship from the ARIES DTP, funded by the UK Natural Environment Research Council (NERC), supported by and carried out in collaboration with the Marine Biological Association of the UK.

Word Count (main body of text): 36,063

Signed: 

Date: 06/02/2024

Publications:

Branscombe, L., Harrison, E.L., Choong, Z.Y.D., Swink, C., Keys, M., Widdicombe, C., Wilson, W.H., Cunliffe, M. and Helliwell, K. (2023), Cryptic bacterial pathogens of diatoms peak during senescence of a winter diatom bloom. *New Phytologist*. https://doi.org/10.1111/nph.19441

Presentations at conferences:

2021 British Phycological Society Annual Meeting (BPS 2021) – Poster presentation *'Deciphering the impacts of algicidal bacteria on algal physiology, signalling and bloom regulation'*

2021 Marine Biological Association Postgraduate Conference – Oral presentation *'Characterising the diversity and abundance of diatom-bacteria interactions in the Western English Channel'*

2021 Microbiology Society Annual Conference – Poster presentation *'Characterising the diversity and abundance of antagonistic diatom-bacteria interactions in the Western English Channel'*

2021 Molecular Life of Diatoms (MLD7) – Poster presentation *'Uncovering the diversity and seasonal patterns of diatom algicidal bacteria in the Western English Channel'*

2021 Molecular Microbial Ecology Group Meeting (MMEG21) – Oral presentation *'Uncovering the diversity and seasonal patterns of diatom-algicidal bacteria in the Western English Channel'*

2022 Plymouth Marine Science and Education Foundation (PlyMSEF 2022) – Oral presentation *'Uncovering the diversity and seasonal patterns of diatom-algicidal bacteria in the Western English Channel'*

2022 International Society of Microbial Ecology (ISME18) – Poster presentation *'Deciphering the metabolic triggers of broad-range algicidal bacterium Ponticoccus alexandrii'*

2022 Molecular Microbial Ecology Group Meeting (MMEG22) – Oral presentation *'Ecosystem-scale patterns in the diversity and abundance of antagonistic diatom-bacteria interactions in the Western English Channel'* (Awarded the International Society of Microbial Ecology Prize for Best Oral Presentation)

ECOSYSTEM-SCALE PATTERNS IN THE DIVERSITY, SEASONAL DYNAMICS AND PHYSIOLOGY OF ANTAGONISTIC DIATOM-BACTERIA INTERACTIONS IN THE WESTERN ENGLISH CHANNEL

Laura Branscombe

Abstract

Diatoms, a major group of marine and freshwater microalgae, are one of the most successful phototrophic organisms in the oceans. Their ubiquity and abundance pins them as important drivers of marine biogeochemical cycles and significant components of marine food webs. Diatoms exist within a complex web of interactions with other microbes, including equally ubiquitous marine bacteria. Interkingdom interactions between diatoms and bacteria are both diverse and numerous, and they underpin the success of diatoms through their resulting impacts on diatom physiology. Interactions between diatoms and antagonistic bacteria are increasingly recognised to significantly impact diatom growth and physiology, and potentially represent important biotic drivers of diatom bloom dynamics. Nevertheless, our understanding of the diversity, seasonal trends and regulation of antagonistic diatom-bacteria interactions in marine ecosystems remains a significant knowledge gap.

This thesis set out to tackle this knowledge gap through a combination of laboratory and field-based approaches. In doing so, a robust environmental sampling pipeline was developed to systematically assess the diversity and

seasonal trends of diatom-antagonistic bacteria in a highly productive ecosystem, the Western English Channel, utilising a range of bloom-forming diatom species. The result was a library of 18 potential diatom-antagonistic bacteria, abundance of which peaked upon the termination of a winter diatom bloom. Seven isolates were subsequently confirmed to exhibit significant growth inhibitory effects against a range of diatoms. However antagonistic behaviour was only observed when pre-cultivated on media derived of diatom necromass, highlighting cryptic antagonistic behaviour that is conserved across diverse bacterial lineages. Finally, the seasonal dynamics and global biogeography of confirmed antagonistic bacteria was assessed through metabarcoding, revealing confirmed antagonistic bacteria to co-occur with important bloom-forming diatom species both locally and globally.

Together, this work provides an ecosystem scale assessment of antagonistic bacteria within a model ecosystem, and enhances our current understanding of the abundance, distribution and regulation of antagonistic diatom-bacteria interactions at an ecosystem scale. Building a comprehensive picture of these interactions in natural environments will allow us to better understand biotic drivers of diatom ecology, and thus marine food webs and biogeochemical cycling.

List of Figures

Introduction

Chapter 1

Chapter 2

Chapter 3

Appendix

List of Tables

Chapter 1

Chapter 2

Chapter 3

Appendix

Abbreviations

AHL – Acyl-Homoserine Lactone

ANOVA – Analysis of Variance

ASV – Amplicon Sequence Variant

BLAST – Basic Local Alignment Search Tool

CFF – Cell-free Filtrate

DCM – Deep Chlorophyll Maximum

DDM – Dead Diatom Media

DMSO – Dimethyl Sulfoxide

DMSP – Dimethylsulfoniopropionate

DOC – Dissolved Organic Carbon

FSW – Filtered Seawater

GTR – General-Time-Reversable

HAB – Harmful Algal Bloom

HGT – Horizontal Gene Transfer

HNA – High Nucleic Acid

IAA – Indole Acetic Acid

L4 – Station L4

LNA – Low Nucleic Acid

MAFFT – Multiple Alignment using Fast Fourier Transform

MES – Mesopelagic

miTAG – Merged Illumina Reads

ML – Maximum Likelihood

NCBI – National Center for Biotechnology Info

OD – Optical Density

OTU – Operational Taxonomic Unit

pCA – p-Coumaric Acid

PCR – Polymerase Chain Reaction

PR^2 – Protist Ribosomal Reference

QS – Quorum Sensing

rRNA – Ribosomal Ribonucleic Acid

RT – Room Temperature

SRF – Surface

TDA – Tropodithietic Acid

TEP – Transparent Exopolymer Particles

V4 – Variable Region 4

WEC – Western English Channel

WCO – Western Channel Observatory

YTSS – Yeast Tryptone Sea Salts

Introduction:

Diatom-bacteria interactions: biotic drivers of diatom success in the oceans

Introduction

Diatoms – diverse and ecologically significant microalgae

Marine environments are teaming with a hidden diversity of microbial life, from prokaryotic viruses and bacteria to microbial eukaryotes such as fungi and unicellular algae, all of which play a vital role in the everyday functioning of marine ecosystems. Diatoms, a major group of photosynthetic microalgae, are some of the most diverse and abundant organisms in the eukaryotic fraction of the marine microbiome and are known to be ubiquitous in both planktonic and benthic communities throughout the sunlit oceans (Kooistra et al., 2007). Diatoms sit within the heterokont (stramenopile) lineage of eukaryotes (Figure 1), albeit they lack the characteristic double flagella in their adult stages that most other heterokonts possess and also differ from other heterokonts in their unique silica cell wall structure (Round et al., 1990). These ornate silica shells (frustules) range in size from 2 – 200 µm depending on the species and are comprised of two halves (valves), joined by silica bands called a girdle. Each valve differs in size, with one valve, the epitheca, being the larger valve, while the smaller valve, the hypotheca, sits just inside the larger one. These distinctive silica frustules are perhaps one of the most striking features of the diatoms as they appear in an incredibly diverse range of cell formations (Figure 2). Despite their vast diversity, however, diatoms are divided into just two groups, the centric and the pennate diatoms, based on their morphology. Centric diatoms show a radial symmetry across their valves (Figure 2A and B), whereas pennate diatoms, the most diversified of the two groups (Kooistra et al., 2007), display bilateral symmetry along the openings in their frustules, termed raphes (Figure 2C and D).

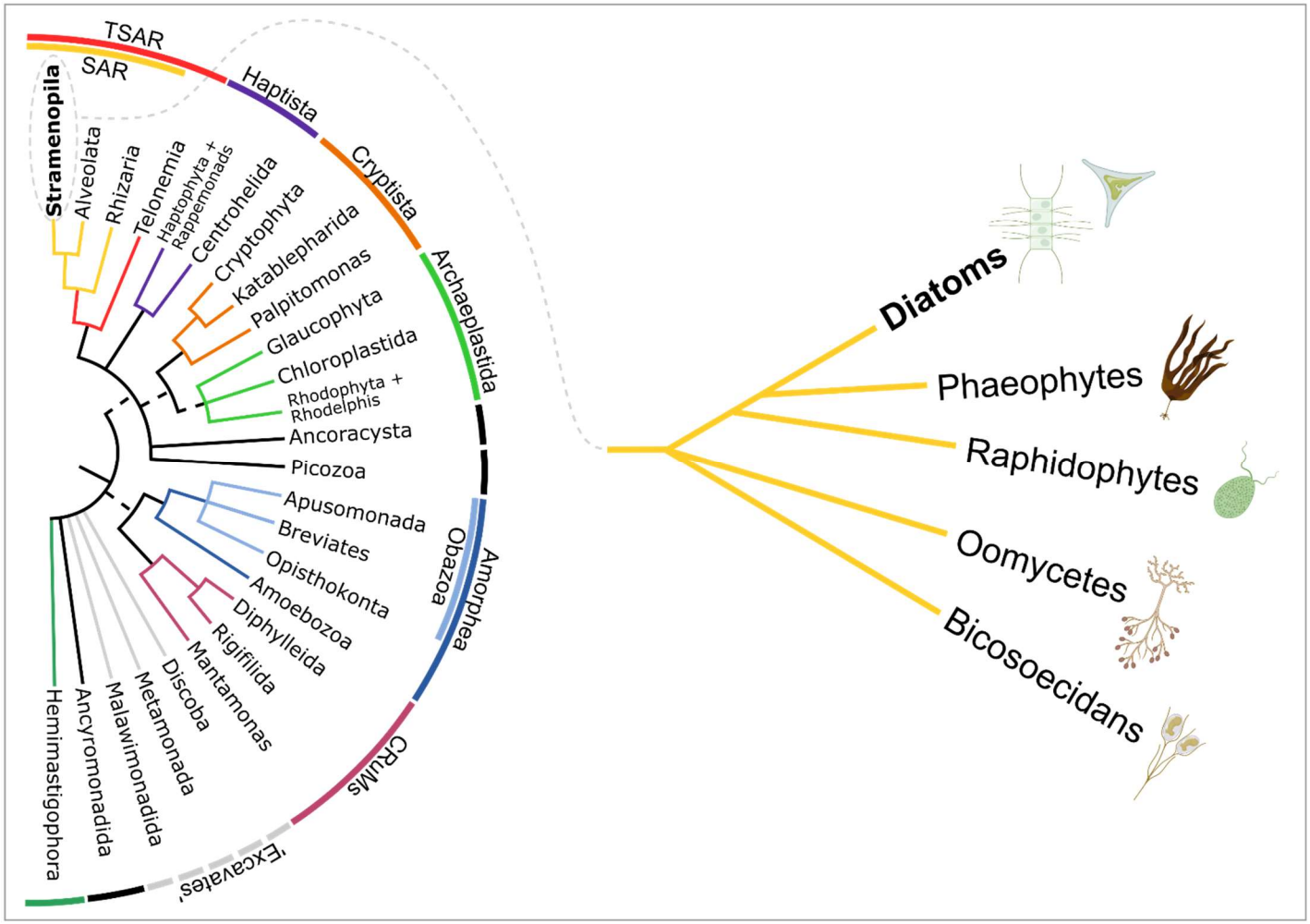

Figure 1. Eukaryote tree of life, adapted from Burki et al., 2020. Coloured bars denote currently accepted eukaryotic 'supergroups'. Highlighted is the Stramenopile lineage in which the diatoms sit, which is expanded to the right of the figure. Stramenopile illustrations were created using Biorender.

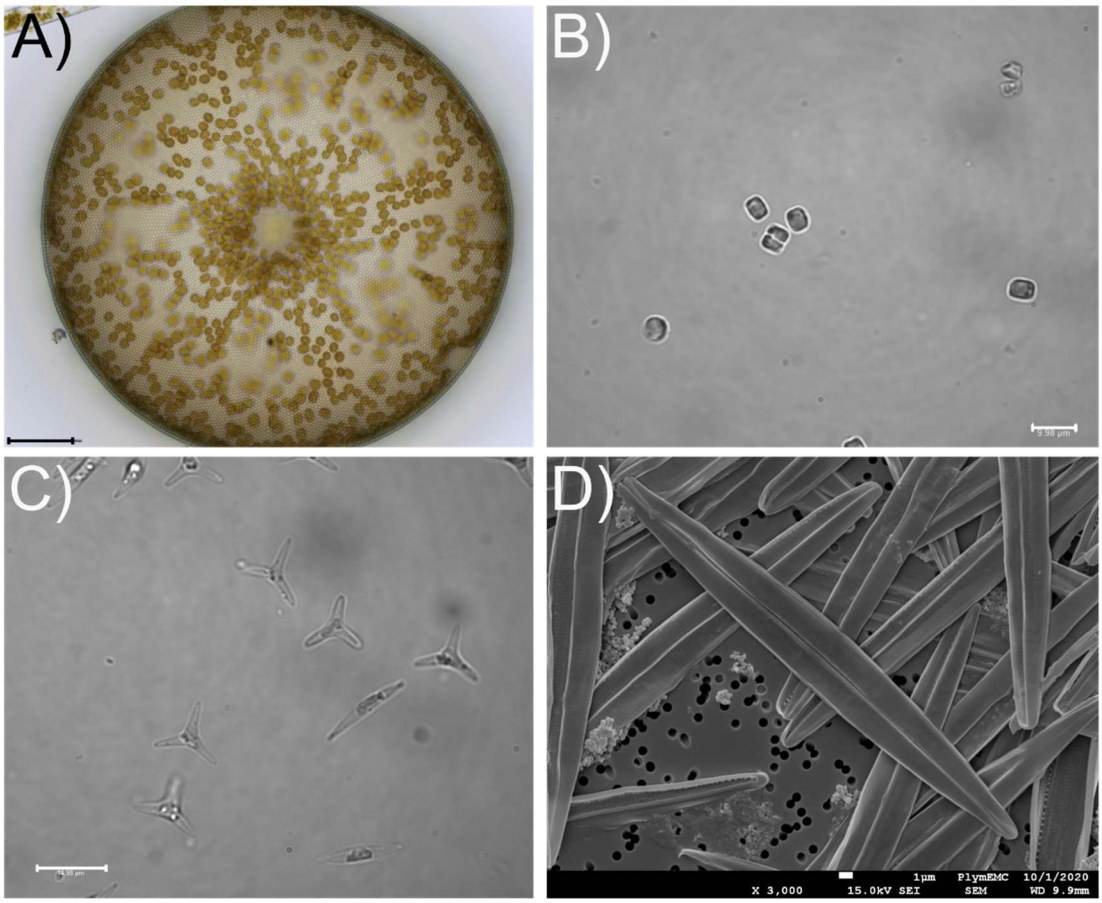

Figure 2. Diversity of cell forms across centric and pennate diatoms as exemplified by images taken of representative diatom species from the MBA culture collection and isolated from natural seawater assemblages. **A)** Centric diatom *Coscinodiscus* sp., (imaged using a Zeiss PALM MicroBeam laser capture microdissection microscope at 40x magnification, scale bar represents 75 µm). **B)** Centric diatom *Thalassiosira pseudonana* (imaged using a Leica DMi8 epifluorescent microscope at 63x magnification, scale bar represents 10 µm). **C)** Pennate diatom *Phaeodactylum tricornutum* (imaged using a Leica DMi8 epifluorescent microscope at 63x magnification, scale bar represents 15 µm). **D)** Pennate diatom *Pseudo-nitzschia delicetissima*, imaged via Scanning Electron Microscopy (image taken in collaboration with Dr Glen Harper, University of Plymouth). Images A – C are differential interference contrast (DIC) images.

Another unique feature of the diatom lineage is their reproductive strategies. Diatom replication is primarily asexual, during which a diatom cell will divide by mitosis to form two daughter cells synthesised from each of its two valves. In this process, both of the original valves of a diatom become the epitheca of the new daughter cells, meaning that each half gains a new hypotheca. This results in a gradual decline in diatom cell size across the whole population. Eventually, a critical size limit is reached (also known as the sexual size threshold, SST), which then triggers a sexual reproduction and restores population size (Round et al., 1990; Chepurnov & Mann 2004).

Evolutionary history

Due to their siliceous cell walls, diatoms have been relatively well preserved in the fossil records, with the oldest recorded appearance of marine diatoms dating back approximately 180 million years ago (Rothplatz et al., 1896). Although fossil records have provided important insights into diatom evolution, more recent advances in molecular techniques such as DNA sequencing have proved incredibly valuable, offering a more detailed picture of diatom evolutionary history. Reference genomes for multiple diatom species, such as the model centric diatom *Thalassiosira pseudonana*, and model pennate diatom *Phaeodactylum tricornutum* (Armbrust et al., 2004; Bowler et al., 2008) were first published almost two decades ago, which facilitated the establishment of these two species as genetically tractable model systems. This enabled the development of a range of molecular tools, including genetic transformations and gene knockouts for gene characterisation (reviewed in Falciatore et al., 2020). Further, these genomes have been instrumental in pinpointing key evolutionary events throughout diatom evolution. Molecular evidence gleamed from diatom genomes suggests that

diatoms may predate their fossil records, dating as far back as approximately 250 million years ago (Sorhannus, 2007).

The evolutionary timeline pieced together from the genomes of both *P. tricornutum* and *T. pseudonana* revealed that diatoms as we know them today are the result of a series of phagotrophic uptakes of various symbionts. The first milestone in the evolution of eukaryotic photosynthesisers in the oceans was the primary uptake of a cyanobacterial symbiont, which was eventually integrated as a permanent organelle, by a eukaryotic heterotrophic host cell, which is believed to have occurred between 1,200 and 1,500 million years ago (Yoon et al., 2004; Knoll et al., 2007). The newly evolved, newly photosynthetic endosymbiont later diverged into the green, the red, and the glaucophyte algae (Bhattacharya & Medlin 1995). A subsequent uptake of a newly diverged red alga by another eukaryotic host somewhere between 700 – 1,200 million years ago resulted in the evolution of a secondary endosymbiont (Gibbs, 1981; Bhattacharya et al., 2007; Parker et al., 2008). Substantial molecular evidence, such as the presence of a number of red algal genes within multiple diatom genomes, supports this timeline of events (Armbrust et al., 2004; Bowler et al. 2008; Deschamps & Moreira, 2012). However more recent genetic evidence hints at the possibility that there may have also been a previously undetected uptake of a green algal endosymbiont uptake that predates the assimilation of the red algal symbiont (Worden et al., 2009; Moustafa et al., 2009). Gradually, this ancestral combination of host and symbiont genes evolved into the stramenopiles from which modern diatoms were born. Around 70 - 90 million years ago, diatom ancestors diversified further into the pennate and the centric diatoms that were discussed in the opening section of this review (Figure 3, Kooistra & Medlin, 1996; Benoiston et al., 2017). Today, there are estimated to be between 30,000 to 100,000 diatom

species throughout marine, freshwater and terrestrial environments (Mann & Vanormelingen 2013).

It is often cited that the repeated assimilation of symbiont DNA is largely responsible for the ecological success of the diatom lineage. While mining the complete genomes of *P. tricornutum* and *T. pseudonana* Bowler and colleagues discovered the presence of over 1700 and 170 genes of green and red algal origin respectively (Bowler et al., 2010). As these diatom genomes consist of between 10,000 and 14,000 genes in total (Armbrust et al., 2004; Bowler et al., 2008), the genes derived from these symbiotic events constitute approximately 13 – 18 % of the total diatom genome. Although the exact number of genes that can be attributed to each symbiont remains uncertain due to a scarcity of red and green algal reference genomes with which to compare, it is overwhelmingly clear that these symbionts have played a significant role in shaping modern diatom genomes and ecological success. Perhaps one of the most prominent examples of endosymbiont derived-genes influencing diatom success is the presence of a large number of membrane transporters in diatom genomes, which allow diatoms to rapidly respond to changing environmental conditions (Chan et al., 2011). Membrane transporters are a vital component of the toolkit that diatoms employ to sense and respond accordingly to fluctuations in essential nutrients such as nitrogen, phosphorous, silica and iron in marine environments (Brownlee et al., 2022). This extensive suite of symbiont-derived genes often allows diatoms to successfully outcompete other phytoplankton species for limiting nutrients and is likely a significant factor in the success of the group.

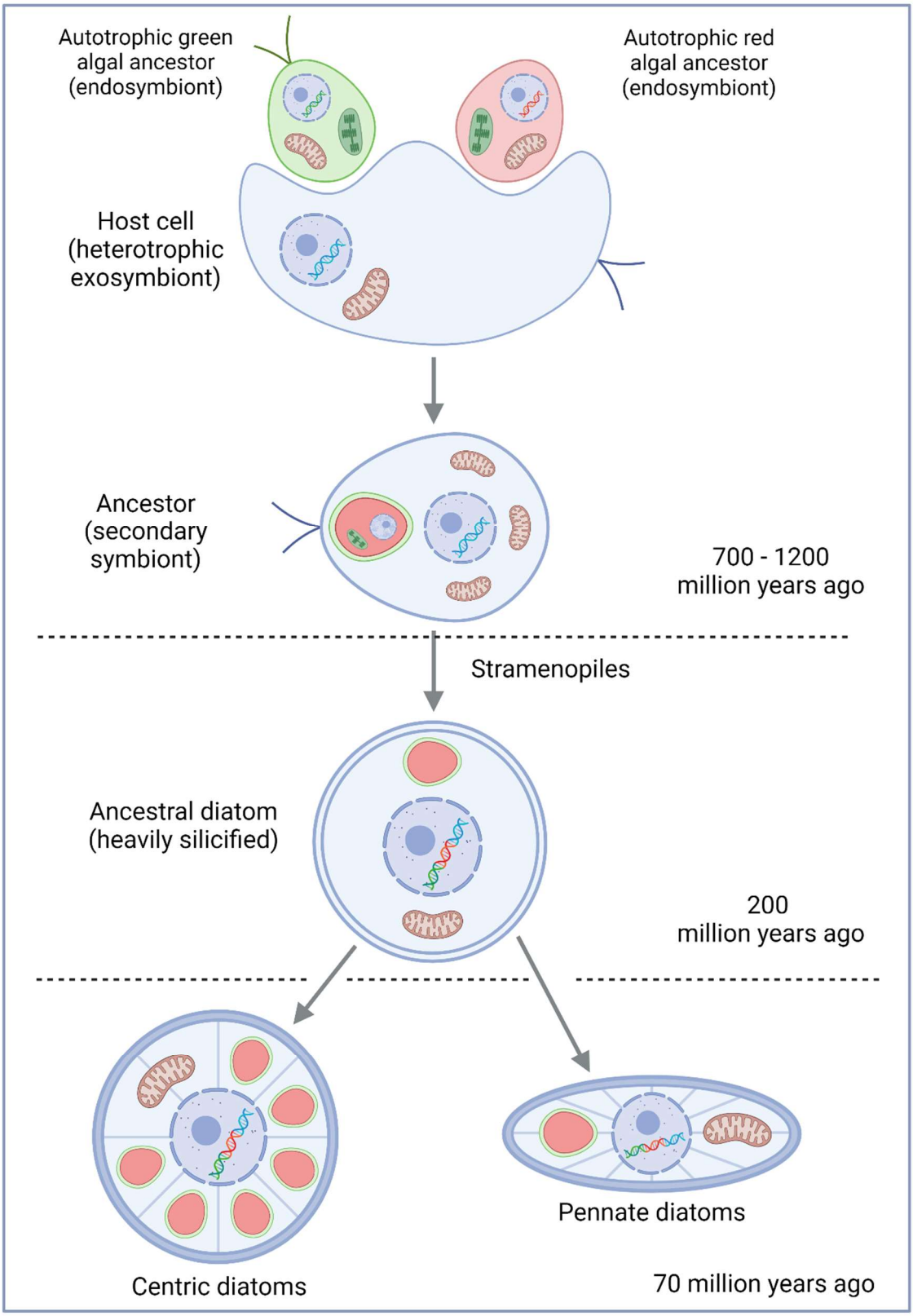

Figure 3. Evolutionary history of the diatom lineage, as told by genomic analysis. Major evolutionary events are shown, including approximate timelines for each step. Figure adapted from Benoiston et al., 2017 and created using Biorender.

Ecological significance

In case there remained any doubt surrounding the significance of diatoms in marine ecosystems, global plankton sampling efforts such as the Tara Oceans project have recently confirmed diatoms to be one of the most abundant groups of obligate photosynthetic organisms in the oceans (Malviya et al., 2016). Diatoms often dominate both marine and freshwater phytoplankton communities and their vital contributions to these ecosystems is widely recognised. In benthic communities, diatoms, typically pennate, are often found within biofilms, where their presence supports microbial communities through the provisioning of organic carbon sources (Underwood & Paterson, 2003), in addition to serving important stabilisers of marine sediments (Holland et al., 1974). In planktonic communities diatoms provide many of the same ecosystem services as their benthic relatives, that is, they serve as the base of marine food webs. As ubiquitous and abundant photoautotrophs diatoms are estimated to be responsible for approximately 20 % of all primary productivity on earth, thus providing a vital source of organic carbon upon which grazers and other microbes, including heterotrophic bacteria, depend (Waksman et al., 1937; Nelson et al., 1995; Haynes et al., 2007). In addition to their role in marine carbon cycles, diatoms are also key players in the cycling of other nutrients, such as silicon and nitrogen. As diatom cell walls are composed of biogenic silica (BSi) their growth is dependent on the availability and uptake of silicic acid (Si(OH)4) and other co-factors such as iron (Moore et al., 2001). Upon diatom cell death, either through grazing, parasitism, or natural senescence, diatom material sinks, thereby transporting approximately 50 % of all biogenic silica (100 - 140 x 10^{12} mol yr^{-1}) in the oceans to deep ocean waters and sediments, while the remaining 50 % remains in surface waters (Nelson et al., 1995). Considering that the

presence of silica cell walls is unique to diatoms, it is said that diatoms in fact drive the cycling of silicon in the world's oceans.

Perhaps one of the most notable features of the diatoms is the ability of many species to form large, sometimes toxic blooms, during which diatoms may constitute as much as 90 % of the total phytoplankton community (Han & Furuya 2000; Costa et al., 2020; Sun et al., 2022). Bloom formation occurs when diatoms are able to exploit optimal nutrient, temperature, and light conditions, resulting in a rapid burst of proliferation that can last anywhere from a few days to a several weeks (Egge & Aksnes, 1992; Kong et al., 2021). The suite of genetic adaptations diatoms have acquired through endosymbioses means that diatoms are often superior competitors for limiting factors such as phosphate and nitrate (Armbrust et al., 2004; Bowler et al., 2008). As such, in the characteristic spring phytoplankton blooms of many coastal regions, diatoms are typically the first and most abundant phytoplankton to appear, later followed by a succession of other microbial groups including grazing dinoflagellates and coccolithophores (Tiselius & Kuylenstierna, 1996; Widdicombe et al., 2010). As diatom blooms terminate, the cell matter left in their wake is either recycled in the surface oceans or forms nutrient-rich aggregates that sink to the sea floor, thus supporting benthic communities (Smetack, 1985). Though common bloom-forming diatom species may vary throughout seasons and geographical locations, there are a number of key bloom-forming genera that appear repeatedly in the literature. For example, in a 15-year time series investigating seasonal phytoplankton trends in the Western English Channel, a highly productive coastal region with annual spring phytoplankton blooms, diatoms belonging to the genera *Chaetoceros*, *Thalassiosira,* and *Skeletonema*, as well as *Pseudo-nitzschia* and *Leptocylindrus* formed regular spring and summer blooms respectively throughout the entire

study period (Widdicombe et al., 2010). Reports of *Chaetoceros*, *Skeletonema* and *Pseudo-nitzschia* blooms are commonplace within the literature and span the world's oceans, indicating that these species are important drivers of marine biogeochemical cycles and marine food webs on a global scale (Bates et al., 1998; Booth et al., 2002; Yoshida et al., 2023).

Given the significance of diatoms in marine ecosystems and the complexity of marine microbial communities, it stands to reason that over time diatoms would form an intricate web of interactions with other microbes, including microalgae, bacteria, fungi and viruses. As two of the major groups within the plankton, diatoms and bacteria have a particularly prevalent history of interkingdom interactions, which range from synergistic to antagonistic. The following sections will discuss the evolution, regulation, and physiological and ecological impacts of some of these interactions.

The good, the bad and the blurry – physiological and ecological impacts of diatom-bacteria interactions

Diatom-bacteria interactions

Diatoms and bacteria have co-occurred in marine environments for millions of years, forming stable interactions that are believed to be fundamental to the evolution and success of both groups (Bowler et al., 2008; Bowler et al., 2010). This is supported by the presence of numerous bacterially derived genes, likely acquired through horizontal gene transfer (HGT), that can be found throughout diverse diatom lineages (Bowler et al., 2008; Marchetti et al., 2008; Bowler et al., 2010). Studies by Bowler et al., (2008; 2010) revealed that the genome of model diatom *P. tricornutum* has 587 genes believed to be of bacterial origin, many of which are shared by the centric diatom *T. pseudonana*. As centric and pennate

diatoms diverged approximately 90 million years ago, this suggests that the acquisition of these bacterial genes occurred sometime prior to this divergence (Kooistra et al., 2007; Bowler et al., 2010).

The acquisition and maintenance of such a large number of bacterial genes implies that these genes provide diatoms with a competitive advantage over other phytoplankton groups, for example by enabling diatoms to exploit niches that are inaccessible to other species. For instance, the acquisition of bacterial polysaccharide synthesis genes has been theorised to have enabled diatoms to colonise open ocean environments by providing an organic coating to the diatom frustule, thereby reducing dissolution of silica from the diatom cell wall and allowing frustules to be thinner and lighter, an advantage in nutrient limited ocean environments (Bowler et al., 2010). Another study by Marchetti et al., (2008) revealed the presence of bacterial genes encoding the protein ferritin, an iron-storage protein, which may provide a competitive advantage for microbes living in iron-deplete environments. Similarly, the ice-binding proteins shared by all sea ice diatoms, but not by non-ice-associated diatoms, appear to be the result of HGT from ice-associated bacteria (Raymond & Kim, 2012), allowing ice diatoms to exploit polar niches that other algae cannot. All this is to say that it is likely that diatoms owe their enormous success in part to their ancient associations and co-evolution with bacteria.

Over many millennia, diatom-bacteria interactions have persisted and evolved along with our ever-changing ocean biome. Today, the literature illustrates a suite of interactions between diatoms and bacteria that exist in modern oceans, which continue to underpin the success of both diatom and bacterial communities. A common feature of many of these interactions is the recurrent isolation of specific bacterial taxa, primarily belonging to the *Alphaproteobacteria* and *Bacteroidetes*,

even from diverse diatom lineages (Schäfer et al., 2002; Bruckner et al., 2008; Amin et al., 2012). In particular, species belonging to the alphaproteobacterial Roseobacter group are commonly reported to be strongly associated with a diverse range of diatoms, both in laboratory cultures and in the field (Riemann et al., 2000; Sapp et al., 2007; Luo & Moran, 2014; Behringer et al., 2018). Further to this, it has been widely demonstrated that diatoms host species-specific bacterial communities, which remain stable throughout varying geographical, temporal, and environmental systems, and that associated microbiome populations are typically phylogenetically distinct from the bacterial communities found in the surrounding seawater (Grossart et al., 2005; Sapp et al., 2007; Sison-Mangus et al., 2014; Sison-Mangus et al., 2016; Behringer et al., 2018; Mönnich et al., 2020). Perhaps one of the most striking studies that supports the idea of host-specific diatom microbiomes comes from Mönnich and colleagues, who carried out a series of exposure experiments to investigate how the microbiome of a diatom host develops in culture (Mönnich et al., 2020). During this study, axenic *Thalassiosira rotula* cultures were exposed to distinct bacterial communities isolated from a range of closely and distantly related diatoms and observed over time to investigate how these bacterial communities shift. Regardless of the composition of the starting inoculum, the bacterial community consistently moved towards a stable core community, comprised largely of *Rhodobacteraceae*, *Alteromonadaceae*, and *Oceanospirillales*, which closely resembled the original microbiome of *T. rotula*. The apparent selection of specific bacterial taxa by diatom hosts implies that such interactions have important implications for host fitness and physiology. An investigation into the microbiomes of three species of *Pseudo-nitzschia* revealed that bacterial communities were phylogenetically distinct even between diatoms belonging to the same genus

(Sison-Mangus et al., 2014). Microbiome transplant experiments resulted in markedly different impacts on the growth of the diatom host when compared to diatoms cultured with their native microbiome, with the introduction of foreign bacterial assemblages to a new host even resulting in parasitic behaviour in some cases. It is therefore likely that microbiome cultivation is an important adaptive strategy that contributes to the ecological success of the diatoms.

At their core, these interactions, like all microbial interactions, are based on a uni- or bidirectional exchange of services to the benefit of one or all partners. Such interactions are regulated by what are sometimes referred to as ‘metabolic currencies’, exogenous compounds that are exchanged between organisms that either signal the presence of a potential microbial associate, or that can be utilised by an associated microbe (Durham, 2021). Perhaps the most simple and well-understood type of algal-bacteria interaction is the mutualistic exchange of essential micronutrients, such as B vitamins, iron or nitrates, from the bacteria in exchange for diatom-derived dissolved organic carbon (DOC) or other algal exudates (Haines & Guillard, 1974; Croft et al., 2005; Amin et al., 2015; Durham et al., 2015). Over time, these interactions appear to have selected for stable, consistent interactions between diatoms and specific groups of bacteria. However, to simplify all diatom-bacteria interactions to the mutual exchange of nutrients would exclude a large portion of the spectrum of synergistic, commensal, antagonistic and variable interactions that are observed between diatoms and marine bacteria. The following sections will examine the types of interactions observed between diatoms and bacteria, in addition to discussing the currencies and regulation of some well-studied examples.

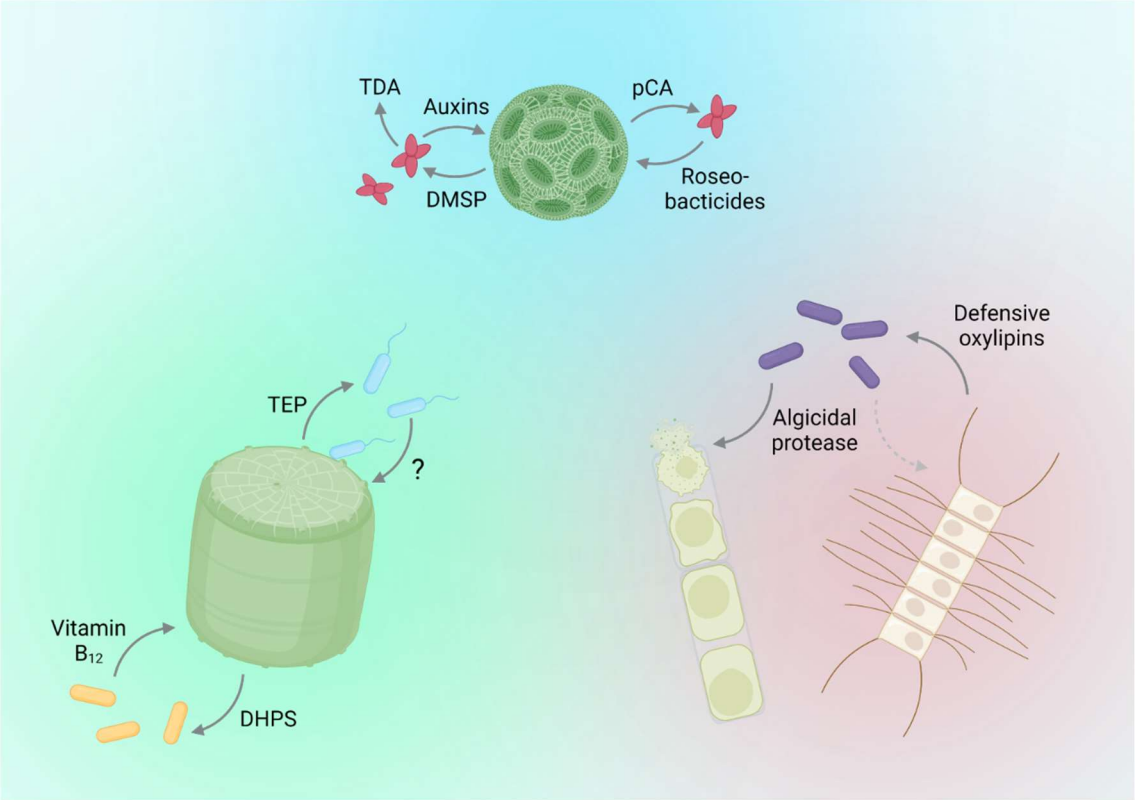

Figure 4. Examples of synergistic (green), antagonistic (red) and 'sliding scale' (blue) interactions between microalgae and bacteria, including some of the metabolic currencies exchanged in the interactions. Synergistic interactions include the exchange of metabolic currencies to the benefit of both partners. Pictured is the provisioning of vitamin B12 by *Roseobacter Ruegeria pomeroyi* to diatom host *Thalassiosira pseudonana* in exchange for 2,3-dihydroxypropane-1-sulfonate (DHPS), a diatom-derived carbon source which sustains the growth of *R. pomeroyi* (Durham et al., 2015). Also pictured is *Marinobacter adhaerens,* which causes an increase in both the growth and the production of transparent exopolymer particles (TEP) by diatom host *Thalassiosira weissflogii*, resulting in increased diatom aggregate formation, which likely benefits the bacteria by increasing their access to diatom-derived dissolved organic carbon (DOC, Sonnenschein et al., 2012; Gärdes et al., 2012). Antagonistic interactions can include the secretion of diatom-lytic compounds by algicidal bacteria, such as *Kordia algicida*, which secretes algicidal proteases with potent lytic activity against *Skeletonema costatum*. Conversely, some diatoms, such as *Chaetoceros didymus*, possess defense mechanisms (in this case, oxylipins), which can protect from algicidal attacks (Paul & Pohnert, 2011; Meyer et al., 2018). Sliding scale interactions are those in which the nature of the interaction is dependent on external variables. *Roseobacter Phaeobacter gallaeciensis* behaves synergistically towards its coccolithophore host *Emiliania huxleyi* during initial stages of the interaction, providing growth promoting auxins and pathogen protection via antimicrobial compound synthesis (Tropodithietic acid, TDA), in return for Dimethylsulfoniopropionate. However, when *E. huxleyi* begins to secrete senescence molecule p-Coumaric acid (pCA), *P. gallaeciensis* switches to an antagonistic lifestyle in which it secretes algicidal compounds known as roseobacticides (Seyedsayamdost et al., 2011). Figure created using Biorender.

The good - examples and mechanisms of synergistic interactions

As previously stated, the most well characterised types of diatom-bacteria interactions are those which are synergistic in nature. Diatom-bacteria synergism is typically based on a mutual exchange of essential resources within the phycosphere, a nutrient-rich microenvironment surrounding a diatom cell (analogous in nature to the rhizosphere, Bell & Mitchell, 1972). Many bacterial species have been reported to use chemotaxis to actively seek out and inhabit these microenvironments in order to exploit the high density of diatom-derived organic carbon sources contained within (Bell & Mitchell, 1972; Sonnenschein et al., 2012; Smriga et al., 2016). In return, bacteria provide their hosts with a diverse array of essential resources, including, but not limited to, B vitamins, nitrogen, iron and even growth promoting auxins and antimicrobial compounds to fend off potential pathogens.

Perhaps the most extensively studied example of diatom-bacteria symbioses is the provision of essential vitamin B_{12} by bacteria in exchange for diatom-derived organic exudates. In 1974, Haines & Guillard conducted a study, which showed that representatives of multiple diatom groups were unable to grow in the absence of vitamin B_{12}. However, growth improved when diatoms were co-cultured with vitamin B_{12} synthesising bacteria, hence pointing to the provisioning of B_{12} by bacteria to the benefit of their diatom hosts (Haines & Guillard, 1974). Roughly 60 % of heterokonts, including many diatoms, require exogenous vitamin B_{12} for growth, which is often reported to be supplied by symbiotic B_{12}-synthesising bacteria (Croft et al., 2005; Tang et al., 2010). In return, bacteria gain access to a steady source of fixed carbon. Indeed, a transcriptional study of a B_{12}-limited phytoplankton community in the Southern Ocean demonstrated that

Oceanospirillaceae, a group of B_{12}-synthesising bacteria, upregulate genes involved in B_{12} synthesis, organic matter acquisition and cell surface attachment when the surrounding diatom community is displaying transcriptional signs of B_{12} starvation (Bertrand et al., 2015). This study thus provides further support for the potential importance of B_{12}-synthesising bacteria in mediating diatom-bacteria interactions, particularly in natural marine ecosystems.

Other nutrients that diatom-associated bacteria may exchange for algal-derived carbon include iron and nitrogen (Amin et al., 2009; Foster et al., 2011). Iron is an essential micronutrient required by all cells, yet bioavailable iron is often present in low quantities in marine environments, often limiting primary productivity (Fung et al., 2000). Many bacteria are able to mitigate this problem by producing iron-chelating compounds called siderophores, which bind iron and transport it into the cell in a bioavailable form (Hider & Kong, 2010). Multiple reports have demonstrated that microalgae are able to utilise bacterial siderophores in exchange for algal-derived organic matter (Amin et al., 2009; Kazamia et al., 2018). Further, as different bacterial and fungal groups produce distinct classes of siderophores (Hider and Kong, 2010), different diatom species appear to favour particular classes of siderophores (Kazamia et al., 2018). While *P. tricornutum* preferentially chelates hydroxamate-type siderophores, *Thalassiosira oceanica* preferentially uptakes catecholate siderophores (Kazamia et al., 2018). Deciphering whether this is the result of the coevolution of each diatom with their species-specific microbiome requires further attention.

While nutrient exchange remains an essential factor in many diatom-bacteria interactions, interkingdom interactions can also be controlled by various other currencies. For instance, bacteria have been reported to provide their hosts with additional services, such as protection from potentially antagonistic microbes

through the synthesis of antimicrobial compounds (Seyedsayamdost et al., 2011; Stock et al., 2019). For example, Stock and colleagues reported that the presence of the natural microbiome of diatom *Cylindrotheca closterium* hindered the antagonistic effects of a growth inhibiting *Marinobacter* strain (Stock et al., 2019). A similar effect is observed between algal-associated Roseobacter *Phaeobacter gallaeciensis* and its coccolithophore host *Emiliania huxleyi* (Seyedsayamdost et al., 2011). In this study, Seyedsayamdost describes not only the production of algal growth promoting stimulants (auxins) by *P. gallaeciensis*, but also the production of antimicrobial tropodithietic acid (TDA), which is hypothesised to deter potential algal pathogens (Seyedsayamdost et al., 2011). The ability to synthesise TDA is a trait shared by a range of different algae-associated *Roseobacters* (Geng et al., 2008; Seyedsayamdost et al., 2011). Combined with the conclusions drawn in other studies about the ability of natural diatom microbiomes to dampen pathogenic activity of other microbes, these results imply that protection from pathogens can be an important factor in diatom-bacteria associations.

Further, advances in molecular techniques, such as transcriptomic analysis, have started to draw a more detailed picture of the intricate regulatory mechanisms employed by diatoms to establish, and perhaps more importantly, maintain associations with beneficial bacterial partners. For example, Shibl et al., (2020) demonstrated that the exposure of universal marine diatom *Asterionellopsis glacialis* to its natural associated bacterial community results in the upregulation of genes involved in the production and secretion of secondary metabolites, including rosmarinic and azelaic acid. While the collection of generic secondary metabolites secreted by *A. glacialis* in this system can be utilised by symbiotic and opportunistic bacteria alike, rosmarinic and azelaic acid both appear to have

a more specific role. Both compounds were found to promote the growth and attachment of symbiotic bacteria, while simultaneously supressing the growth of non-symbiotic bacteria. Utilisation of azelaic acid appears limited to a small handful of symbiotic bacteria (Shibl et al., 2020), and it could therefore be argued that the upregulation of azelaic acid synthesis is part of an intricately regulated system to promote and maintain a symbiotic relationship between diatoms and specific bacterial taxa.

Amin and colleagues provide further evidence for the cultivation of mutualistic interactions between *Pseudo-nitzschia multiseres* and associated *Sulfitobacter* (Amin et al., 2015). In this system, *Sulfitobacter* provides receptive *P. multiseries* strains with ammonium (which is taken up preferentially over alternative nitrate sources) and enhances diatom cell division in return for sulfonated organic compounds. The relationship is suggested to be co-ordinated by the sequential release of diatom-derived tryptophan, and bacteria-derived Indole-3-Acetic Acid (IAA). Transcriptome evidence from *P. multiseries-Sulfitobacter* co-cultures suggest that *Sulfitobacter* converts diatom-derived tryptophan to IAA, which promotes diatom cell division. In turn, IAA is converted back to tryptophan by *P. multiseries*, resulting in a positive feedback loop, which likely maintains this relationship.

The sophisticated regulation of such interactions through the secretion and utilisation of diverse secondary metabolites serves to support the idea that these exchanges are functionally important for both bacteria and their diatom hosts. Although the studies discussed in the previous section demonstrate the beneficial nature of these relationships ex situ, laboratory studies rarely accurately mimic natural environments, and neither confirm nor deny the presence of these interactions in nature. As such, lab-based studies fall short of demonstrating the

true ecological significance of these interactions in natural ecosystems. Combining laboratory studies with field-based examinations will therefore be a vital step in expanding our current knowledge of how diatom-bacteria interactions are mediated in natural marine systems. Although such studies are limited, a few works have started to draw on transcriptional tools and ocean databases to begin to investigate the diversity and distribution of some key components of diatom-bacteria interactions, in the hopes of gaining some insights into their potential ecological significance.

The bad - examples and mechanisms of antagonistic interactions

While synergistic interactions and the benefits that they can confer have been a focal point of the study of diatom-microbe interactions for decades now, it is becoming increasingly apparent that for every synergistic interaction reported that there exists an antagonistic interaction to balance the scales. Reports of diatom pathogens include not only antagonistic bacteria, but also chytrid fungi, oomycetes and viruses, each with substantial physiological impacts on their susceptible diatom hosts (Nagasaki et al., 2004; Hanic et al., 2009; Ibelings et al., 2011; Arsenieff et al., 2019). As such, the literature has seen an increase in studies of diatom-antagonists in recent decades due to the potential value of these organisms as biocontrol agents for controlling Harmful Algal Blooms (HABs, Mayali & Azam, 2004; Kang et al., 2005) and for their use in algal biotechnology systems (Lenneman et al., 2014; Chen et al., 2015), in addition to the potential ecological significance of antagonistic diatom-microbe interactions. For example, chytrid infections of diatoms are widespread, and can cause dramatic reductions in host cell density, thus facilitating shifts in overall diatom

diversity and potentially altering diatom community dynamics (Ibelings et al., 2011). Similarly, although viruses infecting diatoms were discovered only recently (with the first diatom virus being isolated just two decades ago, Nagasaki et al., 2004), lytic diatom viruses are also receiving increased attention for their potential role in diatom bloom demise (Arsenieff et al., 2019).

Given the density and diversity of diatom-associating bacteria hosted within the phycosphere, diatom-antagonistic bacteria have the potential to shape diatom physiology and ecology through antagonistic interactions. The following sections will discuss the types of antagonistic diatom-bacteria interactions reported in the literature and explore some of the mechanisms used in both the attack and defence of diatoms by antagonistic bacteria.

Examples

Possibly the simplest type of any antagonistic microbe-microbe interaction is competition for resources. Essential nutrients in marine environments are often available in short supply, with nutrients such as phosphorous, nitrogen and iron limiting growth and productivity of planktonic organisms (Fung et al., 2000; Bristow et al., 2017). Although research into nutrient competition between diatoms and bacteria is somewhat sparse, environmental and lab-based studies have demonstrated that bacteria appear to compete with diatoms for nutrients including phosphorous and nitrates (Thingstad et al., 1993; Grover, 2000; Diner et al., 2016). Risgaard-Petersen et al., (2004) demonstrated that benthic diatoms are able to outcompete ammonia-oxidising bacteria (AOB) due to their superior rates of nitrogen uptake, thus resulting in decreases of up to 80 % in both the growth and metabolic potential of competing bacteria. Conversely, Diner et al. (2016) investigated nitrate competition between the model diatom *P. tricornutum*

and the heterotrophic bacteria *Alteromonas macleodii* and found that the outcomes of nitrate competition in this system depended heavily on external factors, such as the availability of organic carbon. It was found that while solely utilising *P. tricornutum*-derived carbon, *A. macleodii* was an ineffective competitor for nitrate, whereas when provided with external carbon sources, *A. macleodii* appeared to undergo rapid proliferation to the detriment of *P. tricornutum* (Diner et al., 2016). The diversity and dynamic nature of marine ecosystems means that it is unlikely that diatoms and bacteria will ever interact in a controlled environment where nutrient availability remains favourable and constant. It could therefore be suggested that nitrate or other nutrient competition between diatoms and bacteria will seldom be stable and may vary over spatio- and temporal scales, and that the winners of this type of competition will vary accordingly.

Due to the scarcity of essential nutrients in marine environments, competition for limiting resources is a selection pressure faced by all marine microbes. Over time microbes have evolved various mechanisms to survive in such limited environments. For some, these adaptations have arisen in the form of metabolites that increase scavenging capabilities, such as siderophores that bind iron with a high affinity. A more direct method could be to remove or inhibit a competing microbe entirely, which therefore poses the question, could competition be a pre-cursor for a more active type of antagonistic diatom-bacteria interaction, such as algicidal activity?

Although there exists a wealth of studies on algicidal bacteria, there appears to be no clear definition for what constitutes an algicidal bacterium. Mayali & Azam (2004) propose that true algicidal bacteria are ‘algal pathogens that satisfy Koch’s postulates in an environmental context’. This would stipulate that 1) the pathogen would need to be found in high numbers in all cases of an infected diatom, 2) the

pathogen would need to be isolated in pure culture and demonstrated to be capable of reinfecting a healthy diatom in re-exposure studies, and 3) the pathogen would subsequently need to be reisolated from the diseased diatom and proven to be identical to the strain used in the re-exposure experiment (Loeffler, 1884). It could be argued that some organisms do fit the definition of a true pathogen, i.e., parasitic chytrids and oomycetes are commonly found to infect a broad range of diatoms, with some even showing an obligate parasitic lifestyle (Hanic et al., 2009; Ibelings et al., 2011; Gutiérrez et al., 2016; Buaya et al., 2019). Conversely, others may argue that any bacterium capable of causing algal cell death can be classified as an algicidal bacterium. This definition may be more relevant in an environmental setting, as we have already discussed the range of biotic and abiotic fluctuations in natural ecosystems that can impact the outcomes of diatom-bacteria interactions. If we consider this definition to be more ecologically representative, then the literature reports a suite of studies of diatom-algicidal bacteria. Many marine bacteria possess the ability to produce algicidal compounds, which have been implicated in diatom cell lysis and even the subsequent decline of diatom populations (Park et al., 2010; Paul & Pohnert, 2011; Seyedsayamdost et al., 2011). To date, a range of algicidal compounds and antagonistic mechanisms have been described, which bacteria employ to exploit or gain a competitive advantage over diatoms. For example, two prominent diatom-antagonists, *Kordia algicida* (Sohn et al., 2004; Paul & Pohnert, 2011) and *Croceibacter atlanticus* (Amin et al., 2015; van Tol et al., 2017), each show distinct antagonistic activities with markedly different outcomes on diatom physiology.

K. algicida is a planktonic flavobacteria, which displays algicidal activities against a range of diatom species, including *Thalassiosira weissflogii* (renamed *Conticribra tricircularis*, Stachura-Suchoples & Williams, 2009, however referred

to as *T. weissflogii* throughout this thesis), *P. tricornutum* and bloom-forming *Skeletonema costatum* (Sohn et al., 2004; Paul and Pohnert, 2011). *K. algicida* displays what could be deemed true algicidal activity, i.e., it secretes algicidal compounds resulting in algal cell death. Paul and Pohnert, (2011), revealed the algicidal compounds to be proteases, the efficacies of which are host-specific. While cell-free filtrates of *K. algicida* showed significant activity against *T. weissflogii, P. tricornutum* and *S. costatum*, no activity was observed against bloom-forming diatom *Chaetoceros didymus*.

Conversely, many might argue that ubiquitous marine flavobacterium *C. atlanticus* is a diatom antagonist rather than a true algicidal bacterium, as *C. atlanticus* inhibits diatom growth as opposed to causing cell lysis (Amin et al., 2015; van Tol et al., 2017). *C. atlanticus* has demonstrated an ability to inhibit the growth of multiple diatom species, including *Pseudo-nitzschia multiseries, Pseudo-nitzschia fraudulenta,* and *T. pseudonana* by means of direct contact with its diatom host (Amin et al., 2015; van Tol et al., 2017). In an investigation into the mode of action and physiological impacts of this antagonist, it was found that the attachment of *C. atlanticus* to *T. pseudonana* cells results in an inhibition in diatom cell division. The downstream effect of growth inhibition was a significant increase in the cell size of individual diatom cells and increased chlorophyll a content, suggested to be a mechanism by which *C. atlanticus* can exploit the diatom and its exudates by increasing the surface area to which it can attach (van Tol et al., 2017). Although growth inhibition may seem less significant than diatom cell lysis, van Tol and colleagues theorise that *C. atlanticus* could further contribute to the decline of an already ageing diatom population by halting cell division. Further to this, as many flavobacteria, including *C. atlanticus*, are reported to specialise in organic matter degradation towards the end of algal blooms (Teeling et al., 2012),

their place in diatom bloom decline should not be overlooked. Could it be possible that other members of the Flavobacteria display similar activity, which is simply overshadowed by what is perceived to be the natural termination of a diatom bloom due to ageing?

Unfortunately, one thing that remains clear is that our knowledge of the diversity of diatom-antagonists within natural phytoplankton assemblages is lacking, as only a small handful of studies examine the potential diversity of naturally occurring algicidal bacteria within the phytoplankton. If the antagonistic effects of *C. atlanticus* can go virtually undetected for so long in an ageing diatom population, then there may be a hidden diversity of other diatom-antagonists concealed within the plankton. A lack of proper sampling techniques to isolate algicidal bacteria from phytoplankton communities is a persistent issue slowing the progress of this field.

Mechanisms

As with the synergistic interactions discussed in the previous section of this review, antagonistic interactions are also mediated via the excretion of a spectrum of secondary metabolites (Figure 4). One of the most well characterised examples of such is the protease-mediated algicidal activity of *K. algicida*. During the investigation of the algicidal activity of *K. algicida*, it was discovered that protease synthesis is dependent on the density of the bacterial culture, as opposed to being triggered by the presence of susceptible diatom hosts (Paul & Pohnert, 2011). Proteases were undetectable in early, low density cultures, but saw a rapid increase during the late exponential phase of bacterial growth. Additionally, the introduction of cell free filtrates from an older *K. algicida* culture to freshly cultured *K. algicida* population induced protease synthesis at a much

earlier growth stage than observed in the control culture. A quorum-sensing (QS) like system was suggested to be the responsible regulatory pathway involved in this process. Quorum sensing is a common gene regulation mechanism employed by diverse bacterial lineages, in which singalling molecules called autoinducers, which accumulate in a bacterial medium as cell density increases, trigger the regulation of a metabolic pathway (Miller & Bassler, 2001). A similar type of density-dependent algicidal activity has been reported from an algicidal *Ponticoccus* species (Chi et al., 2017). Chi and colleagues investigated the N-acyl-homoserine lactone (AHL)-based quorum-sensing system of *Ponticoccus* sp. PD-2 and were able to demonstrate that inhibition of AHLs lead to a significant 50 % reduction in algicidal activity. Paul and Pohnert speculate that this type of density-dependent regulation is likely due to the fact that the excretion of a low concentration of algicides in low density bacterial cultures would be inefficient and energetically costly. It could be hypothesised that the presence of low, tolerable levels of potentially lethal compounds could lead to resistance in target hosts.

Ecological impacts

Though still relatively poorly studied, it seems that algicidal bacteria have the potential to significantly shape diatom, and thus wider phytoplankton, communities. For example, it is often speculated that algicidal bacteria may play an important role in diatom bloom termination (Park et al., 2010; Bigalke et al., 2019). Mesocosom experiments by Bigalke et al., (2019) demonstrated that introducing *K. algicida* to a mid-bloom diatom population, taken directly from seawater samples from the North Sea, caused a rapid decline in numbers of bloom-forming *Chaetoceros socialis*. While this result alone has potential ecological implications, Bigalke and colleagues also observed the knock-on effects of the *C. socialis* culture crash on the wider phytoplankton community.

Upon the termination of the *C. socialis* bloom, *Phaeocystis,* a prymnesiophyte resistant to *K. algicida,* was able to exploit the niche left empty by the sudden crash of its competitor. Concurrent observations of the natural phytoplankton bloom from which the initial experimental seawater samples were taken found that the bloom progression of the natural phytoplankton community closely mirrored that of the mesocosm experiment, albeit at a much slower rate.

The blurry – examples and mechanisms of facultative interactions

Despite their limitations, laboratory studies have been instrumental in the study of diatom-bacteria interactions and their metabolic regulation. The ability to control external factors is what has allowed us to disentangle the elaborate regulatory pathways involved in many of the interactions discussed thus far in this review. However, it is such controlled settings that pose perhaps the most significant issue, that is controlled settings cannot possibly accurately mirror the diversity and dynamic nature of natural environments. Marine ecosystems often exhibit annual, seasonal, and even daily fluctuations in a variety of biotic and abiotic factors, including community composition, temperature, salinity and nutrient status. Each of these factors not only impact individual members of the phytoplankton, but also the way in which they interact with their surrounding environment. Many microbes are able to senses fluctuations in their environment and utilise this information to adjust their metabolism or lifestyle accordingly. The result is a range of dynamic, opportunistic interactions between microbial partners that can seemingly shift from synergistic to antagonistic, and vice versa, according to the external factors to which they are exposed (Figure 4).

Examples

Such an opportunistic lifestyle switch is perhaps best demonstrated by members of the ubiquitous roseobacter group. Although the previous discussions of algae-associated roseobacters in this review have been largely positive, various members of the roseobacter lineage have been reported to switch from a synergistic to a pathogenic lifestyle under specific conditions (Seyedsayamdost et al., 2011; Barak-Gavish et al., 2023). In the study by Seyedsayamdost et al., (2011), it was demonstrated that the nature of the relationship between roseobacter *P. gallaeciensis* and its host *E. huxleyi* is highly variable depending on the physiological status of the host cell. The synergistic behaviour observed in this study, i.e., the production of auxins and antimicrobial TDA, occurs only in the primary stages of the relationship, when algal cell health is optimal. As host cells begin to age, *P. gallaeciensis* switches to a pathogenic lifestyle by secreting a class of algicidal compounds known as roseobacticides. Later studies into the distribution of roseobacticides throughout the roseobacter lineage revealed production of these compound to be widespread (Sonnenschein et al., 2018). *Phaeboacter inhibens*, a bacterium commonly associated with diatoms, was found to produce roseobacticides capable of significantly hindering the growth of *T. pseudonana* (Sonnenschein et al., 2018). Despite the potential significance of such compounds on diatoms, the two organisms were not observed in co-culture together, and as such, it is not known whether the same lifestyle switch might be observed in a diatom-bacteria system. Further work is therefore required to investigate if such a lifestyle switch bears any relevance on diatoms.

Mechanisms

By now it is evident that diatom-bacteria interactions, regardless of their nature, are regulated by an elaborate network of metabolic processes, although what these metabolic processes are often remains elusive. Fortunately, both studies discussed in the previous section of this review have been able to provide a comprehensive picture of the metabolic regulation of both systems. For example, in the *E. huxleyi-P. gallaeciens* system, Seyedsayamdost and colleagues were able to link the induction of algicidal activity by *P. gallaeciensis* to algal senescence, whereby an accumulation of algal senescence molecule p-coumaric acid (pCA) is detected by *P. gallaeciensis* and subsequently triggers a lifestyle switch from synergistic (TDA production) to antagonistic (the production of algicidal roseobactecides, Seyedsayamdost et al., 2011).

Similarly, in the *Sulfitobacter* system described by Barak-Gavish and colleagues exposure to algal dimethylsulfoniopropionate (DMSP) was found to be the trigger for algicidal activity. Both of these studies provide an incredibly valuable insight into the regulation of algal-bacteria relationships. The discovery of another example of a ‘Jekyll-and-Hyde’ lifestyle indicates that this regime may be more widespread than initially thought, particularly amongst Roseobacter species. More interestingly, however, is the fact that both of these systems, while similar in nature, appear to be controlled by different metabolic pathways. Could this suggest convergent evolution of an important adaptive strategy within algae-associated heterotrophic bacteria?

Ecological impacts

Unfortunately, studies of lifestyle switches in algal-bacteria relationships still appear to be in their infancy. Although the two algicidal switch systems described in the literature provide a relatively complete picture of how these systems are regulated, the differences in the regulation of each interaction adds an additional barrier to fully understanding algicidal triggers in marine bacteria. Marine environments are a melting pot of microbially-derived metabolites, many of which have yet to be assigned a clear function. It is therefore entirely possible that there are a multitude of other metabolites that trigger shifts in diatom-bacteria interactions that we are currently entirely unaware of. As such, significant further work is required to 1) investigate how common lifestyle switches are within diatom-bacteria relationships, 2) disentangle the diversity of mechanisms that underpin these potentially significant switches, and 3) understand the ecological impacts that these may have on phytoplankton assemblages.

Concluding remarks

It is evident from the range of studies discussed in this review that the coexistence of globally important diatoms and marine bacteria significantly impacts diatom physiology through an extensive range of dynamic interactions. In turn, these interactions have far-reaching impacts not only on phytoplankton ecology, but also on wider marine ecosystems and even biogeochemical cycles. Antagonistic bacteria are certainly capable of significantly influencing diatom growth and physiology, as showcased in this review. Perhaps one of the most significant conclusions to be drawn from some of these studies is the potential of antagonistic bacteria to induce diatom population decline or bloom termination events. Mounting evidence supports the theory that some algicidal bacteria are

indeed capable of causing diatom culture crashes in lab-based studies (Jung et al., 2010; Bigalke et al., 2019). And while Park et al., (2010), have previously hinted at the correlation between increased abundances of algicidal bacteria in natural seawater ecosystems with microalgal population decline, the direct impacts of interactions between diatoms and antagonistic bacteria in natural ecosystems are still unclear. Unfortunately, many of the interactions outlined in the previous sections can be extremely difficult to observe in nature. The root of this issue is likely two-fold. The natural bloom-and-bust life cycles of many diatom species is often attributed to abiotic factors such as temperature and nutrient availability (Egge & Aksnes, 1992; Lomas & Gilbert, 1999; Shipe et al., 2008; Bermejo et al., 2018), and as such, the role of algicidal bacteria in such systems may be easily overlooked. This, combined with a lack of adequate sampling techniques and efforts means that although the significance of antagonistic diatom-bacteria interactions is becoming clear, our understanding of the diversity, abundance and ecological significance of these interactions in natural ecosystems remains poor. The systematic review of diatom-antagonistic bacteria within natural phytoplankton assemblages requires the establishment and routine application of robust sampling methods. Assessing the diversity, seasonal patterns, and metabolic regulation of antagonistic diatom-bacteria interactions in a natural marine ecosystem will not only help predict future trends in a rapidly changing environment but will also help improve our understanding of ecosystem modelling and biogeochemical cycling.

Aims of PhD

The objective of this thesis is to combine laboratory and field-based approaches to characterise antagonistic diatom-bacteria interactions in a model coastal environment, the Western English Channel. As such, there are three main questions this project aims to explore. Firstly, how diverse is the community of antagonistic bacteria present in a diatom-rich ecosystem and do the key players change over a seasonal cycle? Secondly, what are the physiological impacts of antagonistic bacteria on their diatom hosts and how are these interactions metabolically regulated? Finally, how abundant are these antagonistic bacteria and how do they co-exist with their diatom hosts in the natural environment?

1) To explore the diversity of naturally occurring diatom-antagonistic bacteria at the Western Channel Observatory L4 coastal station a robust plaque assay method, designed to isolate a range of antagonistic bacteria, is developed and employed over an annual cycle.

2) To elucidate the physiological impacts of antagonistic bacteria on their diatom hosts, the library of antagonistic bacteria from (1) will be observed in co-culture with a range of model and bloom-forming diatom species. Additionally, the regulation of antagonistic activity under various culture and environmental conditions is investigated.

3) To characterise the seasonal trends and co-occurrence of antagonistic bacteria with their diatom hosts, amplicon sequencing of the whole microbial community at the L4 coastal station is conducted over an annual cycle, and the *Tara* Ocean Barcode Atlas is employed to assess global biogeography.

Chapter 1:

Characterising the diversity and seasonal patterns of bacterial antagonists of bloom-forming diatom species in the Western English Channel

1.1 Introduction

Exploring drivers of diatom bloom succession in coastal ecosystems

As one of the most successful phototrophic groups in the global oceans (Malviya et al., 2016), diatoms fulfill a vital role in marine ecosystems, contributing approximately 40 % of all marine primary productivity, in addition to heavily influencing both nitrogen and silica cycles (Nelson et al., 1995; Tréguer & de La Rocha, 2013; Kamp et al., 2016). Due to their ubiquity and abundance in the oceans, diatoms represent an important source of organic carbon for both higher and lower trophic organisms alike, thus fuelling marine ecosystems through primary productivity. In particular, seasonal diatom blooms are significant events that support an enormous diversity of microbes, including heterotrophic bacteria, which are able to utilise the substantial amounts of organic carbon that result from a diatom bloom. Early studies demonstrated that half of algal derived primary production is utilised by marine bacteria (Prog et al., 1983; Cole et al., 1988; Ducklow et al., 1993), while the remaining carbon is sequestered in marine sediments when diatom aggregates sink out to the sea floor (Jiao et al., 2010). As such, understanding the factors driving diatom success and bloom regulation in marine environments is of paramount importance for understanding microbial community dynamics and global biogeochemical cycles.

The suite of abiotic factors that influence diatom bloom dynamics, such as temperature, light, and nutrient availability have been extensively characterised (Ferris & Lehman, 2007; Edwards et al., 2022). Meanwhile, the significance of biotic factors, such as bacterial antagonism, as drivers of diatom success and bloom regulation has often been underappreciated, despite a multitude of studies observing robust associations between particular bacterial groups and diatom bloom phases over a bloom cycle (Teeling et al., 2012; Taylor et al., 2014;

Klindworth et al., 2014). For example, work conducted by Teeling et al., (2012) on bacterial community composition over a diatom bloom cycle observed high abundances of Alphaproteobacteria that remained stable throughout a North Sea bloom, but saw a significant increase in Flavobacteria (in addition to Gammaproteobacteria) towards the end of the bloom period. The coupling of Alphaproteobacteria, such as Rhodobacterales, and Flavobacteriales with diatom blooms is a common finding of many bloom microbiome studies (Fandino et al., 2005; Teeling et al., 2012; Taylor et al., 2014). The abundance of members of the Alphaproteobacteria is perhaps to be expected due to the range of synergistic relationships Alphaproteobacteria often forge with diverse diatom species (Durham et al., 2015; Amin et al., 2009; 2015). However, more interesting, perhaps, is the association of Flavobacteriales with declining diatom bloom populations, as a mounting number of studies offer insights into the potential significance of antagonistic Flavobacteriales in shaping diatom community dynamics. For example, *Kordia algicida* secretes algicidal compounds that result in the lysis of multiple diatom species, including *Skeletonema costatum*, *Phaeodactylum tricornutum*, and *T. weissflogii* (Sohn et al., 2004; Paul and Pohnert, 2011). Further, Bigalke and colleagues demonstrated that the introduction of *K. algicida* to a mesocosm diatom bloom resulted in a significant restructuring of diatom community composition. Namely, the rapid decline of *Chaetoceros socialis* followed by a sharp increase in *Phaeocystis* species, a pattern which closely mirrored the progression of a natural phytoplankton community over a diatom bloom season (Bigalke et al., 2019). Conversely, *Croceibacter atlanticus*, exhibits growth inhibitory effects as opposed to direct algicidal activity (Amin et al., 2015; van Tol et al., 2017; Bartolek et al., 2022). Nonetheless, cultivations of *C. atlanticus* with multiple *Thalassiosira* species saw

a reduction in diatom cell reproduction and cell wall stability, concurrent with an increase in diatom cell size, chlorophyll content and both intra- and extracellular carbohydrates. This mechanism potentially facilitates increased bacterial colonisation of the larger diatom cells and thus provides more access to increased diatom-derived dissolved organic carbon (DOC). Interestingly, van Tol and colleagues postulate that the interaction between *C. atlanticus* and *T. weissflogii* may accelerate the decline of already ageing diatom blooms via the inhibition of diatom reproduction (van Tol et al., 2017). Additionally, the increase in diatom carbohydrates observed by Bartolek et al., (2022) in the presence of *C. atlanticus* may attract further bacterial degraders, once again accelerating diatom bloom decline.

The repeated occurrence of particular bacterial groups, such as potentially antagonistic Flavobacteria, during distinct diatom bloom phases indicate that certain bacterial orders may be intrinsically linked to diatom bloom succession. Combined with insights gleamed from laboratory studies of diatom-antagonism, such as the parallels drawn between the mesocosm community shift caused by *K. algicida* and the concurrent community shift observed in a natural marine ecosystem, these findings indicate that antagonistic bacteria may indeed be important drivers of diatom bloom regulation. Despite this, the true diversity and prevalence of diatom-antagonists in marine ecosystems remains unclear as ecosystem-scale assessments of diatom-antagonistic bacteria are rare. Many of the currently described diatom-antagonists were isolated either from xenic laboratory cultures (van Tol et al., 2017; Deng et al., 2022), or environmental sampling regimes which utilised a single diatom host species or covered only narrow sampling windows, with a bias towards spring bloom sampling (Mitsutani et al., 2001; Sohn et al., 2004; Wang et al., 2015; Bedoshvili et al., 2021). As

such, these studies often do not represent the true diversity of antagonists within an ecosystem. Characterising the diversity of antagonistic bacteria which inhabit an ecosystem (sometimes referred to as the pathobiome) is fundamental to our understanding of these bacteria as natural drivers of diatom ecology, and requires a robust and systematic sampling approach to capture their true diversity and seasonal dynamics.

The Western English Channel as a model ecosystem

The Western English Channel (WEC) is a highly productive coastal region located off the coast of Plymouth, UK, that has been closely monitored since 1903 by the Western Channel Observatory (WCO) (https://www.westernchannelobservatory.org.uk/). The WCO, as one of the longest running oceanographic time series in the world, collects a variety of *in situ* biological, chemical, and physical data weekly, providing a comprehensive picture of the robust biotic and abiotic annual seasonal trends within this region. As such, phytoplankton and bacterioplankton trends in the WEC have been extensively studied. Phytoplankton communities within the WEC are characterised by annual spring diatom blooms (Figure 1), during which diatoms can contribute up to 83 % of the total phytoplankton biomass. The regions blooms are typically dominated by the genera *Chaetoceros*, *Thalassiosira, Skeletonema*, and to a lesser extent *Pseudo-nitzschia* and *Leptocylindrus* (Widdicombe et al., 2010). The bacterioplankton community of the WEC exhibits similarly robust seasonal trends, typically dominated by Alphaproteobacteria, but displaying annual peaks in bacterial diversity during winter (Gilbert et al., 2012). Further, a study by Taylor et al., (2014) investigated shifts in bacterial community composition over a diatom

bloom period in the WEC. It was observed that members of the Flavobacteriales and Rhodobacterales increased significantly towards the end of the bloom period, and increased abundances of these bacteria were significantly correlated with declining concentrations of phytoplankton-derived transparent exopolymer particles (TEP). These findings, which closely mirror those made in other studies such as Teeling et al., (2012), imply robust associations between WEC channel diatom and bacterioplankton communities.

Given the robust nature of annual diatom spring blooms and tight coupling of the bacterioplankton in the WEC, combined with routine access to weekly sample collection and the wealth of available metadata, the WEC serves as an ideal model ecosystem in which to investigate ecosystem-scale trends in antagonistic diatom-bacteria interactions. As many coastal regions are characterised and sustained by large, seasonal phytoplankton blooms (Dai et al., 2023), it is imperative to better understand how such blooms are regulated. In doing so, we move towards a deeper understanding of the environmental regulators of primary production and coastal ecosystem functioning as a whole.

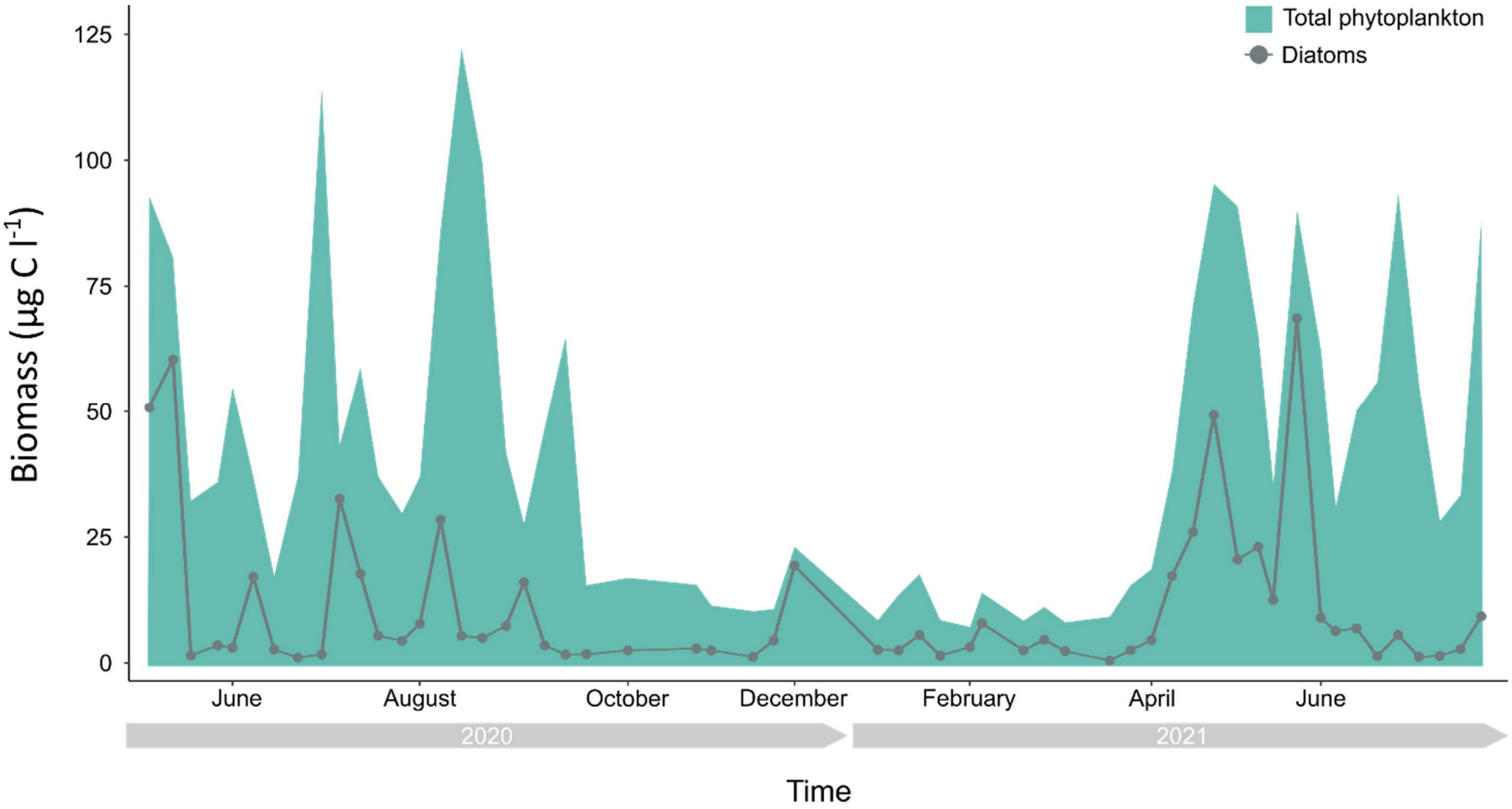

Figure 1. Phytoplankton (turquoise area) and diatom (grey line) biomass in the WEC displays robust seasonal patterns, peaking in late spring and early summer months annually. Smaller winter peaks (blooms), often dominated by diatom species, are also typically observed. Data shown spans June 2020 to July 2021. Data was provided by Claire Widdicombe, Plymouth Marine Laboratory and the WCO (https://www.westernchannelobservatory.org.uk/).

1.2 Aims

As such, this chapter utilises a range of environmentally significant, bloom-forming diatom species to systematically survey the diversity and seasonal patterns of diatom-antagonistic bacteria in a model coastal ecosystem, the WEC. The goal is to provide a clearer picture of the diversity and dynamics of naturally occurring diatom-antagonistic bacterial communities within a highly productive, coastal ecosystem.

1) As one of the most substantial barriers to exploring antagonistic diatom-bacteria interactions in natural ecosystems is the lack of adequate sampling regimes, the first aim of this chapter was to establish a robust sampling method that could be reliably and systematically employed to isolate diatom-antagonistic bacteria from natural seawater assemblages.

2) The resulting plaque assay method, a variation of a soft-agar overlay plaque assay, is employed over an extended sampling period (13 months), using a range of ecologically relevant, bloom-forming diatom species as bait in order to observe seasonal trends and maximise the range of diatom-antagonists captured.

1.3 Materials and methods

1.3.1 Diatom host species and culture conditions

For the establishment of a suitable sampling method and the subsequent isolation of algicidal bacteria, five diatom species were selected for use as antagonist hosts for plaque-assay sampling (Table 1). *Thalassiosira pseudonana* (PLY693), *Thalassiosira weissflogii* (PLY541), *Skeletonema s*p. (PLY627), and *Chaetoceros* sp. (PLY617), were chosen based on their abundance in the Western English

Channel and contribution to seasonal diatom blooms (Widdicombe et al., 2010), in addition to genetically tractable model diatom *Phaeodactylum tricornutum* (PLY100), which was also isolated from the WEC. Host species were obtained from the Marine Biological Association of the UK Culture Collection (Plymouth, UK) and maintained in filtered seawater supplemented with f/2 nutrients (Guillard & Ryther, 1962), at 18 °C under a 16:8 hour light-dark cycle with a light intensity of 50-80 µmol m^{-2} s^{-1}.

Axenic diatom host cultures were generated via three sequential rounds of three-day incubations of 50,000 diatom cells ml^{-1} in f/2 media supplemented with 0.7 mg/ml ampicillin, 0.1 mg/ml streptomycin and 0.5 mg/ml penicillin (Ferrante et al., 2020). Finally, treated diatom cultures were subcultured into fresh f/2 media without antibiotics and allowed to reach exponential growth phase (after approximately four days). Cultures were subsequently examined for bacterial contamination via epifluorescence staining with Hoechst 33342 nucleic acid stain (1 µl per 1 ml, Thermo Fisher) on a monthly basis. Exponential phase treated cultures were incubated with Hoechst 33342 stain and dark adapted for 30 minutes, and cells were then observed using a LEICA DMi8 microscope, excited with 395 nm excitation and 460 nm emission filters (Figure 2). Where bacteria were detected in antibiotic treated cultures, a further single antibiotic treatment of 0.1 mg/ml kanamycin and 0.1 mg/ml neomycin was performed.

Table 1. Diatom taxa used as bait cultures in this study for the isolation of bacterial pathogens from natural seawater samples. Diatom strain and isolation details are also given.

Diatom species	Location of isolation	Latitude and longitude	Isolated by	Date isolated
***Chaetoceros convexicornis* (617)**	L4 Station, Western English Channel	50°15'N 4°13W	R.K. Pipe	11/09/2003
***Phaeodactylym tricornutum* (100)**	Western English Channel	N/A	E.J. Allen	05/12/2007
***Skeletonema sp.* (627)**	L4 Station, Western English Channel	50°15'N 4°13W	R.K. Pipe	17/02/2004
***Thalassiosira pseudonana* (693)**	Moriches Bay, Forge River, Long Island, New York USA	40.7560N 72.8200W	R. Guillard	08/09/1958
***Thalassiosira weissflogii* (541)**	Gorleston -on Sea, Norfolk, England	N/A	J.H. Belcher	1975

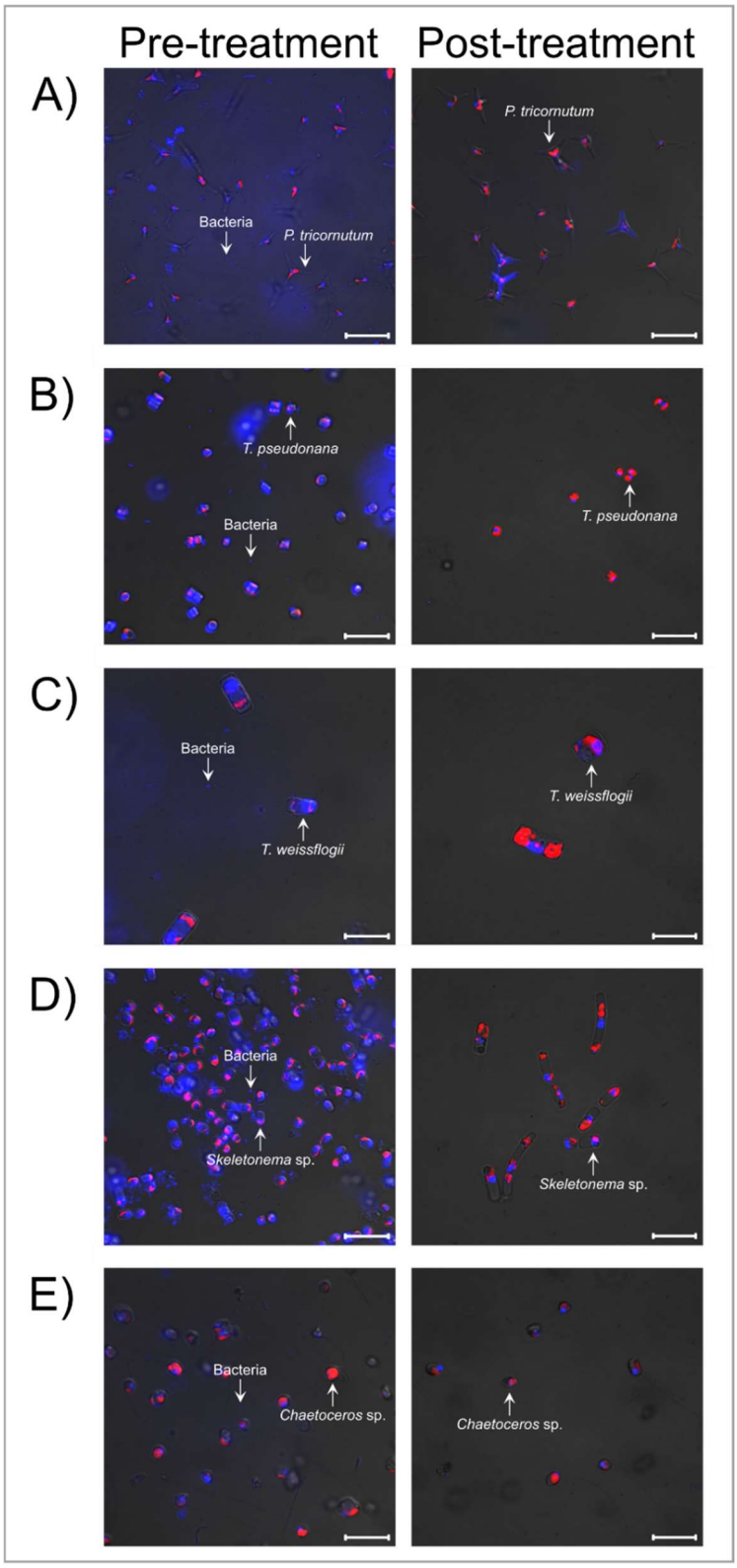

Figure 2. Epifluorescence micrographs of **A)** *P. tricornutum*, **B)** *T. pseudonana*, **C)** *T. weissflogii*, **D)** *Skeletonema* sp. PLY627 and **E)** *Chaetoceros* sp. PLY617 pre- and post-antibiotic treatment. Subsamples of each culture were incubated with Hoechst 33342 nucleic acid and imaged using a LEICA DMi8, excited with 395 nm excitation and 460 nm emission filters. Blue fluorescence represents DNA Hoescht-stained DNA of both bacteria and diatom material and red fluorescence represents diatom chloroplast autofluorescence. Diatom and bacteria cells are indicated by white arrows. Scale bars represent 20 µm.

1.3.2 Development of an environmental sampling pipeline for the isolation of diatom-antagonistic bacteria using bloom-forming diatom species

An adapted soft-agar overlay assay method was developed for the isolation of diatom-antagonistic bacteria from environmental seawater samples, utilising the five diatom host species described in Section 1.3.1 as bait. The development of this method required several rounds of optimisation. The method for trial, including the alterations made at each step, are described below. Each trial was conducted using a single biological replicate (n = 1).

Trial 1 – Serial dilution method (unsuccessful):

Initial plaque assay trials were conducted following a serial dilution method adapted from a viral plaque assay method developed by Wilson et al., (2002). Seawater samples were collected by MBA Sepia from Station L4 (an oceanographic sampling station at 50°15'N; 4°13'W, with a depth of approximately 50 m, Figure 3). Samples were collected from 5 m below the sea surface and 500 µl of untreated seawater was used to inoculate 30 ml of late exponential phase (day four) axenic diatom cultures, with autoclaved filtered seawater (FSW) used as a control. Diatom-bacteria co-cultures were incubated for 24 – 48 hours at 18 °C under a 16:8 hour light-dark cycle at a light intensity of 50-80 µmol m^{-2} s^{-1}. Co-cultures were visually inspected for signs of diatom cell lysis (visible change in colour compared to axenic control culture). Serial dilutions of those cultures that were believed to have lysed were then prepared, ranging from undiluted to a 10^{-4} dilution using FSW as a dilution factor, and used as an inoculum to infect fresh axenic diatom host cultures. One ml of each serial dilution was inoculated into a fresh 30 ml late exponential phase diatom culture and left to incubate under the same conditions for a further 24 – 48 hours. Finally, 10 ml

of fresh late exponential phase diatom cells were concentrated by centrifugation at 3500 rpm and cell pellet was re-suspended in 500 µl sterile f/2 medium. Each concentrated diatom culture was inoculated with 100 µl of the most dilute lysed cultures from the previous round of inoculation and left to incubate at room temperature (RT) for 30 minutes to 1 hour to allow sufficient time for microbial associations to form between potential pathogens and susceptible diatom cells prior to immobilization in agar. The diatom-bacteria culture was added to 4.4 ml of molten semi-solid f/2 agar (f/2 medium supplemented with 0.4 g/l agarose to obtain a final agar concentration of 0.4 % and cooled to 45 °C prior to inoculation with diatom-bacteria culture) and mixed thoroughly by inverting. Agar was poured immediately onto a 1 % f/2 agar plate, incubated at 18 °C under a 16:8 hour light-dark cycle at a light intensity of 50-80 µmol m^{-2} s^{-1} and observed for plaque formation.

Trial 2 – Phaeobacter inhibens (unsuccessful):

Secondary trials were conducted using a known algicidal bacterium, *Phaeobacter inhibens* DSM 17395 (Sonnenschein et al., 2018), as a positive control in order to understand whether plaque assay conditions were suitable. *P. inhibens* was cultured in Marine Broth (Difco, Sigma-Aldrich) for 4 days at 28 °C and serial dilutions, from undiluted to 10^{-8}, were prepared. 10 ml of late exponential phase diatom cultures were concentrated by centrifugation at 3500 rpm for 10 minutes and cell pellets were resuspended in 500 µl sterile f/2 medium. Host cultures (4-day old) were inoculated with 100 µl of the serial dilutions of *P. inhibens*, using autoclaved FSW as a control, and left to incubate at RT for 30 minutes to 1 hour. Diatom-bacteria cultures were mixed with 4.4 ml of 0.4 % molten f/2 agar and mixed thoroughly by inverting and poured immediately onto a 1 % f/2 agar plate.

Plates were incubated according to the conditions listed in Trial 2 and observed for four weeks for plaque formation.

Trial 3 – Increasing inoculum volume (unsuccessful):

As trials with *P. inhibens* were unsuccessful, assays using L4 seawater were resumed using greater quantities of bacterial inoculum. To prepare a bacterial inoculum, 1 L of L4 surface water, collected from a depth of 5 m, was concentrated by centrifugation at 3500 rpm for 10 minutes and supernatant discarded. Ten millilitres (10 ml) of late exponential phase diatom host cultures (4-day old) were also concentrated by centrifugation at 3500 rpm for 10 minutes and cell pellets were re-suspended in 500 µl sterile f/2 medium. Concentrated diatom host cultures were inoculated with 100 µl of concentrated L4 water and left to incubate at room temperature (RT) for 30 minutes to 1 hour. Diatom-bacteria cultures were added to 4.4 ml of 0.4 % molten f/2 agar and mixed thoroughly by inverting, and plaque assays were set up according to Trial 2. Again, this resulted in no plaque formation (Table 2). This was hypothesized to be due to the poor efficiency of centrifugation as a means to concentrate bacteria from environmental samples, and/or due to the relatively young diatom cultures (day four) that were used as bait. A final methodology was therefore trialed (using filtration rather than centrifugation to harvest bacteria, as well as older diatom cultures). This finalized modified method that successfully yielded plaques is outlined below (and described visually in Figure 3).

1.3.3 Isolation of diatom-antagonistic bacteria via a modified plaque assay method

Axenic diatom host species were cultured under standard conditions for 14 days for use as bait in modified plaque assay methodology. For each assay, 100 ml

diatom cell culture was concentrated by centrifugation at 3500 rpm for 10 minutes and cell pellets were re-suspended in 500 µl sterile f/2 medium. One litre (1 L) of surface water collected from station L4 at 5 m depth was filtered sequentially through 100 µm, 40 µm, 10 µm pluristrainers to remove larger cells and debris. Remaining bacterial cells were collected via filtration onto a 0.22 µm membrane. The membrane was subsequently washed with 1 ml sterile seawater to produce a concentrated filtrate of bacterial cells. Soft-agar overlay assays were then prepared by inoculating 100 µl of the concentrated bacterial filtrate into 500 µl of a concentrated diatom host culture (autoclaved filtered seawater was used as a control), which was left to incubate at room temperature (RT) for 30 mins to 1 hr. The diatom-bacteria co-culture was added to 4.4 ml of 0.4 % molten f/2 agar (f/2 medium supplemented with 0.4 g / L agarose) and mixed thoroughly by inversion. Agar was immediately poured onto a 1 % f/2 agar plate and incubated at 18 °C under a 16:8 hour light-dark cycle with a light intensity of 50-80 µmol m^{-2} s^{-1}. Plates were observed for several weeks for plaque formation (Figure 3). This method was employed monthly over the course of an annual cycle.

Upon plaque formation, a sterile loop was used to pick a small amount of material from the centre of the plaque, which was streaked onto 1 % ½ YTSS agar plates (see Appendix Table 1 for media recipe). The same loop was also used to create a new inoculum to be used in reinfection assays (Section 1.3.6) by placing into 500 µl sterile filtered seawater (FSW). Bacterial agar plates were incubated at 18 °C under a 16:8 hour light-dark cycle with a light intensity of 50-80 µmol m^{-2} s^{-1}. Pure bacterial cultures were obtained by streaking single colonies onto fresh ½ YTSS agar a minimum of four times.

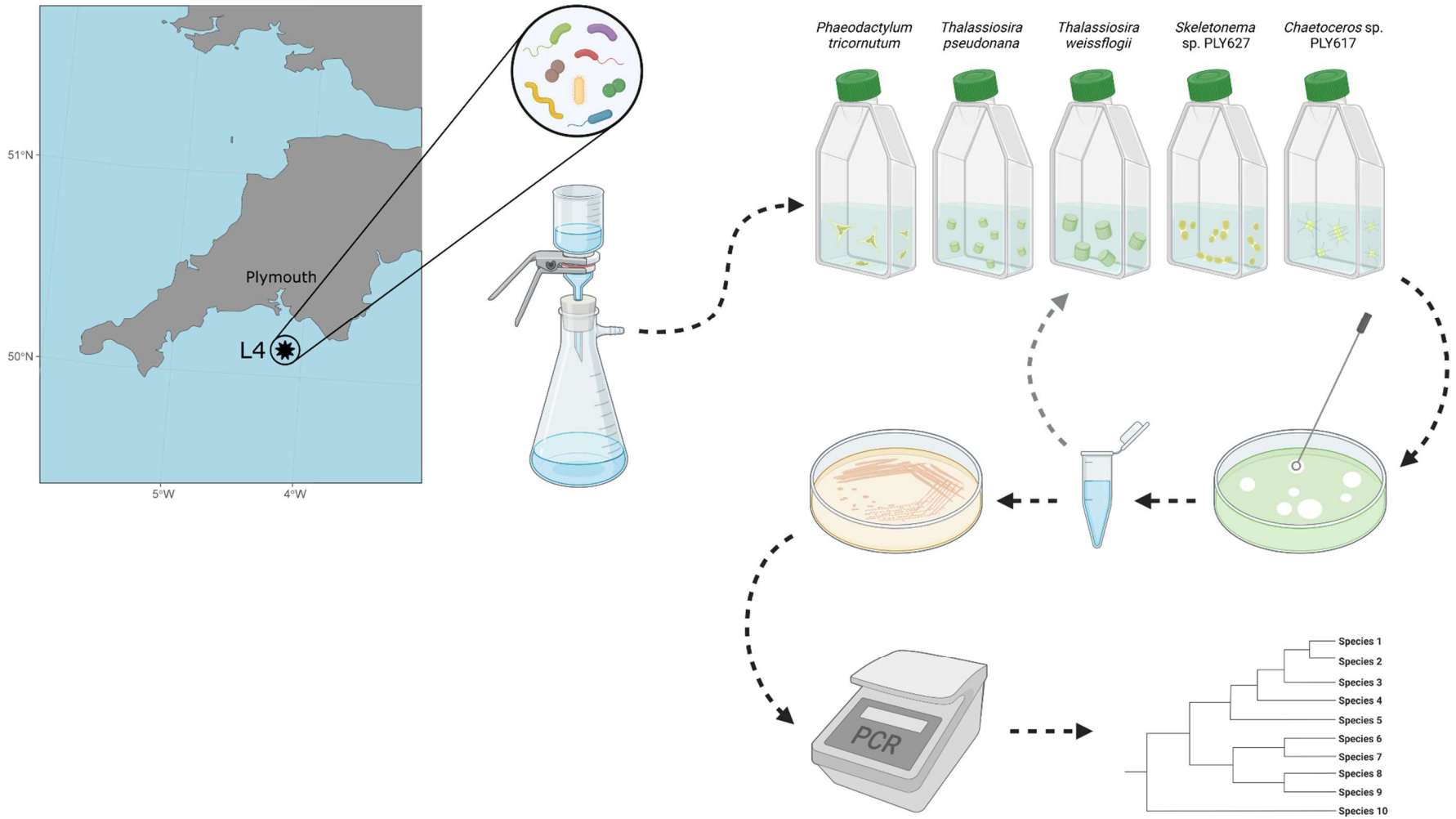

Figure 3. Schematic of the finalised soft-agar overlay method pipeline (Section 1.3.2) for the isolation of diatom-antagonistic bacteria from the Western English Channel (WEC). Seawater samples from Station L4 were sequentially filtered through 100 µm, 40 µm and 10 µm filters and the remaining bacterial fraction was concentrated on 0.22 µm membranes. Axenic diatom bait cultures (14 days old) were infected with the concentrated bacterial suspension and suspended in soft-agar overlay assays. Assays were observed for plaque formation, upon which plaque material was picked and streaked onto ½ YTSS agar for bacterial isolation and identification of pure isolates via 16S rRNA sanger sequencing. Figure was created using BioRender.

1.3.4 Cultivation, identification, and preservation of bacterial isolates

For identification of the isolated bacteria, 16S bacterial rRNA was amplified via a GoTaq (Promega, USA) colony PCR using primers 27f (5′-AGAGTTTGATCMTGGCTCAG-3′) and 1492r (5′-TACGGYTACCTTGTTACGACTT-3′) (Lane, 1985; Turner et al., 1999). PCR cycle conditions were as follows: initial denaturation at 95 °C for five minutes, followed by 32 cycles of i) denaturation at 95 °C for 30 seconds, ii) annealing at 50.1 °C for 30 seconds and iii) extension at 72 °C for 90 seconds, followed by a final extension at 72 °C for five minutes. PCR products were subsequently analysed via gel electrophoresis. Products were run on a 1 % agarose gel at 110 volts for 60 minutes to check for amplification. All 16S rRNA PCR products were purified using a QIAquick PCR Purification kit (Qiagen, UK) and sequenced via Sanger sequencing by Source Bioscience (Cambridge, UK). Retrieved sequences were quality checked, trimmed and forward and reverse sequences aligned using MEGA-11 or Geneious Prime (Tamura et al., 2021; Geneious Prime 2023.0.1, https://www.geneious.com). Trimmed sequences were identified using the NCBI Basic Local Alignment Search Tool (BLAST) nucleotide database (Altschul et al., 1990), and taxonomic assignment of each isolate was subsequently validated by construction of Maximum Likelihood (ML) trees (see Section 1.3.5 for details of phylogenetic tree construction).

Once isolates had received a positive identification, glycerol stocks were prepared for long-term storage at – 80 °C. A 50 % glycerol solution was prepared by diluting pure glycerol with distilled water at a 1:1 ratio and filter sterilising using a 0.2 µM filter membrane. Bacteria were inoculated into 5 ml ½ YTSS broth using a sterile loop and incubated overnight at 30 °C and shaking at 50 rpm.

Subsequently, 500 µl of overnight bacterial culture was mixed with 500 µl of 50 % glycerol solution in 2 ml cryogenic vials and stored at – 80 °C.

1.3.5 Maximum Likelihood tree construction

Maximum Likelihood trees were constructed in Geneious Prime (Geneious Prime 2023.0.1, https://www.geneious.com) for each bacterial isolate to verify taxonomic assignment obtained via NCBI BLAST searches (Appendix Figures 1 – 7). Trees were constructed using full-length 16S rRNA sequences of isolates, in addition to type strains of closely related species and genera obtained from the NCBI Nucleotide Database and the Ribosomal Database Project (Cole et al., 2014; Sayers et al., 2022). Sequences were first aligned using a Multiple Alignment using Fast Fourier Transform (MAFFT) tool (Katoh et al., 2002), alignments were then trimmed to standardise sequence lengths, and finally trees were constructed using the General-Time-Reversable (GTR) substitution model with 1000 bootstraps.

A final tree was constructed following the above protocol containing each isolate, in addition to the type strains of each verified taxonomic assignment.

1.3.6 Confirmation of antagonistic activity via reinfection assays

Reinfection plaque assays were conducted to confirm the antagonistic activity of multiple plaque-forming bacteria. First, a bacterial inoculum was prepared by placing the same loop used to isolate bacteria from original environmental plaques into 500 µl of FSW. Next, 100 µl of the bacterial inoculum was used to reinfect a fresh axenic culture of the original diatom host from which the plaque was observed. A plaque assay was then set up according to Section 1.3.3. Two

of the reinfection assays were used to investigate host range by infecting all five diatom host cultures with the bacterial inoculum.

1.3.7 Analysis of diatom and total phytoplankton abundances at Station L4

Weekly seawater samples were collected by the Western Channel Observatory (https://www.westernchannelobservatory.org.uk/) and analysed by Claire Widdicombe (Plymouth Marine Laboratory, UK) for the enumeration of total phytoplankton abundance (given as cells mL^{-1}) and biomass (given as µg C l^{-1}) at station L4. Samples were collected from a depth of 10 m and fixed in 2 % acid Lugol's iodine solution before enumeration by light microscopy following the Utermohl counting technique (Utermohl, 1958). Phytoplankton counts are further divided into phylogenetic groups, i.e., diatoms, dinoflagellates, coccolithophores etc., with organisms being identified to species level where possible. Phytoplankton and taxa specific biomass calculations were conducted by converting biovolume data (Olenina et al., 2006) to carbon (µg C l^{-1}) following the Menden-Deuer and Lessard formula (Menden-Deuer & Lessard, 2000).

1.4 Results

1.4.1 Establishment of a plaque assay method for the systematic isolation of antagonistic bacteria

The soft-agar overlay assay method, sometimes referred to as the plaque assay method, has been used as a means to investigate inhibition or antagonism between microbial species for over 70 years (Gratia, 1936). The method involves inoculating a host organism (i.e., an axenic diatom culture) with an antagonistic suspension (i.e., a bacterial population containing potential antagonistic species)

and suspending the co-culture in semi-solid (or soft) agar. The host organism will subsequently form confluent lawn within the semi-solid agar layer, and zones of clearing within the lawn (i.e., plaques) indicate inhibition of diatom growth by an infectious agent. The aim of such methods is to isolate and/or identify the bacterial agent responsible for plaque formation as to isolate potential antagonists for further work. Variations of the assay have been developed for a diverse range of applications, as the method can be easily manipulated to provide a robust method by which to investigate the antagonistic relationships of laboratory species or can be used to isolate antagonists from environmental samples using bait host species. As such, a variation of a soft-agar overlay plaque assay was developed in this study to enable the isolation of diatom-antagonists from environmental seawater samples. The establishment this method required several trials, described below and summarized in Table 2, to optimise host and pathogen cell density and host cell age as to maximize the number of antagonistic interactions captured using such a method (the methods for each trial are outlined in full in Section 1.3.2):

Trial 1 – Serial dilution:

Initial plaque assay trials were conducted following a serial dilution method adapted from a viral plaque assay method developed by Wilson et al., (2002). Untreated seawater samples (500 µl) were inoculated into late exponential phase axenic diatom cultures and observed for diatom lysis (indicated by a visible change in colour compared to axenic control cultures). Serial dilutions of lysed cultures were then prepared and used to inoculate fresh axenic diatom host cultures, which, after a further incubation period, were concentrated via centrifugation and subsequently inoculated into soft-agar overlay assays. The aim of the serial dilution method was to avoid obtaining too high a density of

plaques, or total clearance of the diatom lawn, on individual plates, as this would make isolating individual colonies difficult. However, as no plaques were obtained using this method (Table 2), serial dilutions of environmental samples were deemed unnecessary. The lack of plaque formation in this initial trial is likely due to the initial low volume of unconcentrated seawater used (500 µl), which was further diluted in the serial dilution step.

Trial 2 – Phaeobacter inhibens:

In order to more efficiently optimise the plaque assay workflow and culture conditions, secondary trials were conducted using a known algicidal bacterium, *P. inhibens* DSM 17395 (Bramucci et al., 2018), as a positive control. By infecting diatom bait species with a bacterium known to cause algal cell lysis, the limiting factors of the plaque assay method could be more easily identified. However, plaque formation was not observed on any of the plaque assay plates infected with *P. inhibens*.

Trial 3 - Increasing inoculum volume:

As trials with *P. inhibens* were unsuccessful, assays using L4 seawater were resumed, however, this time using a greater volume of seawater to produce a bacterial inoculum. The bacterial fraction of seawater samples was concentrated by centrifugation. Late-exponential phase diatom bait cultures were also concentrated via centrifugation, however, again, no plaque formation was observed.

Trial 4 – Bacterial concentration and increased host age:

Finally, based on multiple trials of the plaque assay method using the above conditions, it was discovered that the main factors key to the success of the protocol were maximizing diatom host cell density, using older diatom host cells, and maximizing bacterial cell density by filtration onto a membrane. As such, a

final trial (Trial 4) was conducted, this time using filtration as the bacteria-concentrating method instead of centrifugation. In addition, a larger volume (100 ml) of older diatom cells (14-day old) were used to inoculate the plaque assay. The resulting successful plaque assay protocol (Figure 3) is described in section 1.3.3.

Table 2. Key variables altered in the optimisation of the soft-agar overlay assay method for the isolation of diatom-antagonistic bacteria, including the number of plaques obtained per trial.

Trial number	Volume of seawater	Volume of bacteria	Bacteria concentration method	Diatom concentration method	Diatom cell age	Number of plaques
1	1 ml	1 ml per 30 ml diatom culture	Not concentrated	Not concentrated	4 days	0
2	N/A	100 µl per 10 ml concentrated diatom culture	Not concentrated, *P. inhibens* grown in MB for 4 days and serial dilutions prepared as inoculum	10 ml concentrated by centrifugation at 3500 rpm for 10 minutes, resuspended in 500 µl f/2	4 days	0
3	1 L	100 µl per 10 ml concentrated diatom culture	Centrifugation at 3500 rpm for 10 minutes, supernatant discarded	10 ml concentrated by centrifugation at 3500 rpm for 10 minutes, resuspended in 500 µl f/2	4 days	0
4	1 L	100 µl per 100 ml concentrated diatom culture	1 L seawater filtered onto 0.2 µm membrane and membrane washed with 1 ml FSW	100 ml concentrated by centrifugation at 3500 rpm for 10 minutes, resuspended in 500 µl f/2	14 days	10

1.4.2 Application of a plaque assay method over an annual cycle for the systematic isolation of algicidal bacteria

The final plaque assay method was employed monthly from June 2020 to July 2021, with the exception of July 2020, January 2021 and June 2021, where sample collection was not possible. Over the course of the sampling period a range of plaque types were obtained across each of the five diatom host species (Figure 4A). In this study, plaque formation was defined as a zone of clearing within the algal lawn where lysis of algal cells or inhibition of algal growth was taking place (Figure 4B). Plaques ranged in size from approximately 3 mm to 4 cm, with the majority of plaques being approximately 1 cm or less in diameter. Plaques were most commonly observed as agar lytic, where degradation of the semi-solid agar in which the diatom lawn was suspended had occurred, followed by non-agar lytic plaques, where a clearing zone of clearing within the diatom lawn could clearly be observed, but where the semi-solid agar layer remained intact. Additionally, in December 2020 four were isolated on *P. tricornutum*, where the semi-solid agar overlay had been separated from the solid agar base layer by the production of a gaseous compound, forming bubble-like plaques (Appendix Figure 8).

In total, 181 plaques were formed over the entire annual cycle (Figure 5). The highest number of plaques were observed on the two *Thalassiosira* species, with *T. pseudonana* and *T. weissflogii* having a total of 56 and 53 plaques respectively. This could be due to the fact that diatoms belonging to the *Thalassiosira* genus were most often present at a higher biomass throughout the sampling period than those belonging to *Chaetoceros* and *Skeletonema* (Figure 6). Conversely, the next highest number of plaques was observed on *Skeletonema* sp. PLY627, with 44 plaques over the annual cycle. This was almost twice the number of plaques

observed on *Chaetoceros* sp. PLY617 (23 plaques), despite *Skeletonema* species contributing a much smaller proportion of overall phytoplankton biomass than *Chaetoceros* and *Thalassiosira*. The lowest number of plaques were isolated on *P. tricornutum*, with a total of just five plaques forming on this host over the entire sampling period.

The sample collected in December 2020 resulted in 125 plaques across all five diatom hosts. Upon inspection of the total phytoplankton data, it was revealed that the December sample point coincided with a winter diatom bloom of *Coscinodiscus* spp. (Figure 7). Data collected a week prior to plaque assay sample collection revealed that *Coscinodiscus* spp., primarily *C. wailesii,* contributed up to 77 % of the total phytoplankton biomass (and 92 % of total diatom biomass) at L4 station. *Thalassiosira* species were also present during this winter bloom, though *Chaetoceros* and *Skeletonema* were not detected. Interestingly, *T. pseudonana* and *T. weissflogii* were the two most susceptible hosts during this sampling period, with 45 and 37 plaques respectively, followed by 32 plaques on *Skeletonema* sp. PLY627, and just 7 and 5 plaques on *Chaetoceros* sp., PLY617 and *P. tricornutum* respectively.

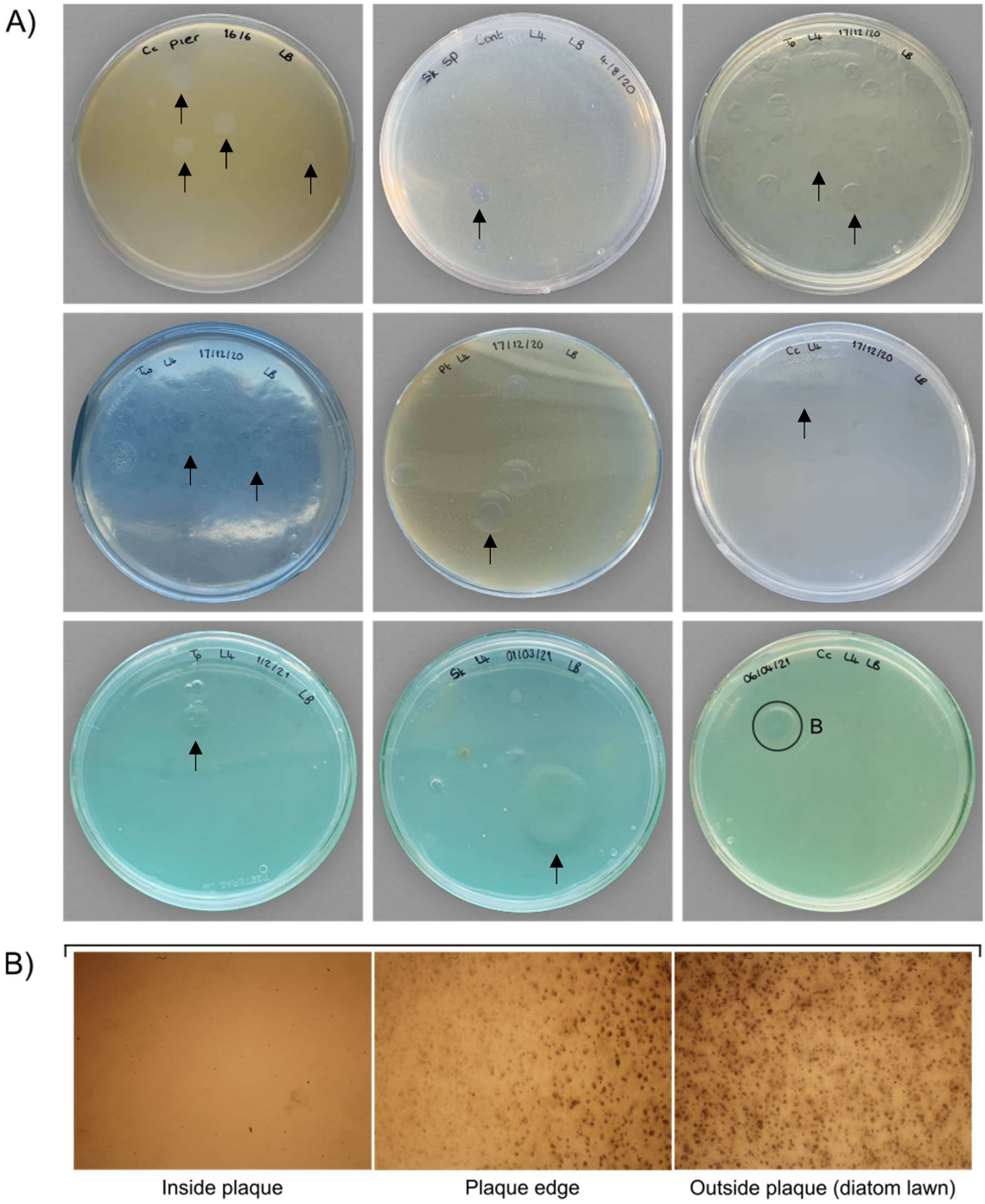

Figure 4. A) Images of soft-agar overlay assay plates across various diatom hosts. Plaques (zones of clearing created by bacterial antagonsits) are indicated by black arrows. B) Light microscope image (x40 objective) of a plaque formed on a *Chaetoceros* sp. PLY617 plate (circled in A). From left to right, centre of plaque showing clearance of diatoms, outer edge of plaque showing gradual appearance of diatoms, and unaffected region of diatom lawn outside of the plaque area.

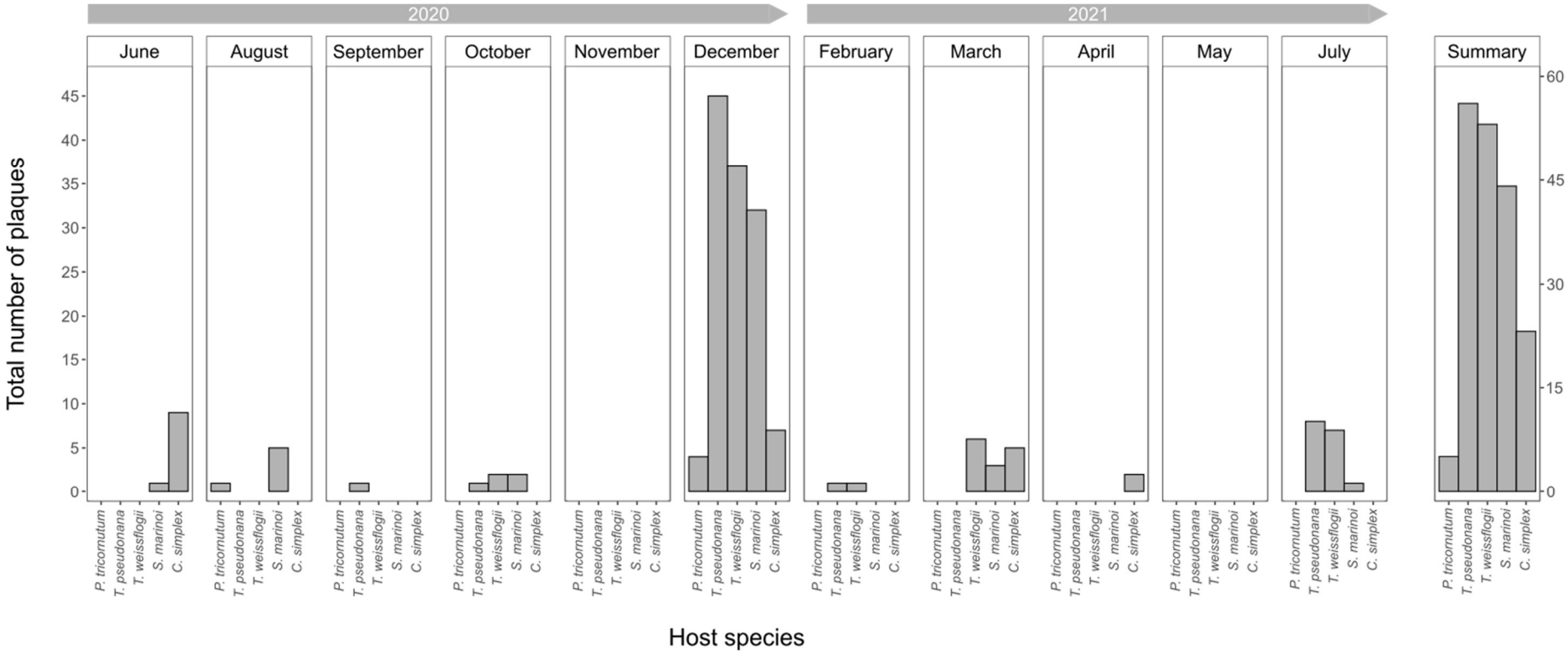

Figure 5. Number of plaques observed in soft-agar overlay assays each month per diatom host, in addition to total number of plaques observed on each diatom host throughout the 13-month sampling period.

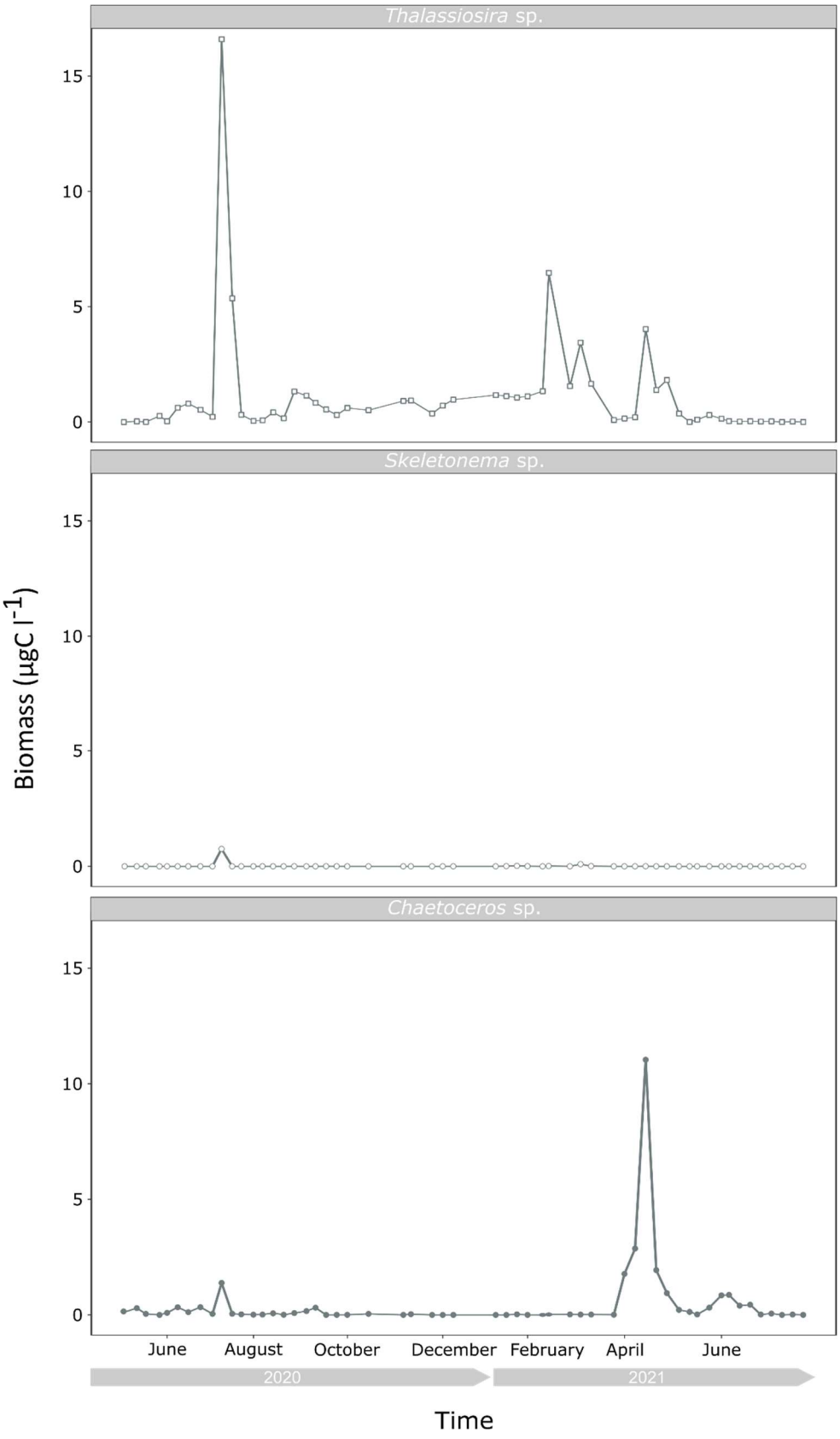

Figure 6. Total biomass (µg C l-1) of common bloom-forming diatom genera (*Thalassiosira* sp., *Skeletonema* sp., and *Chaetoceros* sp.) at station L4 throughout the sampling period of this study (June 2020 to July 2021). Data was provided by Claire Widdicombe, Plymouth Marine Laboratory and the WCO (https://www.westernchannelobservatory.org.uk/).

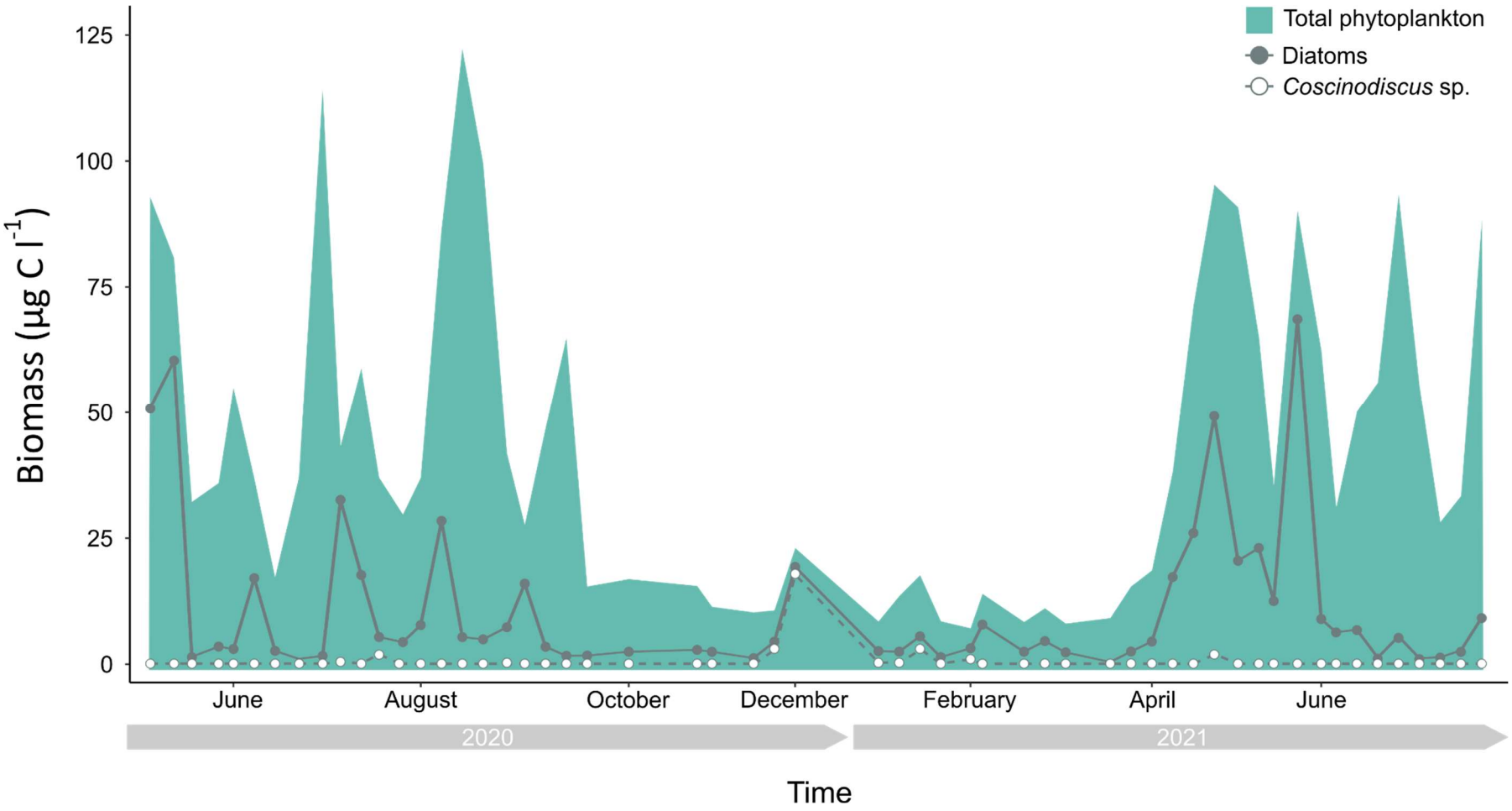

Figure 7. Total biomass (µg C l^{-1}) of phytoplankton (turquoise area), diatoms (grey solid line) and diatoms belonging to the genus *Coscinodiscus* (dashed grey line) throughout the sampling period of this study. WCO sampling was conducted on 7th December 2020, at which point *Coscinodiscus* sp. abundance peaked, comprising up to 92 % of the total diatom biomass at the time of sampling. Plaque assay sampling was conducted on 17th December 2020. Data was provided by Claire Widdicombe, Plymouth Marine Laboratory and the WCO (https://www.westernchannelobservatory.org.uk/).

In order to identify the causative agent of the observed plaques, plaques were picked and streaked onto ½ YTSS agar according to section 1.3.3. All plaques from each sampling point were isolated, with the exception of the December sampling point, where three representative plaques were selected from each plaque assay due to the high number of total observed plaques. Therefore, of the 181 plaques formed, 68 were selected for isolation and identification. Five of the plaques selected for identification (P29, P45, P46, P47 and P49) produced two distinct colony types from a single plaque streak, and as such, both colonies were sequenced. A further three plaques (P60, P65 and P67) could not be identified, and one plaque streak (P41) resulted in a bacteria-fungus co-culture, which was dismissed. In total, the successfully identified isolates comprised 18 distinct bacterial species, spanning four bacterial classes (summarised in Table 3). A full list of plaque isolates can be found in the Appendix (Appendix Table 2).

As a result of the intense peak in algicidal plaques during the December sampling time point, December was shown to have the highest diversity of antagonistic species isolated even in spite of the fact that only a handful of the plaques were sequenced (seven species isolated from 15 sequenced plaques, Figure 8). For comparison, the second highest number of plaques was observed in July 2021 (16 total plaques, all of which were sequenced), which saw the second highest diversity of plaque-forming bacteria, with six distinct species isolated.

Table 3. Each antagonistic bacterial species isolated from soft-agar overlay assay plaques. Nearest hit was determined via examination of 16S rRNA sequences using the NCBI BLAST database and construction of maximum likelihood phylogenetic trees using type strains of closely related species. Diatom hosts and information on whether antagonistic activity has previously been reported for the species is also included.

Nearest Hit	Diatom Host	Bacterial class	Previously reported algal-antagonistic activity	Previously reported susceptible host species	Reference
***Aestuariivita* sp.**	*T. pseudonana, Chaetoceros* sp. PLY617	Alphaproteobacteria	No		
Ahrensia kielensis	*Chaetoceros* sp. PLY617	Alphaproteobacteria	No		
Alteromonas simiduii	*T. pseudonana*	Gammaproteobacteria	*Alteromonas* sp. only	*Karenia mikimotoi* *Skeletonema* sp. (**diatom**)	10.1016/j.scitotenv.2018.03.035 10.1016/j.algal.2015.11.012
Halomonas titanicae	*T. pseudonana, T. weissflogii, Chaetoceros* sp. PLY617	Gammaproteobacteria	*Halomonas* sp. only	*Karenia mikimotoi* *Alexandrium tamarense*	10.1016/j.scitotenv.2018.03.035 10.1016/j.biocontrol.2010.10.004
Hoeflea alexandrii	*T. weissflogii*	Alphaproteobacteria	No		
Hoeflea halophila	*Skeletonema* sp. PLY627	Alphaproteobacteria	No		
Hoeflea phototrophica	*P. tricornutum, Chaetoceros* sp. PLY617	Alphaproteobacteria	No		
Maribacter dokdonensis	*P. tricornutum, Chaetoceros* sp. PLY617	Flavobacteria	Yes	*Skeletonema* sp. (**diatom**)	10.1016/j.algal.2015.11.012
Maribacter spongiicola	*P. tricornutum*	Flavobacteria	No		
Marinobacter adhaerens	*Chaetoceros* sp. PLY617, *T. weissflogii*	Gammaproteobacteria	Yes	*Coscinodiscus radiatus* (**diatom**)	10.1128/aem.01619-22
Marinobacter algicola	*T. pseudonana, T. weissflogii, Skeletonema* sp. PLY627	Gammaproteobacteria	Yes	*Karenia mikimotoi*	10.1016/j.scitotenv.2018.03.035
Metabacillus idriensis	*P. tricornutum*	Bacilli	No		
Oceanicaulis alexandrii	*T. weissflogii*	Alphaproteobacteria	No		
Ponticoccus alexandrii	*T. pseudonana, T. weissflogii, Skeletonema* sp. PLY627, *Chaetoceros* sp. PLY617	Alphaproteobacteria	*Ponticoccus* sp. only	*Prorocentrum donghaiense* *Phaeocystis globose* *Alexandrium tamarense*	10.1186/s13568-017-0357-6
Pseudomonas lurida	*Skeletonema* sp. PLY627	Gammaproteobacteria	*Pseudomonas* sp. only	*Chaetoceros ceratosporum* (**diatom**)	10.1007/s12562-011-0345-8
Roseovarius mucosus	*Chaetoceros* sp. PLY617	Alphaproteobacteria	No		
Thalassospira lohafexi	*T. pseudonana, T. weissflogii, Skeletonema* sp. PLY627	Alphaproteobacteria	*Thalassospira* sp. only	*Karenia mikimotoi*	10.1007/s00253-016-7352-8
Vibrio diazotrophicus	*T. pseudonana*	Gammaproteobacteria	*Vibrio* sp. only	*Alexandrium tamarense* *Akashiwo sanguinea*	10.1371/journal.pone.0091201 10.1016/j.biortech.2019.122246

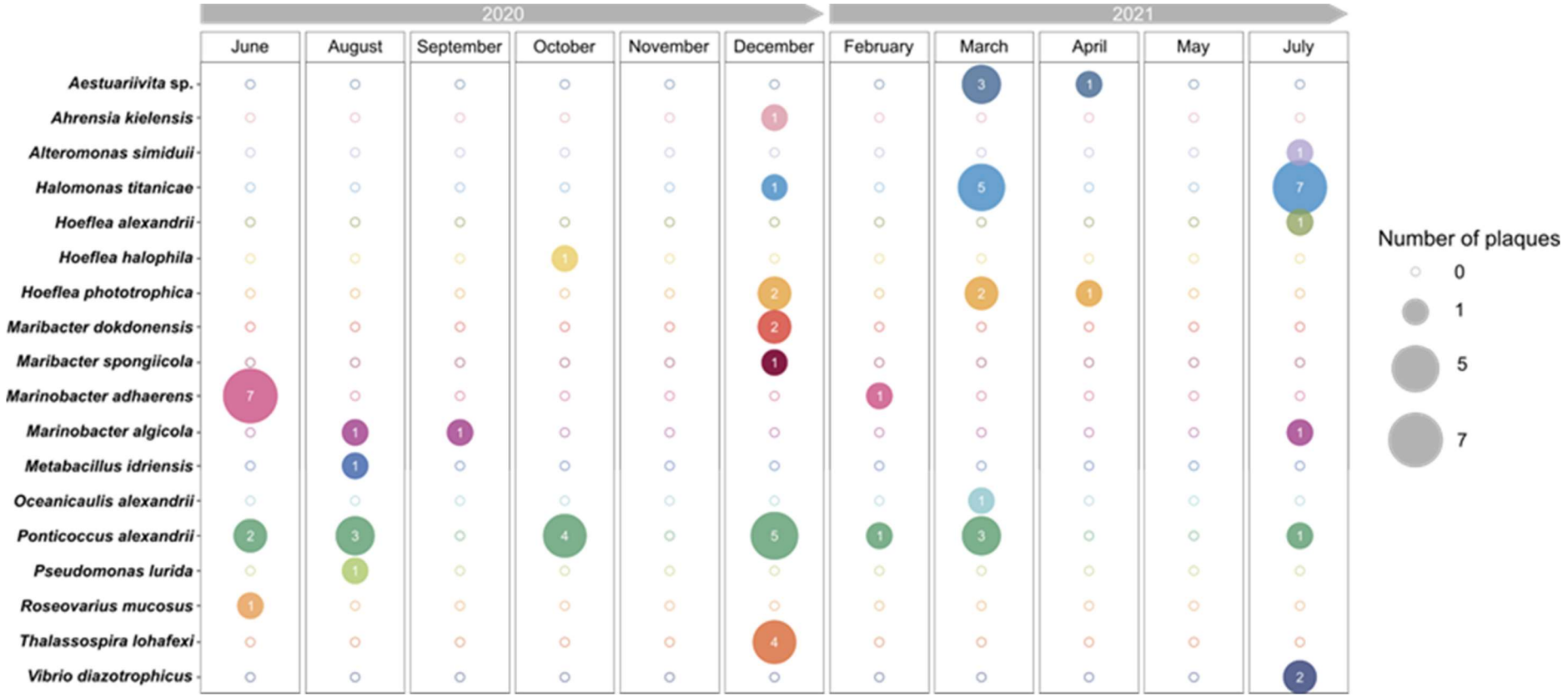

Figure 8. Bubble plot displaying diversity of bacterial species isolated from soft-agar overlay assays at each month of the sampling period. Open circles indicate that a species was not detected at a given sampling point. Note given the large number of plaques observed in Dec 2020 (125) only a sub-sample were processed for identification.

The majority of the sequenced isolates (51.4 %) belonged to the Alphaproteobacteria, with 37 plaques belonging to nine species being detected throughout the sequencing period (Figure 9). Gammaproteobacteria was the second most abundant class (37.5 %) of the sequenced plaques with 27 sequenced isolates belonging to six species. Meanwhile three Flavobacteria belonging to two species were isolated (4.17 %), and a single bacilli isolate was observed (1.4 %).

In addition to being the most frequently isolated and diverse group, species belonging to the Alphaproteobacteria were isolated from all five diatom host species (Figure 10), suggesting potentially wide-reaching impacts of Alphaproteobacteria as pathogens of a diverse range of diatom species. Gammaproteobacteria antagonists were also widespread amongst diatom hosts, being isolated from four of the five host species.

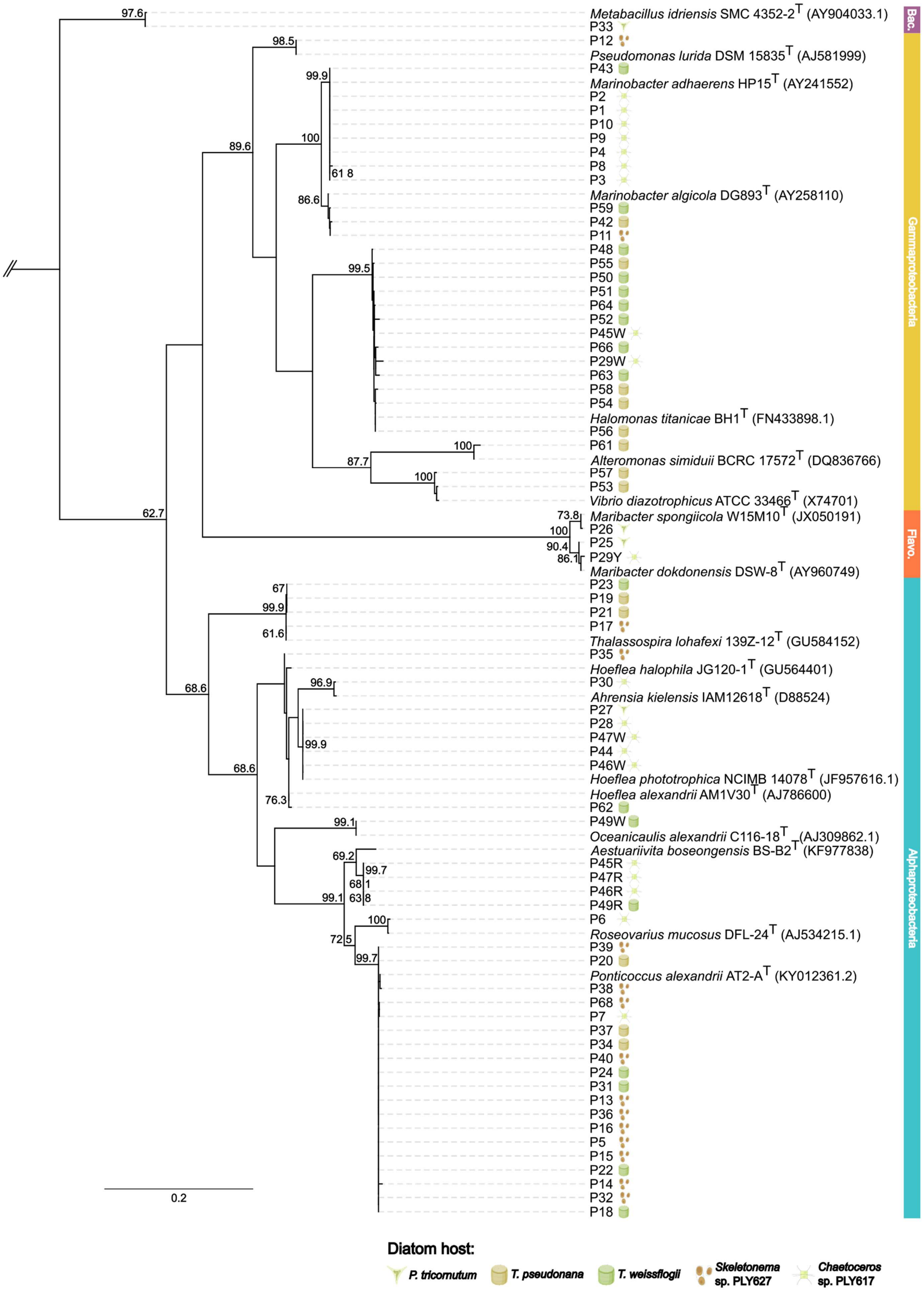

Figure 9. Phylogenetic tree of bacterial antagonists isolated from 65 identifiable plaques formed in soft-agar overlay assays. Five plaques yielded two distinct colony types, in which case both colonies were sequenced and labelled according to their morphology, red ('R'), white ('W') or yellow ('Y'). P indicates plaque number. Phylogenetic tree was constructed from the 16S rRNA gene sequences of bacterial isolates and the type strains of closely related taxa, using the maximum likelihood method with 1000 bootstrap replicates (bootstrap values above 60 % are indicated at branch nodes). Diatom host from which each bacterium was isolated is also indicated.

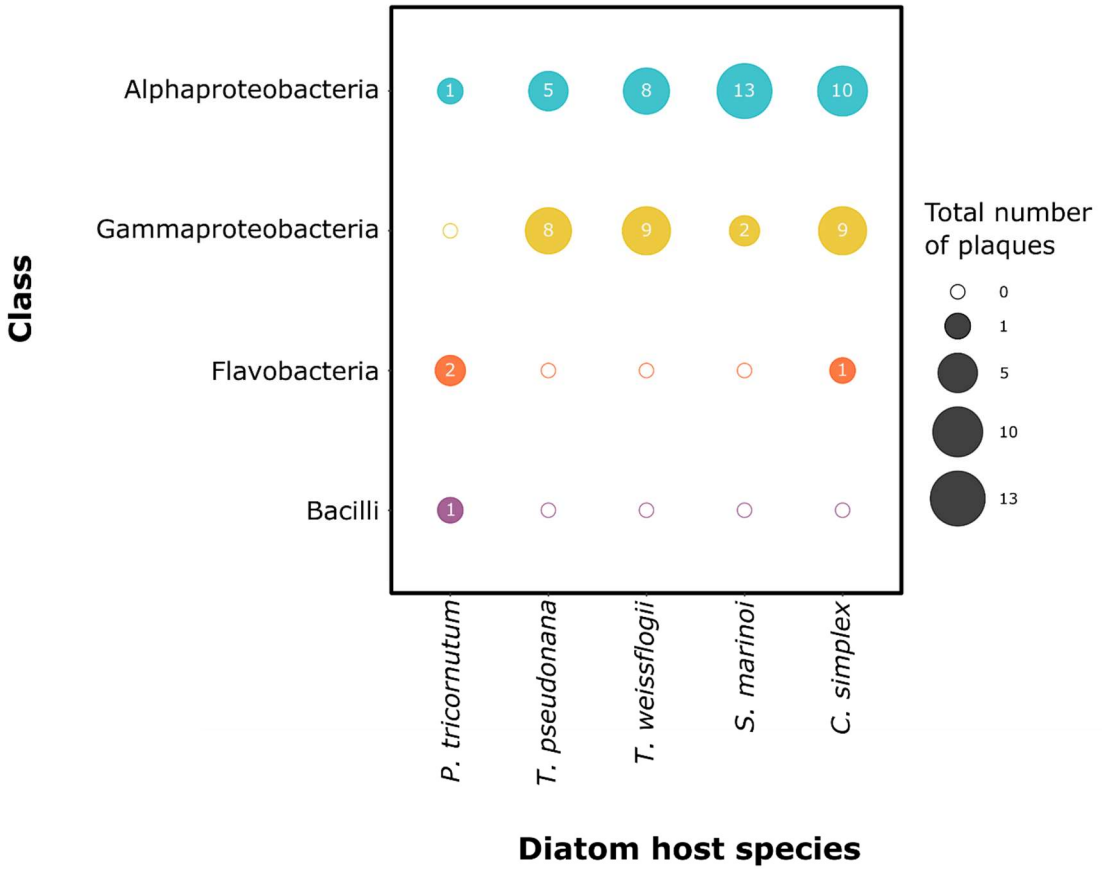

Figure 10. Bubble plot indicating the number of occasions on which a bacterial class was isolated from each diatom host throughout the 13-month sampling period. Open circles indicate that a bacterial class was not isolated from a given diatom host.

1.4.3 Host specificity

Not accounting for the plaques that were not sequenced (December 2020), *Chaetoceros* sp. PLY627 and *T. weissflogii* were the two host species which hosted the highest diversity of plaque-forming bacteria (Figure 11). Eight antagonistic species were isolated from each host, despite *Chaetoceros* sp. having the second lowest total plaque number (23 versus 53 plaques on *T. weissflogii*). Surprisingly, *P. tricornutum* hosted a relatively large diversity of antagonistic species considering the low number of plaques observed on this host, with each of the four plaques sequenced resulting in a different isolate.

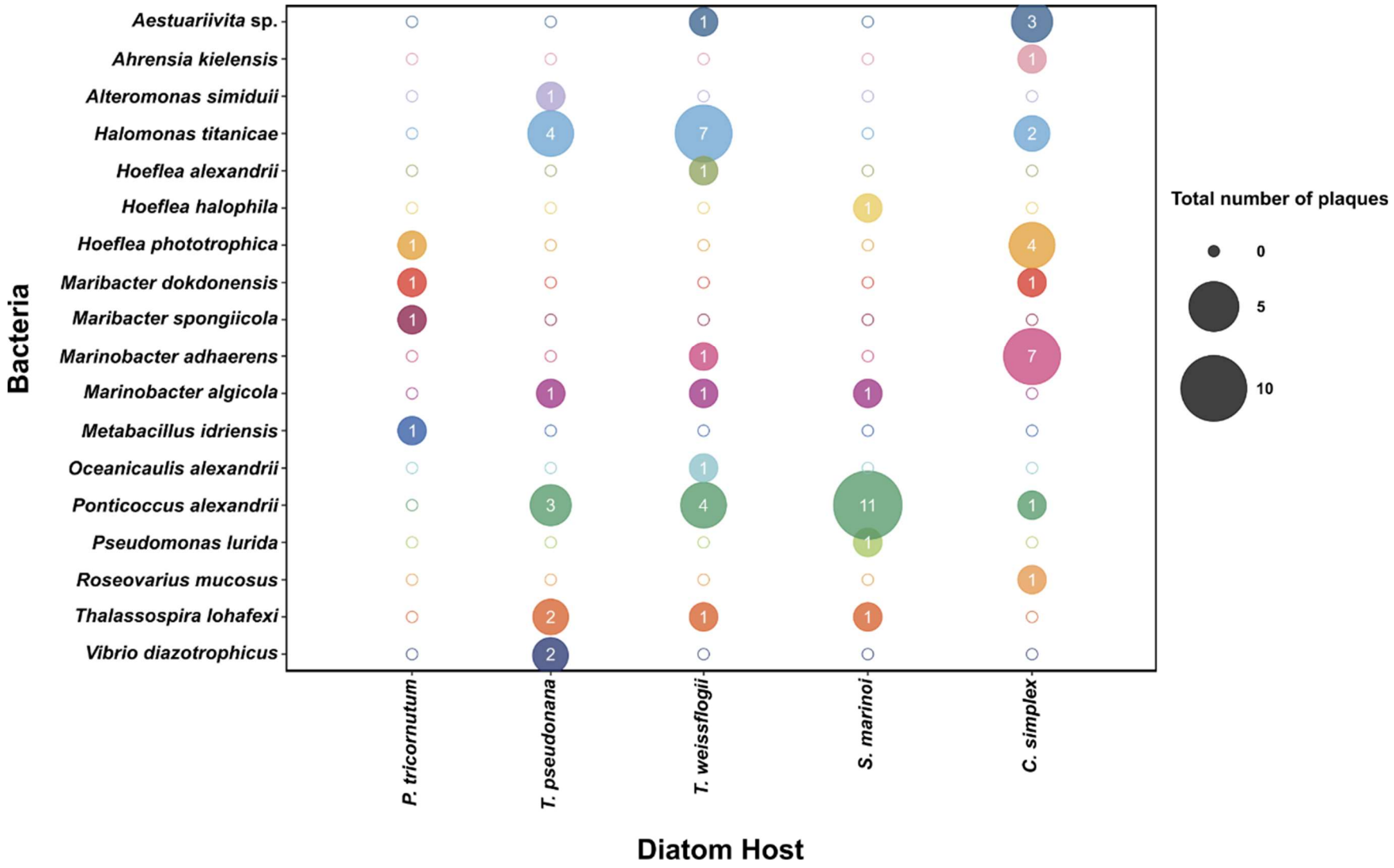

Figure 11. Bubble plot of the number of instances a bacterial species was isolated from each diatom host in soft-agar overlay assays. Open circles indicate that a species was not isolated from a given diatom host.

1.4.4 Reporting novel diatom-antagonistic activity

A literature review was conducted to determine whether antagonistic activity had been previously reported for the plaque-forming isolates obtained in this study. Reports of antagonism were found for seven of the isolated genera, though many of these studies were unable to identify the algicidal agent to species level (Table 3). Four of the studies citing antagonistic activity reported diatom-specific antagonism (Sakata et al., 2011; Wang et al., 2016; Deng et al., 2022), however of those strains, only two were able to be identified to species level, *M. dokdonensis* and *M. adhaerens* (Wang et al., 2016; Deng et al., 2022). In the study by Wang and colleagues, antagonistic *Maribacter* sp. EC-2 was also isolated from station L4, which demonstrated algicidal activity against a *Skeletonema* sp. In order determine whether *Maribacter* sp. EC-2 was phylogenetically related to the *M. dokdonensis* strains isolated in this study, a Maximum Likelihood reference tree was constructed, in which *Maribacter* sp. EC-2 aligned with both the type strain of *M. dokdonensis* and the two strains isolated in this study (Figure 12). This study therefore not only successfully captured known diatom antagonists, but also reports novel diatom-antagonistic activity across a diverse range of bacterial lineages.

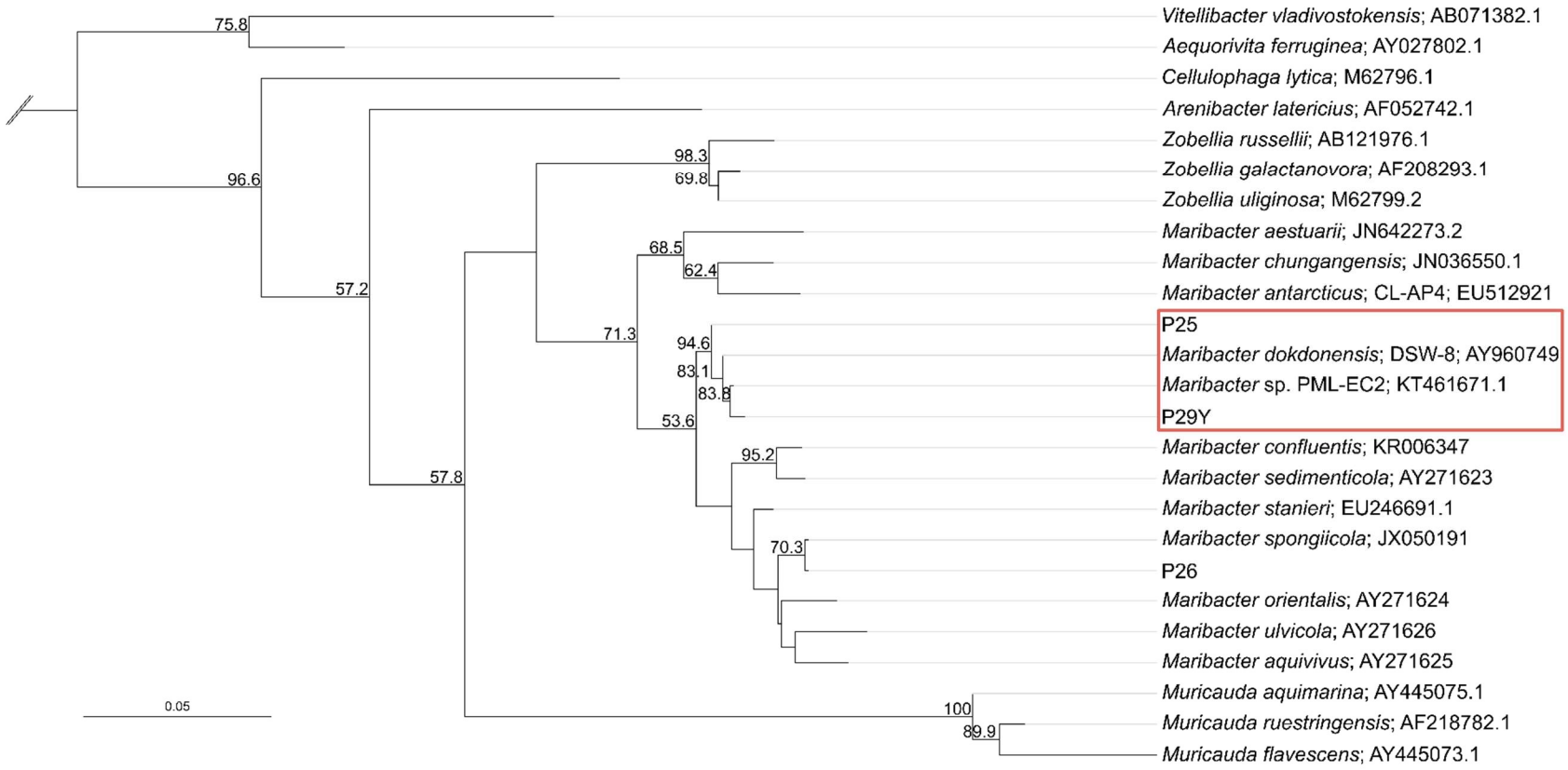

Figure 12. Maximum Likelihood tree constructed to verify the taxonomic assignment of plaque assay isolates P25 and P29Y, and for P26, for which the top NCBI hit were *Maribacter dokdonensis* and *Maribacter spongiicola* respectively. Also included is the diatom-antagonistic *Maribacter* sp. strain (*Maribacter* sp. PML-EC2) isolated at Station L4 by Wang et al., 2016. ML trees were constructed using full-length 16S rRNA sequences of plaque assay isolates and type strains of top NCBI BLAST hit and closely related species. Branch support values above 50 % are shown (calculated from 1000 bootstraps). *Flavobacterium aquatile* was used as an outgroup.

Further, one of the first isolates obtained during the application of this sampling regime was *Marinobacter adhaerens*, a marine Gammaproteobacterium, which is typically regarded as a commensal diatom-associated bacterium (Gärdes et al., 2010; Sonnenschein et al., 2012). *M. adhaerens* was isolated eight times throughout the sampling period from seven plaques on *Chaetoceros* sp. PLY627 in June 2020, followed by a single plaque on *T. weissflogii* in February 2021 (Figure 8).

1.4.5 Seasonal persistence of *P. alexandrii* across a seasonal cycle

Over the course of the sampling period six species, *M. adhaerens*, *M. algicola*, *H. titanicae*, *H. phototrophica*, *Aestuariivita* sp. and *P. alexandrii,* were isolated from multiple temporally distinct samples (Figure 8). However, the most notable of these repeat isolates was *P. alexandrii*, which was isolated on four of the five host species, and seven of the 11 months where samples were collected (Figure 13). *P. alexandrii* produced the highest number of plaques during the winter sampling periods (October and December 2020, with four and five plaques respectively), when it was also isolated from the highest number of host species (three of the five diatom hosts). Of the four host species *P. alexandrii* was isolated from, *Skeletonema* sp. PLY627 appeared to be the most susceptible, with 11 plaques over six sampling points. This repeated isolation from a diverse range of host species indicates that *P. alexandrii* is a broad-range, seasonally persistent diatom-antagonist.

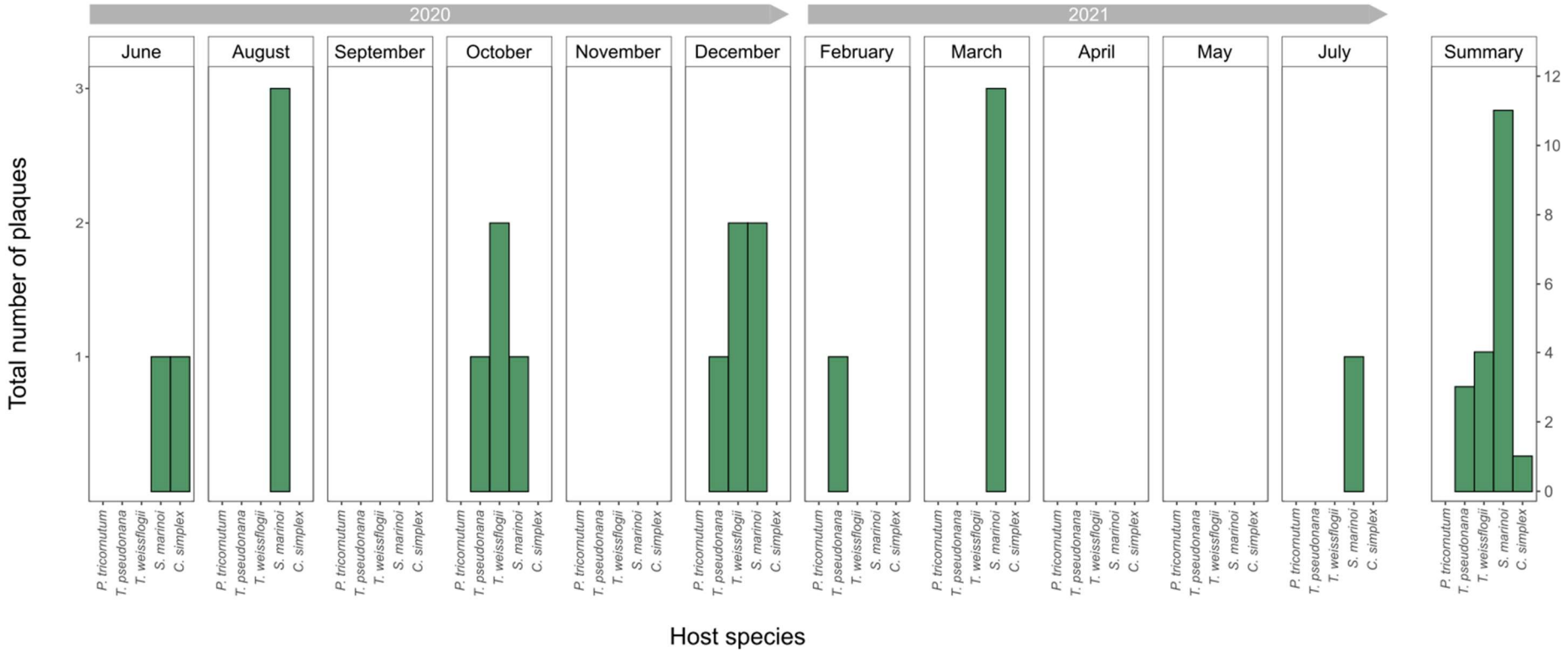

Figure 13. *P. alexandrii* was isolated from seven of the 11 sampling points (across a 13-month sampling period), on all diatom host species except *P. tricornutum*. The total number of occasions on which *P. alexandrii* was identified from plaques on each host is indicated in the summary panel.

1.4.6 Reinfection assays

In order to confirm antagonistic activity, representative plaques were selected to be reinoculated into fresh axenic diatom cultures immediately upon isolation. Four plaques were selected and subsequently identified as *M. adhaerens*, *P. alexandrii* and *M. algicola* (Table 4). *M. adhaerens* and *P. alexandrii* were tested across the range of diatom host species, whereas *M. algicola* was only tested against the original host species.

Although reinfection assays were not performed quantitatively (due to having no knowledge of cell numbers within bacterial inoculum used), in all four cases an increased number of plaques (comparative to the plaque number observed on original environmental plaque assays) were observed on susceptible hosts (Table 4). Interestingly, reinfection assays using *P. alexandrii* was unable to produce plaques on *T. weissflogii*, despite being isolated from *T. weissflogii* on four occasions.

Further characterisation confirming antagonistic activity is outlined in Chapter 2.

Table 4. Re-infection of axenic diatom hosts with plaque material facilitates plaque propagation. Plaque material picked from original soft-agar overlay assays and resuspended in filtered seawater was used to re-infect axenic diatom cultures. Re-infection assays were conducted with plaque material later confirmed to be *M. adhaerens*, *P. alexandrii* and *M. algicola*. *M. adhaerens* and *P. alexandrii* were re-inoculated into all five diatom hosts, while *M. algicola* was only tested against *T. pseudonana*.

Bacteria	**Number of plaques per diatom host species**				
	P. tricornutum	*T. pseudonana*	*T. weissflogii*	*Skeletonema* sp.	*Chaetoceros* sp.
M. adhaerens	0	> 100	0	0	> 100
M. algicola	N/A	60	N/A	N/A	N/A
P. alexandrii	0	38	0	> 100	47

1.5 Discussion

The lack of systematic assessments of antagonistic diatom-bacteria interactions in marine ecosystems poses a significant obstacle to our understanding of the ecological roles of diatom-antagonistic bacteria. The literature demonstrates that a diverse range of diatom-antagonistic bacteria exist that clearly possess the ability to detrimentally impact diatom growth, physiology and potentially even regulate bloom succession (Paul & Pohnert, 2011; van Tol et al., 2017; Bigalke et al., 2019). Nonetheless, field assessments of the diversity and prevalence of antagonists co-occurring with diatoms in natural ecosystems are rarely conducted, thus their contribution to diatom community structuring and bloom regulation is often overlooked. This study takes crucial first steps to rectify this knowledge gap by exploring the diversity and seasonal trends of antagonistic bacteria in a highly productive, coastal marine ecosystem. Using a modified plaque assay method with a range of ecologically relevant, bloom-forming diatom species, 18 antagonistic bacteria were isolated over the course of a 13-month sampling period. Currently, only a handful of studies have investigated the diversity of algal or diatom-antagonists in natural environmental samples, and many of these studies have been limited to a single host species or short sampling periods (Sohn et al., 2004; Kang et al., 2005; Amin et al., 2015). Conversely, the broad host-range and extended sampling period covered in this study (i.e., sampling outside of more typically studied spring phytoplankton blooms) captured a striking increase in plaque formation following a winter diatom bloom, comprised primarily of *C. wailesii*, during which 125 plaques were formed. Not only does this unexpected peak in antagonism highlight the power of long-term monitoring efforts for capturing unexpected trends, but it could also provide

important clues as to which species may be significantly impacted by antagonistic bacteria. While *C. wailesii* was not used as a diatom host species in the present study, the fact that it constituted 77% of the total phytoplankton biomass at the peak of the bloom certainly hints that it may be intrinsically linked to bacterial antagonism detected at the time. As such, monitoring dominant diatom taxa throughout environmental sampling regimes such as these may prove a useful tool for identifying potentially ecologically significant interactions. Despite only being able to identify a sub sample of these plaques (three representative plaques from each host), seven distinct bacterial species were obtained. This corresponded to the highest diversity of plaque-forming bacteria isolated in this study, a result that would likely have increased had more plaques been able to be identified. A study of WEC bacterial community dynamics showed annual increases in bacterioplankton diversity of each winter (Gilbert et al., 2012). It could therefore be hypothesised that an increase in the richness of a bacterial community correlates to increased opportunistic pathogenic activity. Combined with a sudden increase in the availability of potential diatom hosts during a period when phytoplankton biomass, and thus likely phytoplankton-derived DOC, is typically low, the alignment of these conditions could prompt the high rates of diatom-antagonism observed during this sampling point.

In total, 10 bacterial species were isolated from the two *Thalassiosira* hosts, a result which is perhaps to be expected given the relatively large contribution of the *Thalassiosira* genus to total L4 phytoplankton biomass (Figure 6). The increased availability of *Thalassiosira* species as hosts may facilitate greater opportunities for bacteria to evolve antagonistic metabolic pathways. On the contrary, there appeared to be a negative correlation between the low total *Skeletonema* biomass at station L4 and increased plaque number (44), relative

to the higher biomass and lower number of plaques formed on *Chaetoceros* (23). This could be indicative of increased susceptibility of *Skeletonema* species, as opposed to the increased antagonistic opportunities that may preclude the high instances of plaque formation on the two *Thalassiosira* species. Meanwhile, the comparatively low plaque number of *Chaetoceros* could potentially be explained by the complex algicidal defence mechanisms employed by some *Chaetoceros* species (Paul & Pohnert, 2013; Meyer et al., 2018), theoretically providing a line of defence against many pathogenic bacterial species but potentially falling short of defending against opportunistic pathogens when immobilised in a semi-solid plaque assay medium. Further, though *P. tricornutum* was selected as a host species for this study due to the fact that it is a genetically tractable model species, it is not found to be present in significant quantities in pelagic phytoplankton communities in the WEC. As such, *P. tricornutum* may not represent a common target of the pathogenic fraction of the pelagic bacterioplankton community, which could explain why *P. tricornutum* represented just 2.8 % of all plaques observed in this study.

In a study of algicidal bacteria by Coyne et al., (2022), the greatest number of diatom-antagonists belong to the Gammaproteobacteria, with 16 reported species, followed by Flavobacteria, with eight reported species. While 37.5 % of the sequenced plaque-forming bacteria isolated in this study belonged to the Gammaproteobacteria (the second highest contribution), only 4.2 % belonged to the Flavobacteria. Additionally, known diatom-antagonists such as *K. algicida* and *C. atlanticus*, both belonging to the Flavobacteria, were not isolated in this study. While this could simply indicate that Flavobacteria constitute a smaller portion of the diatom pathobiome in this region than in others (for example, open ocean systems, or polar or tropical waters), there are multiple other possible

explanations behind the unexpectedly low contribution of Flavobacteria to plaque formation in this study. Primarily, the three Flavobacteria isolates of this study were obtained during the winter plaque peak, and given that only a fraction of these plaques were sequenced, it is possible that a larger diversity or abundance of Flavobacteria isolates were missed. Other factors that may have hindered Flavobacteria isolation are biases of the sampling method employed, such as the range of diatom host species used, or the use of a single nutrient-rich culture media type (½ YTSS) on which all bacteria were isolated. Interestingly, however, *M. dokdonensis*, a flavobacterium previously isolated from station L4 and shown to be capable of lysing diatom host *Skeletonema marinoi* (Wang et al., 2016), was also detected in this study. *M. dokdonensis* was isolated from *P. tricornutum* and *Chaetoceros* sp., but not from the *Skeletonema* host. However, as *M. dokdonensis* was only isolated during the December 2020 bloom episode, it is possible that *M. dokdonensis* was amongst some of the 29 *Skeletonema* plaques that formed that were not isolated. Further, the detection of Flavobacteria only after the peak of a winter diatom bloom is in-keeping with the literature that reports increased abundances of Flavobacteria towards the end of phytoplankton blooms (Teeling et al., 2012).

In contrast to the high reported number of Gamma- and Flavobacteria, Coyne and colleagues reported only three currently described diatom-antagonists belonging to the Alphaproteobacteria (Coyne et al., 2022). It was therefore surprising to find that Alphaproteobacteria was the most commonly isolated class throughout this study, with nine different species. To the best of our knowledge, this study is the first to report diatom-antagonistic activity in the nine Alphaproteobacteria isolated here. Alphaproteobacteria are typically regarded as diatom-synergists due to the suite of benefits conferred by various diatom-

alphaproteobacteria interactions, such as the provisioning of essential vitamin B12 or iron (Durham et al., 2015; Amin et al., 2009; 2015). However, the significant contribution of Alphaproteobacteria to plaque formation in this study challenges our current understanding of synergistic diatom-bacteria interactions and highlights the importance of ecosystem-scale sampling efforts for uncovering previously undetected antagonists.

Further to this, the isolation of *M. adhaerens* on two diatom hosts, *T. weissflogii* (once) and *Chaetoceros* sp. PLY627 (seven times) from temporally distinct sampling points was particularly surprising. *M. adhaerens,* originally isolated from phytoplankton aggregates in the North Sea*,* is commonly associated with marine diatoms and has often been regarded as a commensal bacterium (Gärdes et al., 2010; Sonnenschein et al., 2011; Kaeppel et al., 2012). The association between *M. adhaerens* and *T. weissflogii* has been extensively studied, and yet, to date, only one study reports diatom-antagonistic activity of this species (Deng et al., 2022). Deng and colleagues demonstrate that *M. adhaerens* strain CS1 was capable of causing a subtle reduction in the growth rate of *Coscinodiscus radiatus* in the early stages of a co-culture, though *C. radiatus* cultures were eventually able to recover and reach cell densities matching axenic control cultures. While this result could simply be attributed to host-specificity of *M. adhaerens*, it was noted that factors such as the age of an algal culture also impacted the behaviour of a range of bacteria in co-culture with a diatom host, alluding to a hidden complexity of diatom-bacteria interactions. Reports of antagonistic activity from unexpected taxa further demonstrates the significance of concerted sampling efforts of diatom-associated bacteria in a broader environmental context.

In addition to uncovering novel antagonistic activity across diverse bacterial lineages, this study also highlights the seasonal persistence of multiple species

of antagonists. Most notably, the Roseobacter *P. alexandrii* was isolated on 19 occasions from four diatom hosts throughout the entire annual cycle. *P. alexandrii*, originally isolated from the toxic dinoflagellate *Alexandrium tamerense* (Yang et al., 2018), has been previously reported to produce algicidal compounds with potent effects against various microalgal species, including *Prorocentrum donghaiense, Phaeocystis globosa* and *A. tamarense* (Chi et al., 2017). While there are currently no reports of algicidal activity against diatom species, the frequent, recurrent isolation of this bacterium across diverse hosts throughout our sampling regime indicates that *P. alexandrii* may be a prevalent diatom-algicidal bacterium within the WEC. Further investigations into the overall abundance and co-occurrence of this pathogen with potential diatom hosts will help elucidate the ecological significance of such a broad-range, seasonally persistent diatom-algicidal bacterium.

The isolation of diverse novel diatom antagonists in this study is an important first step in broadening our understanding of ecologically relevant antagonistic diatom-bacteria interactions. Moreover, the isolation of a known WEC diatom-antagonist (*M. dokdonensis*, isolated seven years ago from the same location, Wang et al., 2016) here not only confirms the soft-agar plaque assay method to be a valuable and reliable tool for the isolation of antagonistic bacteria, but also suggests that the WEC may host a temporally stable community of diatom-antagonistic bacteria. Further, the unexpected peak in bacterial antagonism following a winter diatom bloom raises significant questions about the role of antagonistic bacteria in diatom bloom decline. Are antagonistic bacteria simply opportunistically exploiting an already declining bloom, as is suggested by van Tol and colleagues (van Tol et al., 2017), or is there more direct involvement of these bacteria in bloom decline? The confirmation of antagonistic activity of *M.*

adhaerens, *P. alexandrii* and *M. algicola* in plaque-to-plaque assays certainly hints at the antagonistic nature of these bacteria, however further physiological studies must be conducted with pure isolates in order to gain insight into their mechanism and potential role in impacting diatom physiology (Chapter 2). Nonetheless, this work provides a valuable foundation on which further investigations into the diatom pathobiome can be built. In addition to shedding light on previously undetected diatom-antagonistic activity of diverse bacterial lineages, the collation of a library of ecologically relevant diatom-antagonistic bacteria from this work will enable downstream examination of their impacts on diatom physiology, thus significantly expanding the current landscape of research into antagonistic diatom-bacteria interactions.

Chapter 2:

Investigating the physiological impacts of a library of antagonistic bacteria on bloom-forming diatoms

2.1 Introduction

Elucidating the significance of antagonistic bacteria as drivers of diatom success requires an understanding of both the physiological impacts and regulation of such interactions. The current literature details a diverse range of antagonistic mechanisms and subsequent physiological (and potential population level) impacts suffered by susceptible diatoms, ranging from altered cell sizes, to weakened cell wall structures, to arrested cell division, and even cell lysis (Paul & Pohnert, 2011; van Tol et al., 2017; Bedoshvili et al., 2021). For example, a study of diatom-antagonist *Bacillus mycoides* demonstrated that in the presence of a freshwater diatom host, *Ulnaria acus*, the bacterium produces extracellular compounds capable of inhibiting diatom growth and increasing the fragility of diatom frustules (Bedoshvili et al., 2021). It could be reasonably suggested that this may serve as a mechanism to facilitate cell lysis in order to obtain diatom-derived dissolved organic carbon (DOC), as microscopic observations of diatoms in co-culture with *B. mycoides* showed significant disintegration of diatom frustules. However, increased frustule fragility may also benefit additional microbes within planktonic communities, for example, by increasing accessibility of diatom-derived organic matter to the grazing dinoflagellates that typically proceed a diatom bloom (Widdicombe et al., 2010). Such interactions therefore have the potential to drive marine biogeochemical cycles by influencing the way in which diatom-derived carbon is processed.

Exploring the literature of antagonistic diatom-bacteria interactions with such cascading effects in mind reveals a wealth of potential ecological implications. For example, in mesocosm experiments conducted with algicidal bacterium *Kordia algicida* and a natural phytoplankton assemblage, Bigalke and colleagues

demonstrated that *K. algicida* caused a rapid decline in cell numbers of bloom-forming diatom *Chaetoceros socialis*, which was followed by an increase in numbers of the resistant prymnesiophyte *Phaeocystis*, a trend that mirrored natural bloom succession in nearby waters (Bigalke et al., 2019). Other studies of model systems have also postulated that antagonistic bacteria may impact diatom bloom succession. Van Tol and colleagues demonstrated that flavobacterial diatom-antagonist *Croceibacter atlanticus* exhibits algi-static activity by inhibiting cell division of *Thalassiosira pseudonana* and raise the question of whether such activity towards the end of a diatom blooms life cycle may further contribute to the natural decline of a bloom (van Tol et al., 2017). Indeed, many phytoplankton associated flavobacteria have been demonstrated to possess a diverse suite of polymer degradation pathways, which is suggested to be linked to their prevalence towards the end of diatom bloom periods, where diatom-derived polysaccharides are abundantly available (Teeling et al., 2012; Klindworth et al., 2014). While these seasonal trends are routinely observed, often little consideration is given to the regulation of such interactions. A study into the metabolic and transcriptional regulation of the antagonistic *T. pseudonana-C. atlanticus* system revealed that bacterial metabolites produced by *C. atlanticus* result in increased production of diatom carbohydrates that support bacterial growth (Bartolek et al., 2022). As previously mentioned, this interaction not only alters diatom metabolism, but simultaneously arrests diatom division. This therefore begs the question, are diatom-associated flavobacteria playing a more active role in diatom bloom demise when they are found to be present in such high numbers alongside aging blooms? Indeed, the two Flavobacteria species isolated in the present study, *Maribacter dokdonensis* and *Maribacter spongiicola*, were isolated only in December from a sampling point

that coincided with the decline of a winter *Coscinodiscus* bloom. Interestingly, *M. dokdonensis* is one of just two bacterial antagonists isolated in Chapter 1 that has previously been proven to be algicidal against diatoms (Wang et al., 2015). Wang and colleagues isolated *M. dokdonensis* from Station L4 in the Western English Channel (WEC, the sampling site used in the current study) and demonstrated that the bacterium was capable of producing extracellular metabolites with significant algicidal (lytic) activities against a *Skeletonema* sp. host. Nevertheless, while *M. dokdonensis* displays strong antagonistic activity against a significant WEC diatom species (Widdicombe et al., 2010), little is understood about the regulation of this interaction or it's ecological significance.

Although model laboratory studies of bi- or tri-partite diatom-bacteria systems have indeed proven to be invaluable in the exploration of the mechanisms and physiological consequences of antagonistic microbial interactions, well-characterised interactions are currently limited to a handful of antagonistic species (e.g., *K. algicida*, *C. atlanticus*, Paul & Pohnert, 2011; van Tol et al., 2017). This is, in part, due to the lack of adequate sampling techniques discussed in Chapter 1, however, the current sampling bias towards antagonists of other groups, such as dinoflagellates and cyanobacteria, is perhaps a larger constraint of characterising antagonistic diatom-bacteria interactions (Coyne et al., 2022). For example, the environmental sampling pipeline developed and applied in Chapter 1 has provided a library of 18 potential diatom antagonistic bacteria spanning 10 orders and four classes (Figure 1). Currently, diatom-specific antagonistic activity is novel to a large number of the bacteria isolated in Chapter 1, with nine of the 14 genera isolated having no previous literature reports of diatom-antagonistic activity. However, while literature reports of diatom-antagonism are lacking for the majority of the antagonistic library isolated in this

study, insights can be gleamed from interactions between these species and other microalgae, i.e., dinoflagellates or other microalgae. For example, while the algicidal mechanism of seasonally persistent *Ponticoccus alexandrii* has yet to be investigated in co-culture with diatoms, a study into the antagonistic mechanism of a *Ponticoccus* sp. revealed significant growth inhibitory effects against *Prorocentrum donghaiense*, the prymnesiophyte *Phaeocystis globosa* and the dinoflagellate *Alexandrium tamarense* (Chi et al., 2017). The algicidal nature of *Ponticoccus* sp. appears to be density-dependent, regulated by a quorum-sensing mechanism similar to that of algicidal *Aeromonas* sp. strain GLY-2107 and unidentified gammaproteobacteria MS-02-063 (Nakashima et al., 2006; Guo et al., 2016). Currently, little is known about the bacterial cell densities required for the induction of algicidal activity in *Ponticoccus* sp., thus whether sufficient densities are reached naturally within the phycosphere of a host organism remains unclear. However, certainly given the significant inhibitory effects against a diverse range of microalgae, and the seasonal persistence of *P. alexandrii* as a diatom-antagonist in the Western English Channel (WEC), understanding the mechanism, regulation, and physiological impacts of *Ponticoccus* on susceptible diatom hosts will help elucidate its role in shaping diatom population dynamics and marine ecosystems.

Further, Zheng and colleagues conducted a survey of algicidal bacteria associated with harmful algal bloom forming dinogflagellate *Karenia mikimotoi* (Zheng et al., 2018). The study reports 14 bacteria from estuarine soil and seawater that display growth inhibitory effects against *K. mikimoto*, with three of the isolates belonging to genera that were also isolated in the current study, *Alteromonas* sp., *Halomonas* sp., *Marinobacter* sp. The isolation of diverse antagonistic bacteria from natural seawater communities, like the present study,

supports the idea that there is a hidden diversity of potentially significant algicidal bacteria that have gone undetected due to a lack of adequate sampling techniques.

As such, libraries of potential diatom antagonists, such as that compiled in Chapter 1, serve as an important tool to study antagonistic diatom-bacteria interactions at an ecosystem scale. A better understanding of not only the physiological impacts of such bacteria, but also how antagonistic activity is regulated is imperative for a comprehensive understanding of ecosystem functioning and better predicting drivers of diatom bloom regulation and ecology.

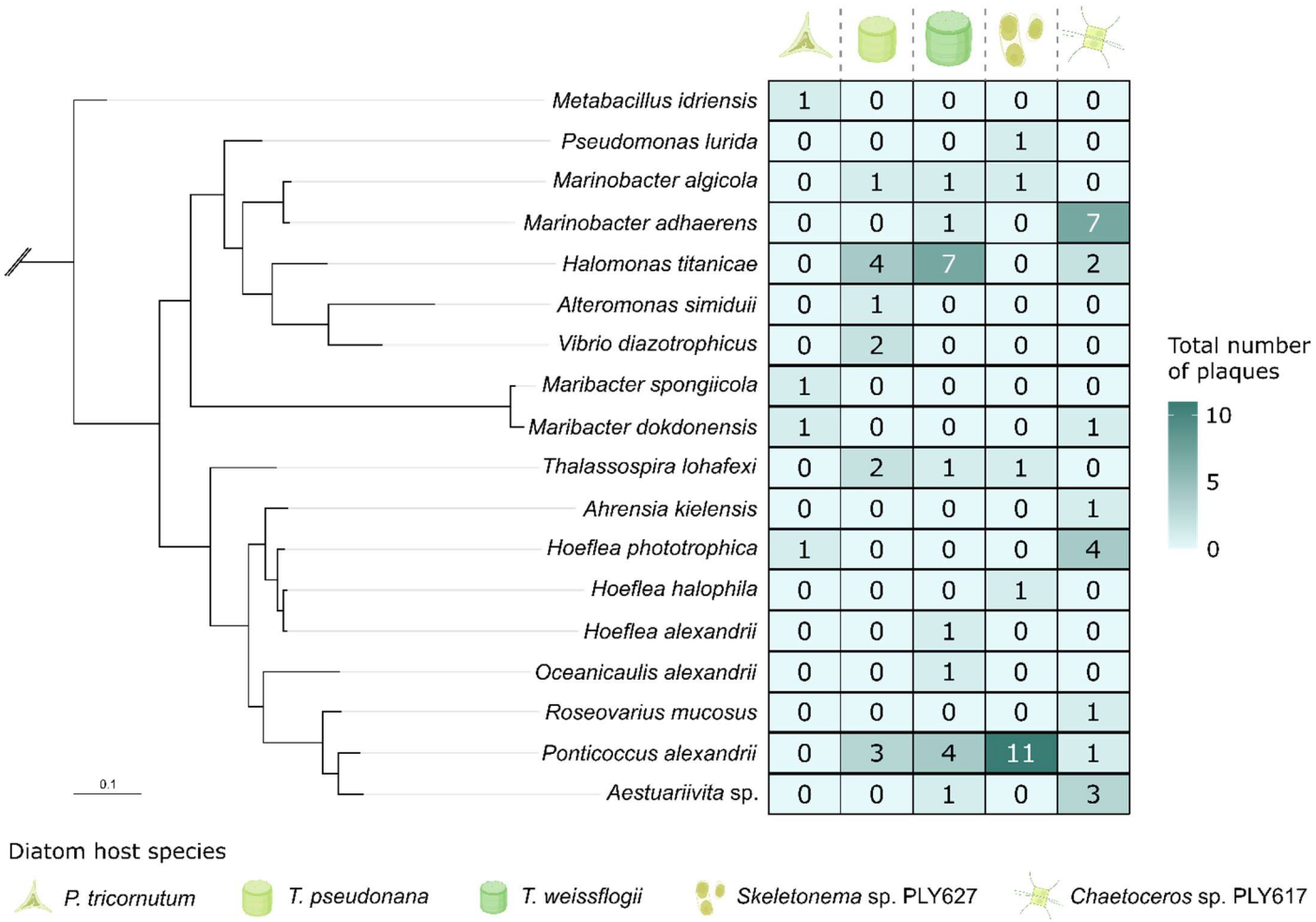

Figure 1. Phylogenetic tree of representatives of each bacterial species isolated from soft-agar overlay assay pipeline isolated in Chapter 1 (left). Number of instances each species was isolated from each of the five diatom hosts is also displayed (right).

2.2 Aims

The objective of this chapter is to build on the long-term sampling efforts of Chapter 1 by exploring the antagonistic activity of a library of ecologically relevant diatom-antagonistic bacteria. As many of the bacterial antagonists isolated in Chapter 1 were found to be novel diatom-antagonists, co-cultivation experiments are conducted in order to investigate how the library bacteria interact with and impact diatom physiology and growth.

1) Observations of bloom-forming diatom species in co-culture with a library of bacterial antagonists shed light on how diatom physiology is impacted by antagonistic activity.

2) Bacterial pre-treatment experiments are conducted to understand the regulation of antagonistic activity across different bacterial lineages.

This chapter serves to both assess the physiological impacts suffered by susceptible diatoms and untangle the ways in which antagonistic interactions are regulated.

2.3 Materials and methods

2.3.1 Algal and bacterial culture conditions

Axenic diatom host species, *Phaeodactylum tricornutum* PLY100, *Thalassiosira pseudonana* PLY693, *Thalassiosira weissflogii* PLY541, *Skeletonema* sp. PLY627 and *Chaetoceros* sp. PLY617 were maintained in filtered seawater supplemented with f/2 nutrients (Guillard & Ryther, 1962), at 18 °C under a 16:8 hour light-dark cycle with a light intensity of 50-80 µmol m^{-2} s^{-1}. All diatom host strains were subjected to three sequential rounds of antibiotic treatment (for details of antibiotic treatment see Chapter 1, Section 1.3.1) and examined

monthly for bacterial contamination via epifluorescence staining using Hoechst 33342 nucleic acid stain (1 µl per 1 ml, Thermo Fisher).

The library of purified bacterial isolates from Chapter 1 were maintained on 1 % ½ YTSS agar (for recipe see Appendix Table 1) at 18 °C under a 16:8 hour light-dark cycle with a light intensity of 50-80 µmol m^{-2} s^{-1}.

2.3.2 Co-cultivation of diatoms in co-culture with a library of antagonistic bacteria

The physiological impacts of a library of antagonistic bacteria on their diatom hosts were investigated. As antagonistic activity of WEC isolates was not readily detectable upon early experimentation, multiple different trials were conducted with various i) bacterial and diatom species (trials 1-3), ii) diatom health and culture ages (trials 4-5), iii) physical environments (trial 6), and iv) pre-treatments on different media types (trials 7-8), as described in detail below:

i) Testing a range of bacterial antagonists with varying diatom hosts

Trial 1

Initial experiments were conducted using *T. pseudonana* as a host species, co-cultured with either *Marinobacter adhaerens*, *Ponticoccus alexandrii or Roseovarius mucosus.* Co-cultures were prepared by inoculating late-exponential phase (day five) *T. pseudonana* cultures into fresh f/2 media at a cell density of 2000 cells ml^{-1}. Bacteria were grown on ½ YTSS agar plates at 18 °C for four days, scraped from plates using a sterile loop and re-suspended in filtered seawater (FSW). Each bacterium was inoculated separately into *T. pseudonana* cultures at a final OD_{600} of 0.01 (axenic *T. pseudonana* cultures were used as a control). *T. pseudonana* growth was observed via cell counts taken at regular

intervals using a Beckman Coulter Counter (Beckman Coulter Life Sciences, UK). The photosynthetic efficiency (Fv/Fm) of photosystem II (PSII) was measured using a PSI AquaPen AP100 (Photon Systems Instruments, Czech Republic) as a proxy for cell stress status, as the activity of PSII is often sensitive to biotic and abiotic environmental stressors, typically resulting in lower and more variable Fv/Fm values in stressed cells (Murchie & Lawson, 2013).

Trial 2

Secondary co-culture experiments were conducted using *Skeletonema* sp., co-cultured with *P. alexandrii*. Late-exponential phase (day four) *Skeletonema* sp. cells were inoculated into fresh f/2 media at a cell density of 30,000 cells ml^{-1}. *P. alexandrii* cells was grown on ½ YTSS agar plates for four days at 18 °C. Cells were scraped from plates using a sterile loop, re-suspended in FSW and washed three times by centrifugation for one minute at 13,000 rpm in FSW to remove residual ½ YTSS nutrients. After washing, *P. alexandrii* cells were again re-suspended in FSW and inoculated into *Skeletonema* cultures at a final OD_{600} of 0.01. *Skeletonema* sp. growth was monitored via cell counting at regular intervals using a haemocytometer (Hawksley, United Kingdom), and Fv/Fm monitored as described in Trial 1).

Trial 3

A third round of co-culture experiments were conducted following the method described in Trial 2), using *Chaetoceros* sp. as a host species, co-cultured with either *M. adhaerens* or *R. mucosus*.

ii) Assessing the impacts of diatom cell health and culture age on antagonistic activity of bacterial isolates

Trial 4

Primary co-cultures were set up according to 2.3.2 Trial 1) with the addition of algal senescence molecule p-coumaric acid (pCA). Each of the three treatments were supplemented with 1 mM pCA dissolved in dimethyl sulfoxide (DMSO). DMSO and pCA controls were run using axenic *T. pseudonana* cultures alongside the standard axenic control. *T. pseudonana* growth and Fv/Fm was monitored at regular intervals.

Trial 5

Further co-cultures were set up to assess culture age, using exponential- and stationary-phase *Skeletonema* sp. cultures with *P. alexandrii* or *T. pseudonana* cultures with *M. adhaerens*. Four or 14-day old diatom cultures were inoculated into fresh f/2 media at a concentration of 30,000 cells ml^{-1}. *P. alexandrii* or *M. adhaerens* was grown for 3 days in ½ YTSS broth at 28 °C and 50 rpm and subsequently washed three times by centrifugation with FSW at 13,000 rpm for one minute. Bacteria were added to their respective diatom host cultures at a final OD_{600} of 0.01, and axenic diatom cultures were used as controls. Cell counts were taken at regular intervals using a Luna Automated Cell counter (Logos Biosystems), using SYTOX Green stain NucGreen™ Dead 488 (ThermoFisher Scientific). Fv/Fm was also measured as previously described.

iii) Assessing the impacts of physical environment on antagonistic activity of bacterial isolates

Trial 6

To assess whether the physical environment of the plaque assay method from Chapter 1 impacted antagonistic activity, soft-agar overlay assays were conducted with *P. alexandrii* and the library of diatom host species.

P. alexandrii was picked from ½ YTSS plates using a sterile loop and inoculated into 200 ml liquid ½ YTSS. Liquid *P. alexandrii* cultures were grown for four days at 28 °C and 100 rpm. *P. alexandrii* cultures were washed three times by centrifugation in FSW for one minute at 13,000 rpm and resuspended in FSW. A cell-free filtrate (CFF) was produced by filtering half of the washed *P. alexandrii* cells through a 0.22 µm sterifilter and collecting the supernatant. Dilutions of the cell-free filtrate were then prepared by diluting CFF in FSW to the following concentrations; 100% CFF; 50% CFF; 25% CFF; 10% CFF; 1% CFF. The remaining unfiltered *P. alexandrii* cells were left untreated and dilutions were prepared using FSW to achieve the following optical densities; OD_{600} 0.1; 0.05; 0.02; 0.01; 0.005.

For each assay 100 ml of 14-day old diatom cell culture was concentrated by centrifugation at 3500 rpm for 10 minutes and cell pellets were re-suspended in 500 µl sterile f/2 medium. Concentrated diatom cultures were mixed with 0.4 % f/2 agar and plated onto 1 % f/2 agar, once set, 20 µl of cell-free filtrate or live *P. alexandrii* culture was pipetted onto a 6 mm Whatmann filter disc and laid on top of the soft-agar diatom lawn. For both live and cell-free treatments, FSW was used as a control. Plates were incubated at 18 °C under a 16:8 hour light-dark cycle (with a light intensity of 50-80 µmol m^{-2} s^{-1}) and observed for zones of inhibition surrounding the discs within the soft-agar diatom lawn.

iv) Assessing antagonistic activity in library of antagonistic bacteria pre-grown on different media

Antagonistic activity of bacteria pre-grown on different media types was investigated in soft-agar overlay assays and in liquid co-cultures.

Trial 7

P. alexandrii was grown on ½ YTSS agar plates or 'Dead Diatom Media' (DDM) agar plates for four days at 18 °C. DDM was prepared by autoclaving 14-day old *T. pseudonana* cultures with agarose at a final weight per volume of 1 %. Bacteria were scraped from agar plates using a sterile loop and re-suspended in 1 ml FSW without nutrients. Plaque assays were prepared by inoculating 500 µl of concentrated 14-day old *T. pseudonana* culture with *P. alexandrii* (or autoclaved filtered seawater for the control) following a concentration gradient of a final estimated OD_{600} of 0.0002 to 0.01. *T. pseudonana-P. alexandrii* co-cultures were left to incubate at room temperature for 30 mins to 1 hr and then mixed with 4.4 ml of 0.4 % molten f/2 agar (f/2 medium supplemented with 0.4 g / L agarose) and mixed thoroughly by inversion. Agar was poured immediately onto a 1 % f/2 agar plate, incubated at 18 °C under a 16:8 hour light-dark cycle with a light intensity of 50-80 µmol m^{-2} s^{-1} and observed for a minimum of four weeks for plaque formation.

Trial 8

For investigation of antagonistic activity in liquid co-cultures, *P. alexandrii* was co-cultured with each of the library of diatom host species. *P. alexandrii* was grown on ½ YTSS agar plates or DDM agar plates comprised of the host species to be infected (e.g., *T. pseudonana* DDM for *T. pseudonana-P. alexandrii* co-cultures) for four days at 18 °C. *P. alexandrii* was scraped from agar plates with a sterile loop and re-suspended in 1 ml FSW without nutrients. Exponential phase diatom cultures were inoculated into fresh f/2 media at a concentration of 30,000 cells ml-1 and *P. alexandrii* was inoculated into diatom cultures at a final OD_{600} of 0.01 (FSW was used as a control). Diatom cell counts were taken at regular intervals using a haemocytometer, and Fv/Fm was monitored.

10 additional bacteria, *M. adhaerens*, *Thalassospira lohafexi*, *Halomonas titanicae*, *Metabacillus idriensis*, *Maribacter spongiicola*, *Vibrio diazotrophicus*, *Marinobacter algicola*, *Hoeflea phototrophica* and *Oceanicaulis alexandrii* were subsequently selected for investigation of antagonistic activity in liquid co-culture. Co-cultures were set up according to the previous *P. alexandrii* liquid co-culture trials, with each bacterium being co-cultured with the diatom species on which it was originally isolated. Bacteria were inoculated into diatom host cultures at a final OD_{600} of 0.05 and diatom cell counts were collected during the exponential growth phase using a haemocytometer.

2.3.3 Epifluorescence imaging of diatom-bacteria interactions

Microscopic observations of live co-cultures were carried out via epifluorescence imaging using Hoechst 33342 nucleic acid stain (1 µl per 1 ml, Thermo Fisher). Subsamples of co-cultures were incubated with the nucleic acid stain in the dark for 30 minutes and imaged using a LEICA DMi8, excited with 395 nm excitation and 460 nm emission filters.

2.3.4 Statistical analysis

Growth rates of diatoms in co-culture with bacterial antagonists was calculated according to the following formula:

$$\mu = \frac{(\ln C_2 - \ln C_1)}{(T_2 - T_1)}$$

Where µ is the bacterial growth rate (per hour), ln is the natural logarithm, C_2 is the cells (ml^{-1}) of a diatom culture taken at the end time point (T_2) and C_1 is the

cells (ml^{-1}) at the initial time point (T_1). $T_2 - T_1$ is the time between measurements (hours).

Statistical significance of growth rates between treatments was calculated using a one-way ANOVA with Tukey's HSD in R Studio (R Core Team, 2019).

Growth inhibition of diatoms in co-culture with bacterial antagonists was calculated according to the following formula:

$$\% = \frac{NC - NT}{NC}\ x\ 100$$

Where % is the percentage by which diatom growth has been inhibited, NC is the cells (ml^{-1}) at a given time point in the axenic control culture, and NT is the cells (ml^{-1}) at the same time point in the bacterial treatment culture.

Statistical significance of rates of inhibition between treatments was calculated using a one-way ANOVA with Tukey's HSD in R Studio (R Core Team, 2019).

2.4 Results

2.4.1 Investigating the impacts of antagonistic bacteria on diatoms in liquid co-cultures

A series of liquid co-cultivation experiments were conducted to investigate the physiological impacts of the library of antagonistic bacteria from Chapter 1 on a range of diatom host species. As growth inhibitory effects of WEC bacterial isolates towards diatoms were not immediately observable during initial experiments, various trials were conducted to investigate further, as described below.

Trial 1

T. pseudonana was selected as the host species for initial experiments due to its use as a genetically tractable model organism (Armbrust et al., 2004) and susceptibility to a range of plaque forming species as demonstrated in Chapter 1 (45 total plaques formed by at least five distinct species). *T. pseudonana* was cultured with either *M. adhaerens*, *P. alexandrii* and *R. mucosus* (with axenic *T. pseudonana* cultures used as a control) and diatom growth and photosynthetic efficiency was monitored at regular intervals (Figure 2). The growth rate of *T. pseudonana* was significantly lower at day two (Figure 2A) when cultured with each of the three tested bacteria (*M. adhaerens* P = 0.0015, *P. alexandrii* P = 0.000433 and *R. mucosus* P = 0.025), when compared to the growth rate of the axenic control. By day five, growth rates of *T. pseudonana* in co-culture with *M. adhaerens* and *P. alexandrii* were significantly higher than that in axenic controls (Figure 2B, P = 0.0046 and P = 0.0016 respectively). *T. pseudonana* growth had recovered (no significant differences in average total cell numbers) by day nine in all three treatments and cell numbers remained comparable to or above that of the axenic control until the end of the observation period (day 28, Figure 2C).

Photosynthetic efficiency (Fv/Fm) was also monitored during the co-cultivation experiment (Figure 2D). Initially (day five) photosynthetic efficiency was higher in bacterial co-cultures than in control culture, though not significantly (P > 0.05). By day seven, photosynthetic efficiency of *T. pseudonana* in co-culture with *P. alexandrii* and *R. mucosus* declined rapidly to 0.135 and 0.07 respectively, compared to 0.48 in control cultures and 0.55 in the *M. adhaerens* treatment. At day nine, the Fv/Fm of *T. pseudonana* in co-culture with *M. adhaerens* decreased to just 0.003. Although the photosynthetic efficiency of a diatom naturally declines as the population ages (as evidenced by the more delayed decline in axenic

control cultures), the decline was both more rapid and more pronounced in the bacterial co-culture treatments.

Despite initial reductions in growth rates and photosynthetic efficiency of *T. pseudonana* cultured with *M. adhaerens*, *P. alexandrii* and *R. mucosus* compared to the axenic control, antagonism in these co-cultures was less pronounced than expected. Final *T. pseudonana* cell densities in antagonistic co-cultures were similar to that of control cultures.

As only subtle effects of the bacteria on *T. pseudonana* were observed, further co-culture experiments were conducted using the diatom hosts on which *M. adhaerens*, *P. alexandrii* and *R. mucosus* were originally isolated. *Skeletonema* sp. was co-cultured with *P. alexandrii*, and *Chaetoceros* sp. was co-cultured with *M. adhaerens* and *R. mucosus*. Growth and photosynthetic efficiency of each diatom host was monitored at regular intervals, and microscopic observations were made on day 7 of the incubation period.

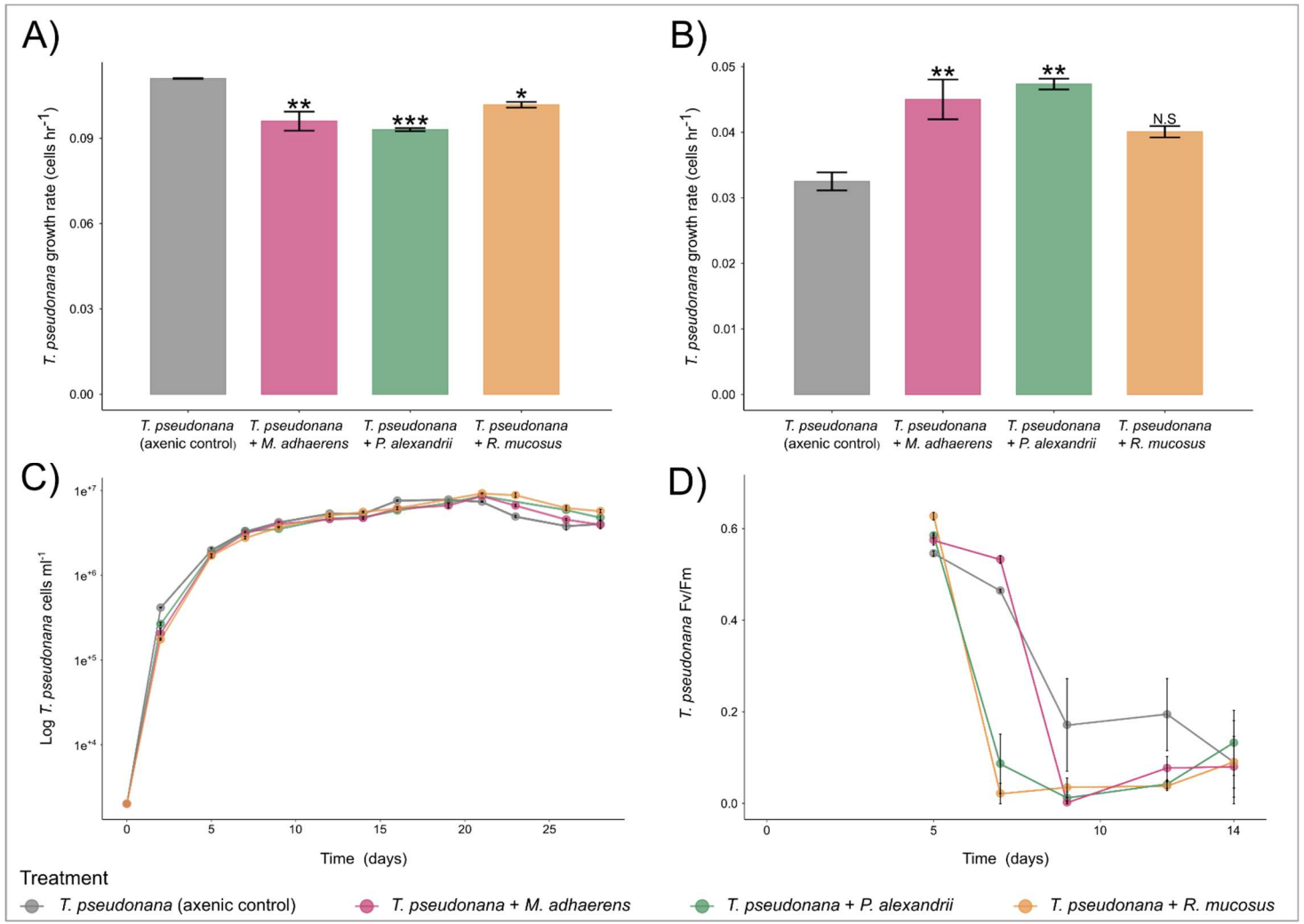

Figure 2. A) Growth rates of *T. pseudonana* between day 0 and day 2 were significantly lower in co-culture with *M. adhaerens* (**, P = 0.0015), *P. alexandrii* (***, P = 0.000433), and *R. mucosus* (*, P = 0.025) compared to an axenic control. **B)** Growth rates of *T. pseudonana* between day 2 and day 5 were significantly higher in co-culture with *M. adhaerens* (**, P = 0.0046), and *P. alexandrii* (**, P = 0.0016) compared to an axenic control. **C)** Growth (cells ml^{-1}) and **D)** photosynthetic efficiency (Fv/Fm) of *T. pseudonana* in axenic culture and in co-culture with *M. adhaerens*, *P. alexandrii* and *R. mucosus*. Error bars represent ± S.E, n = 3 and statistical significance was determined using a one-way ANOVA.

Trial 2

Growth rates of axenic and co-cultured *Skeletonema* sp. showed similar trends to the previous trials with *T. pseudonana*, with growth rates calculated at day two being slightly lower in the *P. alexandrii* treatment than the control (Figure 3A), although this difference was not significant ($P > 0.05$). By day four, the growth rate of Skeletonema sp. in the *P. alexandrii* treatment was slightly higher than that of the axenic control (Figure 3B), although again, this difference was not significant. The growth of *Skeletonema* sp. PLY627 in co-culture with *P. alexandrii* closely mirrored that of the axenic control culture (Figure 3C).

In contrast to the previous co-cultivation experiment, however, photosynthetic efficiency (Figure 3D) of *Skeletonema* sp. PLY627 co-cultured with *P. alexandrii* was significantly higher than that of the control culture by day four of the co-cultivation experiment ($P = 0.015$). Photosynthetic efficiency of both the control and *P. alexandrii* treatment declined steadily throughout experiment, with the *P. alexandrii* treatment remaining significantly higher than the control throughout. No crash in photosynthetic efficiency was observed.

Examination of the cultures by epifluorescence microscopy at day seven revealed numbers of bacterial cells in the treatment co-culture to be low (Figure 4B). Additionally, there was very little attachment of or association between diatom and bacterial cells observed. *Skeletonema* sp. cells in both the control and *P. alexandrii* treatments appeared to be healthy, as evidenced by intact cells and bright chloroplast fluorescence (red fluorescence).

Trial 3

Similar observations were made throughout the *Chaetoceros* sp. co-cultivation experiments, with no significant effects of the bacteria on their diatom hosts being observed (Figure 5). *Chaetoceros* sp. growth rates calculated between time of inoculation and day two were lower in bacterial treatments than control treatments, though these differences were not statistically significant (Figure 5A). By day four *Chaetoceros* sp. growth rates in bacterial treatments had improved and surpassed that

of control cultures, as per the previous trials, however, again, this was not statistically significant (Figure 5B). Total final cell numbers were not significantly different between treatments (Figure 5C).

Despite there being no significant differences between treatments in initial stages of co-cultivation, by day nine the photosynthetic efficiency of *Chaetoceros* sp., in co-culture with *R. mucosus* was significantly higher than that of both the control and the *M. adhaerens* cultures ($P = 0.000027$, Figure 5D). By day 11, photosynthetic efficiency of *Chaetoceros*-*M. adhaerens* co-cultures was also significantly higher than control cultures ($P = 0.02$), despite all three treatments steadily declining in efficiency. Co-cultures remained at a higher photosynthetic efficiency compared to control cultures until the end of the observation period.

Microscopic observations of *Chaetoceros* cultures and bacterial treatments at day seven also revealed low densities of both bacteria (Figure 6).

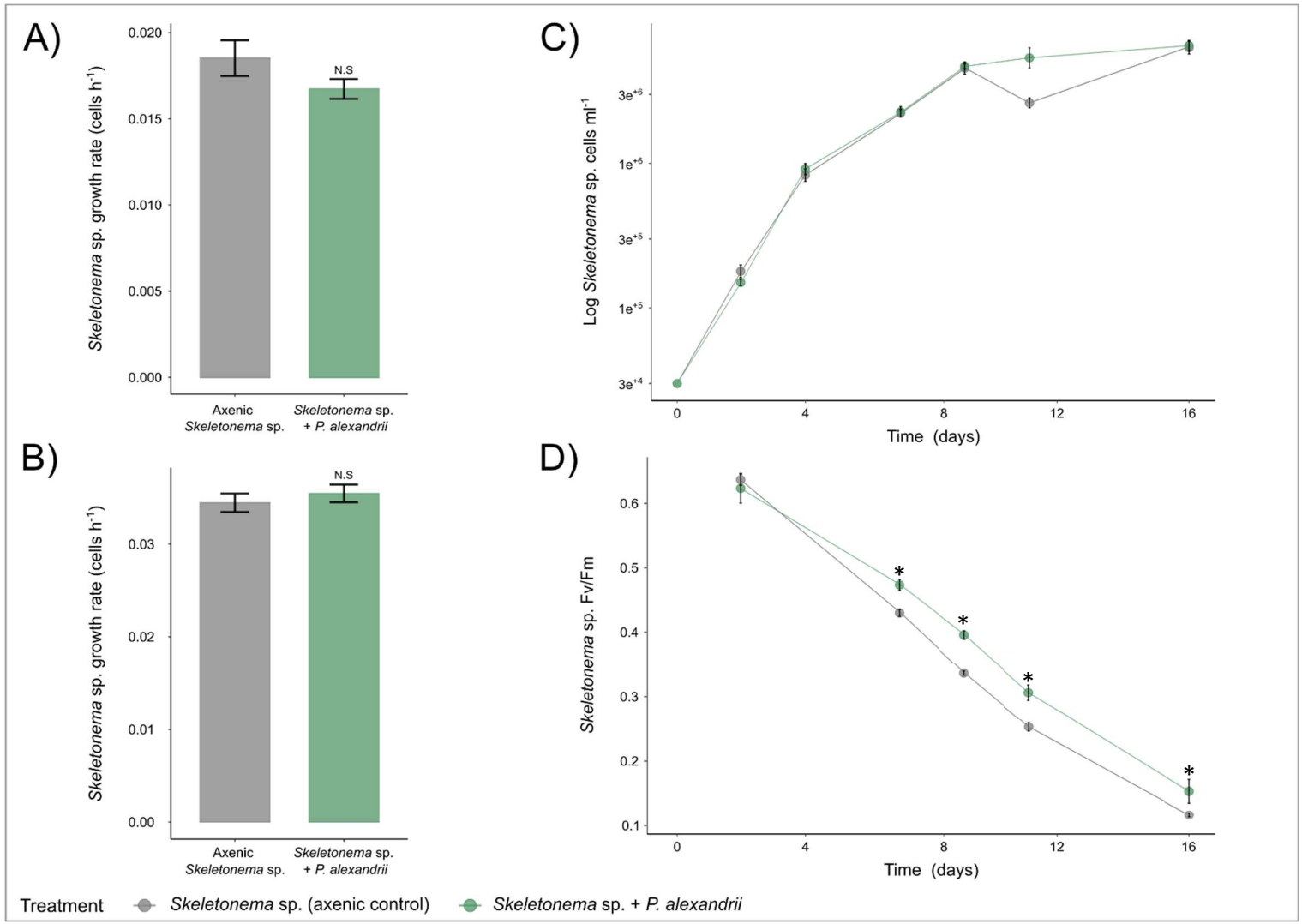

Figure 3. A) Growth rates of *Skeletonema* sp. PLY627 between day 0 and day 2 were not significantly different in co-culture with *P. alexandrii* (N.S, P > 0.05) compared to an axenic control. **B)** Growth rates of *Skeletonema* sp. PLY627 between day 2 and day 4 were not significantly different in co-culture with *P. alexandrii* (N.S, P > 0.05) compared to an axenic control. **C)** Growth (cells ml^{-1}) and **D)** photosynthetic efficiency (Fv/Fm) of *Skeletonema* sp. PLY627 in axenic culture and in co-culture with *P. alexandrii***.** Error bars represent ± S.E, n = 3 and statistical significance was calculated using a one-way ANOVA.

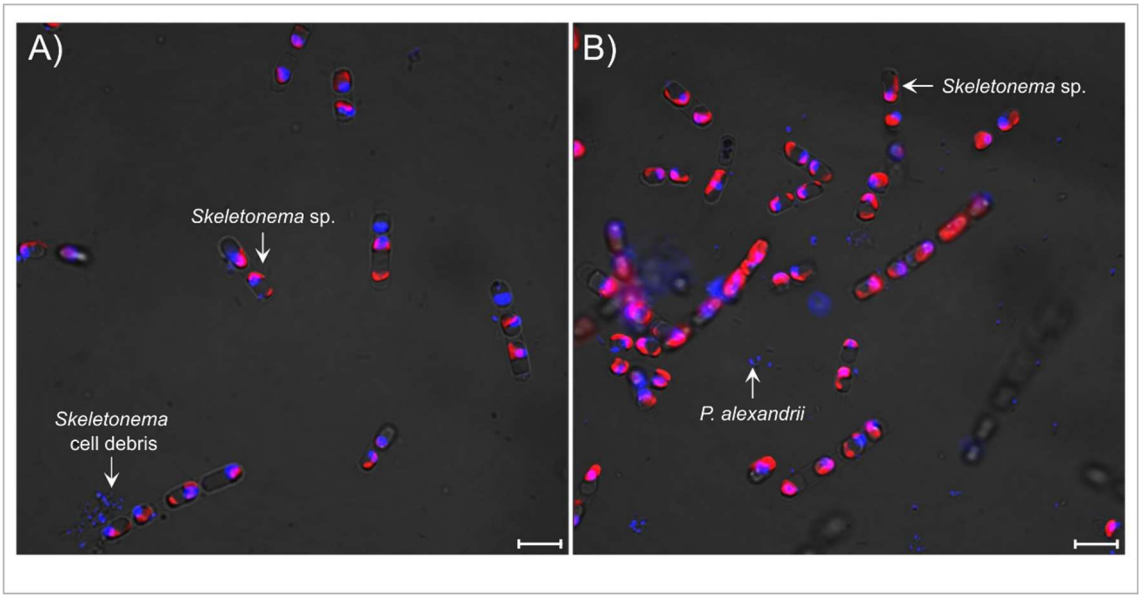

Figure 4. Epifluorescence micrographs of **A)** *Skeletonema* sp. PLY627 control culture and **B)** *Skeletonema* sp. PLY627 co-cultured with *P. alexandrii* at day 7 of growth experiment. Subsamples of each culture were incubated with Hoechst 33342 nucleic acid and imaged using a LEICA DMi8, excited with 395 nm excitation and 460 nm emission filters, at 63x. Blue fluorescence represents DNA Hoescht-stained DNA of both bacteria and diatom material and red fluorescence represents diatom chloroplast autofluorescence. *Skeletonema* sp. and *P. alexandrii* cells are indicated by white arrows. Scale bars represent 10 µm.

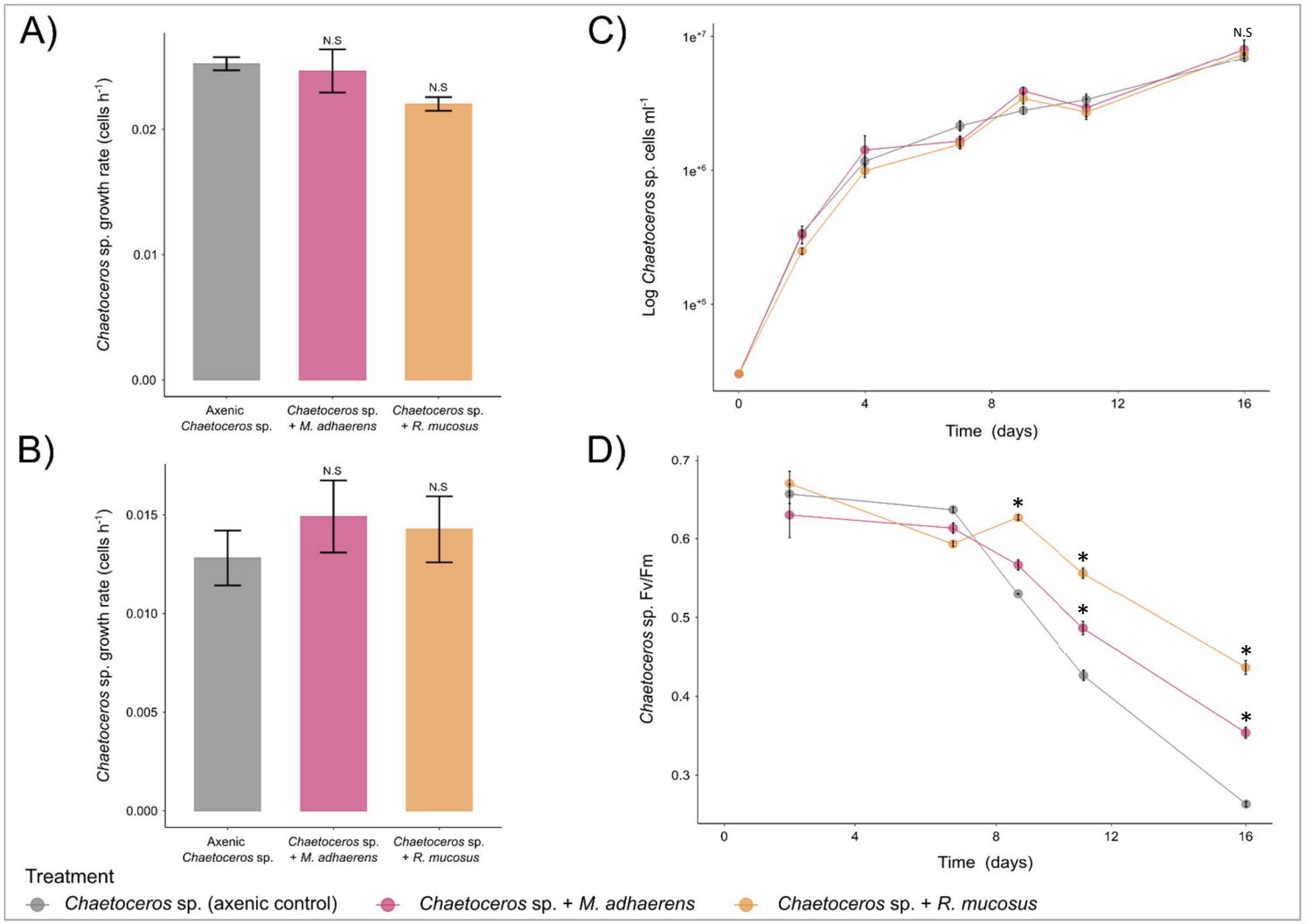

Figure 5. Growth rates of *Chaetoceros* sp. PLY617 between **A)** day 0 and day 2, and **B)** day 2 and day 4 were not significantly different in co-culture with *M. adhaerens* or *R. mucosus* (N.S, P > 0.05) compared to an axenic control. **C)** Growth (total cells ml^{-1}) of *Chaetoceros* sp. PLY617 in axenic culture and in co-culture with *M. adhaerens* or *R. mucosus* were not significantly different (N.S, P > 0.05). **D)** Photosynthetic efficiency (Fv/Fm) of *Chaetoceros* sp. PLY617 in axenic culture was significantly lower than in co-culture with *R. mucosus* by day nine (P = 0.000027) and significantly lower than in co-culture with *M. adhaerens* by day 11 (P = 0.02). Error bars represent ± S.E, n = 3, and statistical significance was calculated using a one-way ANOVA.

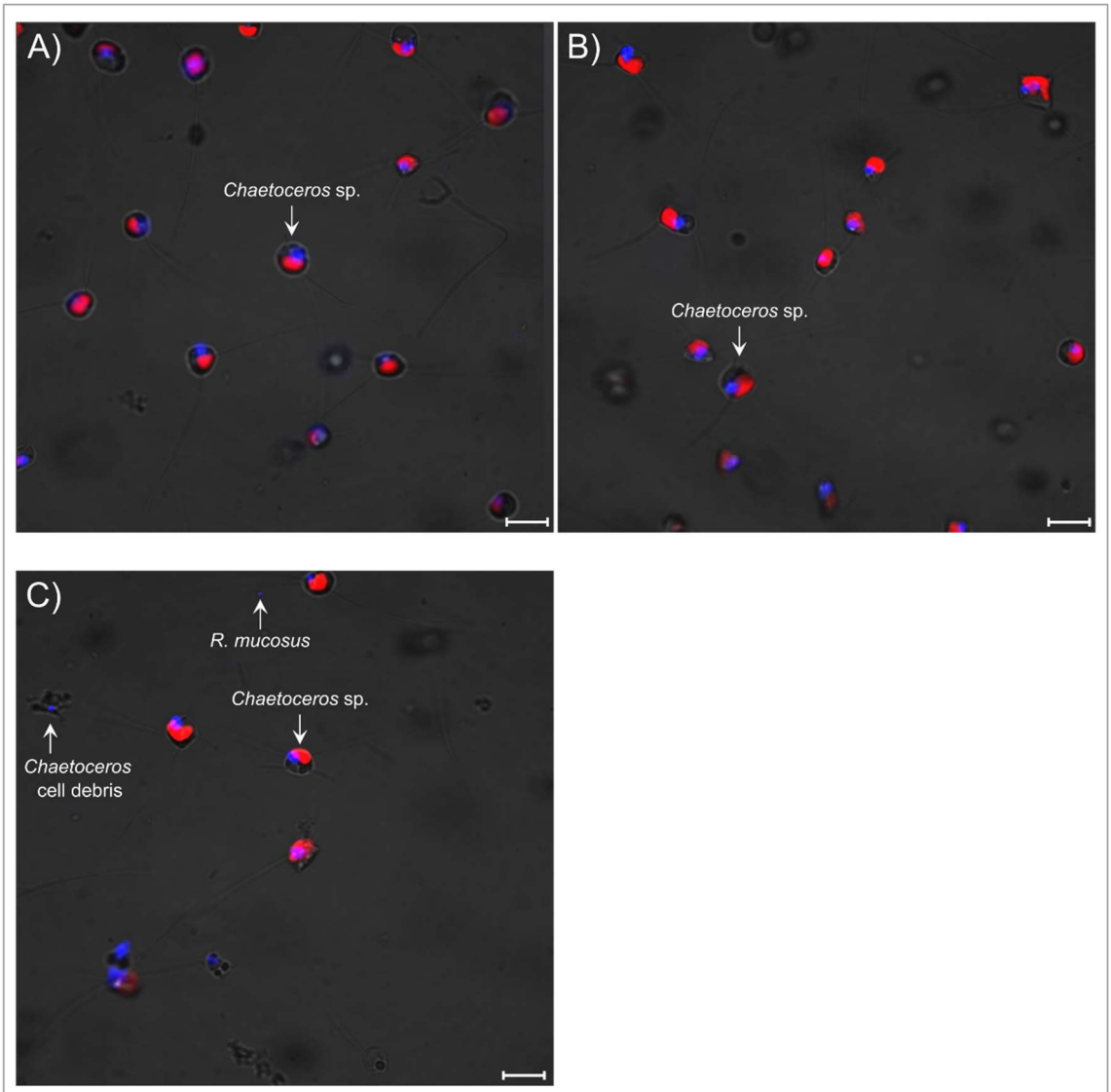

Figure 6. Epifluorescence micrographs of **A)** *Chaetoceros* sp. PLY617 control culture, **B)** *Chaetoceros* sp. PLY617 co-cultured with *M. adhaerens* and **C)** *Chaetoceros* sp. PLY617 co-cultured with *R. mucosus* at day 7 of growth experiment. Subsamples of each culture were incubated with Hoechst 33342 nucleic acid and imaged using a LEICA DMi8, excited with 395 nm excitation and 460 nm emission filters, at 63x. Blue fluorescence represents DNA Hoescht-stained DNA of both bacteria and diatom material and red fluorescence represents diatom chloroplast autofluorescence. *Chaetoceros* sp., *M. adhaerens* and *R. mucosus* cells are indicated by white arrows. Scale bars represent 10 µm.

2.4.2 Assessing the impacts of diatom cell health on antagonistic activity of bacterial isolates

Due to the lack of antagonistic activity observed in the previous three trials, further co-cultures were set up to assess whether diatom cell health impacted susceptibility to bacterial antagonism, as multiple species of the commonly diatom-associated Roseobacter group have been reported to sense and respond to the physiological state of microalgae and adjust their lifestyle from commensal or synergistic to antagonistic accordingly (Seyedsayamdost et al., 2011; Barak-Gavish et al., 2023). As such, co-cultivation trials were set up with the addition of algal senescence molecule p-coumaric acid (pCA) in an attempt to imitate diatom senescence and induce antagonism in the library of bacterial isolates.

Trial 4

T. pseudonana cultures were co-cultured with *M. adhaerens*, *P. alexandrii* or *R. mucosus* and cultures were supplemented with 1 mM pCA dissolved in DMSO (a concentration known to stimulate production of the anti-algal compounds roseobacticides in *Phaeobacter gallaeciensis* (Seyedsayamdost et al., 2011)). Axenic *T. pseudonana* cultures were used as a control, and axenic *T. pseudonana*-DMSO and *T. pseudonana*-pCA controls were also run. Diatom growth and photosynthetic efficiency were monitored at regular intervals for a three-week period. Similar to initial *T. pseudonana* co-cultivation trials in 3.4.1, *T. pseudonana* cultures seemed largely unaffected by the presence of the three bacteria, with no significant differences in total cell numbers between treatments and axenic control (Figure 7A). Conversely, although photosynthetic efficiencies of *T. pseudonana*-bacteria co-cultures were significantly higher than the axenic control at day eight (*M. adhaerens* P = 0.0000024, *P. alexandrii* P = 0.0000140 and *R. mucosus* P = 0.0001071), co-cultures exhibited a much more rapid decline in Fv/Fm from day 11 compared to axenic cultures (Figure 7B).

Comparing growth rates at day two revealed that only one of the co-cultures had a significantly reduced growth rate (*T. pseudonana*-*M. adhaerens*, P = 0.04, Figure 7C). However, in contrast to the initial non-pCA trials in 2.4.1, *P. alexandrii* and *R. mucosus* did not significantly reduce growth rates of *T. pseudonana* when supplemented with pCA. As such, the addition of pCA to diatom-bacteria co-cultures did not appear to increase antagonistic activity.

Microscopic observations of these co-cultures revealed a much higher density of bacteria in all three bacterial treatments than was observed with previous trials (Figure 8B, C and D). However, this could be due to the fact that imaging was conducted on day 15 of this trial, in comparison to day seven in the previous trials (the bacteria were inoculated to the same final density (equivalent to and OD_{600} of 0.05). Nonetheless, epifluorescence imaging of *T. pseudonana*-*M. adhaerens* cultures appeared to show clusters of *M. adhaerens* cells surrounding *T. pseudonana* cells (Figure 8B, circled), potentially indicating *T. pseudonana*-*M. adhaerens* associations.

Interestingly, comparing the three axenic controls (*T. pseudonana*, *T. pseudonana*-DMSO and *T. pseudonana*-pCA), the growth rate of axenic *T. pseudonana* supplemented with pCA was significantly lower at day two than the standard axenic control (P = 0.033), but not than the DMSO control (P > 0.05), suggesting *T. pseudonana* growth is negatively impacted by pCA but not DMSO. Nevertheless, by day eight there was no significant difference in cell numbers between either of the three controls. On the other hand, while DMSO did not significantly impact *T. pseudonana* growth rates or total cell numbers, the decline of photosynthetic efficiency in the DMSO control was slower than in the bacterial treatments, more closely mirroring the trend of the non-DMSO axenic control.

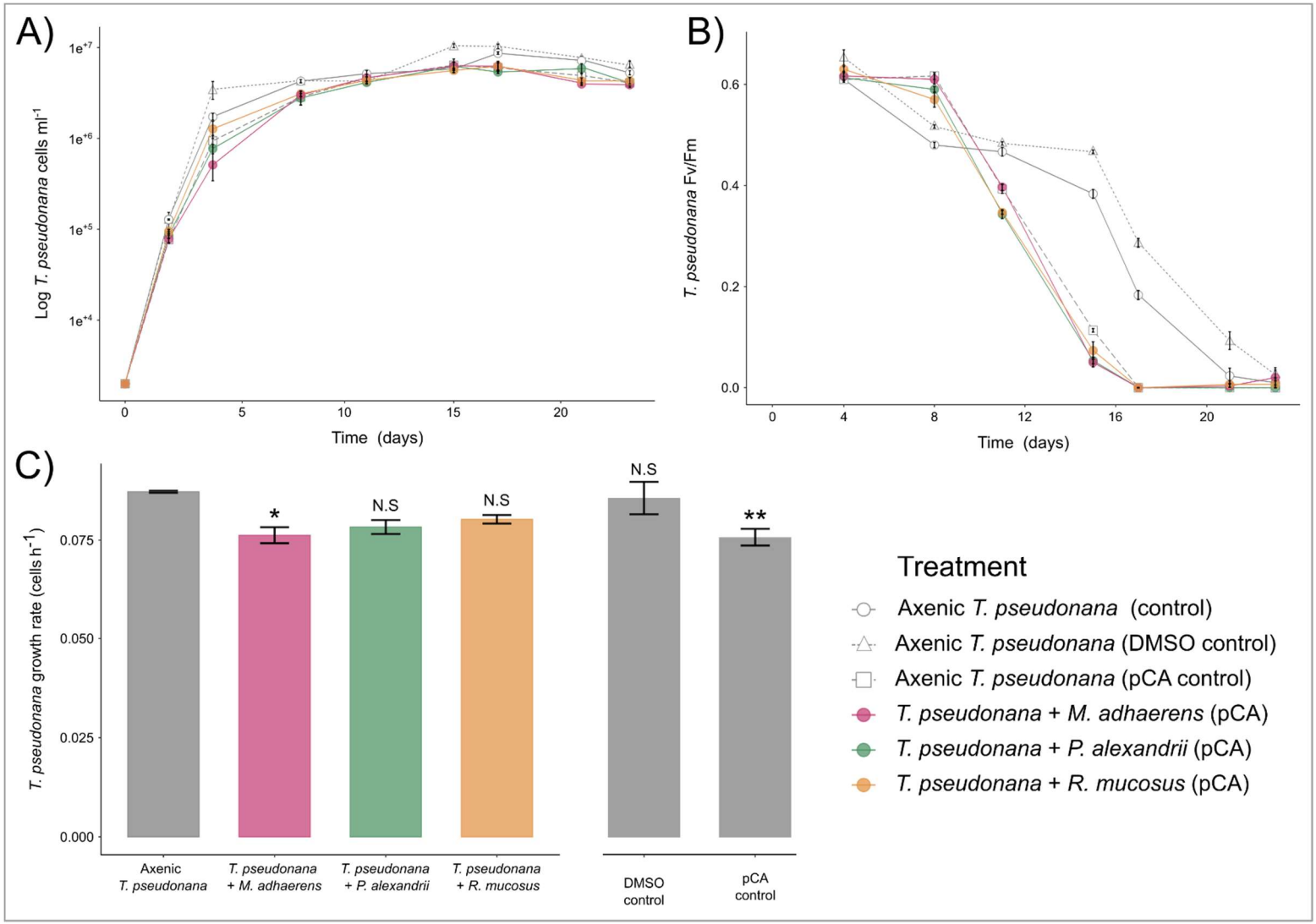

Figure 7. A) Growth (cells ml^{-1}) and **B)** photosynthetic efficiency (Fv/Fm) of *T. pseudonana* in axenic culture and in co-culture with *M. adhaerens*, *P. alexandrii* or *R. mucosus*, in addition to axenic *T. pseudonana* cultures supplemented with either 1 mM pCA or an equal volume of DMSO **C)** Growth rates of *T. pseudonana* between day 0 and day 2 were significantly lower in co-culture with *M. adhaerens* (P = 0.04) and in axenic culture supplemented with pCA (P = 0.033) compared to standard axenic control, however no significant differences were observed in the DMSO control or in co-culture with either *P. alexandrii* or *R. mucosus* (N.S, P > 0.05). Error bars represent ± S.E, n = 3, and statistical significance was calculated using a one-way ANOVA.

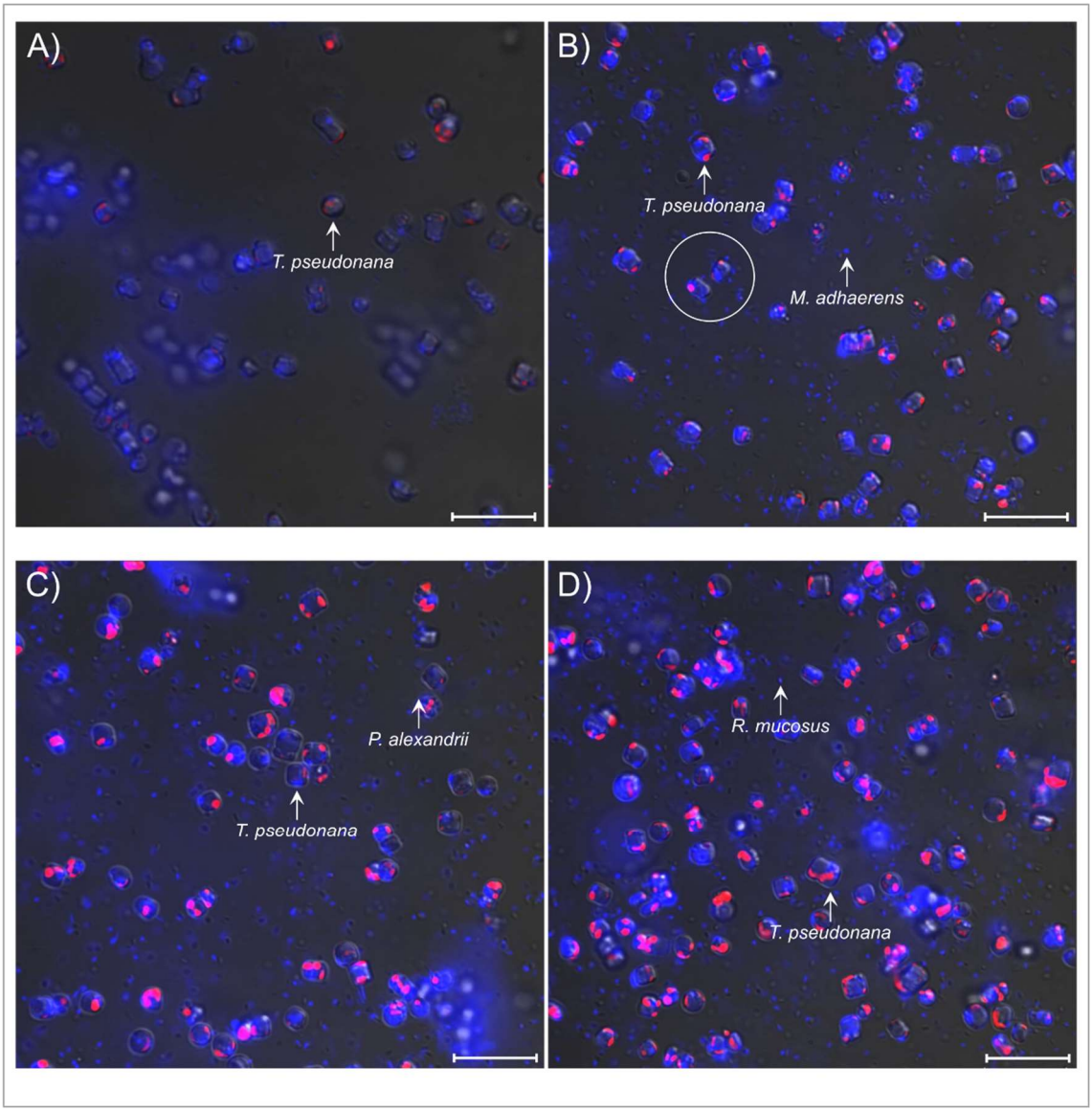

Figure 8. Epifluorescence micrographs of **A)** *T. pseudonana* axenic control culture, **B)** *T. pseudonana* co-cultured with *M. adhaerens* supplemented with 1 mM pCA **C)** *T. pseudonana* co-cultured with *P. alexandrii* supplemented with 1 mM pCA, and D) *T. pseudonana* co-cultured with *R. mucosus* supplemented with 1 mM pCA. All images were captured at day 15. Subsamples of each culture were incubated with Hoechst 33342 nucleic acid and imaged using a LEICA DMi8, excited with 395 nm excitation and 460 nm emission filters, at 63x. Blue fluorescence represents DNA Hoescht-stained DNA of both bacteria and diatom material and red fluorescence represents diatom chloroplast autofluorescence. *T. pseudonana*, *M. adhaerens*, *P. alexandrii* and *R. mucosus* cells are indicated by white arrows. Scale bars

Despite slightly reducing growth rates of *T. pseudonana* at day two, the addition of pCA was not deemed to have a significant impact on overall diatom health, nor bacterial antagonism. As initial plaque assays were conducted with older (14-day), it was hypothesised that older diatom cultures would potentially be less healthy and consequently more susceptible to antagonistic activity. Therefore, co-culture assays were conducted to compare antagonistic activity against older versus younger diatom cultures. These trials were conducted with *P. alexandrii* and original host *Skeletonema* sp., and with *M. adhaerens* and model *T. pseudonana*. Co-cultures were conducted in a similar manner to previous trials, whereby four or 14-day old diatom cells were inoculated into fresh f/2 media with a chosen bacteria, and four and 14-day old axenic diatoms were used as a control.

Trial 5

As expected, *Skeletonema* sp. cultures (both axenic controls and bacterial treatments) that were inoculated from four-day old stock cultures reached and mostly maintained higher cell densities than cultures that were inoculated from 14-day old stocks (Figure 9A). For both the four and 14-day treatments, *Skeletonema* sp. cell densities were typically lower in bacterial treatments than in their respective axenic controls, though this was not significant ($p > 0.05$). Interestingly, photosynthetic efficiency (Fv/Fm) was highest in the two 14-day cultures, with the exception of 14-day *Skeletonema-P. alexandrii* at day two (Figure 9B). Photosynthetic efficiency of 14-day axenic cultures and bacterial treatments were similar throughout the course of the experiment, with the exception of a significant increase in photosynthetic efficiency of the bacterial treatment at day 16 ($p = 0.00003$). However, this by the end of the observation period the photosynthetic efficiency in the bacterial treatment had decreased to below that of the axenic control ($p > 0.05$). Similarly, photosynthetic efficiency of 4-day axenic cultures was closely mirrored by that of the bacterial treatments until day 16, which saw a steep increase of 0.12 in the bacterial treatment ($p = 0.005$), which persisted until the end of the observation period (day 18, $p = 0.015$).

Growth rates of *Skeletonema* sp. inoculated from 14-day old stock cultures were not significantly different when co-cultured with *P. alexandrii* compared to the axenic control (Figure 9C and d, $p > 0.05$). Similarly, *Skeletonema* sp. incoulated from 4-day stock cultures also showed no significant difference in growth rates between axenic controls and *P. alexandrii* co-cultures (Figure 9C and d, $p > 0.05$). Significance was not calculated between the two age groups.

Epifluourescence imaging of *Skeletonema* sp. cultures at day 11 revealed little difference between the four and 14-day cultures in both axenic and bacterial treatments (Figure 10) in terms of cell morphologies and bacterial numbers. In both bacterial treatments, *P. alexandrii* cells were observed attached or close to *Skeletonema* cells (Figure 10B and D). In 14-day *P. alexandrii* treatments, a higher number of 'dead' *Skeletonema* cells could be observed (in-tact cells lacking characteristic red chlorophyll of living or healthy cells, Figure 10E), although there did not appear to be a higher number of bacterial cells associated with these dead cells than was observed with live cells.

In contrast to the *Skeletonema-P. alexandrii* trial, both axenic and co-cultured 14-day *T. pseudonana* cultures displayed more rapid growth than the 4-day cultures, however, by the end of the observation period (day 14), the cell densities in all four treatments were similar (Figure 11A). Growth of the 14-day *T. pseudonana-M. adhaerens* co-culture closely mirrored that of the axenic control throughout the course of the experiment. Growth of the 4-day *T. pseudonana-M. adhaerens* co-culture also followed a similar pattern to the axenic control. Growth of the co-culture was initially lower at day four, however not significantly ($p > 0.05$), but recovered by day seven. Similarly, photosynthetic efficiency was initially higher in both the axenic and co-cultured 14-day treatments compared to the 4-day treatments (Figure 11B). However, while both of the 14-day treatments only displayed a slight decrease in photosynthetic efficiency, both the axenic and co-cultured 4-day treatments displayed marked increases in photosynthetic efficiency, and values had surpassed those of both 14-day treatments by the end of the observation period. Nevertheless, photosynthetic efficiencies of *T. pseudonana* co-

cultured with *M. adhaerens* were not significantly different compared to their respective axenic controls. Finally, growth rates of *T. pseudonana* between day zero and day four were not significantly different between co-culture treatments and their respective axenic controls ($p > 0.05$).

As such, it was deemed that the age of diatom cultures did not have any significant impact on bacterial antagonism in these trials.

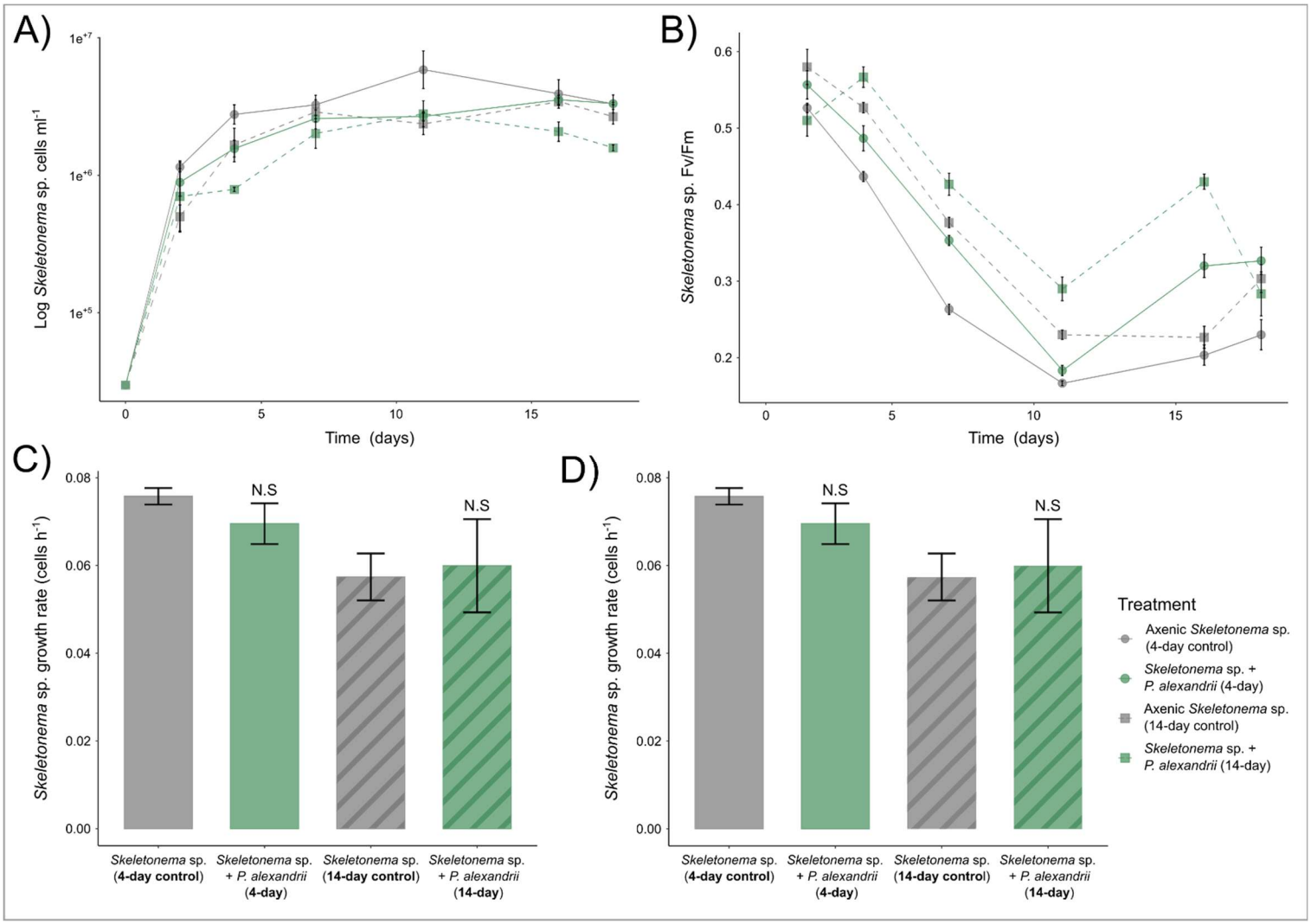

Figure 9. A) Growth (cells ml^{-1}) and **B)** photosynthetic efficiency (Fv/Fm) of exponential and stationary phase *Skeletonema* sp. PLY627 in axenic culture and in co-culture with *P. alexandrii* **C)** Growth rates of *Skeletonema* sp. PLY627 between day 0 and day 2 were not significantly different in co-culture with *P. alexandrii* in either treatment (N.S, $P > 0.05$) compared to their respective axenic controls. **D)** Growth rates of *Skeletonema* sp. PLY627 between day 2 and day 4 were also not significantly different in co-culture with *P. alexandrii* in either treatment (N.S, $P > 0.05$) compared to their respective axenic controls. Error bars represent ± S.E, n = 3, and statistical significance was calculated using a one-way ANOVA.

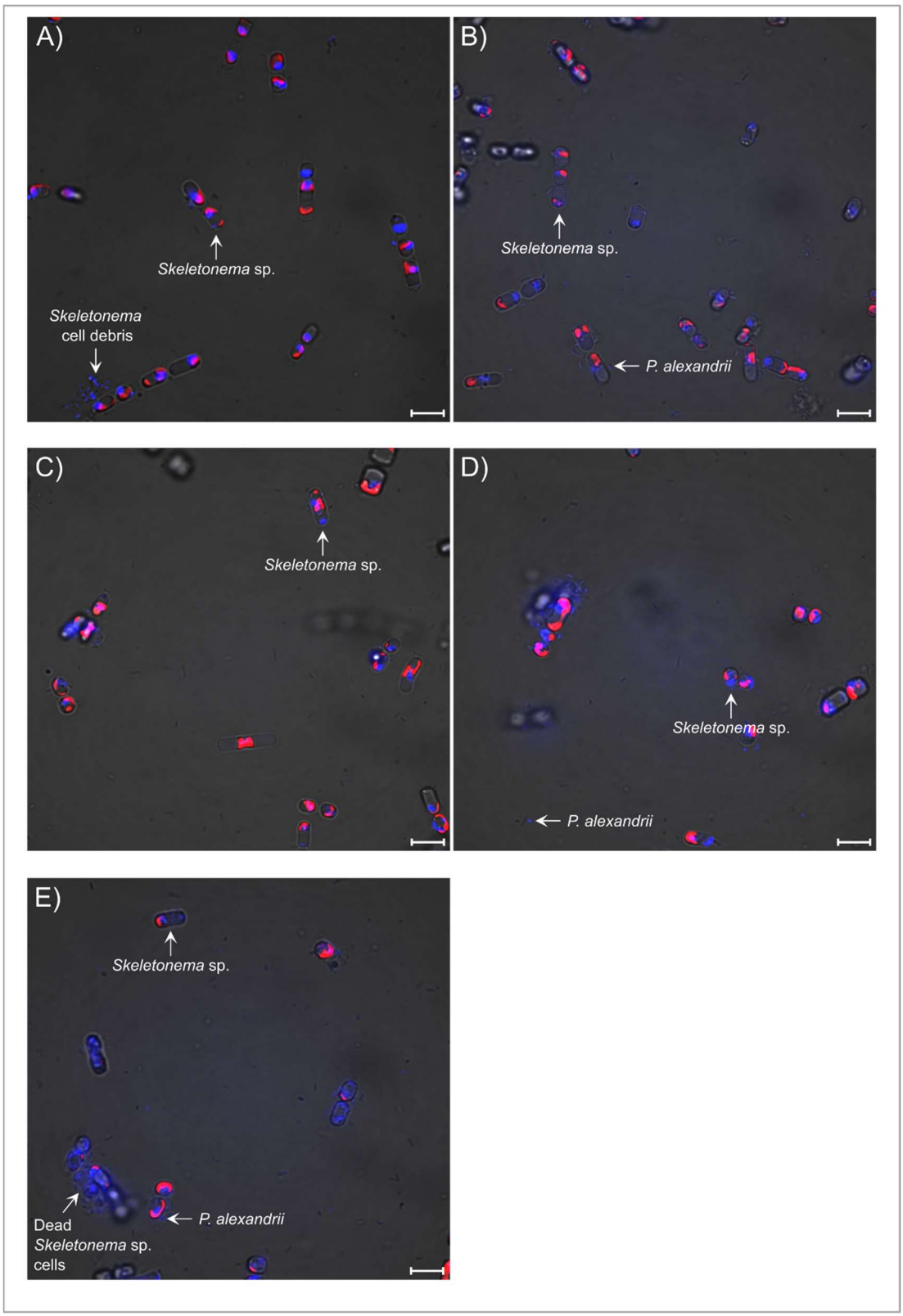

Figure 10. Epifluorescence micrographs of **A)** *Skeletonema* sp. PLY627 (4-day) axenic control culture **B)** *Skeletonema* sp. PLY627 (4-day) co-cultured with *P. alexandrii* **C)** *Skeletonema* sp. PLY627 (14-day) axenic control culture, and **D)** *Skeletonema* sp. PLY627 (14-day) co-cultured with *P. alexandrii* and **E)** *Skeletonema* sp. PLY627 (14-day) co-cultured with *P. alexandrii* showing dead *Skeletonema* cells (lacking chlorophyll fluorescence). All images were captured at day 11. Subsamples of each culture were incubated with Hoechst 33342 nucleic acid and imaged using a LEICA DMi8, excited with 395 nm excitation and 460 nm emission filters. Blue fluorescence represents DNA Hoescht-stained DNA of both bacteria and diatom material and red fluorescence represents diatom chloroplast autofluorescence. *Skeletonema* sp., and *P. alexandrii* cells are indicated by white arrows. Scale bars represent 10 µm.

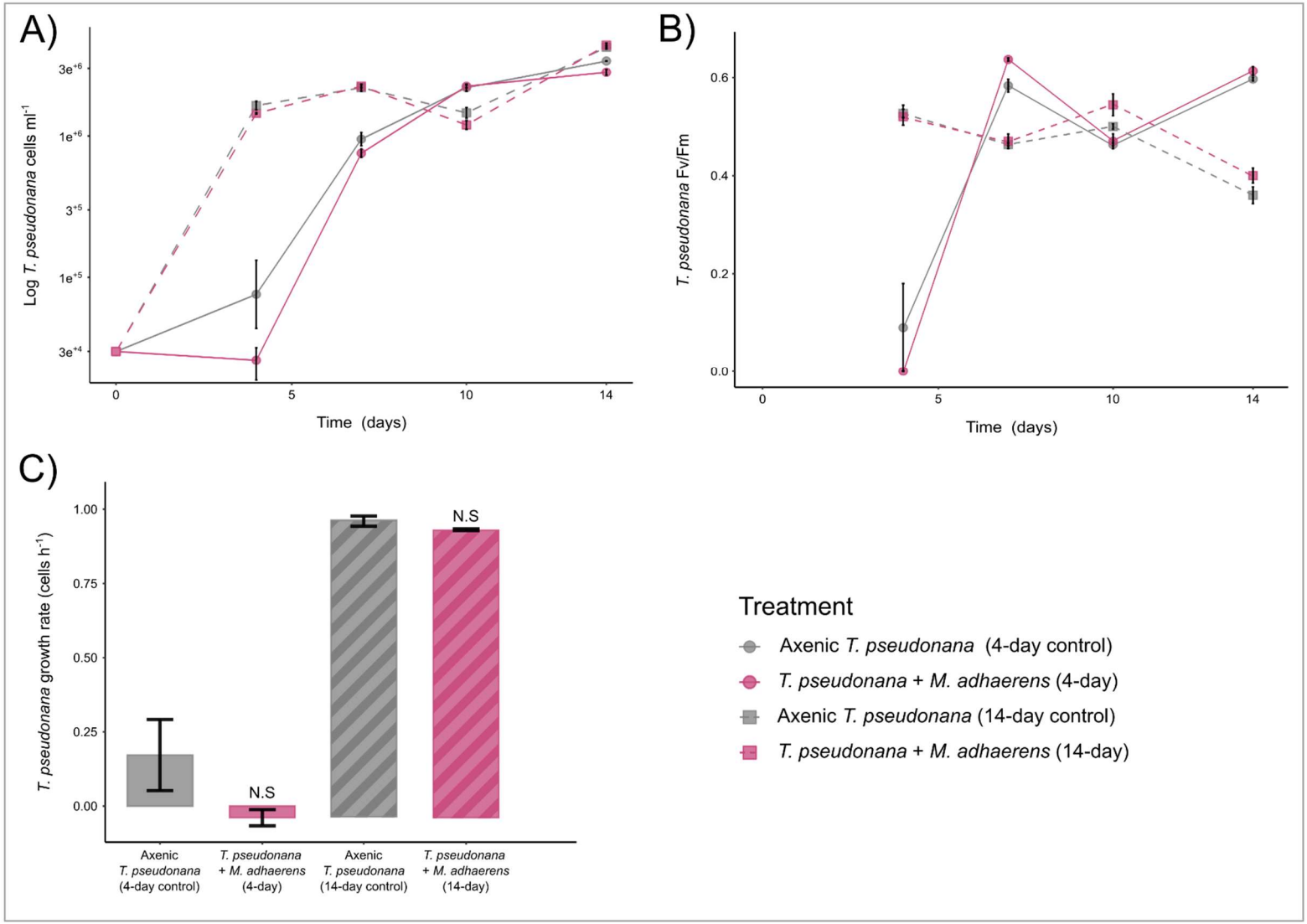

Figure 11. A) Growth (cells ml^{-1}) and **B)** photosynthetic efficiency (Fv/Fm) of exponential and stationary phase *T. pseudonana* in axenic culture and in co-culture with *M. adhaerens* **C)** Growth rates of exponential and stationary phase *T. pseudonana* between day 0 and day 2 were not significantly different in co-culture with *M. adhaerens* in either treatment (N.S, $P > 0.05$) compared to their respective axenic controls. Error bars represent ± S.E, n = 3, and statistical significance was calculated using a one-way ANOVA.

2.4.3 Assessing the impacts of physical environment on antagonistic activity of bacterial isolates

Trial 6

To assess whether the physical environment of the soft-agar overlay assay played a role in antagonistic activity, soft-agar overlay assays were conducted with *P. alexandrii* and the suite of diatom hosts immobilised in semi-solid agar. Live *P. alexandrii* cells or cell-free filtrate was pipetted onto filter discs at various optical densities (live cells) or dilutions (cell-free filtrate, diluted with FSW), and placed on top of 14-day old diatom hosts suspended in semi-solid agar. The diatom lawns were observed for zones ('halos') of clearing surrounding the filter discs, which would indicate that *P. alexandrii* was lysing the diatom cells within the agar. Cultures were observed for four weeks, with no signs of clearing observed on any of the live *P. alexandrii* inoculated or cell-free filtrate inoculated plates, across any of the diatom host species.

2.4.4 Induction of antagonistic activity in *P. alexandrii* through pre-exposure to diatom necromass

Trial 7

Following the initial soft-agar overlay assays with *P. alexandrii* (2.4.3), further soft-agar assays were conducted with *T. pseudonana* and *P. alexandrii* pre-grown on different media types. For these assays, ½ YTSS (that has been used to pre-cultivate bacteria prior to inoculation into co-culture in all preceding experiments) was used as a control medium, while Dead Diatom Media (DDM, 14-day old diatom cultures autoclaved with 1 % agarose) was selected as an alternative medium. *P. alexandrii* was grown on the two media types and re-inoculated at various optical densities into 14-day old *T. pseudonana* cultures suspended in semi-solid agar. Plates were observed for plaque formation as with original soft-agar plaque assays in Chapter 1.

Plaque formation was observed with DDM grown *P. alexandrii* at all five cell densities tested (Figure 12), whereas only a small number of plaques were observed for ½ YTSS grown *P. alexandrii* only at the highest bacterial cell density (0.01). Plaques were small in diameter, typically < 1 cm, and all plaques were agar lytic, resembling those observed in original soft-agar plaque assays of Chapter 1 (Figure 13). In total, across the two DDM versus ½ YTSS plaque assay trials that were conducted, 69 plaques were observed in *T. pseudonana* lawns inoculated with DDM-grown *P. alexandrii*. When compared to the five plaques observed with ½ YTSS-grown *P. alexandrii*, this indicates that growing *P. alexandrii* on diatom necromass increases antagonistic activity.

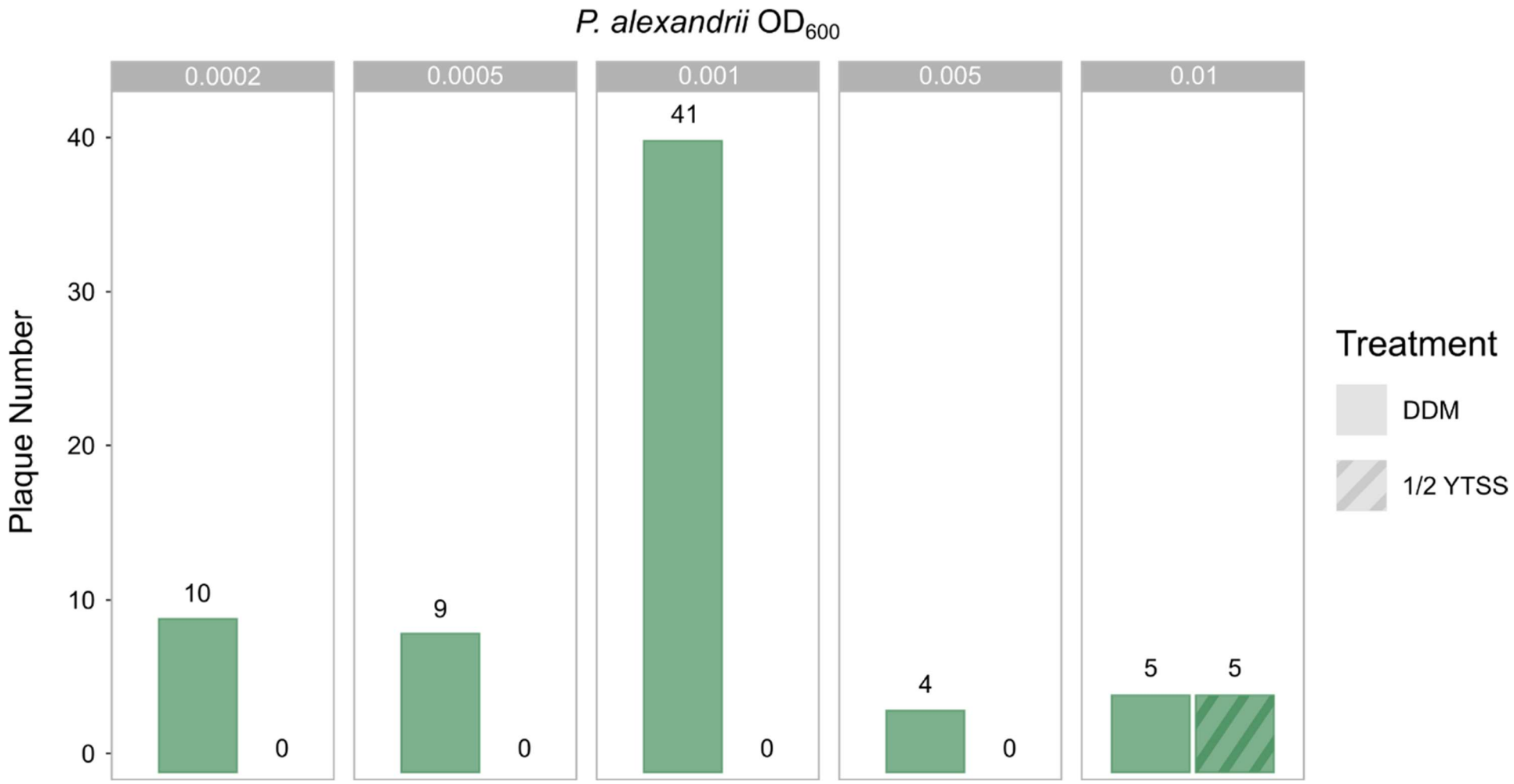

Figure 12. Number of plaques observed in *T. pseudonana* lawns when inoculated with *P. alexandrii* grown on DDM (solid colour bars) or ½ YTSS (hatched bars), at various bacterial optical densities (OD_{600}, ranging from 0.0002 to 0.01). Plaque number is the sum of two comparable rounds of soft-agar overlay assays conducted using the same parameters.

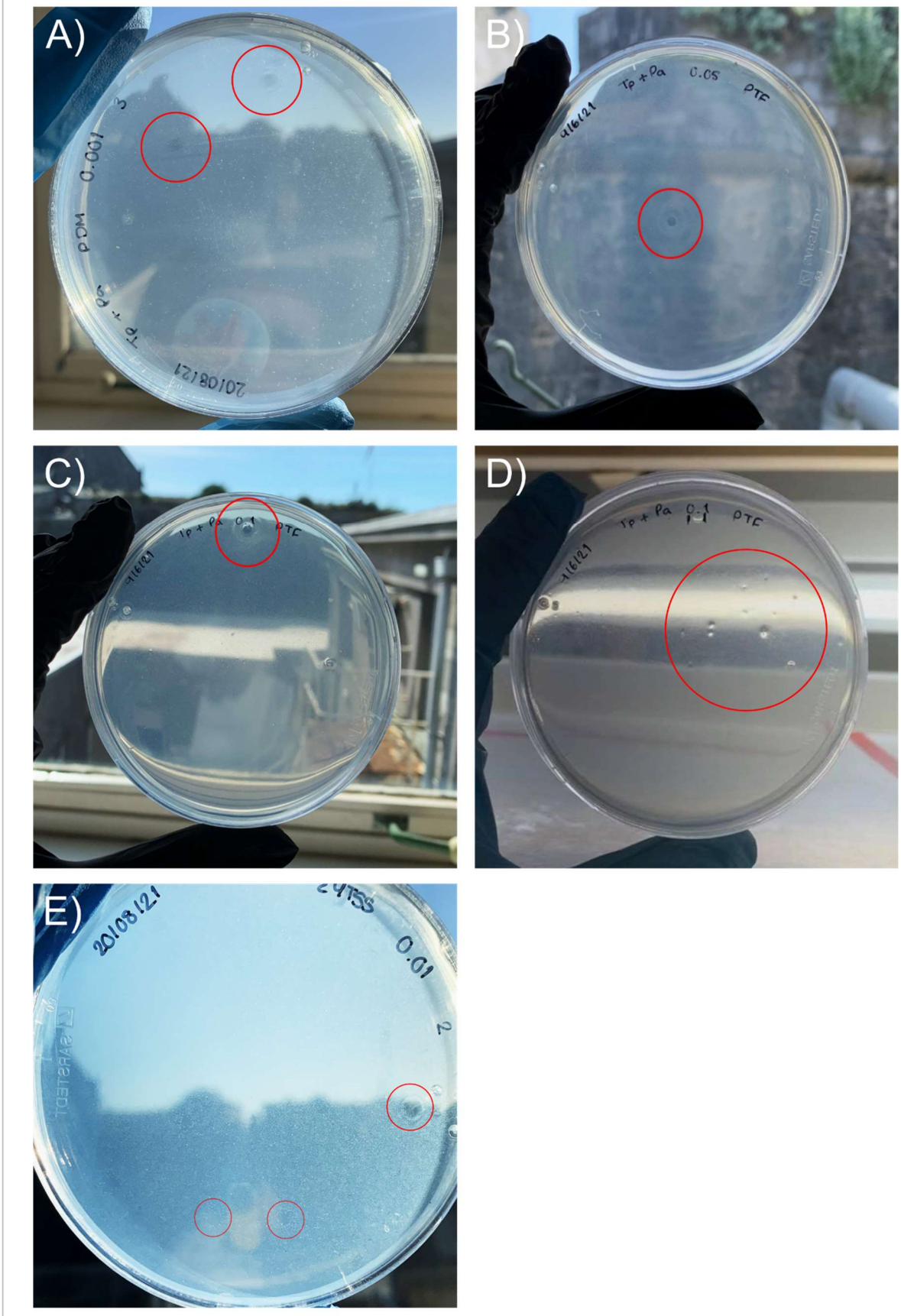

Figure 13. Images of plaques (zones of diatom growth inhibition) within lawns of *T. pseudonana* suspended in soft-agar, caused by the presence of DDM-grown *P. alexandrii* at varying concentrations.

In order to assess whether cultivation on DDM could induce antagonistic activity in an environment that more closely resembles the marine planktonic environments where the diatom hosts are typically found, liquid co-cultures were conducted with *P. alexandrii* and the suite of diatom host species. Co-cultures were set up according to previous trials, by inoculating 4-day old diatom monocultures into fresh f/2 media with *P. alexandrii* grown on either ½ YTSS or DDM (and an axenic diatom culture used as a control).

DDM-grown *P. alexandrii* showed inhibition of diatom growth in three of the five host species, *T. pseudonana*, *Skeletonema* sp., and *Chaetoceros* sp., whereas ½ YTSS-grown *P. alexandrii* exhibited no inhibitory effects against any of the five host species.

The largest inhibitory effects was observed against *T. pseudonana* (Figure 14A), with final (day 23) total cell numbers of *T. pseudonana* in co-culture with DDM-grown *P. alexandrii* being 99.2% lower than in the axenic control ($p = 0.0005$). Conversely, growth of *T. pseudonana* in co-culture with ½ YTSS-grown *P. alexandrii* closely followed the growth curve of the axenic control, with final cell numbers actually being 24.3% higher than in the axenic control cultures (though this was not significant, $p > 0.05$). Photosynthetic efficiency was also undetectable in DDM-grown co-cultures, though slightly (but not significantly) enhanced in ½ YTSS-grown co-cultures (Figure 14B).

Skeletonema sp. was also inhibited by DDM-grown *P. alexandrii* (Figure 15A). Final cell numbers in *Skeletonema* sp.-*P. alexandrii* (DDM) co-cultures were 98.3 % lower than in the axenic control, though interestingly, this inhibition was significant only when comparing DDM co-cultures with ½ YTSS co-cultures ($p = 0.012$), and not when comparing DDM co-cultures to the axenic control ($p > 0.05$). Again, in DDM-grown co-cultures, photosynthetic efficiency of *Skeletonema* sp. was undetectable, but slightly (though not significantly) enhanced in ½ YTSS-grown cultures (Figure 15B, $p > 0.05$).

As with the previous two host species, the addition of ½ YTSS-grown *P. alexandrii* did not significantly impact the growth (Figure 16A) or photosynthetic efficiency (Figure 16B) of *Chaetoceros* sp. cultures. Growth of *Chaetoceros* sp. inoculated with DDM-grown *P.*

alexandrii was initially substantially inhibited (Figure 16A), with cell numbers in DDM treatments at day two being 83.7% lower than in the axenic control. Inhibition persisted until day 16, at which point the cell density of DDM cultures were 96.7% lower than the axenic control. However, at this point the growth of DDM cultures began to recover, and by day 23 was 70% lower than the axenic control (note the log scale on Figure 16A). While final cell numbers in DDM cultures were still significantly lower than the control ($p = 0.0007$), growth recovery was mirrored by a sharp increase in photosynthetic efficiency in the DDM cultures, from undetectable at day 16 to 0.69 at day 18 (Figure 16B), indicating the presence of live, healthy *Chaetoceros* sp. cultures.

When co-cultured with *P. tricornutum* (Figure 17) and *T. weissflogii* (Figure 18), no growth inhibitory effects were observed on with either DDM or ½ YTSS grown *P. alexandrii*, with DDM and ½ YTSS co-culture growth curves closely resembling their respective axenic controls (Figure 17A and 18A respectively). Likewise, no significant differences were observed in the photosynthetic efficiencies of *P. tricornutum* and *T. weissflogii* in co-culture treatments (Figure 17B and 18B respectively).

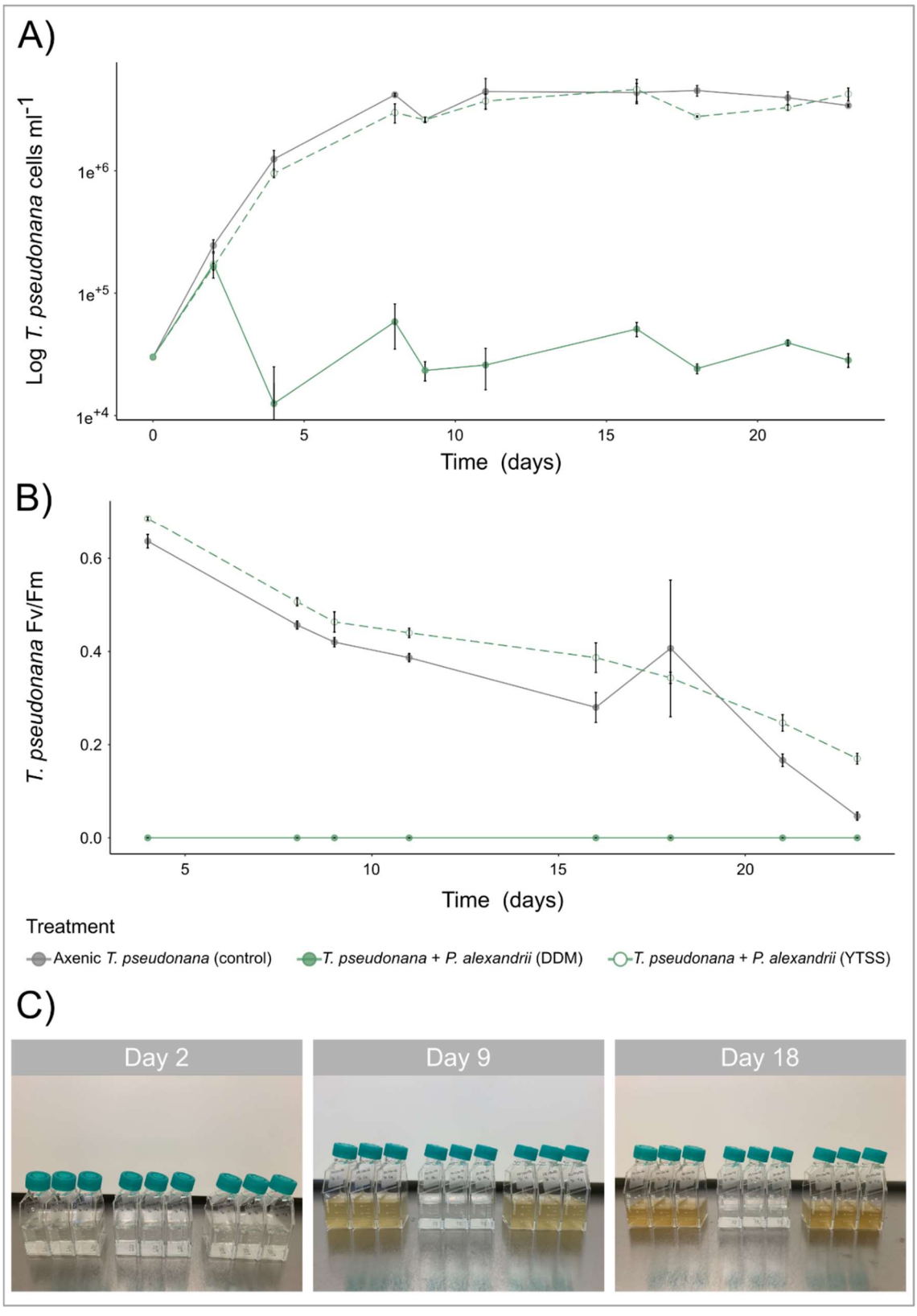

Figure 14. A) Growth (cells ml^{-1}) and **B)** photosynthetic efficiency (Fv/Fm) of *T. pseudonana* in axenic culture (grey) and in co-culture with *P. alexandrii* cultured on DDM (green) or ½ YTSS (open circle) **C)** *T. pseudonana* cultures imaged on day 2, 9 and 18 of the co-cultivation period. Error bars represent ± S.E, n = 3.

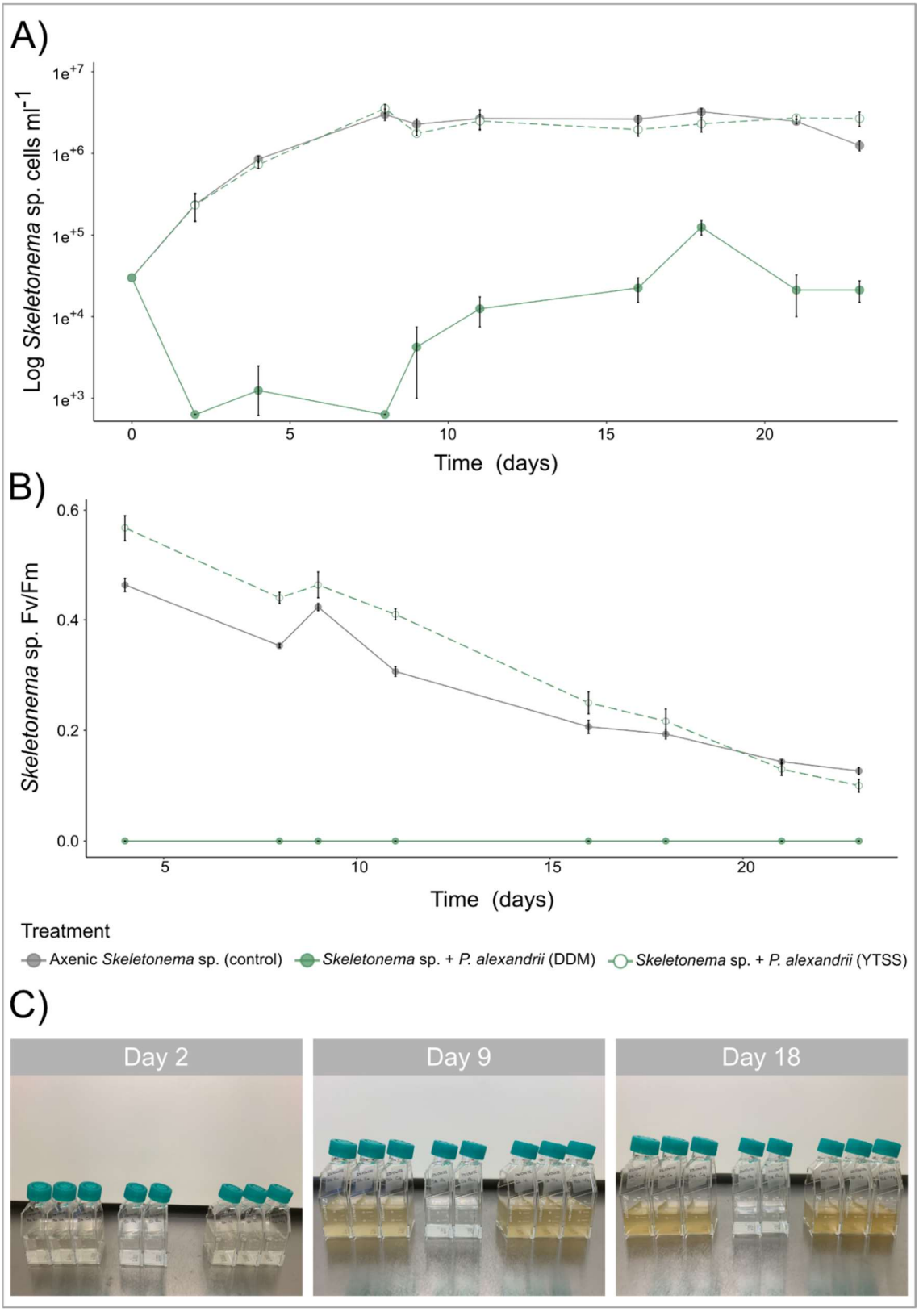

Figure 15. **A)** Growth (cells ml^{-1}) and **B)** photosynthetic efficiency (Fv/Fm) of *Skeletonema* sp. PLY627 in axenic culture (grey) and in co-culture with *P. alexandrii* cultured on DDM (green) or ½ YTSS (open circle). **C)** *Skeletonema* sp. PLY627 cultures imaged on day 2, 9 and 18 of the co-cultivation period. Error bars represent ± S.E, n = 3, with the exception of DDM-grown *P. alexandrii*, where n = 2.

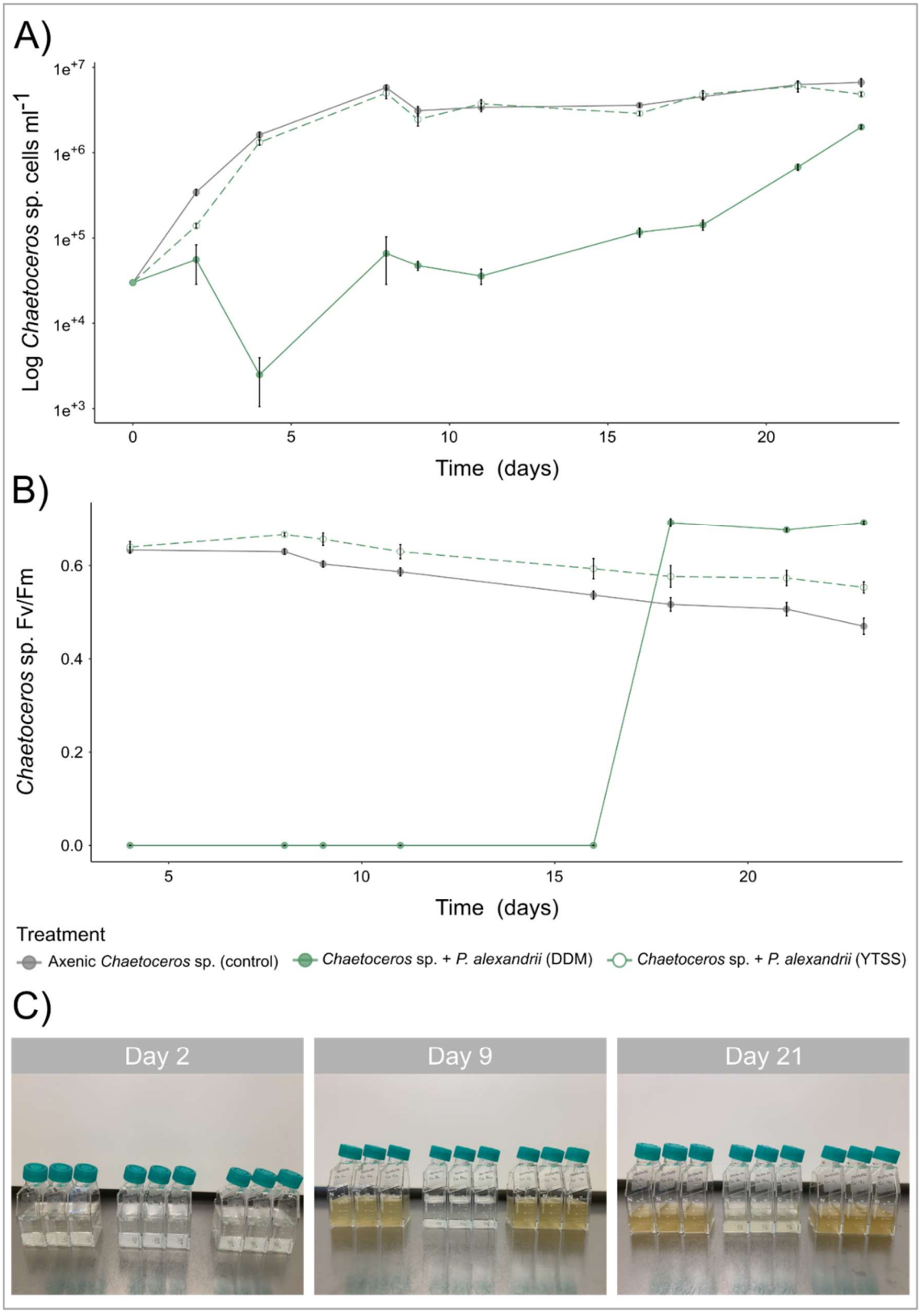

Figure 16. A) Growth (cells ml^{-1}) and **B)** photosynthetic efficiency (Fv/Fm) of *Chaetoceros* sp. PLY617 in axenic culture (grey) and in co-culture with *P. alexandrii* cultured on DDM (green) or ½ YTSS (open circle) **C)** *Chaetoceros* sp. PLY617 cultures imaged on day 2, 9 and 18 of the co-cultivation period. Error bars represent ± S.E, n = 3.

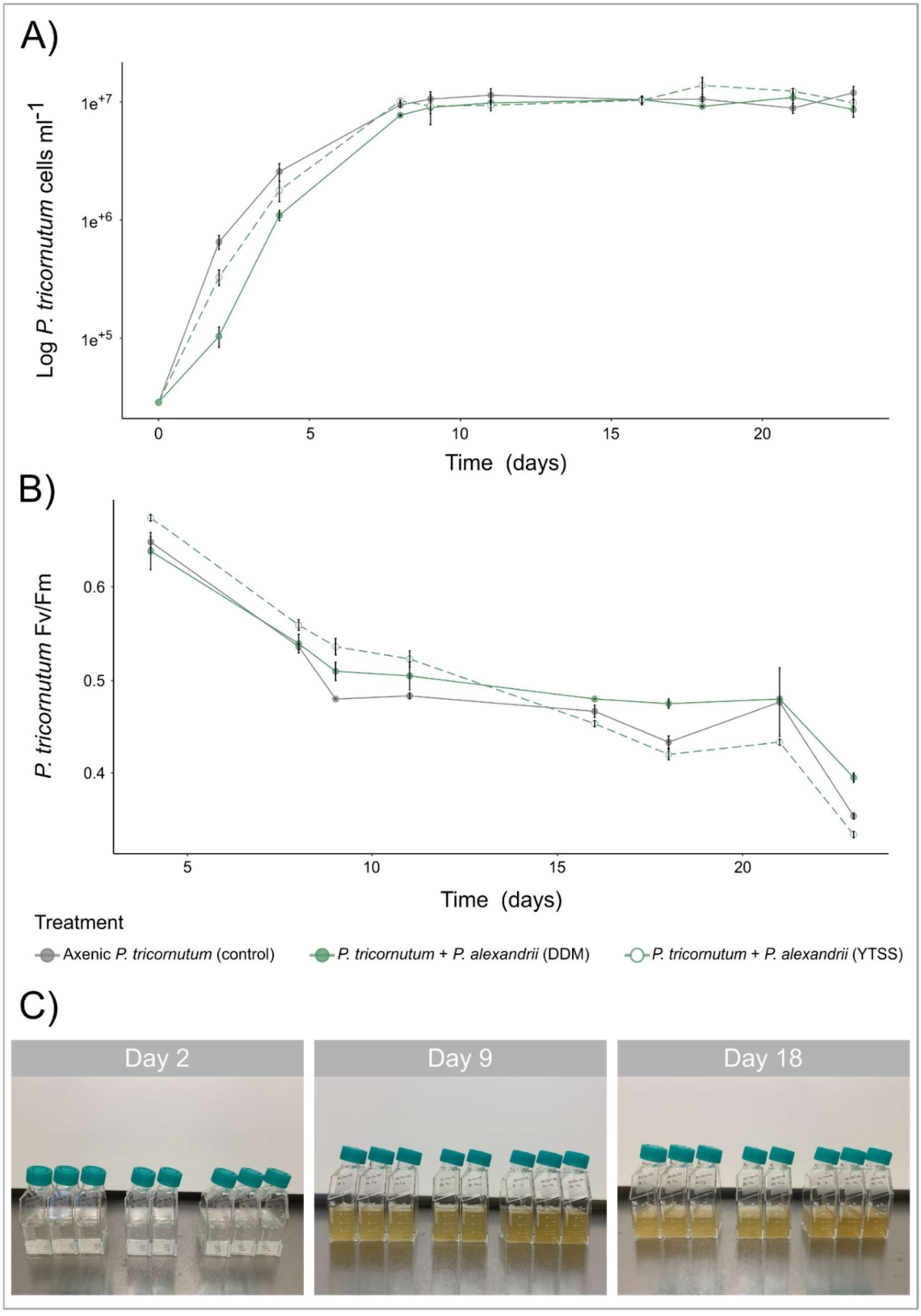

Figure 17. A) Growth (cells ml^{-1}) and **B)** photosynthetic efficiency (Fv/Fm) of *P. tricornutum* in axenic culture (grey) and in co-culture with *P. alexandrii* cultured on DDM (green) or ½ YTSS (open circle) **C)** *P. tricornutum* cultures imaged on day 2, 9 and 18 of the co-cultivation period. Error bars represent ± S.E, n = 3, with the exception of DDM-grown *P. alexandrii*, where n = 2.

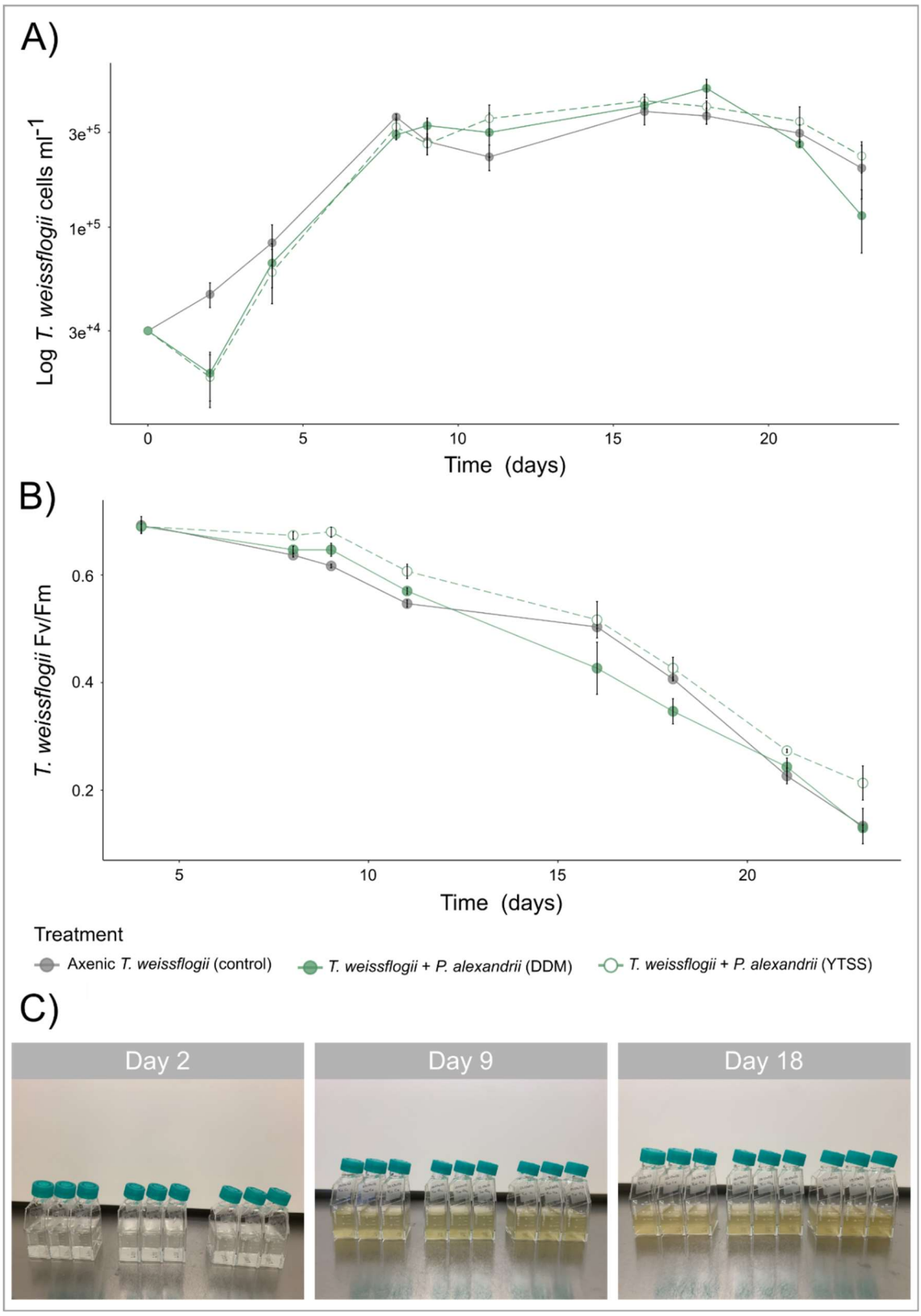

Figure 18. A) Growth (cells ml^{-1}) and **B)** photosynthetic efficiency (Fv/Fm) of *T. weissflogii* in axenic culture (grey) and in co-culture with *P. alexandrii* cultured on DDM (green) or ½ YTSS (open circle) **C)** *T. weissflogii* cultures imaged on day 2, 9 and 18 of the co-cultivation period. Error bars represent ± S.E, n = 3.

2.4.5 Antagonistic switch is conserved across multiple bacterial lineages

To determine whether antagonistic activity could be induced in other bacterial isolates through cultivation on DDM, 10 additional antagonists were also investigated in liquid co-cultures with at least one of their original diatom hosts. Bacteria were selected for verification based on a combination of their abundance throughout the plaque assay time series of Chapter 1 and whether or not diatom-antagonistic activity had previously been reported (Table 1). *P. alexandrii* was also used as a 'positive control' with diatom hosts against which it had previously displayed antagonistic activity (*T. pseudonana*, *Skeletonema* sp., and *Chaetoceros* sp.). Six of the 11 bacteria tested (including *P. alexandrii*) exhibited growth inhibitory effects against their respective hosts when grown on DDM (Figure 19). Microscopic observations of co-cultures were also conducted (Appendix Figures 9 – 13)

Table 1. Bacterial antagonists tested for induction of antagonistic activity via cultivation on DDM. Diatom hosts used in co-culture experiments, as well as original plaque assay hosts are also listed.

Isolate	Co-culture host	Original plaque assay hosts	Number of plaques isolated from	Previously reported antagonistic activity
Halomonas titanicae	*T. weissflogii*, *Chaetoceros* sp.	*T. pseudonana*, *T. weissflogii*, *Skeletonema* sp. *Chaetoceros* sp.	13	Genus only
Hoeflea phototrophica	*Chaetoceros* sp.	*P. tricornutum*, *Chaetoceros* sp.	5	No
Maribacter spongiicola	*P. tricornutum*	*P. tricornutum*	1	Genus only
Marinobacter adhaerens	*Chaetoceros* sp.	*T. weissflogii*, *Chaetoceros* sp.	8	Yes
Marinobacter algicola	*T. weissflogii*, *Skeletonema* sp.	*T. pseudonana*, *T. weissflogii*, *Skeletonema* sp.	3	Yes
Metabacillus idriensis	*P. tricornutum*	*P. tricornutum*	1	No
Oceanicaulis alexandrii	*T. weissflogii*	*T. weissflogii*	1	No
Ponticoccus alexandrii	*T. pseudonana*, *Skeletonema* sp., *Chaetoceros* sp.	*T. pseudonana*, T. *weissflogii*, *Skeletonema* sp., *Chaetoceros* sp.	19	Genus only
Pseudomonas lurida	*Skeletonema* sp.	*Skeletonema* sp.	1	Genus only
Thalassospira lohafexi	*T. pseudonana*	*T. pseudonana*, *T. weissflogii*, *Skletonema* sp.	4	Genus only
Vibrio diazotrophicus	*T. pseudonana*	*T. pseudonana*	2	Genus only

DDM-grown *Metabacillus idriensis* and *Maribacter spongiicola* inhibited the growth of *P. tricornutum* by 98.7 % and 57 % respectively (Figure 19). The impacts of ½ YTSS-grown *M. idriensis* significantly differed from DDM-grown cultures (p = 0.0000095), resulting in a 3.1 % increase in growth compared to the axenic control (though this increase was not significantly different from the axenic control). *M. spongiicola* was only tested on DDM.

P. alexandrii, *T. lohafexi* and *V. diazotrophicus* all exhibited significant growth inhibitory effects against *T. pseudonana* (Figure 19). DDM-grown *P. alexandrii* resulted in an inhibition of 99.8 %, whereas ½ YTSS-grown cultures only caused an 8.2 % inhibition. Similarly, DDM-grown *T. lohafexi* resulted in a 99.8 % inhibition, compared to the 32.3 % inhibition caused by ½ YTSS-grown cultures. *V. diazotrophicus* also resulted in a 99.7 % inhibition of *T. pseudonana* when cultured on DDM, but only a 21.7 % inhibition when cultured on ½ YTSS. In all three cases, inhibition by DDM-grown bacteria was significantly higher than by ½ YTSS-grown bacteria (p = 0.0000001, p = 0.0000094, and p = 0.000001 respectively).

Of the three bacteria tested against *T. weissflogii*, *Marinobacter algicola*, *Halomonas titanicae* and *Oceanicaulis alexandrii*, no significant inhibitory effects were observed by either DDM- or ½ YTSS-grown bacteria (Figure 19).

A further three bacteria, *P. alexandrii*, *M. algicola* and *Pseudomonas lurida*, were tested against *Skeletonema* sp. DDM-grown *P. alexandrii* resulted in a significant 98.7 % inhibition (P = 0.0000502), whereas a non-significant reduction of 22.4 % was observed in co-cultures inoculated with ½ YTSS-grown bacteria (Figure 19). Again, the difference in inhibition between DDM- and ½ YTSS-grown cultures was significant (p = 0.0000502). Neither *M. algicola* or *P. lurida* inhibited *Skeletonema* sp. growth when cultured on either media type.

Finally, *Chaetoceros* sp. was co-cultured with *M. adhaerens*, *P. alexandrii*, *Hoeflea phototrophica* and *H. titanicae*. DDM-grown *M. adhaerens* displayed a significant growth inhibitory effect of 99.8 % (P = 0.0000062), however, interestingly, ½ YTSS-grown

cultures resulted in an increase of 36.2 %, though this increase was not significant (Figure 19). Nevertheless, the difference in inhibition was significantly different between the DDM and ½ YTSS treatments ($p = 0.0000062$). *P. alexandrii* cultured on DDM resulted in a less pronounced inhibition of 60.6 %, and ½ YTSS-grown bacteria resulted in an 18.6 % inhibition. Neither inhibitory rate was significant when compared to the axenic control, and the differences between the two media types were also non-significant. Similarly, although DDM-grown *H. titanicae* caused a 31.8 % inhibition of *Chaetoceros* sp. growth, the difference in activity was significantly different between DDM-grown and ½ YTSS-grown *H. titanicae* ($p = 0.049$). Both DDM- and ½ YTSS-grown *H. phototrophica* resulted in a slight, but not significant, increase of 4.3 % and 20.2 % respectively.

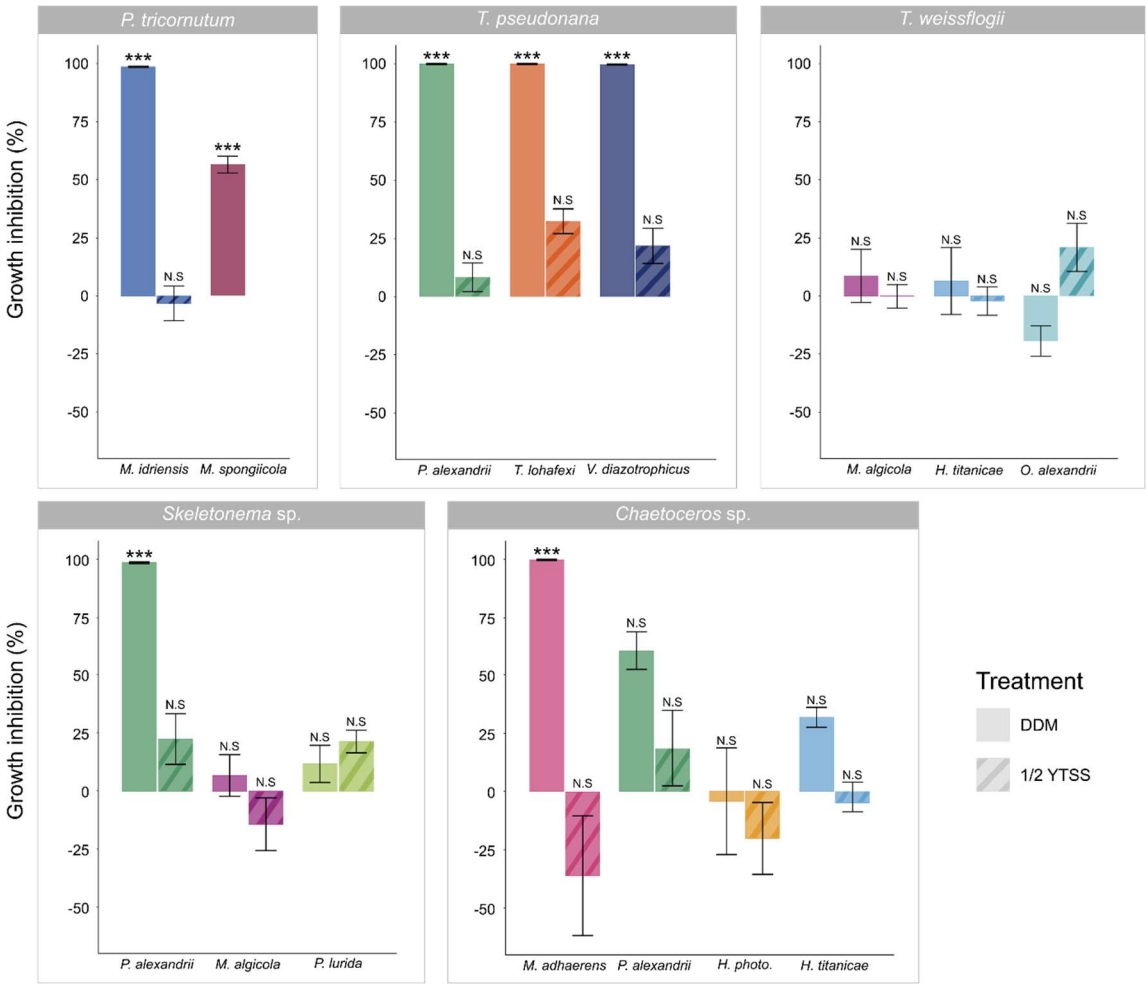

Figure 19. Growth inhibition (%) of diatoms in co-culture with different bacterial antagonists grown on DDM (solid colour bars) or ½ YTSS (hatched bars), compared to an axenic diatom control culture. Error bars represent ± S.E, n = 4.

A secondary experiment was conducted to investigate whether culturing bacterial antagonists on media consisting of both DDM and ½ YTSS at a 1:1 ratio (thus diluting both DDM and ½ YTSS to half strength) would induce antagonism. This trial was set up according to the co-cultivation trials in Section 2.4.5 using *P. alexandrii* with *T. pseudonana* as a host species, as this was the most robust model system investigated in this study. While DDM-grown *P. alexandrii* resulted in a 99.8 % inhibition of *T. pseudonana* growth, *P. alexandrii* grown on the DDM/YTSS mix resulted in a non-significant increase of 2.8 % (Figure 20). Further, while the difference in activity of DDM-grown and DDM/YTSS mix-grown *P. alexandrii* was found to be significant ($p = 0$), there was no significant difference between the ½ YTSS and DDM/YTSS mix ($p > 0.05$), suggesting that pre-exposure to diatom hosts at the current concentration is not sufficient to induce antagonism.

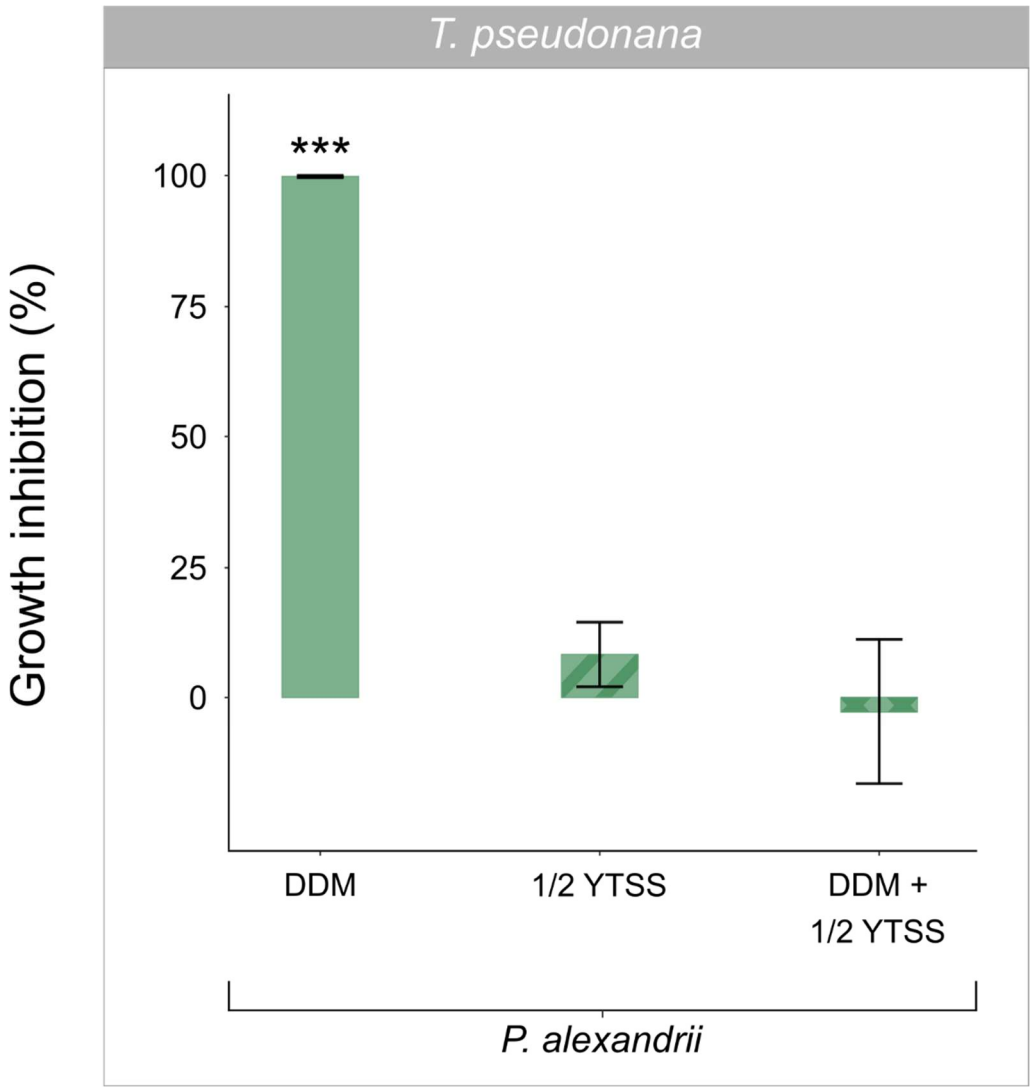

Figure 20. Growth inhibition (%) of *T. pseudonana* in co-culture with *P. alexandrii* grown on DDM (solid colour bar), ½ YTSS (hatched bar), or 1:1 DDM-½ YTSS mixture (crossed bar), compared to an axenic diatom control culture. Error bars represent ± S.E, n = 4.

2.5 Discussion

As primary producers, phytoplankton are a vital component of marine ecosystems, sustaining both higher trophic organisms, such as grazing zooplankton, in addition to smaller heterotrophic organisms, such as bacteria and archaea through the provisioning of DOC (Fry & Wainright, 1991; Buchan et al., 2014). As such, the interactions of phytoplankton with other microbes drive marine carbon cycling, with current estimates suggesting that approximately 50% of all phytoplankton-derived organic matter is catabolised by bacteria (Cole et al., 1988; Ducklow et al., 1993). As one of the most abundant microbial eukaryotic groups in the oceans, diatoms are a globally important component of the phytoplankton (Malviya et al., 2016). Nevertheless, the biotic factors controlling diatom ecology and bloom succession remain poorly understood. In particular, the physiological impacts of antagonistic bacteria on diatoms and the ways in which these interactions are regulated are largely overlooked from an ecological perspective.

Using a library of ecologically relevant diatom-antagonistic bacteria isolated from the WEC (Chapter 1), the present study demonstrates facultative diatom-antagonistic activity of six bacteria spanning four classes. The six bacteria, *P. alexandrii*, *M. idriensis*, *M. spongiicola*, *T. lohafexi*, *V. diazotrophicus* and *M. adhaerens*, displayed significant growth inhibitory effects against various bloom-forming diatom species only when pre-cultured on dead diatom media. Pre-cultivation on ½ YTSS media resulted in no significant growth inhibitory effects against any diatom species, and in the case of *M. adhaerens*, actually resulted in a slight, though not significant, growth promoting effect of 36.2 %.

Initial co-cultivation trials with ½ YTSS-grown *M. adhaerens*, *P. alexandrii* and *R. mucosus* (Sections 2.4.1 and 2.4.2) exhibited only minor reductions in growth rates, however no impacts were observed on overall population densities or photosynthetic efficiency. While this is likely largely due to the facultative nature of these interactions,

these minor reductions in early growth rates should not be dismissed. In a study of the parasitism of a *Chaetoceros* sp. by a common marine thraustochytrid, it was discovered that only older or unhealthy diatom cells were targeted by the parasite, while younger, healthy cells remained unaffected (Laundon et al., 2021). Though direct evidence of parasitism was observed in this study, the resulting *Chaetoceros* populations suffered no negative impacts in overall population densities, and photosynthetic efficiency was improved in diatom-parasite co-cultures. It is therefore believed that the parasitic removal of old and unhealthy diatom cells from culture actually improves overall population health. Interestingly, in initial co-culture experiments (Section 2.4.1), growth rates of diatoms in co-culture with *M. adhaerens*, *P. alexandrii* and *R. mucosus* appeared lower than that of axenic controls at day two but were higher than control culture growth rates by day four. Though this result was only significant with *T. pseudonana*-*M. adhaerens*/*P. alexandrii* co-cultures, a similar pattern was observed throughout the secondary and tertiary trials with *Skeletonema* sp. and *Chaetoceros* sp. Live, sustained microscopic observations of diatom-bacteria interactions could help elucidate whether the observations made in these trials result from the removal of old or unhealthy diatom cells.

Considering the impacts of diatom age and cell health on parasitic activity, it could be reasonably expected that the addition of algal senescence molecule pCA would increase such activity, as has been demonstrated in the *Emiliania huxleyi*-*Phaeobacter gallaeciensis* system (Seyedsayamdost et al., 2011). In this system, the presence of pCA induces a switch from bacterial synergism to antagonism. However, the addition of pCA to *T. pseudonana* co-cultured with *M. adhaerens*, *P. alexandrii* or *R. mucosus* did not increase antagonism of any of the bacteria tested when compared to the previous trials conducted without pCA. It is interesting to note that the addition of pCA initially significantly reduced growth rates of axenic pCA-supplemented control cultures (though final cell densities were unaffected, Section 2.4.2), suggesting that cells may have been in a weakened physiological state in the early stages of the experiment. In spite of this, the addition of pCA failed to increase bacterial antagonism. While pCA production has

been reported in model diatom *P. tricornutum*, it is possible that pCA is not as widely produced by diatoms and therefore less effective at inducing similar opportunistic antagonism as other diatom-derived compounds may be (Rico et al., 2012). Interestingly, Barak-Gavish and colleagues have reported a similar bacterial lifestyle switch in *Sulfitobacter* sp. D7, from commensal to pathogenic, in response to *E. huxleyi* derived DMSP (Barak-Gavish et al., 2023). This report of a pathogenic switch in response to an alternative algal metabolite suggests that bacteria may possess diverse mechanisms by which they are able to sense and respond to the physiological state of algal hosts and subsequently upregulate antagonistic pathways.

In the present study, the lifestyle switch from commensal to antagonistic was observed in seven bacteria (*M. idriensis*, *M. spongiicola*, *P. alexandrii*, *T. lohafexi*, *V. diazotrophicus*, *H. titanicae*, and *M. adhaerens*, Section 2.4.5) when pre-cultured on 'low nutrient' DDM. The induction of antagonism via this method across multiple species suggests conserved facultative pathogenicity across diverse bacterial lineages. Of these seven antagonists, this study is the first to report such a 'lifestyle switch' in six of the strains. In previous studies into the antagonistic mechanism of *Ponticoccus* sp. PD-2, bacterial cultures grown in Marine Broth (MB) were able to inhibit the growth of algal host *P. donghaiense* by up to 84.8 % (Chi et al., 2017). However, while MB-cultured PD-2 also exhibited antagonism against a prymnesiophyte and a dinoflagellate, diatom-antagonism was not tested. Further, many studies of the interactions of *T. weissflogii* and *M. adhaerens* report commensalism or synergism, with *M. adhaerens* promoting growth and transparent exopolymer particle (TEP) production of *T. weissflogii* in co-cultures (Gärdes et al., 2012; Sonnenschein et al., 2012). However, a more recent study of a *Coscinodiscus radiatus*-*M. adhaerens* system reported that MB-grown *M. adhaerens* was capable of supressing the growth of *C. radiatus* (Deng et al., 2022). Interestingly, however, *C. radiatus* growth in co-cultures eventually (after 13 days) was able to fully recover, potentially indicating an induction of diatom defence mechanisms.

While the capability of bacteria to sense and respond to differential algal physiological states is certainly not a novel idea, identifying a conserved lifestyle switch amongst multiple bacterial lineages is a key step towards understanding the distribution of bacterial antagonism at an ecosystem scale. While bacterial antagonism was induced through pre-cultivation on dead diatom matter, preliminary experiments conducted in this study demonstrated that extended pre-exposure to live diatoms did not appear to induce antagonistic activity. Similarly, cultivation on a ½ YTSS-DDM mix did not induce antagonism of *P. alexandrii* against *T. pseudonana* (Section 2.4.5). While it remains difficult to draw conclusions from these preliminary trials, it could be speculated that the induction of bacterial antagonism is the result of nutrient limitation as opposed to exposure to a diatom metabolite. Certainly, significant differences in the synthesis of antimicrobial compounds in response to different carbon, nitrogen and phosphate sources have been widely demonstrated amongst many bioactive *Actinobacteria* species (for a comprehensive review, refer to van der Heul et al., 2018). Perhaps most interestingly, suppression of antimicrobial compound synthesis in the presence of high-energy carbon sources, such as glucose, has been observed in various species of *Streptomyces* (Demain and Inamine, 1970; Bhatnagar et al., 1988). In these instances, it is suggested that high-energy carbon sources are preferentially catabolised by bacteria, resulting in little need for the production of antimicrobial compounds that would aid in resource 'protection'. Hence, cultivation of bacteria with live, healthy diatom cells could potentially provide sufficient diatom-derived nutrients to survive without the need for antagonism. Similarly, the addition of ½ YTSS to DDM agar, particularly at a high 1:1 ratio, could be explained in a similar manner. As nutrient availability in marine environments tends to be not only sparse, but also highly patchy, nutrient limitation is an important factor regulating interkingdom competition throughout marine ecosystems (Thingstad et al., 1993; Grossart, 1999; Grover, 2000; Diner et al., 2016). Subsequently, microbes have evolved a diverse suite of secondary metabolites, such as antimicrobial compounds, that provide a fitness advantage over competing microbes and allow producing bacteria to monopolise limiting resources. Nevertheless, synthesis of such

compounds is often energetically costly, and therefore tightly regulated, selectively expressed only under certain environmental conditions. Could facultative diatom-antagonism therefore serve as an adaptive strategy for select bacteria to monopolise limiting nutrients in unfavourable conditions? Such strategies could prove particularly prominent in environments where nutrient limitation is standard, such as oligotrophic open oceans regions.

The remaining four bacteria (*M. algicola*, *P. lurida*, *O. alexandrii* and *H. phototrophica*) tested in this study did not exhibit an antagonistic switch under cultivation on DDM. While there are a myriad of possible explanations for this, such as requiring the physical environment of the soft-agar assay to facilitate activity or insufficient bacteria inoculated into co-culture trials to induce activity, the lack of activity under DDM-cultivation could reasonably indicate the presence of an alternative regulatory pathway altogether. The discovery of a DDM-induced antagonistic switch in the present study that differs from the two well-characterised algal-bacteria switches described in the literature highlights the diversity of regulatory pathways involved in mediating algal-bacterial interactions. However, as antagonistic bacteria can also display density dependent effects (e.g., as demonstrated with Ponticoccus PD-2, Chi et al., 2017), it could also be speculated that further optimisation is required to detect the antagonistic activity of these bacteria.

Although the antagonistic mechanisms employed by the library of bacterial isolates from this study remain unclear, the discovery of a conserved ‘antagonistic switch’ in seven diverse bacteria hints at a hidden diversity of opportunistic pathogens in marine ecosystems. The complexity of diatom-bacteria interactions in nature is often poorly represented in controlled laboratory systems, and as such, many crucial phases of these interactions may be going undetected. Characterising the spectrum of interactions that may exist within a single diatom-bacteria system under varying environmental conditions, and elucidating the factors underpinning the regulation of bacterial lifestyle switches is paramount to a better understand how such interactions may play out in

nature and for understanding the contribution of bacteria to the bloom-and-bust lifestyle of natural diatom populations.

Chapter 3:

Prevalence and seasonal trends of diatom-antagonistic bacteria in the Western English Channel

3.1 Introduction

Diatom-bacteria interactions, whether synergistic or antagonistic in nature, are widely understood to be significant drivers of diatom success in the global oceans. Laboratory-based studies have been instrumental in exploring the physiological impacts bacteria impose on their diatom hosts, from supporting diatom growth via the provisioning of essential nutrients, such as vitamin B12 (Haines & Guillard, 1974; Croft et al., 2005), to growth suppression or even cell lysis (Mitsutani et al., 2001; Kang et al., 2005; Paul and Pohnert, 2001; van Tol et al., 2017). These interactions can confer fitness advantages or disadvantages for diatoms at the population level, with subsequent ramifications for wider microbial communities and ecosystem functioning. For example, a study conducted with cosmopolitan bloom-forming diatom *Pseudo-nitzschia multiseries* and an associated *Sulfitobacter* species revealed a tight coupling of the two partners co-ordinated by the sequential release of diatom-derived tryptophan, and bacteria-derived Indole-3-Acetic Acid (IAA, Amin et al., 2015). Transcriptome evidence from *P. multiseries*-*Sulfitobacter* co-cultures suggest that *Sulfitobacter* converts diatom-derived tryptophan to IAA, which promotes diatom cell division of this harmful alga. In turn, IAA is converted back to tryptophan by *P. multiseries*, resulting in a positive feedback loop, likely maintaining the relationship. Metabolic and metatranscriptome analysis of natural seawater samples revealed IAA, which previously had no known function in marine ecosystems, to be widely synthesised in coastal waters by *Sulfitobacter* and related bacteria. Amin and colleagues postulate that given the significant distribution of IAA production in coastal oceans, this could be a potential widespread mechanism for the cultivation and maintenance of a mutually beneficial relationship between an abundant marine

Roseobacter and a ubiquitous diatom species. The combination of laboratory and field-based approaches in studies such as these not only provides essential insight into the mechanisms underpinning interkingdom interactions, but also provides important ecological context, which allows for a more in-depth understanding of the potential significance of such in ecosystem functioning.

Investigating the ecological role and significance of such interactions in the natural environment is no easy feat, largely due to the complexity and diversity of marine microbial communities, as well as the microscale nature of these interactions. Nevertheless, advances in environmental sampling techniques, such as metabarcode sequencing, metatranscriptome and metabolic analyses in recent decades have allowed microbial ecologists to explore microbial community dynamics at a much greater depth. For example, techniques such as short-read amplicon sequencing provide microbial ecologists with a high throughput method with which to explore the diversity and composition of microbial communities at the ecosystem scale. Increased accessibility to such technologies has improved our understanding of microbial communities and their seasonal or even annual patterns. A prime example is the exploration of both the prokaryotic and eukaryotic microbial communities within the Western English Channel (WEC). Phytoplankton biodiversity data has been collected on a weekly basis by the Western Channel Observatory (WCO) since 1992, providing a wealth of information not only of community composition, but also seasonal trends (Widdicombe et al., 2010). Microscopic analyses of these samples demonstrates that the WEC experiences regular diatom spring blooms (typically dominated by species belonging to *Chaetoceros*, *Thalassiosira* and *Skeletonema*) that are characteristic of many highly productive coastal regions (Widdicombe et al., 2010). While the diatom community within the WEC did display some inter-annual

variability, primarily in the timings that blooms would occur, the presence of the top diatom genera remained largely consistent. However, a recent study using a seven-year eukaryotic metabarcoding dataset collected at the SOMLIT-Astan station in the WEC highlights the importance of often over-looked nano-diatoms in these environments (Arsenieff et al., 2020). Analysis of the dataset demonstrated that nano-diatoms, such as those belonging to the genera *Minidiscus* and *Thalassiosira* species exhibit regular small winter blooms. Nano-diatoms are often overlooked in microscopic analyses of phytoplankton communities due to issues in identification due to their small size (typically 2 – 5 µm). Interestingly, these trends of winter nano-diatom blooms highlighted through metabarcode analysis by Arsenieff and colleagues is consistent with findings from similar metabarcode analyses that also demonstrate the importance of overlooked nano-diatoms in the global oceans (Leblanc et al., 2018), further highlighting the power of such molecular sampling techniques.

High throughput sequencing techniques have also been instrumental in the exploration of prokaryotic communities. Bacteria, archaea, and viruses, though a fundamental component of marine planktonic communities, are difficult to study in depth utilising traditional methods such as cell counting, as, unlike eukaryotic phytoplankton, prokaryotic species are typically indistinguishable using microscopy or traditional cell counting techniques such as flow cytometry or cell staining. Nevertheless, bacterial abundance data has been collected via flow cytometry on a weekly basis in the WEC since 2007 (https://www.westernchannelobservatory.org.uk/). As flow cytometry can only distinguish between high nucleic acid (HNA) and low nucleic acid (LNA) cells, in-depth analysis of the diversity and seasonality of the prokaryotic community relies primarily on molecular techniques, such as pyrosequencing/metabarcoding.

Such techniques have been instrumental in revealing that, like the phytoplankton community in the WEC, bacterial communities also exhibit seasonal patterns that are stable inter-annually. These communities, typically dominated by bacteria belonging to just four groups/phyla (*SAR11*, *Rhodobacterales*, *Flavobacterales* and *Pseudomonadales*, Gilbert et al., 2009), are also shown to be tightly coupled to phytoplankton community structure, with *Rhodobacterales* and *Flavobacterales* exhibiting robust increases in abundance following seasonal diatom blooms (Taylor et al., 2014), hence, understanding the composition and seasonal dynamics of microbial communities through high-throughput sequencing not only provides a picture of microbial diversity within marine environments but can also help build a picture of functional diversity. Despite extensive monitoring of the WEC over several decades uncovering the coupling of bacterial community composition with seasonal trends of phytoplankton, particularly diatoms, exploration of the diatom pathobiome of this region is still lacking.

In addition to enabling in-depth analysis of microbial communities on a local scale, improvements in sequencing technologies, and subsequently sequencing efforts, have facilitated the development of invaluable global-scale datasets, advancing our knowledge in this field globally. Perhaps the most prominent example of this is the *Tara* Oceans project, a global sampling effort aiming to catalog the microbial diversity of the world's oceans through metagenomic Illumina sequencing (Sunagawa et al., 2015). The data collected during this project has been compiled into an invaluable database, the Ocean Barcode Atlas, against which researchers can query species or gene sequences of interest to aid in answering fundamental questions about the global distribution of specific taxa or even functional genes (Vernette et al., 2021). Databases such as these

provide a reliable and efficient tool by which researchers can add important ecological context, such as geographic distribution, to model laboratory systems. For example, through an investigation of interactions between globally distributed diatom *Asterionellopsis glacialis* and its natural bacterial consortia it was discovered that diatom-derived azelaic acid both inhibited the growth of *Alteromonas macleodii* (a potential diatom pathogen, see Chapter 1 of this work and Wang et al., 2016), but also stimulated the growth of potential symbiotic *Roseobacter* bacteria (Shibl et al., 2020). A search of the *Tara* Oceans database was subsequently conducted to assess the geographic distribution and abundance of genes involved in the bacterial response to this diatom metabolite throughout the global oceans. This revealed that these genes, while limited to a small number of bacterial taxa, are ubiquitous in the oceans, thus potentially representing an important metabolic pathway regulating interactions between a globally important diatom and its microbiome. Studies such as these highlight the power of high throughput metagenomic sequencing techniques, and the wealth of information that can be learned from these studies about the diversity and seasonality of microbial communities, and the distribution of functional taxa and genes of interest.

Despite the current literature pertaining to antagonistic diatom-bacteria interactions highlighting the potential significance of such bacteria in shaping diatom communities, our understanding of the role of diatom-antagonistic bacteria in ecosystem functioning remains limited by a lack of investigations of these interactions in nature. The previous two chapters of this work described the isolation and confirmation of seven naturally occurring diatom-antagonistic bacteria in a highly productive coastal ecosystem (the WEC). Given that six of the seven confirmed isolates were revealed to be novel diatom antagonists, the

distribution and co-occurrences of these bacteria with potential diatom hosts is yet to be explored. Here, the application of environmental sequencing techniques, such as metabarcode analysis, will take these laboratory-verified diatom-bacteria systems ‘back to sea’ to work towards a clearer picture of the functional diversity of diatom-antagonists both in the WEC and globally.

3.2 Aims

The final chapter of this work aims employ metabarcoding techniques and publicly available databases to build a comprehensive picture of the abundance, distribution, and co-occurrence of a library of environmentally derived diatom-antagonistic bacteria with their hosts on both a local and global scale.

1. Amplicon sequencing of the microbial communities at Station L4 is conducted over an annual cycle to elucidate trends in prokaryotic and eukaryotic communities around peak diatom bloom times, e.g., characteristic spring blooms, in addition to smaller winter blooms where peak antagonistic activity was detected in previous chapters.

2. The *Tara* Ocean Barcode Atlas will be employed to explore the distribution of WEC diatom-antagonists and assess their co-occurrence with diatom hosts globally.

3.3 Materials and methods

3.3.1 Amplicon sequencing sample collection and processing

For the assessment of the bulk eukaryotic and prokaryotic communities in the Western English Channel, seawater samples were collected from Station L4 by *R.V MBA Sepia* for 16S and 18S amplicon sequencing. Samples were collected bi-monthly (where possible, with the exception of March and April 2021, where samples were collected weekly) for 13 months from a depth of 5 m. For each sampling point, four 1 L seawater replicates were filtered onto a 0.22 µm Whatman filter paper membrane (Sigma-Aldrich, UK), which was immediately stored in DNA/RNA shield (Zymo Research, USA) at –80 °C until DNA extraction.

3.3.2 DNA extraction and metabarcoding

Samples were thawed on ice and DNA was extracted from the filters using a ZymoBIOMICS DNA Miniprep kit (Zymo Research, USA). Thawed filters were cut into smaller sections and extractions were carried out according to the manufacturer's instructions, with the addition of a mechanical bead-beating step. For eukaryotic community analysis, 18S rRNA gene amplification of the V9 region was conducted via PCR using the primers 1391F (GTACACACCGCCCGTC) and EukB (TGATCCTTCTGCAGGTTCACCTAC) (Lane, 1991; Medlin et al., 1988), an initial denaturation step at 95 °C for three minutes, followed by 35 cycles of i) denaturation at 95 °C for 45 seconds, ii) annealing at 57 °C for one minutes, and iii) extension at 72 °C for one minute and 30 seconds. Final extension was carried out at 72 °C for ten minutes. For prokaryotic community analysis, 16S rRNA gene amplification of the V4 region was conducted via PCR using the primers 515F (GTGCCAGCMGCCGCGGTAA) (Caporaso et al., 2011; Parada et al., 2016) and 806R (GGACTACHVGGGTWTCTAAT) (Apprill et al., 2015). PCR cycle conditions were as follows: an initial denaturation step at 94 °C for two minutes, followed by 35 cycles of i) denaturation at 94 °C for 45 seconds, ii) annealing at

50 °C for one minute, and iii) extension at 72 °C for one minute and 30 seconds. PCR products were then analysed via gel electrophoresis by running on a 1 % agarose gel at 110 volts for 60 minutes to check for amplification. Final DNA concentrations were quantified using a NanoDrop spectrophotometer (ThermoFisher). PCR products were subsequently sequenced via Illumina MiSeq sequencing, performed by NUOMICS, Northumbria, UK.

3.3.3 Data processing of amplicon sequence data

Amplicon sequence data was processed in R Studio (R Core Team, 2019) following the DADA2 pipeline (Callahan et al., 2016). 16S and 18S samples were processed independently of each other following the same pipeline: primers and low-quality sequences were removed by filtering and trimming demultiplexed reads, before merging paired ends to produce full denoised sequences. Chimeric sequences were subsequently removed prior to taxonomic assignment of amplicon sequence variants (ASVs) using the PR^2 database (release 4.140, Guillou et al., 2013) for 18S sequences, and the SILVA database (Quast et al., 2013) for 16S sequences. Chloroplast and mitochondria sequences were removed from both data sets, and non-eukaryote sequences were removed from the 18S data set. Quality profiles for both the forward and reverse 16S reads are displayed in Appendix Figures 14 and 15.

The phyloseq package (McMurdie & Holmes, 2013) was then used to create a phyloseq object by combining ASV tables, taxonomic assignments and environmental metadata. Read depths of each sample were inspected, and sequences were rarefied to a depth of 10,443 reads per sample for 16S sequences, and 10,716 for 18S sequences. To avoid losing diversity of samples

with higher read depths, four samples with comparatively low read depths (< 10,000 reads) were removed from the 16S dataset (discarded samples are listed in Appendix Table 3). As a result, the total number of ASVs increased 3,488 to 3785.

3.3.4 Investigating the occurrence of bacterial antagonists and their diatom hosts within the Western English Channel

To assess the abundance and seasonal trends of bacterial antagonists and their diatom hosts in the Western English Channel, separate 16S and 18S BLAST databases were created in Geneious Prime (Geneious Prime 2023.0.1, https://www.geneious.com), against which 16S or 18S rRNA sequences could be queried.

For bacterial isolates with confirmed antagonistic activity (*Metabacillus idriensis*, *Maribacter spongiicola*, *Ponticoccus alexandrii*, *Thalassospira lohafexi*, *Vibrio diazotrophicus*, *Marinobacter adhaerens* and *Halomonas titanicae*, Chapter 2), full-length 16S rRNA gene sequences were queried against the 16S ASV database, and ASVs with a percentage pairwise identity above 97 % (query cover 100 %) were collated. Taxonomic assignment of each ASV was subsequently validated by constructing Maximum Likelihood (ML) trees (for details on phylogenetic tree construction see section 3.3.6).

In addition, amplicon sequence analysis of diatom diversity and abundance was verified by analysis of total phytoplankton counts provided by Claire Widdicombe, Plymouth Marine Laboratory. For total phytoplankton counts, seawater samples were collected bi-weekly (where possible) by Plymouth Marine Laboratory from Station L4 from a depth of 10 m. Samples were fixed in 2 % Lugol's iodine solution for enumeration by light microscopy according to the Utermohl counting

technique (Utermohl, 1958). Organisms were classified into taxonomic groups (i.e., diatoms, coccolithophores, dinoflagellates, ciliates, etc.) and identified to species level where possible.

3.3.5 Assessing the global distribution and co-occurrence of bacterial antagonists with diatom host species using the *Tara* Oceans database

The global distribution of bacterial isolates with confirmed antagonistic activity, including *P. alexandrii*, *T. lohafexi*, *V. diazotrophicus*, *M. idriensis*, *M. spongiicola*, *M. adhaerens*, and *H. titanicae*, was assessed using the Ocean Barcode Atlas portal of the *Tara* Oceans database (Vernette et al., 2021). Full-length 16S rRNA gene sequences of query isolates were searched against the 16S/18S miTAG metabarcode database using the 'vsearch' function. For miTAG hits with a percentage pairwise identity of above 97 % and query cover of 97 % and above, taxonomic assignment was verified via the construction of ML trees (Section 3.3.6). The distribution of miTAG hits which were demonstrated to be phylogenetically similar to query sequences was subsequently assessed using sample locations listed in the associated sample metadata. Hits from all size fractions (0.22 – 3 µm) and sampling depths (surface [SRF], deep chlorophyll maximum [DCM] and mesopelagic [MES]) were pooled to assess geographic distribution.

3.3.6 Verification of taxonomic assignment of L4 ASV and *Tara* Oceans miTAG hits via construction of Maximum Likelihood phylogenetic trees

Maximum Likelihood trees were constructed in Geneious Prime (Geneious Prime 2023.0.1, https://www.geneious.com) to verify the taxonomic assignment of ASV hits

obtained through local BLAST searches of the bacterial amplicon sequence dataset (Section 3.3.4), and miTAG hits obtained through BLAST searches of the *Tara* Ocean Barcode Atlas (Section 3.3.5).

For taxonomic validation of ASV hits from the L4 amplicon dataset ML trees were constructed using the full-length 16S rRNA bacterial query sequence, the V4 region of each nearest ASV hit, and full-length 16S rRNA sequences of type strains of closely related species and genera obtained from NCBI and the Ribosomal Database Project (Cole et al., 2014; Sayers et al., 2022). Sequences were aligned using a Multiple Alignment Fast Fourier Transform (MAFFT) tool (Katoh et al., 2002), and alignments were then manually trimmed to standardise sequence lengths, before using the General-Time-Reversable (GTR) substitution model with 1000 bootstraps to construct Maximum Likelihood trees.

For miTAG hit validation ML trees were constructed using only full-length 16S rRNA sequences of bacterial query isolates, miTAG hits and closely related species and genera obtained from NCBI and the Ribosomal Database Project (Cole et al., 2014; Sayers et al., 2022). Sequences were aligned using a MAFFT alignment tool, trimmed to standardise sequence lengths and a GTR substitution model with 1000 bootstraps was used to construct ML trees.

3.4 Results

3.4.1 Analysis of seasonal trends in eukaryotic microbial communities at Station L4 over an annual cycle

Metabarcode analysis of the microbial eukaryotic community at Station L4 was conducted over a 13-month period from March 2021 – March 2022. Diatoms (Bacillariophyta) constituted a numerically important component of the phytoplankton community year-round (Figure 1). Relative abundance of diatoms

compared to other major phytoplankton groups peaked, as expected, in spring (March – April 2021), and again in the winter months (December 2021 – January 2022).

The diversity and seasonal trends of diatom taxa was further investigated (where possible) at genus level throughout the sampling period (Figure 2). Early spring (March 2021) samples were dominated primarily by species belonging to *Thalassiosira*, and to a lesser extent *Minidiscus*. This was followed by an increase in the relative abundance of *Chaetoceros* throughout late March and early April. Late April was characterized by an intense yet brief peak in *Lauderia* (comprised of a single species*, Lauderia annulata*). Early summer months (June – July 2021) were heavily dominated by *Leptocylindrus*, followed by a peak in the relative abundance of *Pseudo-nitzschia* species, which is characteristic of the diatom community at Station L4 (Widdicombe et al., 2010). Finally, the late autumn and winter diatom community was heavily dominated by diatoms belonging to the polar-centric Mediophyceae (class). The *Thalassiosira* population also begins to increase in number during this period and remains a relatively abundant component of the diatom community throughout the autumn and early winter months (October 2021 – January 2022). Additionally, diatoms belonging to the *Coscinodiscus* genus also began to increase in relative abundance towards the end of the winter period (January 2022 – March 2022), peaking in March, where they constituted approximately 20 % of the total diatom relative abundance. It is important to note that the difference between the relative abundance and biomass of *Coscinodiscus* sp. observed is likely due to the large cell size of *Coscinodiscus* species. Interestingly, diatoms belonging to the genus *Minidiscus* also comprised an important part of the diatom community throughout winter months (late March 2021 and November 2021 – March 2022), findings which were concurrent with

analysis conducted by Arsenieff and colleagues in the WEC (Arsenieff et al., 2020).

The abundance and seasonal trends In diversity (Figure 3) of WEC diatoms throughout an annual cycle was further scrutinized via microscopic counting of fixed seawater samples (Figure 3A, data provided by Claire Widdicombe, Plymouth Marine Laboratory) and analysis of metabarcoding diversity data (Figure 3B). Microscopic cell counts showed characteristic peaks in diatom biomass in mid-late spring (April – early June 2021), with peaks in *Chaetoceros* and *Thalassiosira* biomass also being observed, concurrent with both previous literature (Widdicombe et al., 2010) and the metabarcoding data presented here. A second, more intense diatom bloom was observed in late May 2021 (Figure 3A), which was comprised of an increased diversity of diatom genera (Figure 3B) compared to the previous April bloom. The smaller summer bloom that was observed in August coincided with increased relative abundance of *Pseudo-nitzschia* (Figure 2), a finding that was also concurrent with prior literature on the region (Widdicombe et al., 2010). Finally, a characteristic much smaller winter bloom was observed in January 2022 that was comprised almost entirely of diatoms belonging to the genus *Coscinodiscus* (85 %), as seen in previous years.

Alpha diversity (Shannon's *H* index) of the diatom community at Station L4 was assessed using the amplicon sequence data, revealing that seasonal variations in diversity were positively correlated with diatom biomass, i.e., community diversity increases with increasing biomass, and vice versa. Interestingly, however, the winter diatom community, while low in biomass (Figure 3A) remains high in diversity.

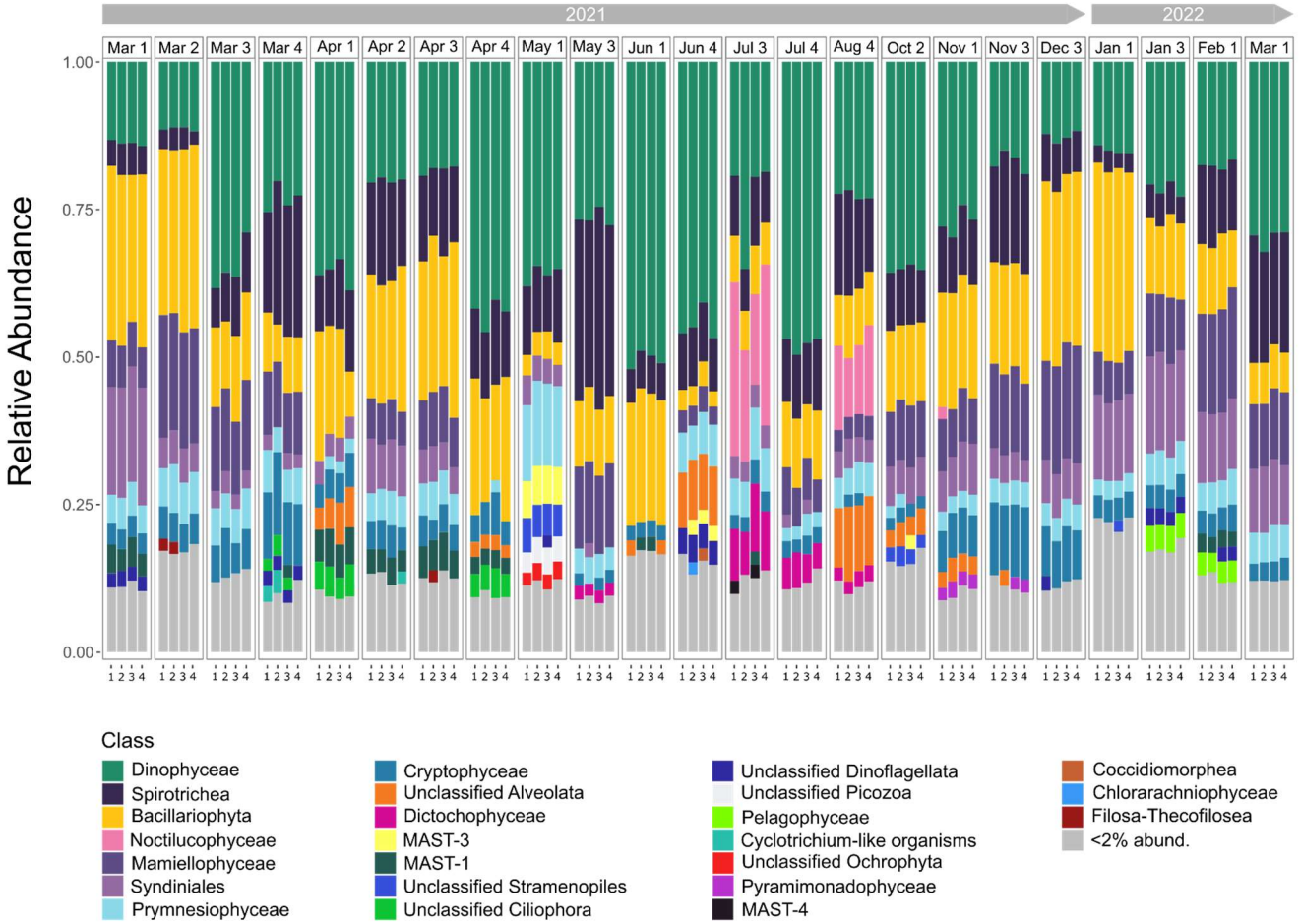

Figure 1. Relative abundance of amplicon sequencing variants (ASVs) belonging to major phytoplankton classes over an annual cycle (March 2021 – March 2022), highlighting the seasonal persistence and abundance of diatoms (Bacillariophyta, yellow). Bars represent the four replicates processed at each sampling point. Taxa that constituted less than 2 % of the total ASVs are grouped into the <2% abundance category.

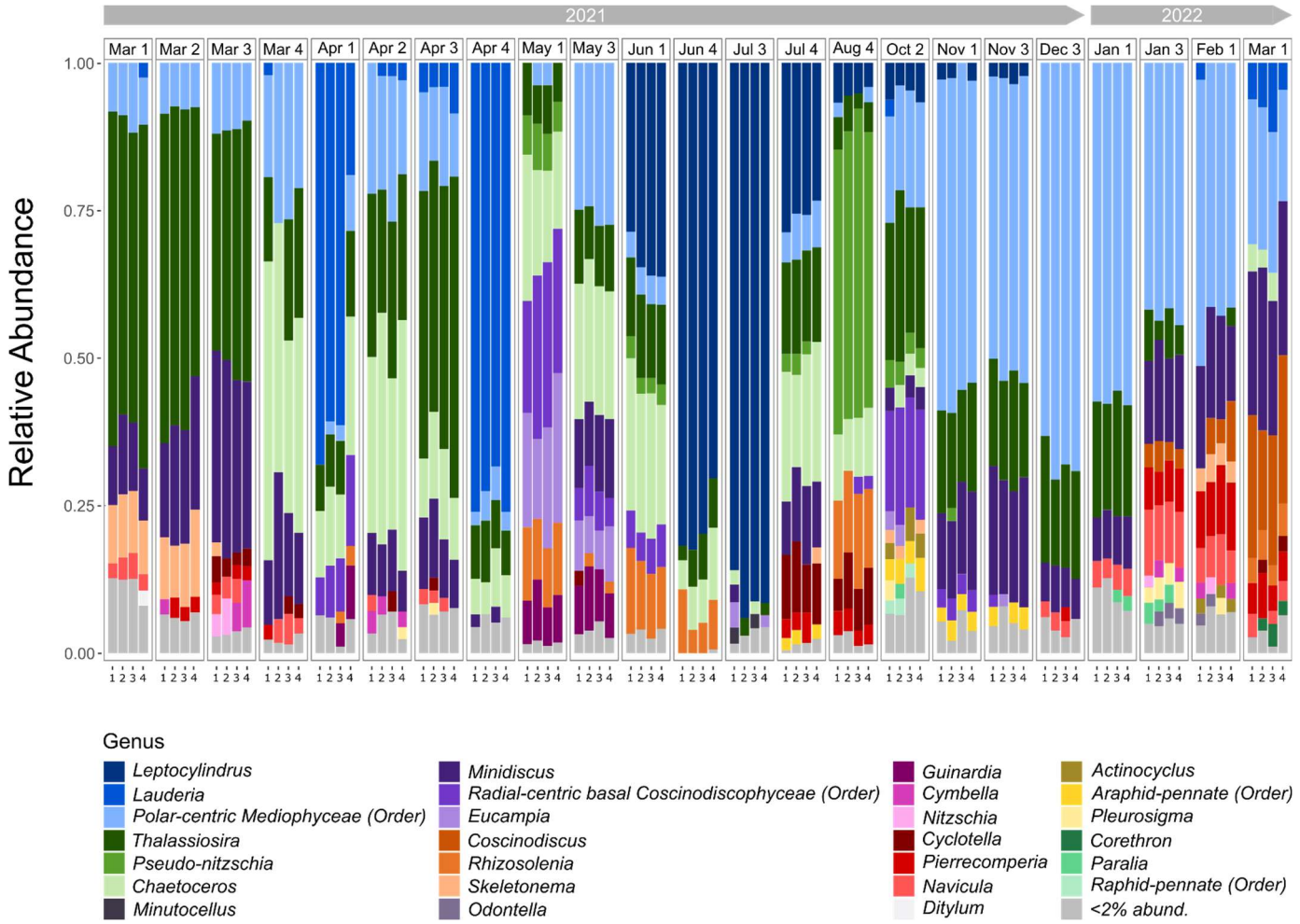

Figure 2. Relative abundance of amplicon sequencing variants (ASVs) belonging to major diatom genera over an annual cycle (March 2021 – March 2022). Each sampling point contains four replicates. Taxa that constituted less than 2 % of the total ASVs are grouped into the <2% abundance category.

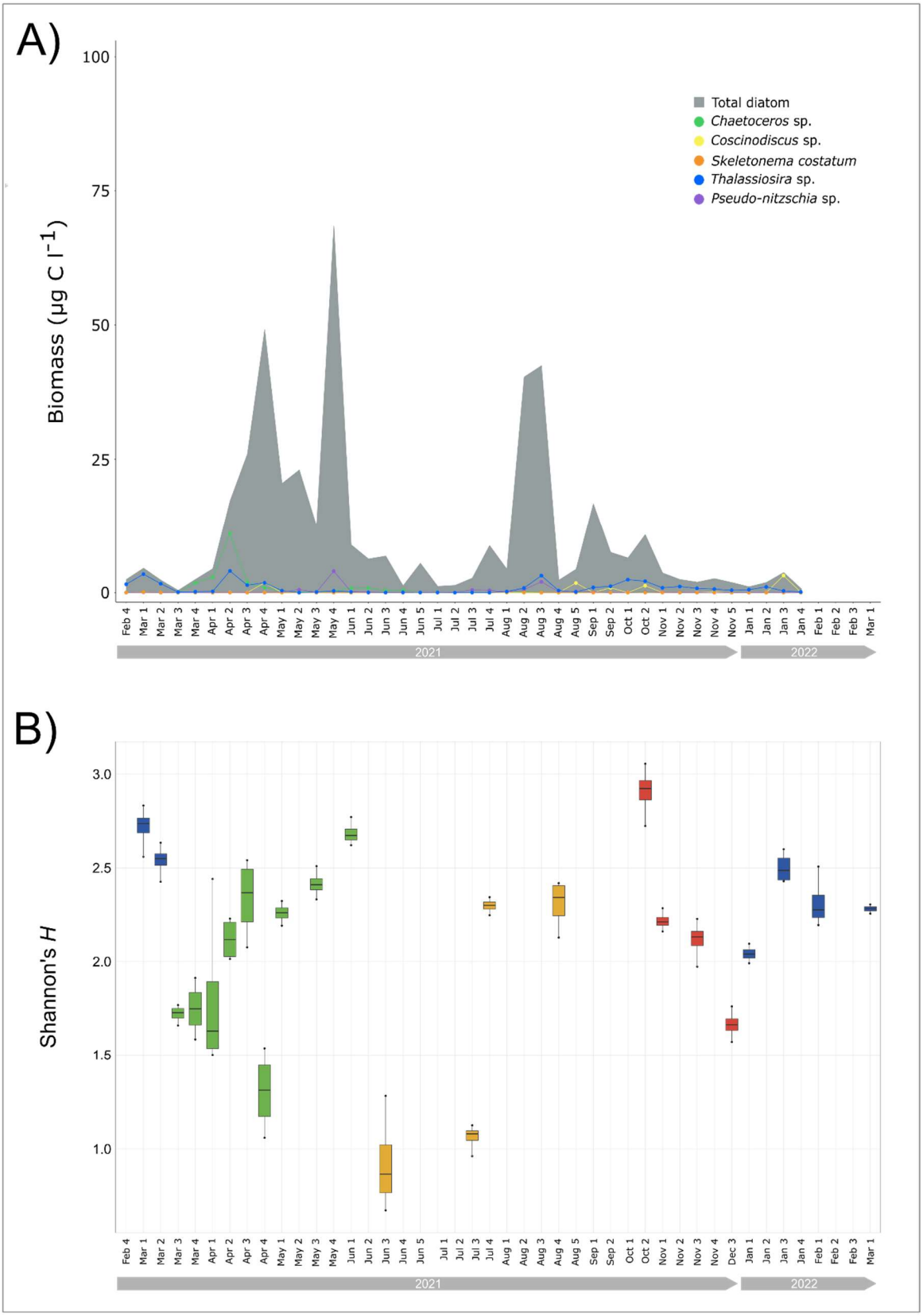

Figure 3. A) Biomass (µg C l^{-1}) of total diatoms, as well as five diatom genera, *Chaetoceros*, *Thalassiosira*, *Skeletonema* (comprised of just *Skeletonema costatum* in this dataset), *Pseudo-nitzschia* and *Coscinodiscus* between February 2021 and January 2022. Biomass was calculated by converting biovolume data (Olenina et al., 2006) to carbon (µg C l^{-1}) following the Menden-Deuer and Lessard formula (Menden-Deuer & Lessard, 2000). **B)** Alpha diversity (Shannon's H index) of diatom community (amplicon sequence dataset). Bars represent the standard error of the four replicates at each sampling point.

3.4.2 Analysis of seasonal trends in prokaryotic community at Station L4 over an annual cycle

The relative abundance of the prokaryotic community at Station L4 was also monitored over a 13-month period (March 2021 – March 2022) via metabarcode sequencing. Analysis of the prokaryotic amplicon sequence data revealed that the bacterial community was consistently largely dominated by four orders, *Flavobacteriales*, *SAR11* clade, *Rhodobacterales* and *Pseudomonadales* (Figure 4). These four groups remained the most abundant taxa throughout the entire annual cycle, with the exception of the May 2021 sampling points, where the *SAR11* clade constituted less than 2 % of the total relative abundance of the prokaryotic community. The decrease in *SAR11* clade abundance during the early May sampling point was concurrent with increases in the relative abundance of the *Flavobacteriales* and the *Rhodobacterales*. Bacteria belonging to the *Pseudomonadales* were also seasonally persistent throughout the entire sampling period. However, unlike the *Flavobacteriales*, *Rhodobacterales* and *SAR11*, the relative abundance of *Pseudomonadales* remained more stable across the annual cycle, often constituting approximately 20 % of total prokaryotic reads (with the exception of the first sampling point in May 2021, where relative abundance decreased).

Rhodospiralles, the order containing confirmed diatom antagonist *T. lohafexi*, made up a much smaller percentage of the total bacterial community throughout the annual cycle, though was routinely observed throughout the winter months (October 2021 – March 2022). Interestingly, however, the largest *Rhodospiralles* peak was observed in July. *Bacillales*, the order to which confirmed antagonist *M. idriensis* belongs, were also typically low in abundance only exceeding the 2 % relative abundance threshold in August 2021. *Vibrionales* and

Alteromonadales (two orders also containing confirmed diatom antagonists *V. diazotrophicus,* the present study, and *Alteromonas* sp. PML-EC-1, Wang et al., 2016) remained below the 2 % relative abundance threshold throughout the entire sampling period.

Total bacterial abundance (cell counts) was also monitored via flow cytometry (Figure 5A). Bacterial abundance peaked in late June 2021 at 3.8 x 10^6 cells per ml, during which, interestingly, bacterial diversity (Shannon's *H* index) was relatively low in comparison to early spring and summer samples (Figure 5B). This peak in abundance and concurrent decrease in diversity coincided with an increase in the relative abundance of *SAR11* bacteria (Figure 4). Despite bacterial abundance remaining low throughout winter and early spring, the diversity of the bacterial community was typically higher in these sampling points than when bacterial abundance was at its highest, a result which mirrors previous literature on the prokaryotic community of the WEC (Gilbert et al., 2012).

Comparison of the bacterial diversity and abundance with diatom biomass in the WEC revealed that the large increase in the relative abundance of both *Flavobacteriales* and *Rhodobacterales* coincided with the termination of the first diatom spring bloom (heavily dominated by *L.*158aters158n*a*) of the season (late April 2021, Figure 6A). This finding is in line with previous reports of both local and global sites, which highlight increases in the two groups following diatom bloom decline (Teeling et al., 2012; Taylor et al., 2014; Klindworth et al., 2014). Interestingly, however, maximum bacterial numbers were not observed until after the second diatom bloom (late May 2021). The bacterial community during peak abundance was again comprised largely of *Flavobacteriales* and *Rhodobacterales*, in addition to *Pseudomonadales*.

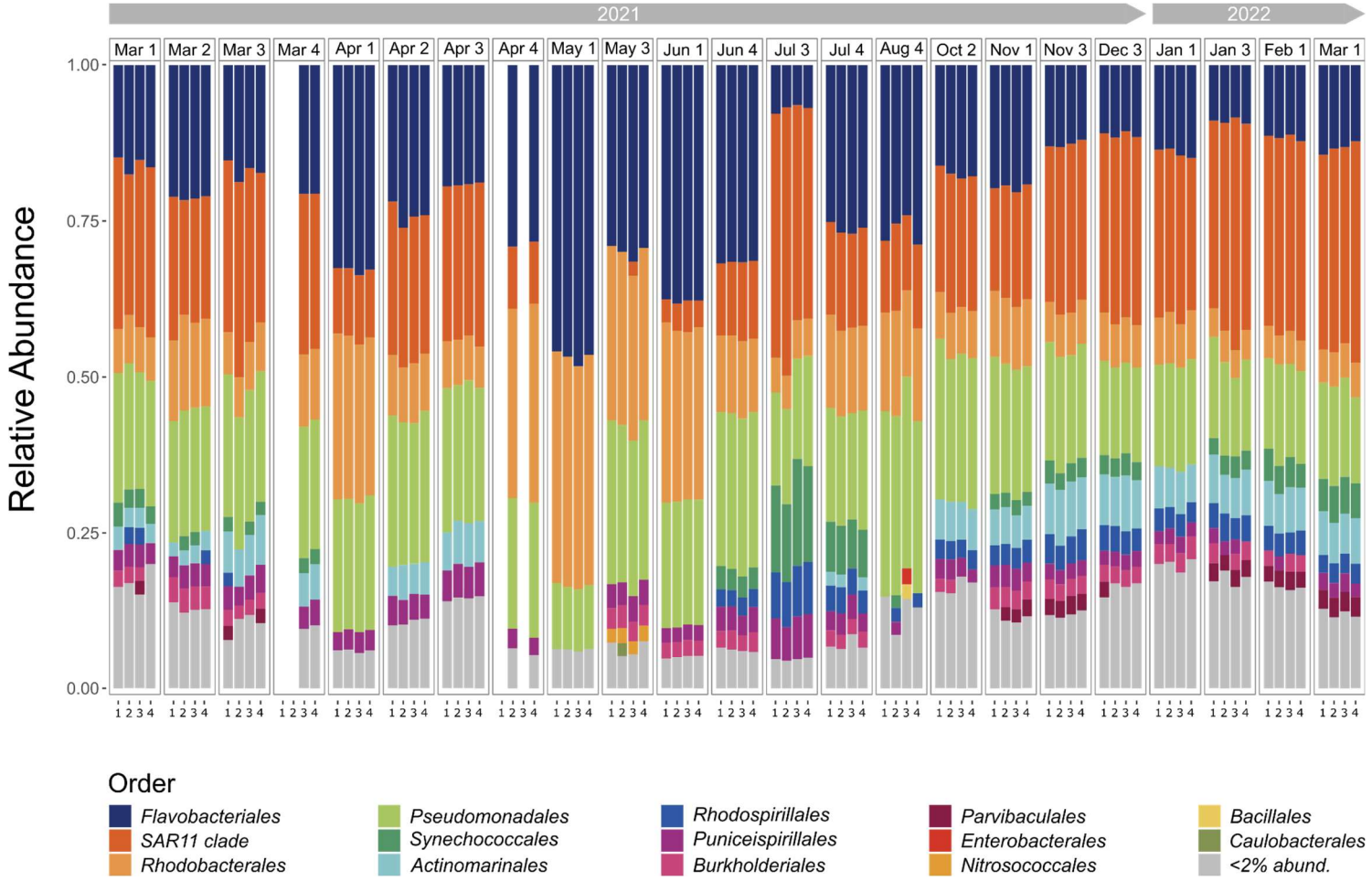

Figure 4. Relative abundance of amplicon sequencing variants (ASVs) belonging to major bacterial orders over an annual cycle (March 2021 – March 2022). Each sampling point contains four replicates. Taxa that constituted less than 2 % of the total ASVs are grouped into the <2% abundance category. Samples (replicates) with read depths < 10,000 were removed to avoid losing diversity of samples with higher read depths in the rarefication step of the sequencing pipeline.

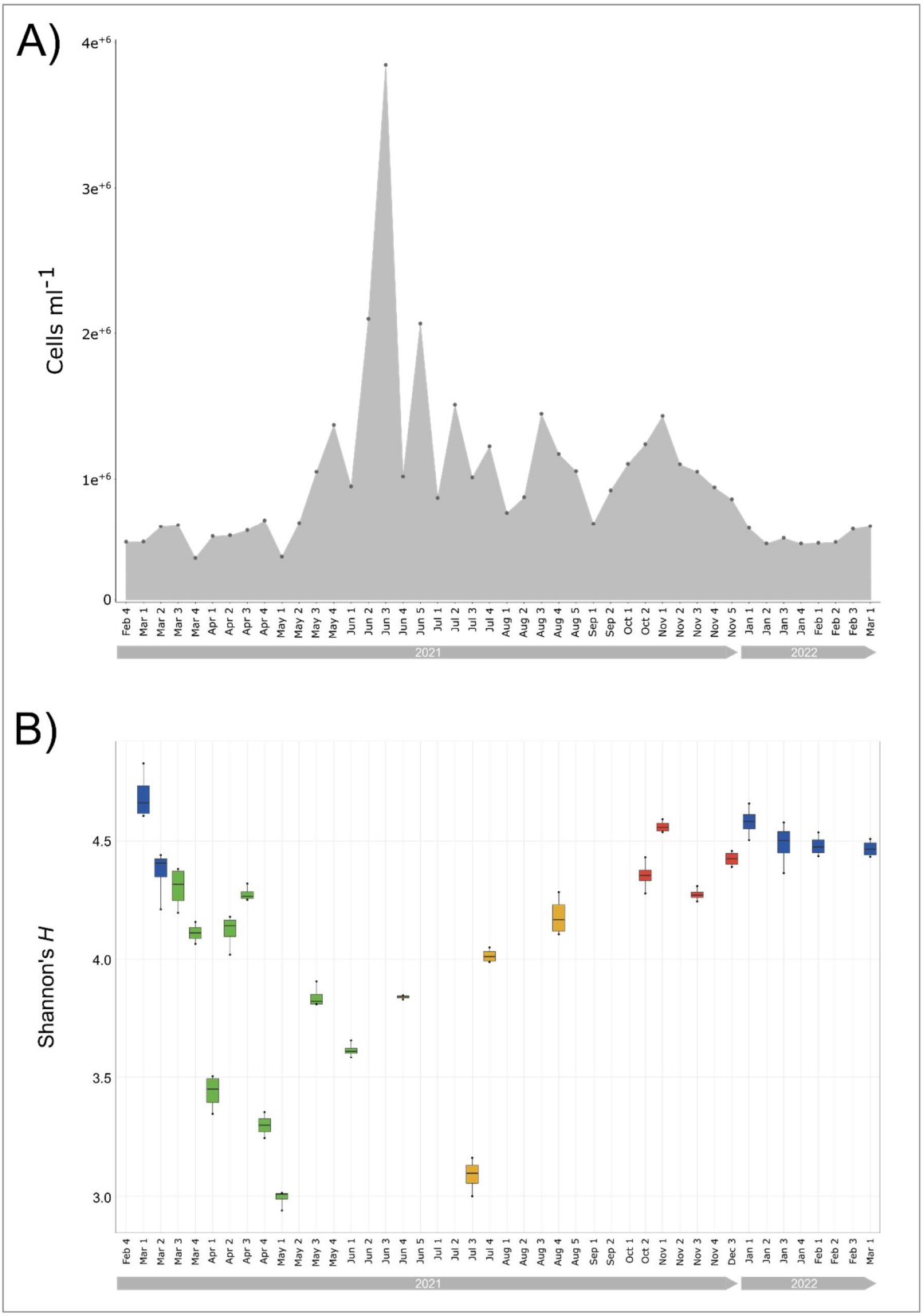

Figure 5. A) Total abundance (cells ml^{-1}) of bacteria in seawater samples collected weekly from 2 m depth between February 2021 and March 2022. Abundance is the sum of high nucleic acid (HNA) and low nucleic acid (LNA) bacteria as counted by flow cytometry. **B)** Alpha diversity (Shannon's *H* index) of bacterial community (amplicon sequence dataset). Bars represent the standard error of the four replicates at each sampling point.

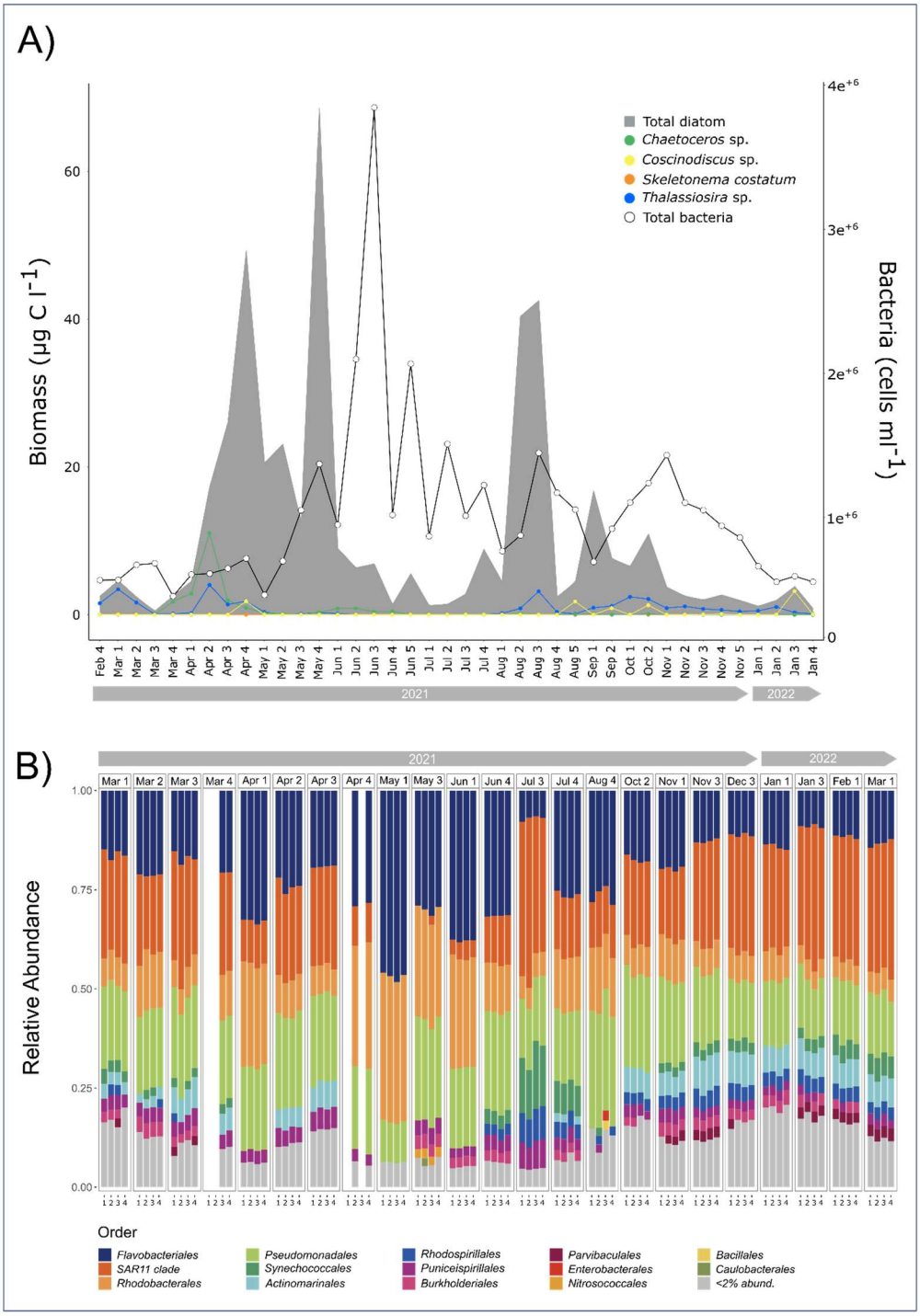

Figure 6. ***A)*** Biomass (µg C l^{-1}) of total diatoms, as well as four diatom genera, Chaetoceros, Thalassiosira, Skeletonema (comprised of just Skeletonema costatum in this dataset), and Coscinodiscus between February 2021 and January 2022. Biomass was calculated by converting biovolume data (Olenina et al., 2006) to carbon (µg C l^{-1}) following the Menden-Deuer and Lessard formula (Menden-Deuer & Lessard, 2000). Also included is total bacterial abuncance (Cells ml^{-1}), demonstrating peak abundance upon the termination of a diatom bloom. ***B)*** Relative abundance of bacterial orders in the prokaryotic amplicon sequence dataset over an annual cycle (March 2021 – March 2022), highlighting increase in *Flavobacteriales* and *Rhodobacterales* upon the termination of a diatom bloom. Each sampling point contains four replicates. Taxa that constituted less than 2 % of the total ASVs are grouped into the <2 % abundance category.

3.4.3 Assessment of seasonal trends in confirmed bacterial antagonists in the Western English Channel

The primary goal of this chapter was to assess the seasonal trends and co-occurrences of confirmed diatom-antagonistic bacteria (Chapter 2) with their diatom hosts in natural seawater assemblages. As such, 16S rRNA gene sequences of *P. alexandrii*, *T. lohafexi*, *M. spongiicola*, *H. titanicae*, *M. adhaerens*, *M. idriensis* and *V. diazotrophicus* were queried against the non-rarefied 16S amplicon sequence dataset, and top hits (ASVs) of each antagonist were subsequently monitored throughout the sampling period.

In order to verify the taxonomic assignment of ASV hits (as assigned by the SILVA database in the DADA2 pipeline), Maximum Likelihood trees were constructed. Positive hits were identified for five of the seven query sequences (summarised in Table 1), *P. alexandrii*, *T. lohafexi*, *M. adhaerens*, *M. idriensis* and *V. diazotrophicus* (Figures 7, 8 and 9). Upon phylogenetic analysis of the top ASV hit for *H. titanicae*, it was revealed that despite having a percentage pairwise identity of 100 % with the *H. titanicae* query sequence and clustering closely on the ML tree, it was more closely related to *Halomonas sulfidaeris* (Figure 7A). Further, the top two ASV hits for *M. spongiicola* were discovered to be most closely related to *Maribacter dokdonensis* (Figure 7B). Despite *M. dokdonensis* not being verified as a diatom antagonist in Chapter 2 of this study, an *M. dokdonensis* strain isolated from the WEC has previously been confirmed to display growth inhibitory affects against a *Skeletonema* species. As such, the two *M. dokdonensis* hits were tracked in place of *M. spongiicola*.

Table 1. Top amplicon sequencing variants (ASVs) hits for each bacterial antagonist when queried against the raw (non-rareified) 16S amplicon sequence dataset. ASV number, taxonomic assignment (according to SILVA taxonomic assignment via DADA2 pipeline), percentage pairwise identity when aligned with query sequence, and the bacterial sequence that an ASV most closely aligns with under Maximum Likelihood tree construction are also provided. Percentage pairwise identity covers a 254 base pair fragment as this was the maximum length of ASVs in the amplicon sequence dataset.

Bacterial antagonist	**Amplicon sequence ASV hits**	**% Pairwise identity**	**ASV assigned taxonomic identity**	**Phylogenetic grouping**	**Reference tree**
Halomonas titanicae	asv_775	100	*Halomonas* sp.	*H. sulfidaeris*	Figure 7A
Maribacter spongiicola	asv_3491	97.6	*Maribacter* sp.	*M. dokdonensis*	Figure 7B
	asv_3288	95.7	Flavobacteriaceae	*M. dokdonensis*	Figure 7B
Marinobacter adhaerens	asv_989	100	*Marinobacter* sp.	*M. adhaerens*	Figure 7C
	asv_990	99.6	*Marinobacter 'manganoxydans'*	*Marinobacter 'manganoxydans'*	Figure 7C
Metabacillus idriensis	asv_418	99.3	*Bacillus* sp.	*Metabacillus mangrovi*	
	asv_1597	98.5	*Bacillus* sp.	*M. idriensis*	Figure 8A
Ponticoccus alexandrii	asv_1208	100	*Phaeobacter* sp.	*P. alexandrii*	Figure 8B
	asv_1257	98.8	*Phaeobacter* sp.	*Phaeobacter inhibens*	Figure 8B
	asv_1259	97.6	*Sulfitobacter dubius*	*Sulfitobacter dubius*	Figure 8B
Thalassospira lohafexi	asv_1398	100	*Thalassospira* sp.	*T. lohafexi*	Figure 8C
Vibrio diazotrophicus	asv_1535	100	*Vibrio* sp.	*V. diazotrophicus*	Figure 9
	asv_1850	99.2	*Vibrio* sp.		Figure 9

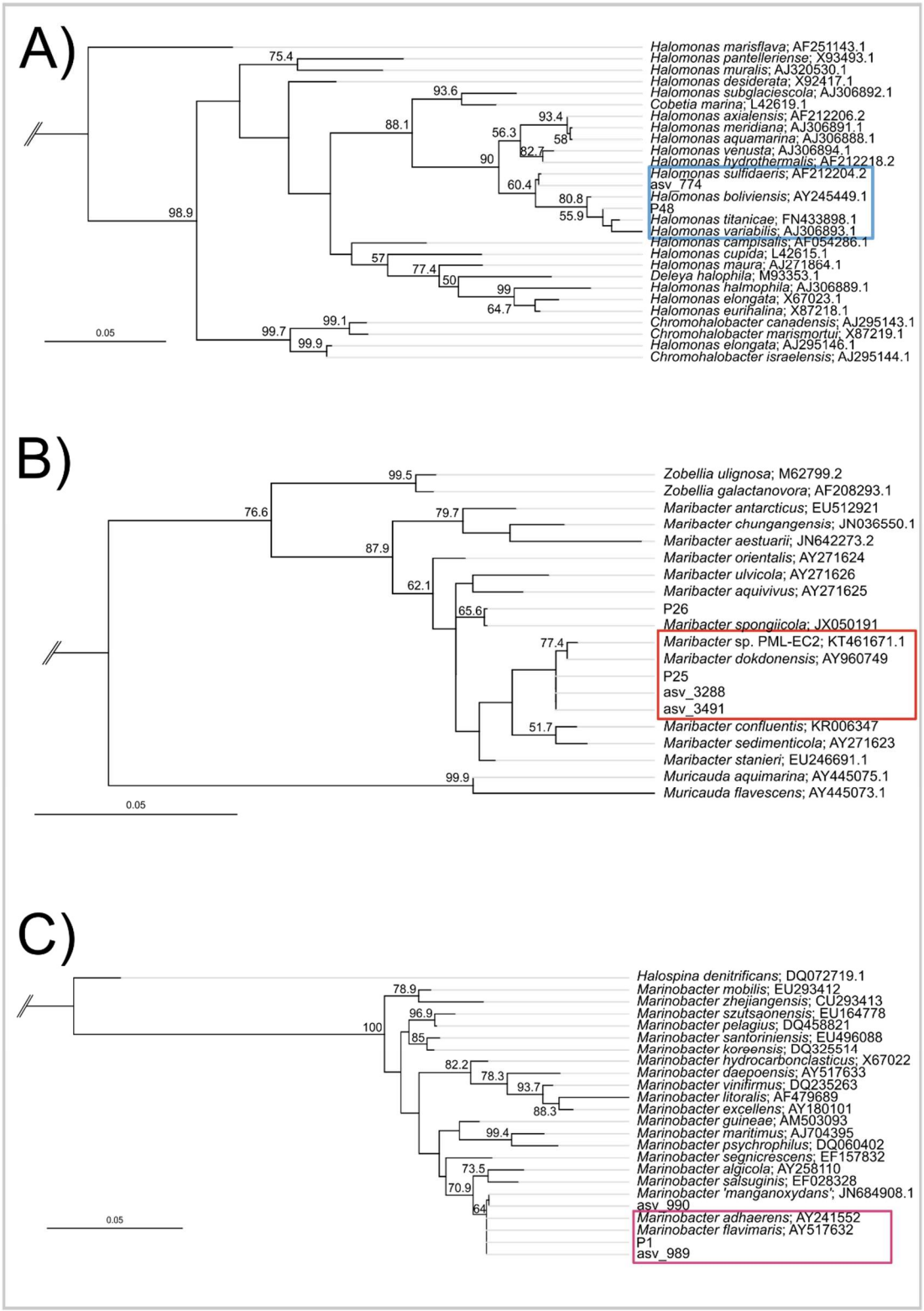

Figure 7. Maximum Likelihood trees constructed to verify the identity of amplicon sequence dataset ASVs most closely related to ***A)*** *Halomonas titanicae* (P48) using *Zymobacter palmae* as an outgroup ***B)*** *M. dokdonensis* (P25) using *Flavobacterium aquatile* as an outgroup. *Maribacter spongiicola* (P26 query sequence) is also included. ***C)*** *Marinobacter adhaerens* (P1 query sequence) using *Salicola marasensis* as an outgroup, and ML trees were constructed using ASV sequences (V4 region), full-length 16S rRNA sequences of query bacteria (bacterium with confirmed antagonistic activity), and type strains of closely related species. Branch support values above 50 % are indicated at branch nodes (calculated from 1000 bootstrap replicates).

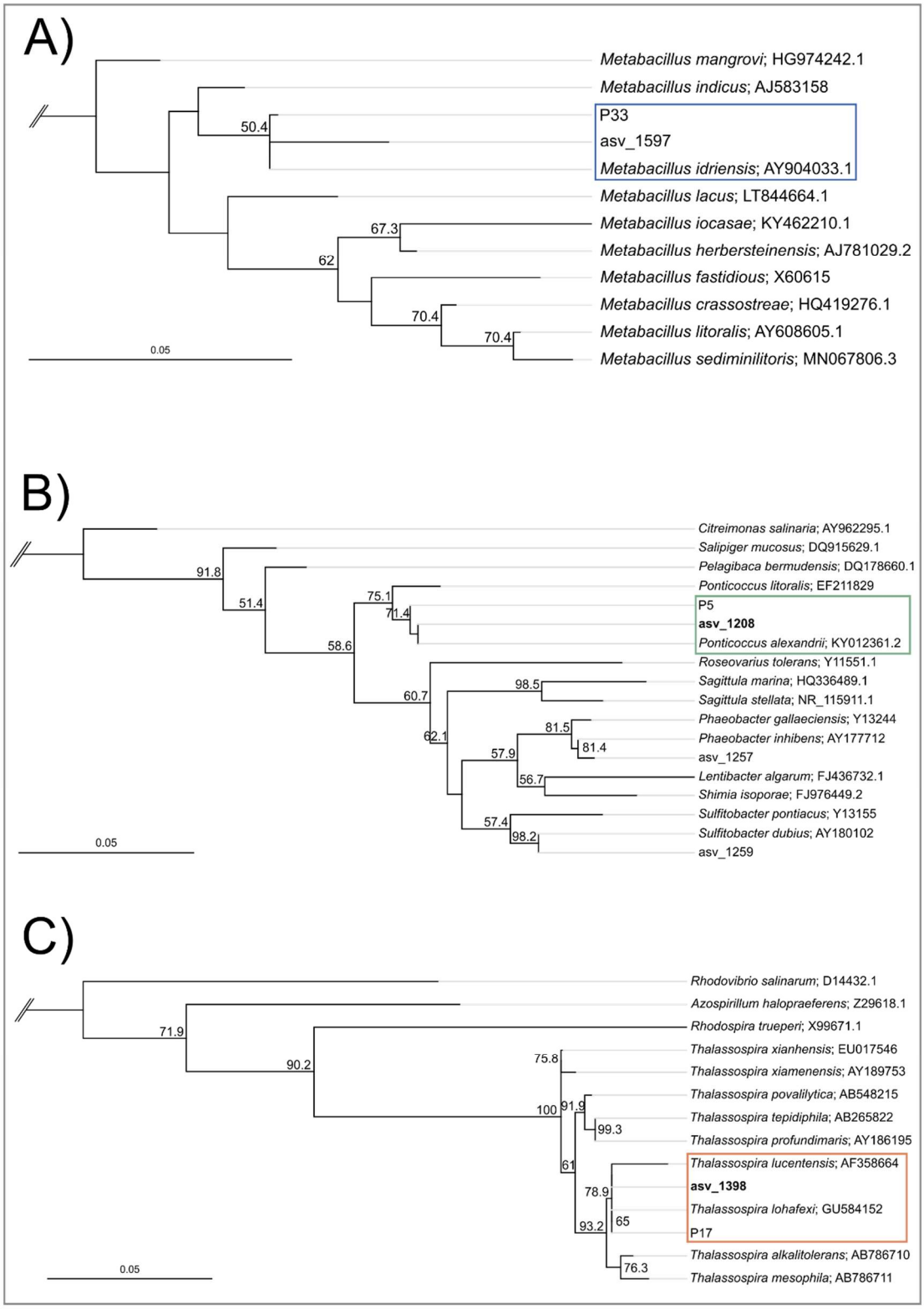

Figure 8. Maximum Likelihood trees constructed to verify the identity of amplicon sequence dataset ASVs most closely related to **A)** *Metabacillus idriensis* (P33 query sequence) using *Lysinibacillus boronitolerans* as an outgroup. **B)** *Ponticoccus alexandrii* (P5 query sequence) using *Rubellimicrobium aerolatum* as an outgroup. **C)** *Thalassospira lohafexi* (P17 query sequence) using *Azorhizobium caulinodans* as an outgroup. ML trees were constructed using ASV sequences (V4 region), full-length 16S rRNA sequences of query bacteria (bacterium with confirmed antagonistic activity), and type strains of closely related bacterial species. Branch support values above 50 % are shown (calculated from 1000 bootstraps).

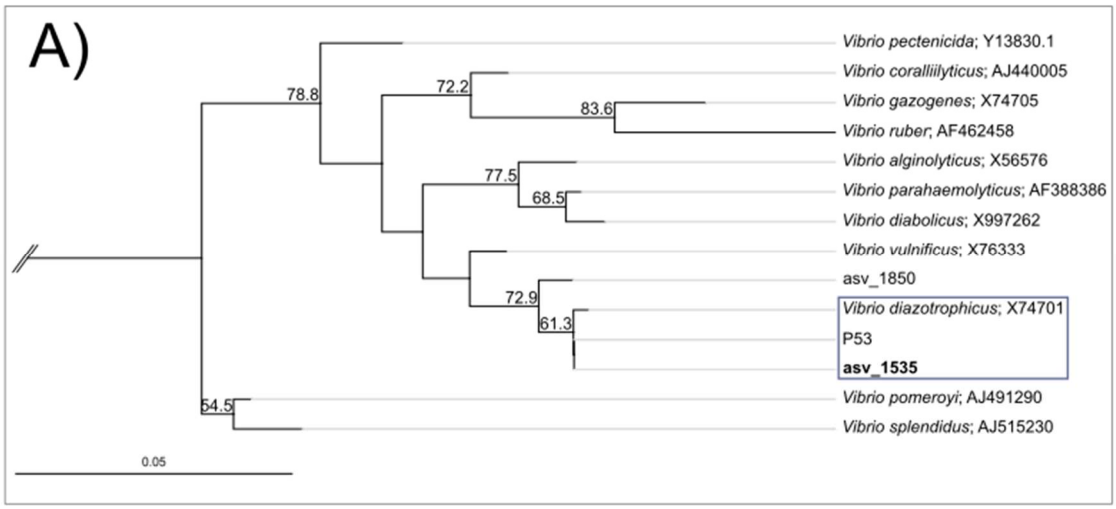

Figure 9. Maximum Likelihood trees constructed to verify the identity of amplicon sequence dataset ASVs most closely related to ***A)*** *Vibrio diazotrophicus* (P53 query sequence) using *Salinivibrio costicola* as an outgroup. ML trees were constructed using ASV sequences (V4 region), full-length 16S rRNA sequences of query bacteria (bacterium with confirmed antagonistic activity), and type strains of closely related bacterial species. Branch support values above 50 % are shown (calculated from 1000 bootstraps).

Each confirmed ASV was subsequently monitored throughout the amplicon sequencing sampling period. Surprisingly, the ASVs, though detected in temporally distinct samples from spring to the following winter, were detected in just nine of the 23 sampling points of this time series. The first ASV to be detected was that which was closely related to *H. titanicae*, which was detected in early March and again in late March and mid-April (Figure 10A). *Thalassiosira* sp. and/or *Chaetoceros* sp. were amongst the most abundant diatom taxa during these sampling points where the closest *H. titanicae* hit was detected in early Spring. The next two ASVs to be detected were those belonging to *P. alexandrii* and *M. dokdonensis*, which were both present in late March 2021 and late June 2021 (Figure 10A). Interestingly, at the time of sampling when *P. alexandrii* was first detected, diatoms of the *Thalassiosira* genus (one of the original diatom host genera of *P. alexandrii*), and to a lesser extent *Minidiscus*, dominated the diatom community (Figure 10B). During the second sampling point, however, the diatom community was heavily dominated by *Leptocylindrus*, although *Thalassiosira* species were still present above the 2 % threshold. Despite *Flavobacteriales* abundance peaking during the early May 2021 sampling point, the *Flavobacteria M. dokdonensis* was not detected at this time point, but instead in March 2021 and June 2021. The remaining ASV hits, with the exception of that belonging to *M. idriensis*, were all detected during the summer months (June – August 2021). The *V. diazotrophicus* ASV was detected in late July 2021 (the same month in which it was originally isolated twice in 2020) following the decline of the *Leptocylindrus* bloom. While *Chaetoceros* and *Leptocylindrus* were the dominant diatoms at this time point, *Thalassiosira* (again, the original host genus of *V. diazotrophicus*) was also abundant within the same samples. Both the *T. lohafexi* and *M. adhaerens* ASVs were detected in late August, along with that of *H.*

titanicae, where *Pseudo-nitzschia* and *Rhizoselenia* species dominated the diatom community. Although *Thalassiosira* species (the original host of *T. lohafexi* and one of the hosts on which *M. adhaerens* was detected) were present in the August sampling point, they constituted a relatively minor component of the diatom community at the time. The *H. titanicae*, *T. lohafexi* and *M. adhaerens* ASVs were also the most abundant (by read number) of all the ASVs detected throughout the sampling period. *M. adhaerens* was also present in the mid-October sample, though as no sample collection took place in September, it is difficult to know whether this correlated with a persistence of this ASV in the environment or was simply detected on two distinct occasions at these time points by chance. Finally, the *M. idriensis* related ASV was detected only in the early November sampling point, where the diatom community was dominated largely by polar-centric Mediophyceae, and to a lesser extent, *Thalassiosira* and *Minidiscus* species.

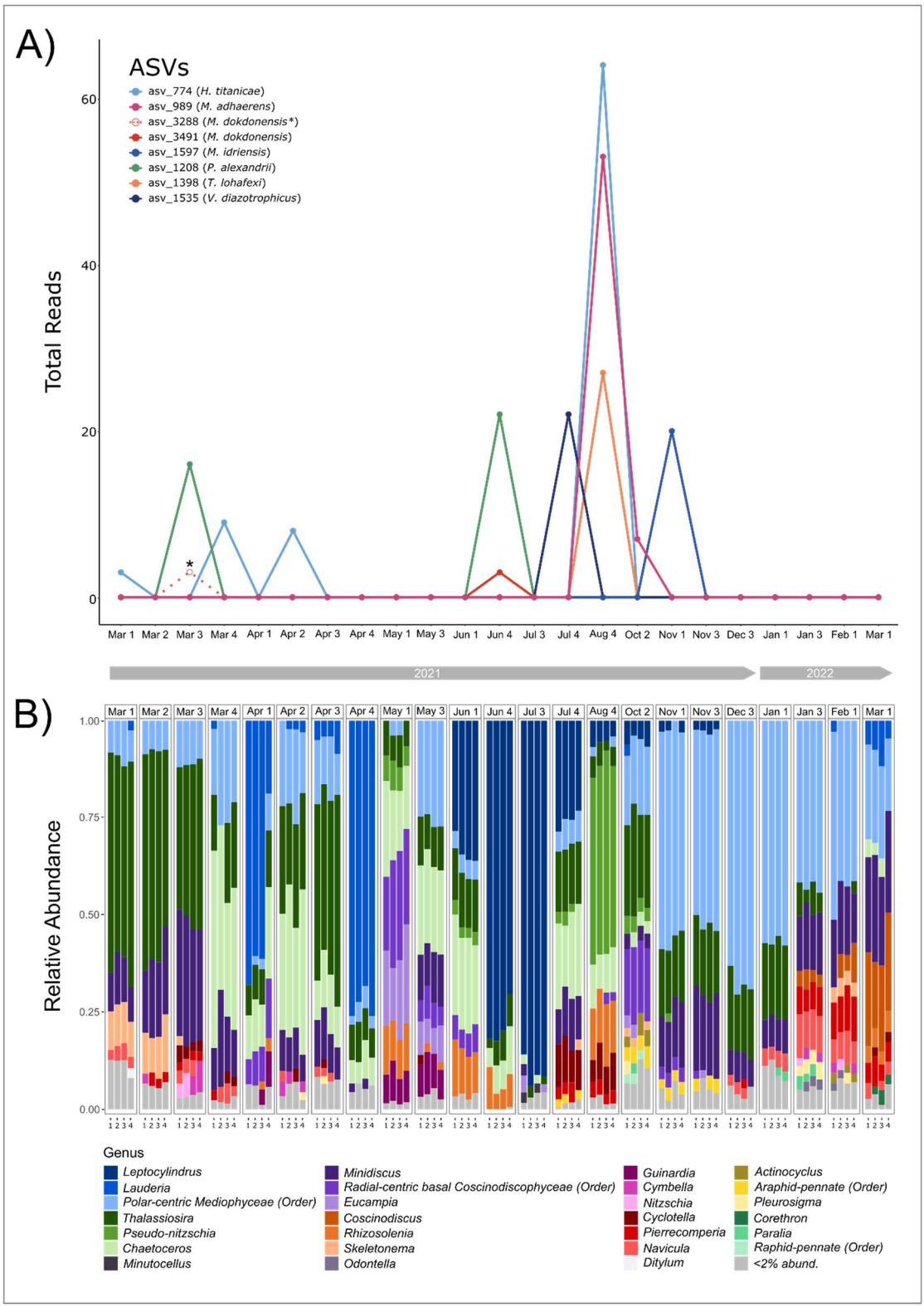

Figure 10. A) Total number of reads (sum of reads detected in each four replicates collected per sampling point) of ASVs phylogenetically related to query sequences of bacterial antagonists with confirmed antagonistic activity over an annual cycle (March 2021 – March 2022). * indicates detection at a secondary sampling site, Plymouth Sound, rather than L4. **B)** Relative abundance of major diatom genera over an annual cycle (March 2021 – March 2022), highlighting dominant taxa present during sampling points where diatom-antagonistic bacteria were detected. Each sampling point contains four replicates. Taxa that constituted less than 2 % of the total ASVs are grouped into the <2% abundance category.

3.4.4 Assessing the geographic range of antagonistic bacteria and their diatom hosts

The *Tara* Oceans 'Ocean Barcode Atlas' was employed to assess the geographic range of WEC bacterial antagonists and their diatom hosts in the global oceans. As with the WEC queries in Section 3.4.2, full-length 16S rRNA sequences of bacterial antagonists were searched against the *Tara* Oceans 16S/18S miTAG metabarcode database. The identity of miTAG hits was subsequently verified via the construction of ML phylogenetic trees.

Positive hits were obtained for *H. titanicae*, *M. adhaerens*, *M. dokdonensis* and *T. lohafexi* and *V. diazotrophicus* (Figure 11 and 12, three, one, two, one, and two miTAG hits respectively). The single miTAG hit obtained for *M. spongiicola* were revealed through phylogenetic analysis to be more closely related to *M. dokdonensis* (Figure 11B), and as such, the global distribution of *M. dokdonensis* was assessed instead. Similarly, the single miTAG hit obtained for *P. alexandrii,* despite being closely related, grouped more closely with *Ponticoccus litoralis* (Figure 12A), and no miTAG hit could be verified for *M. idriensis* (Appendix Figure 16).

For the assessment of the biogeography of diatom hosts, full-length 18S rRNA gene sequences of the diatom hosts, or closest relatives, used in Chapters 1 and 2 (*Thalassiosira pseudonana*, *Chaetoceros calcitrans* and *Skeletonema marinoi*) were also queried against the *Tara* Oceans OTU 18S V9 database (Version 2). As the closest OTU hits obtained for *C. calcitrans* and *S. marinoi* had less than 100 % percentage pairwise identity, the identity of these hits was verified via the construction of ML trees (Figure 13). Phylogenetic analysis revealed that the twoOTU hits for the *C. calcitrans* query sequence did not cluster directly with *C. calcitrans* (Figure 13A), though as these were the closest OTUs available, their

distribution was assessed in place of a *C. calcitrans* OTU. Conversely, the three OTU hits for the *S. marinoi* query sequence did cluster with *S. marinoi* (Figure 13B). A single positive hit (100 % pairwise identity) was obtained for the 18S rRNA gene of *T. pseudonana*, which phylogenetic analysis revealed to also cluster with *T. pseudonana* (Figure 13C).

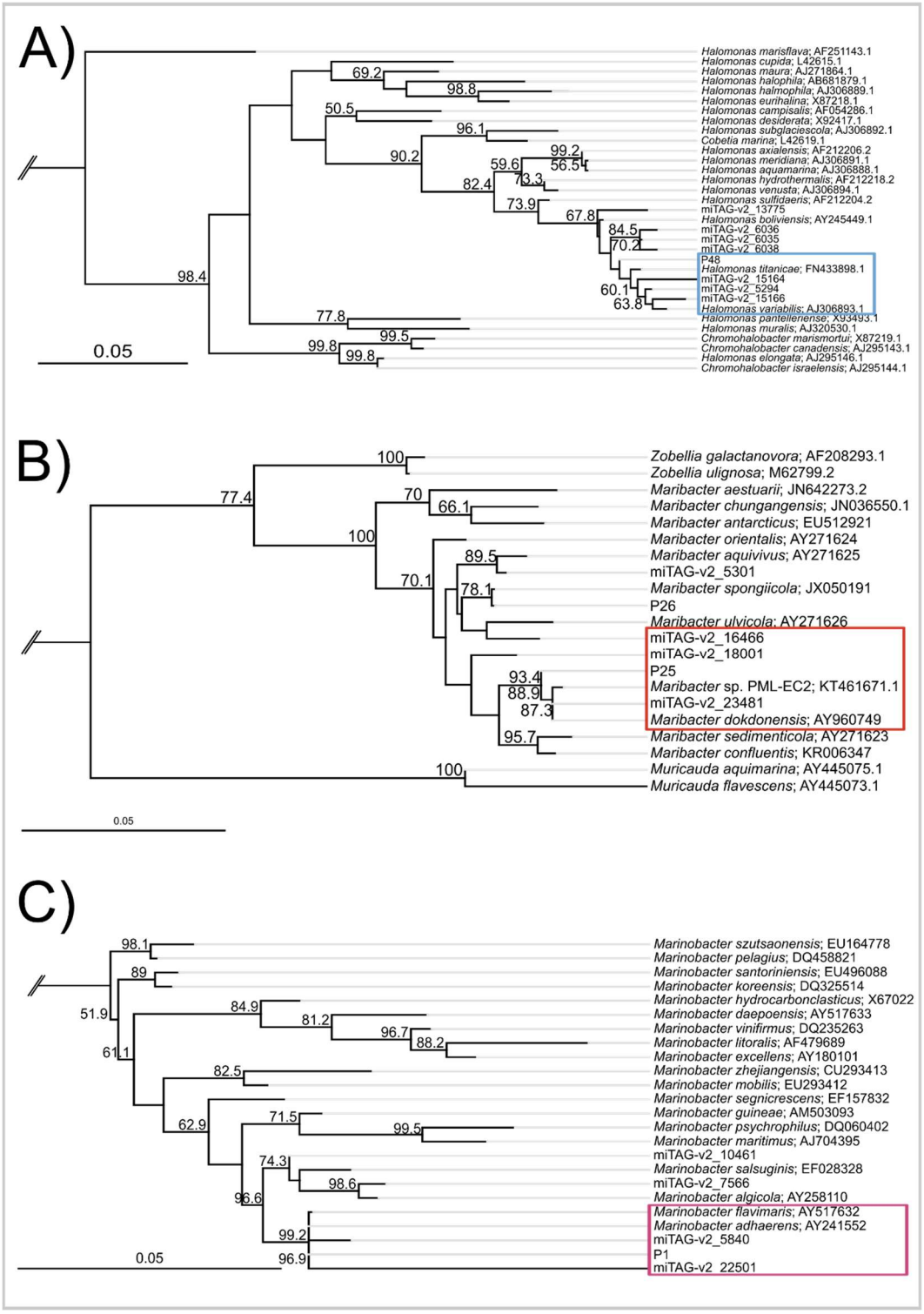

Figure 11. Maximum Likelihood trees constructed to verify the identity of miTAG hits (obtained from the Tara Ocean Barcode Atlas Portal) most closely related to **A)** *Halomonas titanicae* (P48 query sequence) using *Zymobacter palmae* as an outgroup, **B)** *Maribacter spongiicola* (P26 query sequence) and *Maribacter dokdonensis* (P25) using *Flavobacterium aquatile* as an outgroup, and **C)** *Marinobacter adhaerens* (P1 query sequence) using *Salicola marasensis* as an outgroup. ML trees were constructed using full-length 16S rRNA sequences of miTAG hits, query bacteria (bacterium with confirmed antagonistic activity), and type strains of closely related bacterial species. Branch support values above 50 % are shown (calculated from 1000 bootstraps).

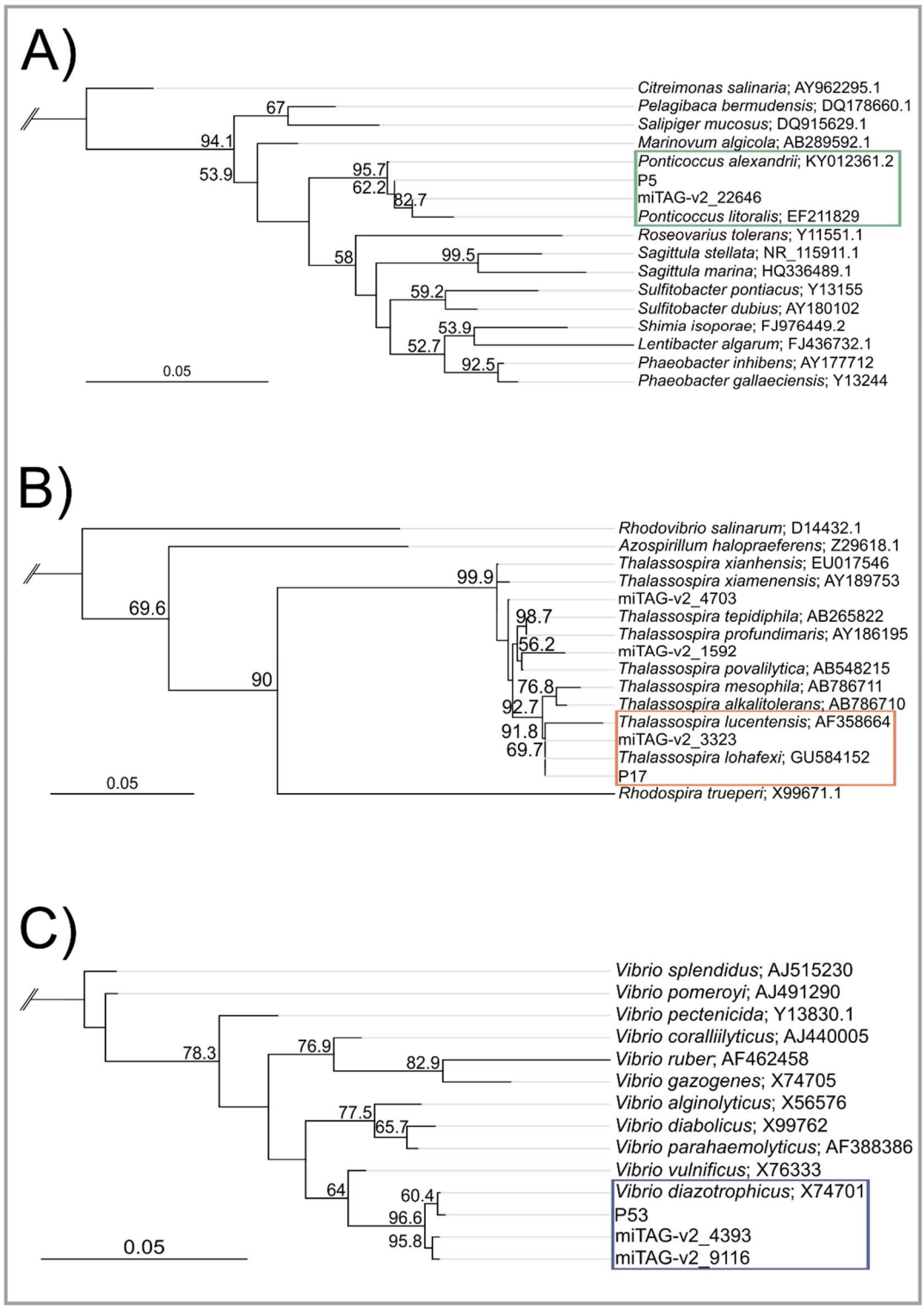

Figure 12. Maximum Likelihood trees constructed to verify the identity of miTAG hits (obtained from the *Tara* Ocean Barcode Atlas Portal) most closely related to **A)** *Ponticoccus alexandrii* (P5 query sequence) using *Rubellimicrobium aerolatum* as an outgroup, **B)** *Thalassospira lohafexi* (P17 query sequence) using *Azorhizobium caulinodans* as an outgroup, and **C)** *Vibrio diazotrophicus* (P53 query sequence) using *Salinivibrio costicola* as an outgroup. ML trees were constructed using full-length 16S rRNA sequences of miTAG hits, query bacteria (bacterium with confirmed antagonistic activity), and type strains of closely related bacterial species. Branch support values above 50 % are shown (calculated from 1000 bootstraps).

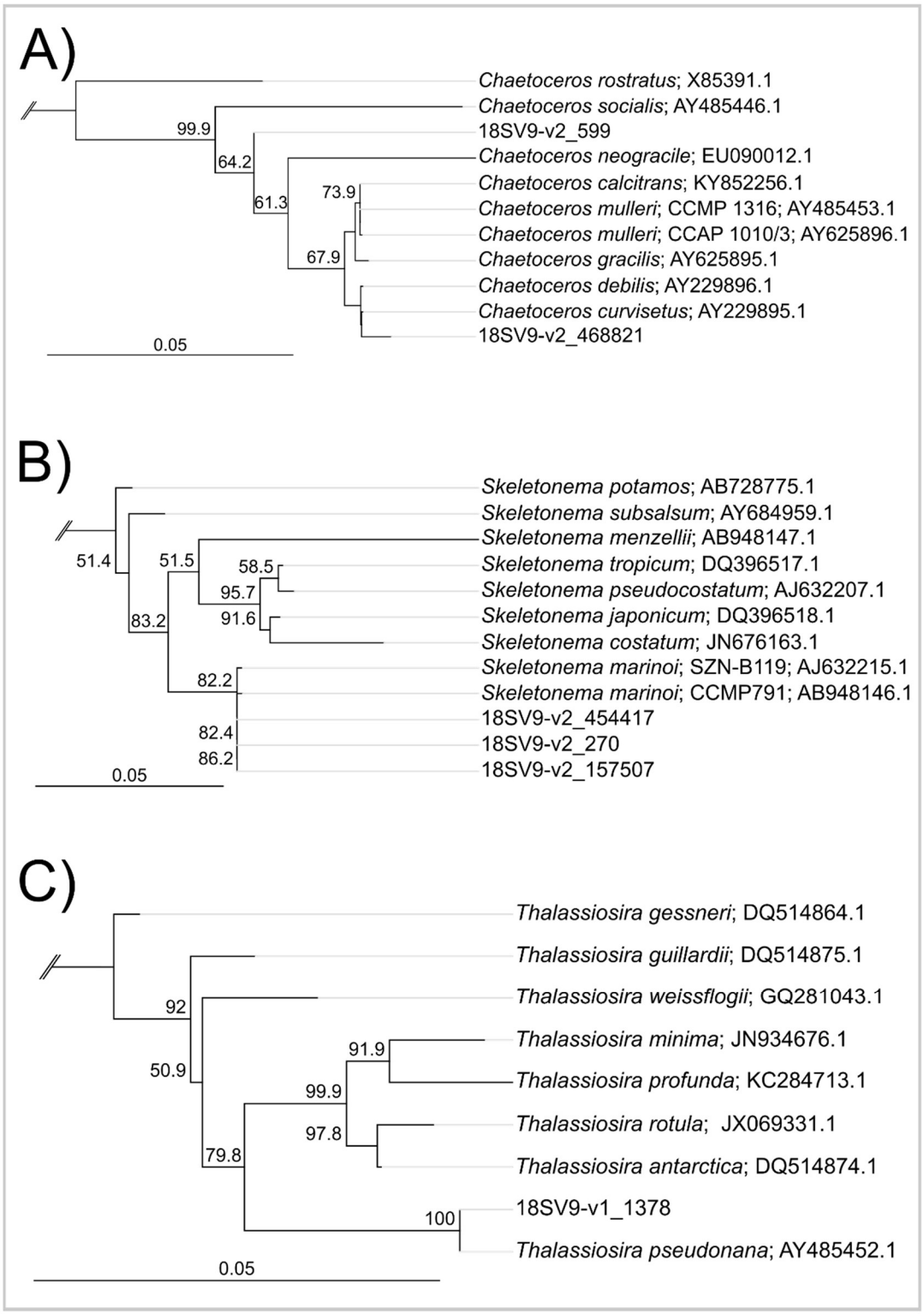

Figure 13. Maximum Likelihood trees constructed to verify the identity of 18S V9 hits (obtained from the Tara Ocean Barcode Atlas Portal) most closely related to **A)** *Chaetoceros calcitrans* (*Chaetoceros* sp. PLY617 proxy query sequence) using *Thalassiosira pseudonana* as an outgroup, **B)** *Skeletonema marinoi* (*Skeletonema* sp. PLY627 proxy query sequence) using *Thalassiosira pseudonana* as an outgroup, and **C)** *Thalassiosira pseudonana* using *Phaeodactylym tricornutum* as an outgroup. ML trees were constructed using V9 regions of 18S rRNA gene of miTAG hits and full-length sequences of query diatom, and type strains of closely related species. Branch support values above 50 % are shown (calculated from 1000 bootstraps).

The distribution of *M. adhaerens*, *H. titanicae*, and the closest hits to their susceptible diatom host, *Chaetoceros* sp., was assessed globally using the Ocean Barcode Atlas (Figure 14). *M. adhaerens* was detected at 19 stations (many coastal) and displayed a wide geographic range, spanning the global oceans. Meanwhile, *H. titanicae* was detected at only six stations and displayed a narrower distribution that *M. adhaerens*, primarily being detected in the South Pacific, North Atlantic and Mediterranean, and a single instance in the Indian Ocean. Assessment of the *Chaetoceros* sp. hit revealed *Chaetoceros* sp. to have an extensive geographic range, including being found in many coastal ocean regions in the Atlantic Ocean and Mediterranean sea. The geographic ranges of both *M. adhaerens* and *H. titanicae* overlapped that of *Chaetoceros* sp., with both bacteria only being detected at two stations where *Chaetoceros* sp. was not present.

The distribution of *M. dokdonensis* and *S. marinoi* was also assessed. *M. dokdonensis* was the most widespread antagonist, being detected at 26 sampling stations across the global oceans (Figure 15). An assessment of the distribution of *S. marinoi* revealed that the ranges of *M. dokdonensis* and *S. marinoi* showed significant overlap, particularly in northern sampling stations, with the two species co-occurring at 13 sites. Additionally, the distribution of the miTAG hit most closely related to *P. alexandrii* was also assessed. While the hit was detected only at a single station in the Atlantic Ocean, the hit did co-occur with *S. marinoi*.

Finally, the distribution of *T. lohafexi*, *V. diazotrophicus* and *T. pseudonana* was assessed (Figure 16). *T. lohafexi* was detected at 12 stations, with high instances in the Mediterranean and Red Sea, and in the Arctic Ocean. On the other hand, *V. diazotrophicus* was detected at only two stations in the Atlantic and Pacific Oceans. An assessment of the distribution of susceptible host *T. pseudonana*

revealed a much smaller distribution than *Chaetoceros* sp., and *S. marinoi*, being detected at only five stations throughout the Atlantic Ocean, Mediterranean Sea and Arctic Ocean. Nevertheless, analysis showed that the geographic ranges of *T. pseudonana* and *T. lohafexi* overlapped in the Arctic Ocean, with both species being detected at three sampling sites. The ranges of *T. pseudonana* and *V. diazotrophicus* did not exhibit any overlap in this assessment.

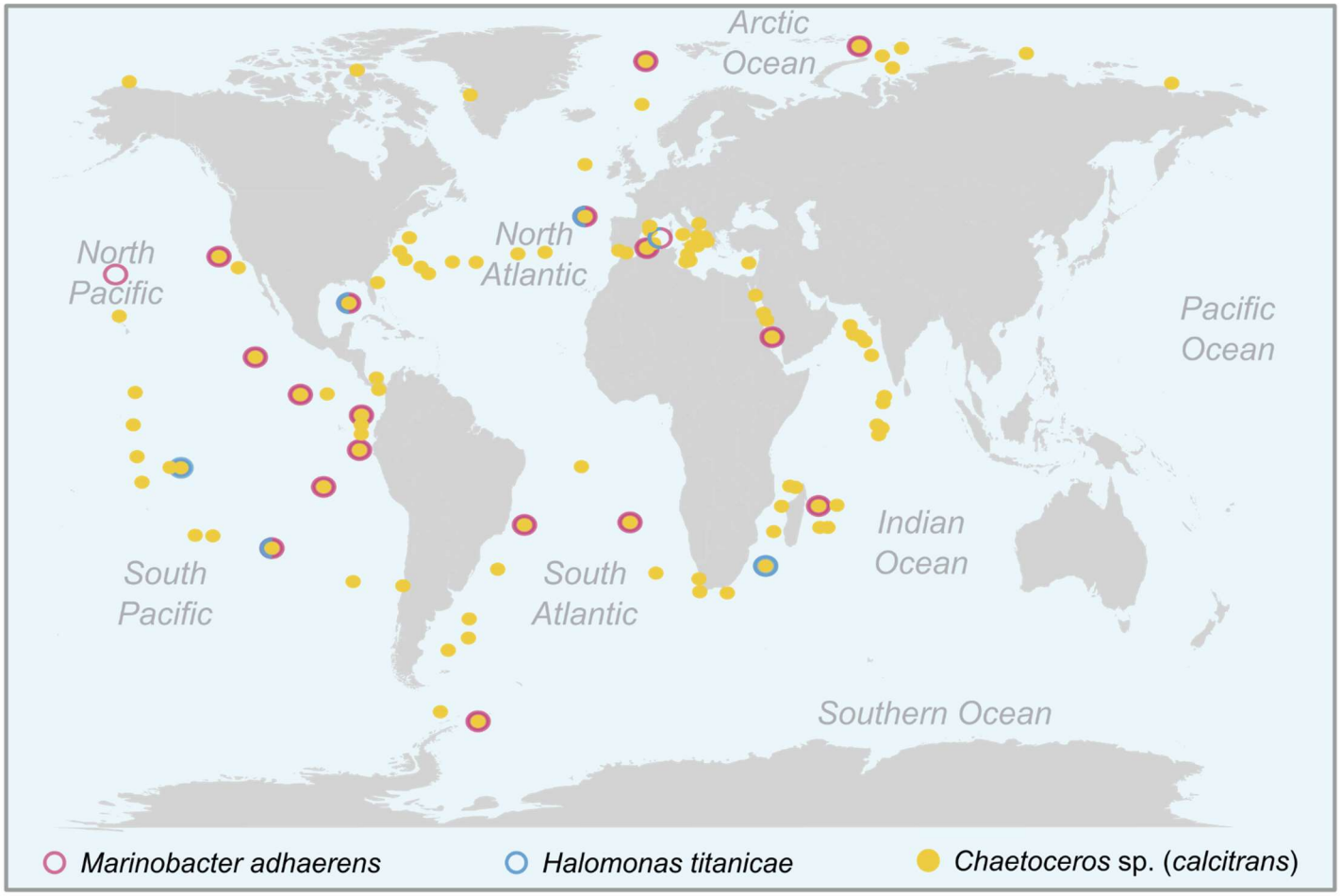

Figure 14. Global distribution of *H. titanicae* and *M. adhaerens* and co-occurrence with proxy diatom host *Chaetoceros* sp. Displayed are the miTAG hits for *H. titanicae* (blue open circles) and *M. adhaerens* (pink open circles), and 18S hits for *Chaetoceros* sp. (yellow circles) detected in surface waters, the deep chlorophyll maxima, and the mesopelagic zone. All hits, sequence data and metadata was obtained from the Tara Ocean Barcode Atlas.

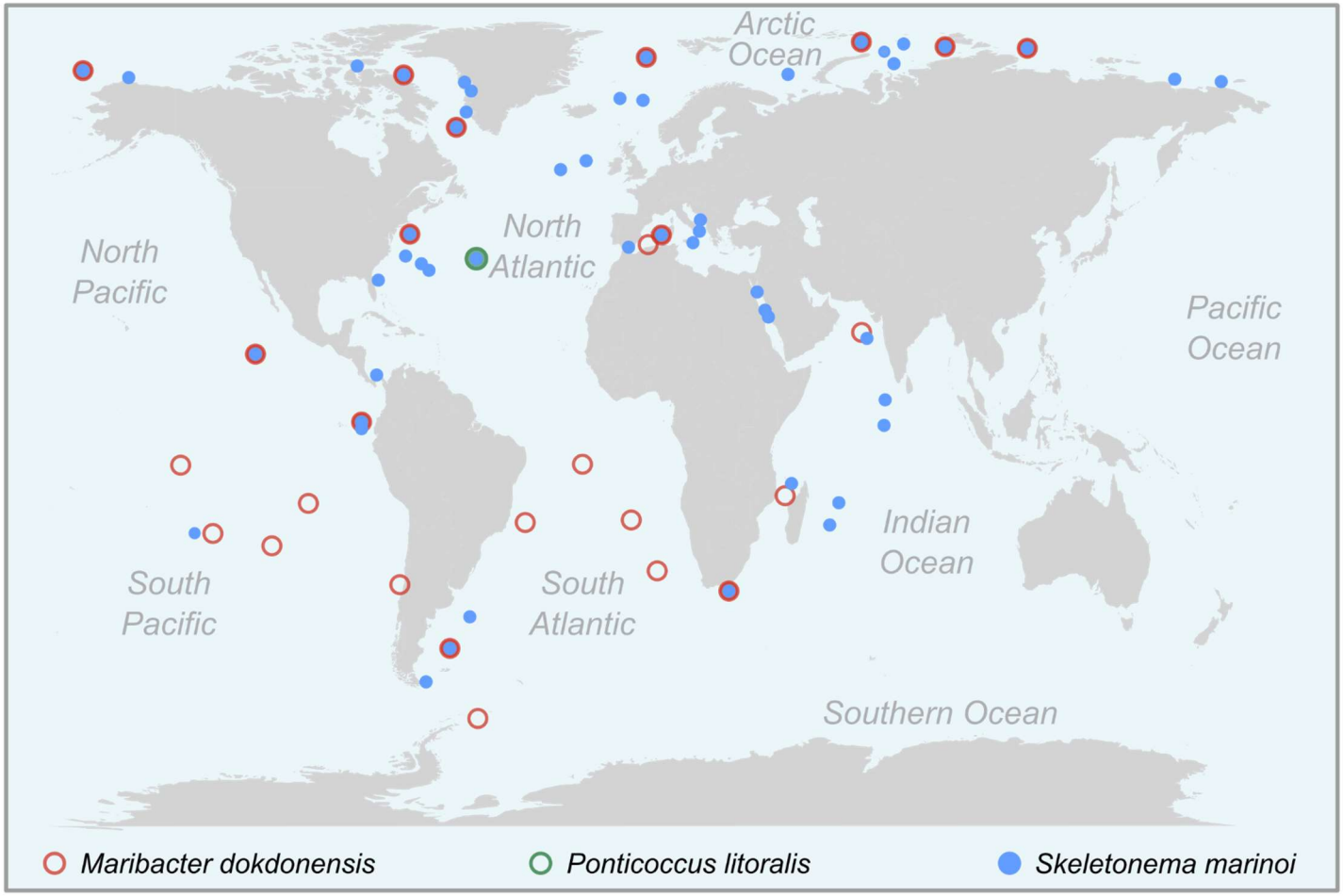

Figure 15. Global distribution of *M. dokdonensis* and co-occurrence with proxy diatom host *S. marinoi*. Displayed are the miTAG hits for *M. dokdonensis* (red open circles) and 18S hits for *S. marinoi* (blue circles) detected in surface waters, the deep chlorophyll maxima, and the mesopelagic zone. The miTAG hit most closely related to *P. alexandrii* is also displayed (green open circle). All hits, sequence data and metadata was obtained from the Tara Ocean Barcode

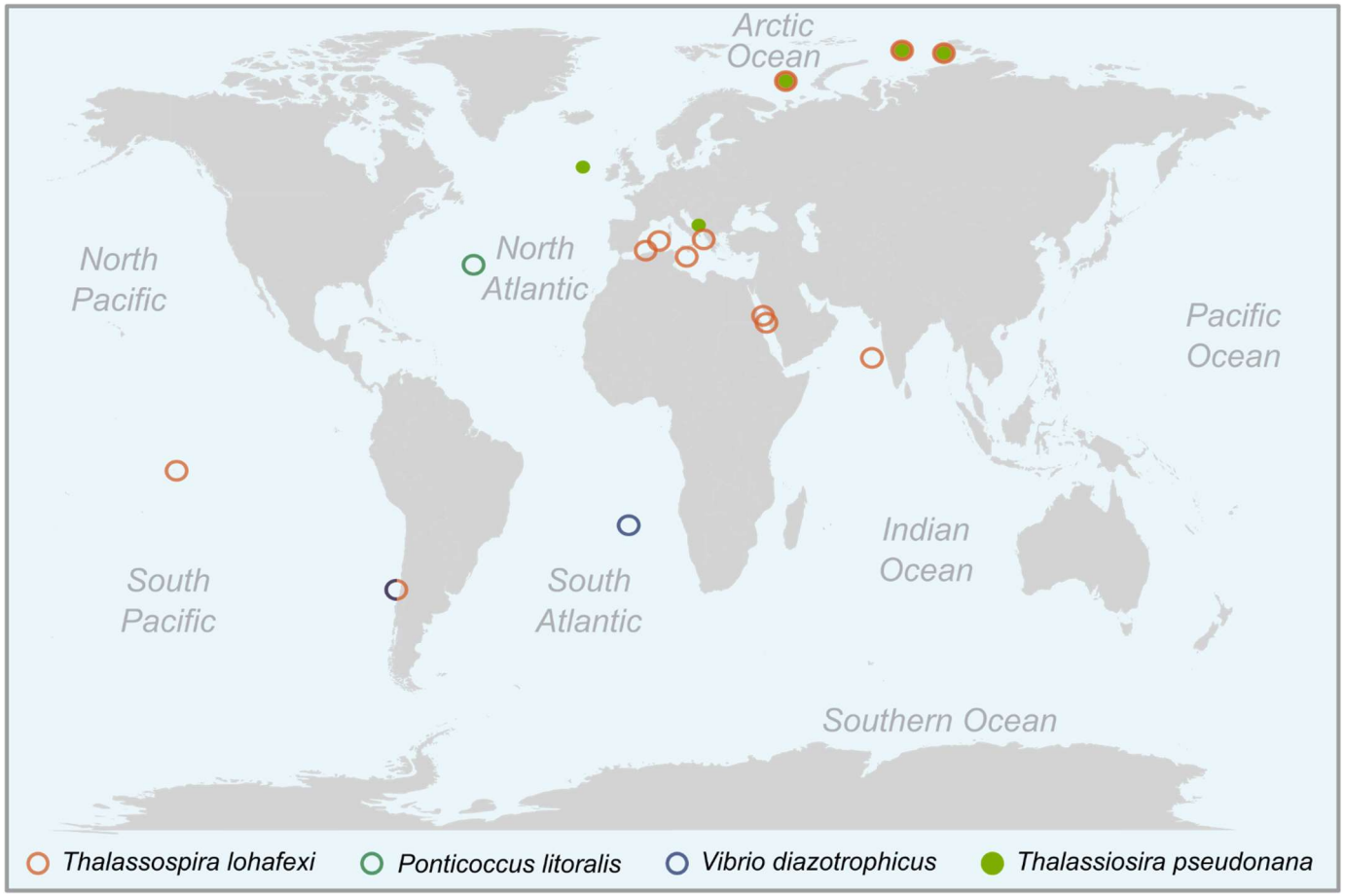

Figure 16. Global distribution of *T. lohafexi* and *V. diazotrophicus* and co-occurrence with diatom host *T. pseudonana*. Displayed are the miTAG hits for *T. lohafexi* (orange open circles) and *V. diazotrophicus* (blue open circles), and 18S hits for *T. pseudonana* (green circles) detected in surface waters, the deep chlorophyll maxima, and the mesopelagic zone. The miTAG hit most closely related to *P. alexandrii* is also displayed (gree open circle). All hits, sequence data and metadata was obtained from the Tara Ocean Barcode Atlas.

3.5 Discussion

Elucidating the ecological significance of laboratory-verified microbe-microbe interactions requires an understanding of their distribution, co-occurrence and seasonal dynamics, and is a fundamental step in characterizing the functional diversity of marine ecosystems. Techniques such as short-read amplicon sequencing and global ocean microbial datasets, such as the *Tara* Oceans databases, are invaluable tools for investigating the dynamics of lab-verified interactions in the natural environment. Utilizing such tools, this work has explored the distribution and seasonal dynamics of seven confirmed diatom-antagonistic bacteria and their host species at both a local and global scale.

Short-read amplicon sequencing of the diatom community at Station L4 revealed a highly dynamic community displaying strong seasonal variations in the dominant diatom taxa. These findings were concurrent with previous literature reports on the eukaryotic community in the WEC (Widdicombe et al., 2010; Arsenieff et al., 2020), where specific genera, such as *Chaetoceros*, *Thalassiosira*, *Coscinodiscus*, and *Pseudo-nitzschia* (amongst others) were found to exhibit seasonal blooms. Amplicon sequence analysis also confirmed the importance of typically overlooked diatom species, such as those belonging to the genus *Minidiscus*, which were found to be seasonally abundant and persistent throughout the entire sampling period of this work.

Meanwhile, the bacterial community was revealed to be consistently dominated by four orders, *Flavobacteriales*, *SAR11*, *Rhodobacterales* and *Pseudomonadales*, again, concurrent with previous literature reports (Gilbert et al., 2009; Taylor et al., 2014). These groups routinely comprised the majority portion of the prokaryotic community throughout the sampling period. Abundance

of both *Flavobacteriales* and *Rhodobacterales* peaked in May 2021, following the decline of a diatom bloom. While a tight coupling of diatom bloom termination processes and increased *Flavobacteriales* and *Rhodobacterales* abundance has been demonstrated in the past, it was interesting to note that the diatom antagonists belonging to the *Flavobacteriales* and *Rhodobacterales* (*M. spongiicola*, *M. dokdonensis*, *P. alexandrii* and *T. lohafexi*) isolated in previous chapters were not detected at this time point. Similarly, while the isolation of bacterial antagonists isolated in Chapter 1 peaked in December 2020, coinciding with a winter bloom of *Coscinodiscus wailesii*, bacterial antagonists were not detected during the winter *Coscinodiscus* bloom of this sampling period (January 2021). One possible explanation for this is that the size of the *Coscinodiscus* bloom during this sampling period (March 2021 – March 2022) was significantly smaller than that detected during the sampling period covered in Chapter 1 (June 2020 – July 2021). *Coscinodiscus* sp. biomass reached 17.8 µg C l^{-1} during the peak of the bloom in December 2020, while peaking at just 3.2 µg C l^{-1} during the bloom detected in January 2022. As such, although *Coscinodiscus* species did constitute 85 % of the total diatom biomass at this time (not too dissimilar from December 2020, where *Coscinodiscus* constituted 92 % of total diatom biomass), overall cell numbers were much lower, thus potential *Coscinodiscus* host cells were markedly fewer during this period. As diatoms are often tightly coupled with host-specific associated bacterial communities often observed in marine environments (Fandino et al., 2005; Teeling et al., 2012; Taylor et al., 2014) a difference in diatom biomass of this size could be a significant factor influencing the abundance of bacteria for which diatom antagonism provides a source of organic carbon.

An additional important consideration is that sample collection during this study was limited to monthly or bi-monthly time points over the course of a 12-month period. Given the stochastic and highly dynamic nature of marine microbial communities, it is possible, if not likely, that a relatively 'infrequent' sample collection such as this could impact the bacterial diversity and abundance detected by amplicon sequencing of single monthly samples. Additionally, while bacterioplankton communities in the WEC typically demonstrate robust seasonal and inter-annual trends in diversity and dominant groups, analysis of longer time series datasets often highlight anomalies. For example, a study of microbial community dynamics at Station L4 over a six-year period demonstrated that while the two most dominant bacterial orders (*Rickettsiales* and *Rhodobacterales*) exhibited largely regular seasonal patterns, *Rhodobacterales* abundance in the summer of 2004 was almost double that of previous and proceeding years (Taylor et al., 2014). Interestingly, this study also highlighted a bacterial 'bloom' in the summer of 2003 that consisted largely (54 %) of a single *Vibrio* sp., despite this species remaining relatively rare (<2 % relative abundance) throughout the rest of the time series. As such, increased sampling frequency and increased sample duration (e.g., weekly samples and multi-year monitoring) may be able to provide further insights into whether the trends observed in this study are typical.

Furthermore, tracking single isolates (ASVs) throughout time in a highly dynamic microbial community, consisting of thousands of species, is inevitably going to be difficult, particularly as short-read amplicon sequencing, while a powerful tool for the exploration of microbial communities at an ecosystem scale, is not without limitations or biases. For example, one of the most prominent issues faced with short-read amplicon sequencing pipelines such as these is the taxonomic assignment of ASVs, particularly at genus or species level. Short-read amplicon

sequencing utilizes subregions of the 16S rRNA gene, termed variable regions, to distinguish separate sequences and assign taxonomy (Ghyselinck et al., 2013; Abellan-Schneyder et al., 2021). Numerous studies have demonstrated the effects of the chosen variable region used for amplicon sequencing, with some regions being able to better discern species than others, thus producing more robust taxonomic assignment (Bukin et al., 2019; Greay et al., 2019; Callahan et al., 2021). The present study utilized variable region 4 (V4), widely used for short-read amplicon sequencing as it is the region of the 16S rRNA gene which contains maximum nucleotide heterogeneity (Ghyselinck et al., 2013; Yang et al., 2016). Nevertheless, multiple studies have reported lower diversity using this variable region compared to other longer regions, for example, the V2-V3 or V3-V4 regions, or even full-length 16S rRNA sequencing, as these longer regions allow for a more robust separation of closely related sequences, hence increasing and better representing the true diversity of microbial communities (Bukin et al., 2019; Greay et al., 2019). Indeed, while taxonomic assignment in the present study was often verified via the construction of ML phylogenetic trees, some ASVs were incorrectly assigned. For example, when *P. alexandrii* was queried against the prokaryotic amplicon sequence dataset, the top ASV (with a 100 % pairwise identity) was identified as a *Phaeobacter* sp., despite ML tree construction consistently placing the ASV with *P. alexandrii*. As such, it is possible that some diversity of the prokaryotic community was lost throughout the sampling pipeline, hindering or dampening the detection of bacterial antagonists within this dataset.

Nevertheless, ASVs which were phylogenetically similar to six of the seven bacterial antagonists with confirmed activity (*M. adhaerens*, *M. dokdonensis*, *M. idriensis*, *P. alexandrii*, *T. lohafexi*, *V. diazotrophicus*, Chapter 2; Wang et al., 2016) were detected in the amplicon sequence dataset bacterial community

during this sampling period. A peak in the detection of multiple antagonists appeared to occur during the summer sampling points (June – August), throughout which the dominant diatom taxa fluctuated from primarily *Leptocylindrus*, to a diverse community of *Thalassiosira*, *Chaetoceros* and *Minidiscus*, to largely *Pseudo-nitzschia*. While each hit was detected alongside one of its original host species, e.g., *P. alexandrii* and *V. diazotrophicus* were detected alongside *Thalassiosira* sp., *M. adhaerens* was detected when *Chaetoceros* sp., were abundant, the dominant taxa present at the time should not be overlooked. Given the unexpected number of antagonists isolated during the winter *Coscinodiscus* bloom of 2020, sampling efforts such as these could provide pertinent groundwork on which to identify potentially ecologically significant antagonistic interactions in the future.

Further, the assessment of the biogeography of six confirmed diatom-antagonistic bacteria via searches of the *Tara* Ocean Barcode Atlas revealed four species (*H. titanicae*, *M. adhaerens*, *M. dokdonensis*, and *T. lohafexi*) to have significant global ranges that overlapped those of their host species (*Chaetoceros* sp., and *Skeletonema* sp.). Perhaps the most widespread of these global distributions were those of *H. titanicae* and *M. adhaerens* with *Chaetoceros* sp. Both *H. titanicae* and *M. adhaerens* were detected at six and 19 stations respectively, ranging from the Pacific to the Arctic oceans. Not only were these bacteria globally distributed, but they were almost exclusively (with the exception of a single station each) detected at stations where *Chaetoceros* sp. was also detected. This highlights numerous ecosystems (including multiple productive coastal regions) where diatom antagonism by *H. titanicae* and *M. adhaerens* could potentially represent an important driver of *Chaetoceros* success. Analysis of *M. dokdonensis* also revealed an extensive distribution, being detected at 26

stations globally. While *M. dokdonensis* was detected at multiple stations where host *S. marinoi* was not found, the two species did co-occur in 13 coastal stations across the Atlantic, Pacific and Arctic oceans, in addition to the Mediterranean and Red Sea. Conversely, while the biogeographic analysis of *T. lohafexi* and host *T. pseudonana* revealed narrower distribution ranges than *M. adhaerens*, *M. dokdonensis*, *Chaetoceros* sp. and *S. marinoi*, co-occurrence was detected at three stations in the Arctic Ocean, potentially hinting at an important relationship in an important yet often understudied ecosystem. Further, it is important to consider the host ranges of bacterial antagonists isolated in this study, as multiple bacteria were isolated on multiple host species throughout the environmental sampling pipeline. For example, while antagonistic activity of *H. titanicae* was assessed only against *Chaetoceros* sp. in Chapter 2, it was originally isolated on both *T. pseudonana* and *T. weissflogii*, in addition to *Chaetoceros* sp. Similarly, *T. lohafexi* was isolated from both *Thalassiosira* species in addition to *Skeletonema* sp. As such, the overlapping ranges of our WEC antagonists and their potential diatom hosts in the global oceans may extend far beyond the analysis included in this thesis.

Assessing trends in the seasonality and biogeography of WEC diatom-antagonistic bacteria and their susceptible hosts hints that many of these species may potentially represent important drivers of diatom community dynamics, particularly in coastal ocean environments. Certainly, the identification of overlapping niches of globally important diatom taxa with antagonistic bacteria, at both a local and global scale, is a vital step towards determining the role of antagonistic bacteria in the shaping of diatom communities in the global oceans. Further, analysis of amplicon sequence datasets, though not without its limitations, may prove useful in monitoring ‘hotspots’ in the abundance of

confirmed bacterial antagonists. Combining this with knowledge of the dominant diatom taxa present when the antagonist abundance peaks could help identify potential diatom hosts, and present future opportunities to explore antagonistic diatom-bacteria interactions at an ecosystem scale.

General Discussion

Interkingdom interactions are key to the success (or failure) of microbial species within the oceans. As such, understanding the diversity, regulation and prevalence of microbe-microbe interactions at an ecosystem scale is paramount to our understanding of the functional ecology of marine environments. Diatoms, as one of the most successful groups of photosynthetic eukaryotes in the global oceans (Malviya et al., 2016) are involved in a broad spectrum of interactions with marine bacteria, which have considerable impacts both on their physiology and ecology (Amin et al., 2012). In particular, antagonistic bacteria have the potential to regulate diatom ecology and bloom succession through their ability to inhibit the growth of, or even kill diatoms (Paul & Pohnert, 2011; van Tol et al., 2017; Bigalke et al., 2019; Bedoshvili et al., 2021). Nevertheless, the significance of antagonistic diatom-bacteria interactions as drivers of diatom life cycles and bloom regulation poses a significant knowledge gap in the field.

This thesis set out to address this knowledge gap by characterising the diatom pathobiome of a highly productive model ecosystem, the Western English Channel (WEC). Through the establishment and application of a robust environmental sampling pipeline over an annual cycle, utilising a range of bloom-forming diatom species as bait, 18 potential diatom antagonistic bacteria were isolated, spanning 10 orders and four classes of bacteria (**Chapter 1**). Subsequently, physiological laboratory studies of seven of these species highlighted a widespread facultative antagonistic lifestyle mode hidden among diverse bacterial lineages (**Chapter 2**). Finally, the biogeography of confirmed diatom antagonists was investigated to assess co-occurrence with diatom hosts on both a local and global scale, revealing many of the antagonistic bacteria to co-occur globally with ecologically important diatom species (**Chapter 3**).

Chapter 1 (From sea…)

Ecosystem scale assessments of microalgae-antagonistic bacteria in natural environments are far and few between, and those studies which do exist are typically focused more on antagonists of other microalgal species, such as harmful algal bloom-forming dinoflagellates (Coyne et al., 2022). As such, the primary aim of this chapter was to survey the diversity and seasonal trends of diatom-antagonistic bacteria in a model ecosystem over an annual cycle. This required the establishment of a robust sampling pipeline for the systematic isolation of diatom-antagonistic bacteria from natural seawater assemblages, utilising diverse diatom host species. In doing so, this chapter not only provided a library of 18 potential diatom-antagonistic bacteria spanning diverse bacterial lineages, but also captured an unexpected peak in bacterial antagonists (both in diversity and abundance) concurrent with the termination of a winter diatom bloom comprised almost entirely of *Coscinodiscus wailesii* (constituting 77 % of the total phytoplankton biomass at the time of sampling). As this peak occurred around a winter bloom, rather than the characteristic spring bloom as one might expect, this work highlights a need for long-term, routine sampling efforts. Past and present sampling efforts typically focus on narrow sampling windows and/or utilise single host species (Mitsutani et al., 2001; Kang et al., 2005; van Tol et al., 2017) and as such, are likely overlooking a hidden diversity of potentially ecologically significant diatom-antagonistic bacteria.

Although *C. wailesii* was not used as a bait species in this study, the co-occurrence of such a high diversity and abundance of antagonistic bacteria upon the termination of such a bloom could provide important ecological context as to which species may be impacted by antagonistic bacteria in a natural ecosystem,

or alternatively, which species may act as environmental reservoirs for antagonistic bacteria. Unfortunately, whether the antagonists isolated from this sampling point were directly involved in the decline of the *C. wailesii* bloom or rather were opportunistically exploiting the dissolved organic carbon (DOC) that results from a diatom bloom decline (Buchan et al., 2014) remains unclear. More frequent sampling throughout an entire bloom cycle (i.e., collecting weekly or even bi-weekly samples for soft-agar overlay assays) would not only increase the chances of capturing diverse antagonistic bacteria, but would perhaps provide a more detailed insight into the dynamics of these antagonists throughout each of the bloom phases. For example, it would be particularly interesting to conduct assays with samples collected during the early and mid-phases of the bloom to determine if any of the antagonists detected during bloom decline were present before, and if so, to also monitor how the abundance of these bacteria changes throughout the bloom cycle.

Of course, a logical next step would be to extend the sampling method employed in this study to include *C. wailesii* as a bait species, and potentially other important WEC bloom-forming species, such as *Pseudo-nitzschia* species (Widdicombe et al., 2010), as this would hopefully increase the diversity of bacterial antagonists isolated and also provide clues into ecologically significant drivers of diatom bloom cycles. Unfortunately, however, the soft-agar overlay method, though proven to be incredibly successful in this chapter, is not conducive to all potential host species. For example, culturing *Pseudo-nitzschia* species in laboratory settings often proves difficult, and cultivation of some *Pseudo-nitzschia* species on agar rather than in liquid has proven to be unreliable (Sabatino et al., 2015). Thus, for species which grow preferentially in liquid media, the soft-agar overlay assay method would need significant adaptation, and these species would likely

require a dilution to extinction method in liquid media instead (similar to techniques often used to propagate viruses of algae, e.g., Wilson et al., 2002).

There are additional important methodological biases to consider when employing the soft-agar overlay assay method. For example, while this pipeline facilitated the successful isolation of 18 potential antagonists (one of which was previously reported to be a diatom antagonist [Wang et al., 2015], and a further seven of which were confirmed as antagonistic in Chapter 2 of this study), some of the taxa which might have been expected were seemingly underrepresented in this study. For example, whereas *Flavobacteria* are often reported to be algicidal (Mayali & Azam, 2004; Paul & Pohnert, 2011; van Tol et al., 2017), only two *Flavobacteria* isolates were detected in this sampling period (although more could have been hidden in the unprocessed December plaques). While it could simply be that antagonistic *Flavobacteria* such as *Croceibacter atlanticus* and *Kordia algicida* are not particularly abundant in the WEC, it could also be explained by limitations posed by the cultivation aspect of the sampling pipeline. As identification of antagonists in this study relied on the cultivation of pure isolates on ½ YTSS agar, which may have precluded the growth of some 'uncultivatable' species. Indeed, not all plaques could be successfully propagated long-term under laboratory conditions, as plaque P30, identified via 16S rRNA sequencing and Maximum Likelihood tree construction as *Ahrensia kielensis*, proved difficult to maintain on ½ YTSS agar, and an additional three plaques (P60, P65, and P67) could not be successfully propagated or identified. There are adaptations which could be applied to the pipeline which may better facilitate the isolation of hard to culture bacteria, such as the use of different media types (e.g., low nutrient media, or media containing host cell material), although using additional media types would be both costly and time consuming. Conversely,

perhaps a more efficient way of maintaining these antagonists is in co-culture with their diatom hosts, either in soft-agar or liquid co-cultures.

A further pertinent obstacle is the isolation of the 'correct' antagonistic agent from a plaque. For example, five of the plaques selected for bacterial isolation and identification yielded two distinct bacterial colonies from each single plaque streak. As not all of the species that were isolated in this study were confirmed to be antagonistic, it cannot be confirmed which of the two isolates obtained from a single plaque, if any, was responsible for the initial plaque formation. On the other hand, one of the plaques which produced two distinct species resulted in *Maribacter dokdonensis* and *Halomonas titanicae*, both of which are confirmed diatom antagonists (Chapter 2; Wang et al., 2015). Using a concentrated bacterial inoculum created using natural seawater bacterial assemblages is undoubtedly going to result in a milieu of species within the diatom-bacteria agar lawn, and obtaining multiple species from a single plaque is inevitable to a certain extent, however, again, perhaps a dilution to extinction method would help eliminate some of the non-antagonistic bacteria.

Despite the methodological challenges faced in this chapter, the isolation of diverse antagonistic bacteria and concurrent identification of trends in their seasonal dynamics provides an excellent framework on which to build a more comprehensive picture of diatom-bacteria interactions at an ecosystem scale. The end result of this chapter was not only an increased understanding of the diversity of antagonistic bacteria, but also a library of ecologically relevant potential antagonists with which further research can be done into the physiology and regulation of such interactions, thus offering insight into the potential ecological significance of these interactions.

Chapter 2 (…to lab…)

Laboratory studies of diatom-bacteria model systems are instrumental in elucidating the physiological impacts of antagonistic bacteria on their diatom hosts, in addition to untangling the regulatory pathways involved in maintaining such interactions. As such, having a diverse library of ecologically derived bacterial antagonists that interact with a range of bloom-forming diatom hosts is an invaluable resource in the investigation of the potential ecological implications of such interactions. Nevertheless, although fundamentally important for the isolation of these antagonistic bacteria, the soft-agar overlay assay, whereby diatom host cells are immobilised in agarose, does not represent a particularly 'natural' planktonic environment, and thus liquid co-cultivation trials were necessary to fully explore the physiological impacts of these associations. Unfortunately, however, investigating 'naturally occurring' interactions in laboratory settings is no easy feat.

Initial co-cultivation trials conducted in Chapter 2 resulted in minor physiological impacts on the diatom hosts, i.e., limited effects were seen on diatom growth, and characteristic signs of algicidal activity, such as diatom cell lysis, were not observed. Multiple subsequent co-culture trials were conducted, altering various parameters in an attempt to induce antagonistic activity. Finally, after iterative co-cultivation trials, it was discovered that pre-cultivation of *Ponticoccus alexandrii* (selected as a model antagonist due to its seasonal persistence in Chapter 1) on dead diatom media (DDM) could induce significant, robust growth inhibitory activity. Although lifestyle switches of this kind are not a novel concept (Seyedsayamdost et al., 2011; Barak-Gavish et al., 2023), this thesis appears to be the first to report a conserved switch across diverse bacterial lineages. This finding not only represents a potentially novel mechanism of lifestyle switch, but

also highlights the cryptic nature of diatom-antagonism and some of the difficulties faced when studying these interactions in laboratory cultures.

While seven distinct species exhibited robust antagonistic activity when pre-cultivated on DDM, this study has unfortunately only begun to scratch the surface of this regulatory pathway. For example, 11 species of bacteria from Chapter 1 were cultivated on DDM, and while seven exhibited growth inhibitory activity, antagonism in the remaining four species could not be induced in this manner. This raises significant questions, for example, as to whether these species are true antagonists, or whether there is simply a different mechanism altogether that is governing these specific interactions. For example, *Marinobacter algicola*, a known algal-antagonist (Zheng et al., 2018), did not demonstrate antagonistic activity under the conditions explored in this thesis (i.e., when cultured on either ½ YTSS or DDM comprised of *Skeletonema* sp. PLY627, and subsequently inoculated into liquid co-cultures of *Skeletonema* sp.), which could indicate that it is regulated by a different mechanism. Indeed, while the current literature reports of lifestyle switches in algal-bacteria systems are limited, two distinct mechanisms are described (Seyedsayamdost et al., 2011; Barak-Gavish et al., 2023). The first describes a switch from synergism to antagonism in response to p-Coumaric acid (pCA), an algal metabolite indicative of algal senescence (Seyedsayamdost et al., 2011), whereas the second describes a similar switch, this time in response to algal-derived dimethylsulfoniopropionate (DMSP, Barak-Gavish et al., 2023). In this thesis, the addition of pCA to diatom-bacteria co-cultures appeared to have no significant impact on the antagonistic activity of three bacteria, *Marinobacter adhaerens*, *P. alexandrii* and *Roseovarius mucosus*, even at previously effective concentrations (1 mM), whereas DMSP was not tested. As such, the induction of antagonistic activity via pre-cultivation on DDM could be the result of the

presence of an unknown diatom metabolite trigger. Alternatively, induction could be the result of nutrient limitation. As discussed in Chapter 2, there are numerous examples of bacteria in which the synthesis of energetically expensive antimicrobial compounds is supressed in the presence of high-energy carbon sources, such as glucose (Demain and Inamine, 1970; Bhatnagar et al., 1988). A simple preliminary trial was conducted to begin to elucidate whether induction was the result of diatom-derived signals or nutrient starvation, whereby *P. alexandrii* was cultured on a media comprised of both DDM and ½ YTSS at a 1:1 ratio. This method was unable to induce antagonism, and ultimately, conclusions were unable to be drawn from this experimental set up, as the DDM-½ YTSS mixture naturally diluted the amount of diatom matter present while still presenting a high ratio of ½ YTSS. Nevertheless, further trials, such as cultivation of antagonists on a dilution series of ½ YTSS concentrations, or the addition of alternative carbon sources to DDM whilst controlling the concentration of diatom matter within DDM plates could help elucidate the trigger which underpins this induction. Further, the impact of pre-culturing *P. alexandrii* on media comprised of autoclaved cultures of other phytoplankton taxa (e.g., dinoflagellates) could be tested to examine the specificity of the response to diatom derived organic matter.

However, perhaps the most comprehensive insights into how this widespread mechanism is regulated could be gained through transcriptome analysis of antagonistic bacteria cultured on DDM versus ½ YTSS. Upon the discovery of an antagonistic lifestyle switch, one of the aims of this thesis was to perform transcriptome analysis using *P. alexandrii-T. pseudonana* as a model system. To do so, *P. alexandrii* was cultivated on DDM (comprised of *T. pseudonana*) to represent ‘actively antagonistic’ *P. alexandrii*, and was also cultivated on ½ YTSS to represent an ‘inactive’ *P. alexandrii* culture, as to gain an insight into which

pathways were being up- or down-regulated in response to the different media types. However, growth of *P. alexandrii* (and indeed the other confirmed species) on DDM was substantially less than on ½ YTSS, and as such it was difficult to obtain sufficient yields of bacteria to produce workable RNA for transcriptome analysis of 'actively' antagonistic DDM-grown *P. alexandrii*. Cultivation of bacteria on DDM would therefore require further optimisation in order to effectively conduct transcriptome analysis.

Being able to elucidate the regulatory pathways that underpin antagonistic diatom-bacteria interactions is not only invaluable in untangling and monitoring ecological interactions but could also provide important insight for biotechnology applications. For example, lytic bacterium *Labrenzia* sp. was demonstrated be beneficial in harvesting lipids and other useful diatom-derived compounds from *P. tricornutum*, pinning it as a useful candidate to use in biotechnology systems such as those aimed at biofuel production (Chen et al., 2015). However, similar to the present study, *Labrenzia* sp. demonstrated lytic activity only under certain oligotrophic conditions, and thus understanding how lytic, or indeed antagonistic activity, is regulated, is vital for optimising such systems.

Further questions remain regarding the interaction between *P. alexandrii* and *Chaetoceros* sp. PLY617, as although *P. alexandrii* appears to initially behave antagonistically towards *Chaetoceros* sp., diatom growth was repeatedly observed to recover in later phases of the co-culture experiments. Unfortunately, the dynamics of this specific interaction are unclear, however, as this study is not the first to report a *Chaetoceros* defence system, perhaps important insights can be gained from previous studies. For example, a study by Meyer and colleagues investigated the mechanism by which *Chaetoceros didymus* is able to defend itself from broad-range algicidal bacterium *Kordia algicida* (Meyer et al., 2018). It

was revealed that the resistance of *C. didymus* is achieved by the production of oxylipins such as hydroxylatedeicosapentaenoic acids (HEPEs), which inhibits the growth, and subsequently antagonistic activity, of *K. algicida.* Studies of diatom defence are currently extremely limited yet represent a potentially significant driver of phytoplankton community dynamics, as many *Chaetoceros* species are incredibly successful bloom-formers (Booth et al., 2002; Begum et al., 2015; Tomaru et al., 2018). Although it remains largely unclear what is responsible for their success, resistance to potential pathogens is certainly an adaptation that could provide *Chaetoceros* species with a competitive advantage over other diatom or phytoplankton species. As such, understanding the dynamics of the interaction between *Chaetoceros* sp. and seasonally persistent *P. alexandrii* observed in this thesis would be pertinent to our understanding of biotic drivers of diatom blooms in the WEC. The growth of *P. alexandrii* in co-culture with susceptible diatoms was not measured in this thesis, however the use of techniques such as flow cytometry to monitor bacterial growth dynamics in co-culture may prove to be particularly illuminating.

Although further work is required to build a comprehensive picture of exactly how antagonistic activity is induced through cultivation on DDM, this chapter provides fundamental insight into the regulation of diatom-antagonism and highlights significant antagonistic activity against important bloom-forming diatom species by seven ecologically derived bacteria.

Chapter 3 (…and back again.)

As the growth inhibitory effects exhibited by the bacteria in Chapter 2 pose significant potential implications for diatom physiology and possibly ecology,

understanding their prevalence and co-occurrence with potential diatom hosts in marine environments is of paramount importance. Therefore, the aim of the final chapter of this work was to investigate the seasonal dynamics and biogeography of these potentially ecologically significant bacteria and their hosts on both a local and a global scale.

Metabarcoding techniques are widely used to investigate co-occurrence trends of microbial species (Sison-Mangus et al., 2014; Taylor et al., 2014; Gibson et al., 2022), as this type of sequencing provides a picture of microbial diversity on a community scale, in addition to facilitating the monitoring of taxa of interest over time. Thus, metabarcoding of the eukaryotic and prokaryotic communities within the WEC was conducted over an annual cycle to monitor the abundance of confirmed bacterial antagonists (Chapter 2), while also monitoring trends in the dominant diatom taxa in order to assess whether bacterial antagonists co-occur with their tested diatom hosts and to what extent. While antagonists of interest were detected concurrent with their diatom hosts, sampling limitations meant that it was difficult to draw conclusions about seasonal trends of these bacteria.

For example, although a peak in the detection of bacterial antagonists occurred during the summer sampling period, detection of antagonists was largely ‘patchy’, likely due to low sampling frequency. Samples were collected monthly where possible throughout a 12-month annual cycle, though this is likely insufficient for capturing the true dynamic nature of marine microbial communities, where fluctuations in diversity and abundance may occur on the scale of days. As such, increased sampling frequency is an important consideration when conducting similar studies. Sampling communities frequently throughout the different phases of a diatom bloom would help build a more comprehensive picture of the dynamics of antagonistic bacteria. As with Chapter 1, it would be interesting to

determine whether bacterial antagonists peak solely upon diatom bloom decline, or whether these bacteria are abundant during earlier bloom phases too.

Furthermore, although identifying co-occurrences of interacting taxa (as demonstrated by laboratory studies) certainly indicates the potential significance of such interactions, further work is required to provide important ecological context as to whether these interactions are representative of those observed in natural environments. While the interactions explored in this study have proven to be robust under laboratory conditions, and widespread co-occurrences of these taxa has been demonstrated by metabarcode analysis, marine planktonic habitats are incredibly varied and dilute. Interactions between marine microbes may result from chance encounters or may be facilitated by motile bacteria utilising chemotaxis in order to seek out and associate with host organisms of interest (Sonnenschein et al., 2012; Li et al., 2016; Smriga et al., 2016). Although the library of antagonists explored in this thesis contains a mixture of both motile and non-motile bacteria (for example, *M. adhaerens* uses chemotaxis to seek out diatom host *Thalassiosira weissflogii*, while *P. alexandrii* is described as non-motile, Sonnenschein et al., 2012; Yang et al., 2018), it is not known how associations are formed between the bacteria and their host organisms investigated in this study, thus it remains unclear whether these associations in natural environments would be likely. Chemotaxis assays may provide evidence of whether motile bacterial antagonists actively seek out their diatom hosts. However, demonstrating physical associations of these interacting taxa in natural seawater assemblages would elevate our understanding of antagonistic diatom-bacteria interactions even further. There are multiple powerful tools available by which these interactions can be explored. For example, fluorescence in-situ hybridization (FISH) could be employed to not only allow the quantification of

absolute abundances of bacteria of interest (as opposed to the relative abundances provided by metabarcoding), but also demonstrate physical proximity of bacterial antagonists to diatom cells in natural seawater samples (Grossart et al., 2005).

Additionally, combining techniques such as FISH with RNA sequencing would allow not only visual confirmation of antagonistic associations, but could also help elucidate whether these bacteria are functionally active throughout these associations (e.g., Sapp et al., 2008; Klindworth et al., 2014). As our knowledge of algicidal mechanisms and gene pathways grows, it would be illuminating to examine the activity and expression of antagonistic pathways by bacteria in close proximity to diatom hosts throughout a bloom cycle. The combination of such techniques throughout a natural diatom bloom would be invaluable in further determining how specific antagonistic bacteria may be interacting with diatom blooms in the oceans, and would be the final puzzle piece in determining their contribution to driving diatom bloom succession.

Concluding remarks

Together, the chapters of this thesis contribute significant insight into our understanding of the abundance, distribution and dynamics of antagonistic diatom-bacteria interactions at an ecosystem scale. Through a combination of both laboratory and field-based approaches, this thesis reports a hidden diversity of novel diatom-antagonistic bacteria in a highly productive coastal ecosystem, as well as the discovery of cryptic facultative behaviour in diverse bacterial lineages. As antagonistic bacteria represent potentially significant drivers of the success of one of the ocean's most important planktonic groups, this work calls

to attention a need for increased efforts in the monitoring and investigation of antagonistic diatom-bacteria interactions in marine ecosystems.

References

Abellan-Schneyder, I., Matchado, M. S., Reitmeier, S., Sommer, A., Sewald, Z., Baumbach, J., List, M., & Neuhaus, K. (2021). Primer, Pipelines, Parameters: Issues in 16S rRNA Gene Sequencing. MSphere, *6*(1). https://doi.org/10.1128/msphere.01202-20

Altschul, S. F., Gish, W., Miller, W., Myers, E. W., & Lipman, D. J. (1990). Basic local alignment search tool. *Journal of Molecular Biology,* 215(3), 403–410. https://doi.org/10.1016/S0022-2836(05)80360-2

Amin, S. A., Green, D. H., Küpper, F. C., & Carrano, C. J. (2009). Vibrioferrin, an unusual marine siderophore: Iron binding, photochemistry, and biological implications. *Inorganic Chemistry*, *4*8(23), 11451–11458. https://doi.org/10.1021/ic9016883

Amin, S. A., Hmelo, L. R., Van Tol, H. M., Durham, B. P., Carlson, L. T., Heal, K. R., Morales, R. L., Berthiaume, C. T., Parker, M. S., Djunaedi, B., Ingalls, A. E., Parsek, M. R., Moran, M. A., & Armbrust, E. V. (2015). Interaction and signalling between a cosmopolitan phytoplankton and associated bacteria. *Nature*, 522(7554), 98–101. https://doi.org/10.1038/nature14488

Amin, S. A., Parker, M. S., & Armbrust, E. V. (2012). Interactions between Diatoms and Bacteria. *Microbiology and Molecular Biology Reviews : MMBR*, *76*(3), 667. https://doi.org/10.1128/MMBR.00007-12

Apprill, A., McNally, S., Parsons, R., & Weber, L. (2015). Minor revision to V4 region SSU rRNA 806R gene primer greatly increases detection of SAR11 bacterioplankton. *Aquatic Microbial Ecology,* 75(2), 129-137. https://doi.org/10.3354/ame01753

Armbrust, E. V., Berges, J. A., Bowler, C., Green, B. R., Martinez, D., Putnam, N. H., Zhou, S., Allen, A. E., Apt, K. E., Bechner, M., Brzezinski, M. A., Chaal, B. K., Chiovitti, A., Davis, A. K., Demarest, M. S., Detter, J. C., Glavina, T., Goodstein, D., Hadi, M. Z., … Rokhsar, D. S. (2004). The genome of the diatom Thalassiosira Pseudonana: Ecology, evolution, and metabolism. *Science*, *306*(5693), 79–86. https:// doi: 10.1126/science.1101156

Arsenieff, L., Simon, N., Rigaut-Jalabert, F., Le Gall, F., Chaffron, S., Corre, E., Com, E., Bigeard, E. and Baudoux, A.C., 2019. First viruses infecting the marine diatom Guinardia delicatula. *Frontiers in microbiology*, 9, p.3235. https://doi.org/10.3389/fmicb.2018.03235

Arsenieff, L., Le Gall, F., Rigaut-Jalabert, F., Mahé, F., Sarno, D., Gouhier, L., Baudoux, A. C., & Simon, N. (2020). Diversity and dynamics of relevant nanoplanktonic diatoms in the Western English Channel. *The ISME Journal*, *14*(8), 1966. https://doi.org/10.1038/S41396-020-0659-6

Azam, F., Fenchel, T., Field, J.G., Gray, J.S., Meyer-Reil, L.A. and Thingstad, F.J.M.E.P.S., (1983). The ecological role of water-column microbes in the sea. Marine ecology progress series. Oldendorf, 10(3), pp.257-263. Raymond, J. A., & Kim, H. J. (2012). Possible Role of Horizontal Gene Transfer in the

Colonization of Sea Ice by Algae. *PLOS* ONE, 7(5), e35968. https://doi.org/10.1371/JOURNAL.PONE.0035968

Barak-Gavish, N., Dassa, B., Kuhlisch, C., Nussbaum, I., Brandis, A., Rosenberg, G., Avraham, R., & Vardi, A. (2023). Bacterial lifestyle switch in response to algal metabolites. *eLife*, *12*. https://doi.org/10.7554/ELIFE.84400

Bartolek, Z., Creveld, S. G. van, Coesel, S., Cain, K. R., Schatz, M., Morales, R., & Virginia Armbrust, E. (2022). Flavobacterial exudates disrupt cell cycle progression and metabolism of the diatom Thalassiosira pseudonana. *The ISME Journal*, 16(12), 2741–2751. https://doi.org/10.1038/S41396-022-01313-9

Bates, S. S., Garrison, D. L., & Horner, R. A. (1998). *Physiological ecology of harmful algal blooms*. 267–292.

Bedoshvili, Y., Bayramova, E., Sudakov, N., Klimenkov, I., Kurilkina, M., Likhoshway, Y., & Zakharova, Y. (2021). Impact of Algicidal Bacillus mycoides on Diatom Ulnaria acus from Lake Baikal. *Diversity 2021, Vol. 13, Page* 469, 13(10), 469. https://doi.org/10.3390/D13100469

Begum, M., Sahu, B. K., Das, A. K., Vinithkumar, N. V., & Kirubagaran, R. (2015). Extensive Chaetoceros curvisetus bloom in relation to water quality in Port Blair Bay, Andaman Islands. *Environmental Monitoring and Assessment*, 187(5), 1–14. https://doi.org/10.1007/S10661-015-4461-2

Behringer, G., Ochsenkühn, M. A., Fei, C., Fanning, J., Koester, J. A., & Amin, S. A. (2018). Bacterial communities of diatoms display strong conservation across strains and time. *Frontiers in Microbiology*, 9(APR), 340664. https://doi.org/10.3389/FMICB.2018.00659

Bell, W., & Mitchell, R. (1972). Chemotactic and growth responses of marine bacteria to algal extracellular. *The Biological Bulletin*, 143(2), 265–277. https://doi.org/10.2307/1540052

Benoiston, A. S., Ibarbalz, F. M., Bittner, L., Guidi, L., Jahn, O., Dutkiewicz, S., & Bowler, C. (2017). The evolution of diatoms and their biogeochemical functions. *Philosophical Transactions of the Royal Society B: Biological Sciences*, 372(1728). https://doi.org/10.1098/RSTB.2016.0397

Bermejo, P., Helbling, E. W., Durán-Romero, C., Cabrerizo, M. J., & Villafañe, V. E. (2018). Abiotic control of phytoplankton blooms in temperate coastal marine ecosystems: A case study in the South Atlantic Ocean. *Science of The Total Environment*, 612, 894–902. https://doi.org/10.1016/j.scitotenv.2017.08.176

Bertrand, E. M., McCrow, J. P., Moustafa, A., Zheng, H., McQuaid, J. B., Delmont, T. O., Post, A. F., Sipler, R. E., Spackeen, J. L., Xu, K., Bronk, D. A., Hutchins, D. A., Allen, A. E., & Karl, D. M. (2015). Phytoplankton-bacterial interactions mediate micronutrient colimitation at the coastal Antarctic sea ice edge. *Proceedings of the National Academy of Sciences of the United States of America*, 112(32), 9938–9943. https://doi.org/10.1073/pnas.1501615112

Bhatnagar, R. K., Doull, J. L., & Vining, L. C. (1988). Role of the carbon source in regulating chloramphenicol production by *Streptomyces venezuelae* : studies in

batch and continuous cultures. *Canadian Journal of Microbiology*, 34(11), 1217–1223. https://doi.org/10.1139/m88-214

Bhatnagar, R. K., Doull, J. L., & Vining, L. C. (2011). Role of the carbon source in regulating chloramphenicol production by Streptomyces venezuelae: studies in batch and continuous cultures. Https://Doi.*Org/10.1139/M88-214*, 34(11), 1217–1223. https://doi.org/10.1139/M88-214

Bhattacharya, D., & Medlin, L. (1995). The phylogeny of plastids: a review based on comparisons of small-subunit ribosomal RNA coding regions. *Journal of Phycology*, 31(4), 489–498. https://doi.org/10.1111/j.1529-8817.1995.tb02542.x

Bigalke, A., Meyer, N., Papanikolopoulou, L. A., Wiltshire, K. H., & Pohnert, G. (2019). The algicidal bacterium Kordia algicida shapes a natural plankton community. *Applied and Environmental Microbiology*, *85*(7). https://doi.org/10.1128/AEM.02779-18

Booth, B. C., Larouche, P., Bélanger, S., Klein, B., Amiel, D., & Mei, Z.-P. (2002). Dynamics of Chaetoceros socialis blooms in the North Water. *Deep Sea Research Part II: Topical Studies in Oceanography*, *49*(22–23), 5003–5025. https://doi.org/10.1016/S0967-0645(02)00175-3

Bowler, C., Allen, A. E., Badger, J. H., Grimwood, J., Jabbari, K., Kuo, A., Maheswari, U., Martens, C., Maumus, F., Otillar, R. P., Rayko, E., Salamov, A., Vandepoele, K., Beszteri, B., Gruber, A., Heijde, M., Katinka, M., Mock, T., Valentin, K., … Grigoriev, I. V. (2008). The Phaeodactylum genome reveals the evolutionary history of diatom genomes. *Nature*, 456(7219), 239–244. https://doi.org/10.1038/nature07410

Bowler, C., Vardi, A., & Allen, A. E. (2010). Oceanographic and Biogeochemical Insights from Diatom Genomes. *Annual Review of Marine Science*, 2(1), 333–365. https://doi.org/10.1146/annurev-marine-120308-081051

Bramucci, A. R., Labeeuw, L., Orata, F. D., Ryan, E. M., Malmstrom, R. R., & Case, R. J. (2018). The bacterial symbiont Phaeobacter inhibens Shapes the life history of its algal host emiliania huxleyi. *Frontiers in Marine Science*, 5(MAY), 364965. https://doi.org/10.3389/FMARS.2018.00188

Bristow, L. A., Mohr, W., Ahmerkamp, S., & Kuypers, M. M. M. (2017). Nutrients that limit growth in the ocean. In *Current Biology* (Vol. 27, Issue 11, pp. R474–R478). Cell Press. https://doi.org/10.1016/j.cub.2017.03.030

Brownlee, C., Helliwell, K. E., Meeda, Y., McLachlan, D., Murphy, E. A., & Wheeler, G. L. (2023). Regulation and integration of membrane transport in marine diatoms. *Seminars in Cell & Developmental Biology*, 134, 79–89. https://doi.org/10.1016/J.SEMCDB.2022.03.006

Bruckner, C. G., Rahul Bahulikar, †, Monali Rahalkar, † ‡, Schink, ‡ Bernhard, & Kroth, P. G. (2008). Bacteria Associated with Benthic Diatoms from Lake Constance: Phylogeny and Influences on Diatom Growth and Secretion of Extracellular Polymeric Substances. Applied and Environmental Microbiology, 74(24), 7740–7749. https://doi.org/10.1128/AEM.01399-08

Buaya, A., Kraberg, A., & Thines, M. (2019). Dual culture of the oomycete Lagenisma coscinodisci Drebes and Coscinodiscus diatoms as a model for plankton/parasite interactions. *Helgoland Marine Re*search, 73(1), 1–6. https://doi.org/10.1186/S10152-019-0523-0

Buchan, A., LeCleir, G. R., Gulvik, C. A., & González, J. M. (2014). Master recyclers: features and functions of bacteria associated with phytoplankton blooms. *Nature Reviews Microbiology 2014 12:1*0, 12(10), 686–698. https://doi.org/10.1038/nrmicro3326

Bukin, Y. S., Galachyants, Y. P., Morozov, I. V., Bukin, S. V., Zakharenko, A. S., & Zemskaya, T. I. (2019). The effect of 16S rRNA region choice on bacterial community metabarcoding results. *Scientific Data 2019 6:1*, *6*(1), 1–14. https://doi.org/10.1038/sdata.2019.7

Burki, F., Roger, A. J., Brown, M. W., Simpson, A. G. B. (2020). *The New Tree of Eukaryotes.* Trends in Ecology & Evolution, 35(1), 43-55. https://doi.org/10.1016/j.tree.2019.08.008

Callahan, B. J., Grinevich, D., Thakur, S., Balamotis, M. A., & Yehezkel, T. Ben. (2021). Ultra-accurate microbial amplicon sequencing with synthetic long reads. *Micr*obiome, 9(1), 1–13. https://doi.org/10.1186/S40168-021-01072-3

Callahan, B. J., McMurdie, P. J., Rosen, M. J., Han, A. W., Johnson, A. J. A., & Holmes, S. P. (2016). DADA2: High-resolution sample inference from Illumina amplicon data. *Nature Methods 2016 13*:7, 13(7), 581–583. https://doi.org/10.1038/nmeth.3869

Caporaso, J.G., Lauber, C.L., Walters, W.A., Berg-Lyons, D., Lozupone, C.A., Turnbaugh, P.J., Fierer, N. and Knight, R., 2011. Global patterns of 16S rRNA diversity at a depth of millions of sequences per sample. *Proceedings of the national academy of sciences*, 108(supplement_1), pp.4516-4522. https://doi.org/10.1073/pnas.1000080107

Chan, C. X., Reyes-Prieto, A., & Bhattacharya, D. (2011). Red and Green Algal Origin of Diatom Membrane Transporters: Insights into Environmental Adaptation and Cell Evolution. *PloS* ONE, 6(12), 29138. https://doi.org/10.1371/journal.pone.0029138

Chen, Z., Zhang, B., Zhang, J., Lei, X., Zhang, H., Li, Y., Yang, L., Zheng, W., Tian, Y., Boughner, L. A., Xu, H., & Zheng, T. (2015). A lytic bacterium's potential application in biofuel production through directly lysing the diatom Phaeodactylum tricornutum cell. *Algal Res*earch, 12, 197–205. https://doi.org/10.1016/j.algal.2015.08.023

Chepurnov, V. A., & Mann, D. G. (2004). Auxosporulation of Licmophora communis (Bacillariophyta) and a review of mating systems and sexual reproduction in araphid pennate diatoms. *Phycological Res*earch, 52(1), 1–12. https://doi.org/10.1111/j.1440-1835.2003.00319.x

Chi, W., Zheng, L., He, C., Han, B., Zheng, M., Gao, W., Sun, C., Zhou, G., & Gao, X. (2017). Quorum sensing of microalgae associated marine Ponticoccus sp.

PD-2 and its algicidal function regulation. *AMB* Express, 7(1), 59. https://doi.org/10.1186/s13568-017-0357-6

Cole, J. J., Findlay, S., & Pace, M. L. (1988). *Bacterial production in fresh and saltwater ecosystems: a cross-system overview*. *43*, 1–10.

Cole, J. R., Wang, Q., Fish, J. A., Chai, B., McGarrell, D. M., Sun, Y., Brown, C. T., Porras-Alfaro, A., Kuske, C. R., & Tiedje, J. M. (2014). Ribosomal Database Project: data and tools for high throughput rRNA analysis. *Nucleic Acids Research*, 42(D1), D633–D642. https://doi.org/10.1093/NAR/GKT1244

Costa, R. R., Mendes, C. R. B., Tavano, V. M., Dotto, T. S., Kerr, R., Monteiro, T., Odebrecht, C., & Secchi, E. R. (2020). Dynamics of an intense diatom bloom in the Northern Antarctic Peninsula, February 2016. *Limnology and Oceanography,* 65(9), 2056–2075. https://doi.org/10.1002/LNO.11437

Coyne, K. J., Wang, Y., & Johnson, G. (2022). Algicidal Bacteria: A Review of Current Knowledge and Applications to Control Harmful Algal Blooms. *Frontiers in Microb*iology, 13, 871177. https://doi.org/10.3389/FMICB.2022.871177

Croft, M. T., Lawrence, A. D., Raux-Deery, E., Warren, M. J., & Smith, A. G. (2005). Algae acquire vitamin B12 through a symbiotic relationship with bacteria. *Nature,* 438(7064), 90–93. https://doi.org/10.1038/nature04056

Dai, Y., Yang, S., Zhao, D., Hu, C., Xu, W., Anderson, D. M., Li, Y., Song, X. P., Boyce, D. G., Gibson, L., Zheng, C., & Feng, L. (2023). Coastal phytoplankton blooms expand and intensify in the 21st century. *Nature 2023 615:7951*, 615(7951), 280–284. https://doi.org/10.1038/s41586-023-05760-y

Demain, A. L., & Inamine, E. (1970). Biochemistry and Regulation of Streptomycin and Mannosidostreptomycinase (a-D-Mannosidase) Formation. *Bacteriological Reviews,* 1–19. https://journals.asm.org/journal/br

Deng, Y., Mauri, M., Vallet, M., Staudinger, M., Allen, R.J. and Pohnert, G., 2022. Dynamic diatom-bacteria consortia in synthetic plankton communities. *Applied and Environmental Microbiology*, 88(22), pp.e01619-22. https://doi.org/10.1128/aem.01619-22

Deschamps, P., & Moreira, D. (2012). Reevaluating the Green Contribution to Diatom Genomes. *Genome Biology and Evolut*ion, 4(7), 683–688. https://doi.org/10.1093/gbe/evs053

Diner, R. E., Schwenck, S. M., McCrow, J. P., Zheng, H., & Allen, A. E. (2016). Genetic manipulation of competition for nitrate between heterotrophic bacteria and diatoms. *Frontiers in Microbi*ology, 7(JUN), 880. https://doi.org/10.3389/fmicb.2016.00880

Ducklow, H. W., Kirchman, D. L., Quinby, H. L., Carlson, C. A., & Dam, H. G. (1993). Stocks and dynamics of bacterioplankton carbon during the spring bloom in the eastern North Atlantic Ocean. *Deep Sea Research Part II: Topical Studies in Oceanography,* 40(1–2), 245–263. https://doi.org/10.1016/0967-0645(93)90016-G

Durham, B. P. (2021). Deciphering Metabolic Currencies That Support Marine Microbial Networks. *Msyst*ems, 6(4), 763–784. https://doi.org/10.1128/msystems.00763-21

Durham, B. P., Sharma, S., Luo, H., Smith, C. B., Amin, S. A., Bender, S. J., Dearth, S. P., Van Mooy, B. A. S., Campagna, S. R., Kujawinski, E. B., Armbrust, E. V., & Moran, M. A. (2015). Cryptic carbon and sulfur cycling between surface ocean plankton. *Proceedings of the National Academy of Sciences of the United States of Americ*a, 112(2), 453–457. https://doi.org/10.1073/pnas.1413137112

Edwards, M., Beaugrand, G., Kléparski, L., Hélaouët, P., & Reid, P. C. (2022). Climate variability and multi-decadal diatom abundance in the Northeast Atlantic. *Communications Earth & Environment 2*022 3:1, 3(1), 1–8. https://doi.org/10.1038/s43247-022-00492-9

Egge, J., & Aksnes, D. (1992). Silicate as regulating nutrient in phytoplankton competition. *Marine Ecology Progress S*eries, 83, 281–289. https://doi.org/10.3354/meps083281

Falciatore, A., Jaubert, M., Bouly, J. P., Bailleul, B., & Mock, T. (2020). Diatom molecular research comes of age: Model species for studying phytoplankton biology and diversity[open]. In *Plant Cell* (Vol. 32, Issue 3, pp. 547–572). American Society of Plant Biologists. https://doi.org/10.1105/tpc.19.00158

Fandino, L. B., Riemann, L., Steward, G. F., & Azam, F. (2005). Population dynamics of Cytophaga-Flavobacteria during marine phytoplankton blooms analyzed by real-time quantitative PCR. *Aquatic Microbial Ecology*, *40*(3), 251–257. https://doi.org/10.3354/AME040251

Ferrante, M, Annunziata, R, Russo, M, T, Manfellotto, F. (2020) Axenic Diatoms cultures protocol. *Protocols.io.* dx.doi.org/10.17504/protocols.io.8pihvke

Ferris, J. A., & Lehman, J. T. (2007). Interannual variation in diatom bloom dynamics: Roles of hydrology, nutrient limitation, sinking, and whole lake manipulation. *Water Research*, 41(12), 2551–2562. https://doi.org/10.1016/J.WATRES.2007.03.027

Foster, R. A., Kuypers, M. M. M., Vagner, T., Paerl, R. W., Musat, N., & Zehr, J. P. (2011). Nitrogen fixation and transfer in open ocean diatom–cyanobacterial symbioses. *The ISME Journa*l, 5(9), 1484–1493. https://doi.org/10.1038/ismej.2011.26

Fry, B., & Wainright, S. C. (1991). Diatom sources of 13C-rich carbon in marine food webs. *Marine Ecology Progress Seri*es, 76(2), 149–157. https://doi.org/10.3354/MEPS076149

Fung, I. Y., Meyn, S. K., Tegen, I., Doney, S. C., John, J. G., & Bishop, J. K. B. (2000). Iron supply and demand in the upper ocean. *Global Biogeochemical Cycl*es, 14(1), 281–295. https://doi.org/10.1029/1999gb900059

Gärdes, A., Iversen, M. H., Grossart, H. P., Passow, U., & Ullrich, M. S. (2010). Diatom-associated bacteria are required for aggregation of Thalassiosira

weissflogii. *The ISME Journal 2011* 5:3, 5(3), 436–445. https://doi.org/10.1038/ismej.2010.145

Gärdes, A., Ramaye, Y., Grossart, H. P., Passow, U., & Ullrich, M. S. (2012). Effects of Marinobacter adhaerens HP15 on polymer exudation by Thalassiosira weissflogii at different N:P ratios. *Marine Ecology Progress* Series, 46*1*, 1–14. https://doi.org/10.3354/MEPS09894

Geng, H., Bruhn, J. B., Nielsen, K. F., Gram, L., & Belas, R. (2008). Genetic dissection of tropodithietic acid biosynthesis by marine roseobacters. *Applied and Environmental Microbiology*, 74(5), 1535–1545. https://doi.org/10.1128/AEM.02339-07/SUPPL_FILE/071219_AEM02339_07_SUPPLEMENTAL_FIGURES.DOC

Ghyselinck, J., Pfeiffer, S., Heylen, K., Sessitsch, A., & De Vos, P. (2013). The Effect of Primer Choice and Short Read Sequences on the Outcome of 16S rRNA Gene Based Diversity Studies. *PLOS* ONE, 8(8), e71360. https://doi.org/10.1371/JOURNAL.PONE.0071360

Gibbs, S. P. (1981). THE CHLOROPLASTS OF SOME ALGAL GROUPS MAY HAVE EVOLVED FROM ENDOSYMBIOTIC EUKARYOTIC ALGAE. *Annals of the New York Academy of Sciences*, *361*(1 Origins and E), 193–208. https://doi.org/10.1111/j.1749-6632.1981.tb54365.x

Gibson, K., Song, H., & Chen, N. (2022). Metabarcoding analysis of microbiome dynamics during a Phaeocystis globosa bloom in the Beibu Gulf, China. *Harmful* Algae, 114, 102217. https://doi.org/10.1016/J.HAL.2022.102217

Gilbert, J. A., Field, D., Swift, P., Newbold, L., Oliver, A., Smyth, T., Somerfield, P. J., Huse, S., & Joint, I. (2009). The seasonal structure of microbial communities in the Western English Channel. *Environmental Microbiology*, 11(12), 3132–3139. https://doi.org/10.1111/j.1462-2920.2009.02017.x

Gilbert, J. A., Steele, J. A., Caporaso, J. G., Steinbrück, L., Reeder, J., Temperton, B., Huse, S., McHardy, A. C., Knight, R., Joint, I., Somerfield, P., Fuhrman, J. A., & Field, D. (2011). Defining seasonal marine microbial community dynamics. *The ISME Journal 2012* 6:2, 6(2), 298–308. https://doi.org/10.1038/ismej.2011.107

Gratia, A. (1936). The Numerical Relation between Lysogenic Bacteria and the Phage Particles which they carry. *Ann. Inst. Pasteur*, *57*, 652–676.

Greay, T. L., Gofton, A. W., Zahedi, A., Paparini, A., Linge, K. L., Joll, C. A., & Ryan, U. M. (2019). Evaluation of 16S next-generation sequencing of hypervariable region 4 in wastewater samples: An unsuitable approach for bacterial enteric pathogen identification. *Science of The Total Environme*nt, 670, 1111–1124. https://doi.org/10.1016/J.SCITOTENV.2019.03.278

Grossart, H. P. (1999). Interactions between marine bacteria and axenic diatoms (Cylindrotheca fusiformis, Nitzschia laevis, and Thalassiosira weissflogii) incubated under various conditions in the lab. *Aquatic Microbial Ec*ology, 19(1), 1–11. https://doi.org/10.3354/AME019001

Grossart, H. P., Levold, F., Allgaier, M., Simon, M., & Brinkhoff, T. (2005). Marine diatom species harbour distinct bacterial communities. *Environmental Microbiol*ogy, 7(6), 860–873. https://doi.org/10.1111/j.1462-2920.2005.00759.x

Grover, J. P. (2000). Resource competition and community structure in aquatic micro-organisms: experimental studies of algae and bacteria along a gradient of organic carbon to inorganic phosphorus supply. *Journal of Plankton Research*, 22(8), 1591–1610. https://doi.org/10.1093/plankt/22.8.1591

GUILLARD, R. R., & RYTHER, J. H. (1962). Studies of marine planktonic diatoms. I. Cyclotella nana Hustedt, and Detonula confervacea (cleve) Gran. *Canadian Journal of Microb*iology, 8, 229–239. https://doi.org/10.1139/m62-029

Guillou, L., Bachar, D., Audic, S., Bass, D., Berney, C., Bittner, L., Boutte, C., Burgaud, G., De Vargas, C., Decelle, J., Del Campo, J., Dolan, J. R., Dunthorn, M., Edvardsen, B., Holzmann, M., Kooistra, W. H. C. F., Lara, E., Le Bescot, N., Logares, R., … Christen, R. (2013). The Protist Ribosomal Reference database (PR2): a catalog of unicellular eukaryote small sub-unit rRNA sequences with curated taxonomy. *Nucleic Acids Research*, 41(Database issue). https://doi.org/10.1093/NAR/GKS1160

Guo, X., Liu, X., Wu, L., Pan, J., & Yang, H. (n.d.). *The algicidal activity of Aeromonas sp. strain GLY-2107 against bloom-forming Microcystis aeruginosa is regulated by N-acyl homoserine lactone-media*ted quorum *sensing*. https://doi.org/10.1111/1462-2920.13346

Gutiérrez, M. H., Jara, A. M., & Pantoja, S. (2016). Fungal parasites infect marine diatoms in the upwelling ecosystem of the Humboldt current system off central Chile. *Environmental Microbiology*, 18(5), 1646–1653. https://doi.org/10.1111/1462-2920.13257

Haines, K. C., & Guillard, R. R. L. (1974). GROWTH OF VITAMIN B $_{12}$ -REQUIRING MARINE DIATOMS IN MIXED LABORATORY CULTURES WITH VITAMIN B $_{12}$ -PRODUCING MARINE BACTERIA [1] [2]. *Journal of Phycolo*gy, 10(3), 245–252. https://doi.org/10.1111/j.1529-8817.1974.tb02709.x

Han, M. S., & Furuya, K. (2000). Size and species-specific primary productivity and community structure of phytoplankton in Tokyo Bay. *Journal of Plankton Research*, 22(7), 1221–1235. https://doi.org/10.1093/PLANKT/22.7.1221

Hanic, L. A., Sekimoto, S., & Bates, S. S. (2009). Oomycete and chytrid infections of the marine diatom Pseudo-nitzschia pungens (Bacillariophyceae) from Prince Edward Island. *Botany*, 87(11), 1096–1105. https://doi.org/10.1139/B09-070

Haynes, K., Hofmann, T. A., Smith, C. J., Ball, A. S., Underwood, G. J. C., & Osborn, A. M. (2007). Diatom-derived carbohydrates as factors affecting bacterial community composition in estuarine sediments. *Applied and Environmental Microbiology*, 73(19), 6112–6124. https://doi.org/10.1128/AEM.00551-07

Hider, R. C., & Kong, X. (2010). Chemistry and biology of siderophores. In *Natural Product Reports* (Vol. 27, Issue 5, pp. 637–657). Nat Prod Rep. https://doi.org/10.1039/b906679a

Holland, A. F., Zingmark, R. G., & Dean, J. M. (1974). Quantitative evidence concerning the stabilization of sediments by marine benthic diatoms. *Marine Biology,* 27(3), 191–196. https://doi.org/10.1007/BF00391943/METRICS

IBELINGS, B. W., GSELL, A. S., MOOIJ, W. M., Van DONK, E., Van Den WYNGAERT, S., & De SENERPONT DOMIS, L. N. (2011). Chytrid infections and diatom spring blooms: paradoxical effects of climate warming on fungal epidemics in lakes. *Freshwater Biology,* 56(4), 754–766. https://doi.org/10.1111/j.1365-2427.2010.02565.x

Jiao, N., Herndl, G. J., Hansell, D. A., Benner, R., Kattner, G., Wilhelm, S. W., Kirchman, D. L., Weinbauer, M. G., Luo, T., Chen, F., & Azam, F. (2010). Microbial production of recalcitrant dissolved organic matter: long-term carbon storage in the global ocean. *Nature Reviews Microbiology 2010* 8:8, 8(8), 593–599. https://doi.org/10.1038/nrmicro2386

Jung, S. W., Kang, Y. H., Katano, T., Kim, B. H., Cho, S. Y., Lee, J. H., Kim, Y. O., & Han, M. S. (2010). Testing addition of Pseudomonas fluorescens HYK0210-SK09 to mitigate blooms of the diatom Stephanodiscus hantzschii in small- and large-scale mesocosms. *Journal of Applied Phycology,* 22(4), 409–419. https://doi.org/10.1007/S10811-009-9473-2/

Kaeppel, E. C., Gärdes, A., Seebah, S., Grossart, H. P., & Ullrich, M. S. (2011). Marinobacter adhaerens sp. nov., isolated from marine aggregates formed with the diatom Thalassiosira weissflogii. *International Journal of Systematic and Evolutionary Microbiology,* 62(1), 124–128. https://doi.org/10.1099/IJS.0.030189-0

Kamp, A., Stief, P., Bristow, L. A., Thamdrup, B., & Glud, R. N. (2016). Intracellular Nitrate of Marine Diatoms as a Driver of Anaerobic Nitrogen Cycling in Sinking Aggregates. *Frontiers in Microbiology,* 7(NOV), 1669. https://doi.org/10.3389/fmicb.2016.01669

Kang, Y.-H., Kim, J.-D., Kim, B.-H., Kong, D.-S., & Han, M.-S. (2005). Isolation and characterization of a bio-agent antagonistic to diatom, Stephanodiscus hantzschii. *Journal of Applied Microbiology,* 98(5), 1030–1038. https://doi.org/10.1111/j.1365-2672.2005.02533.x

Katoh, K., Misawa, K., Kuma, K. I., & Miyata, T. (2002). MAFFT: a novel method for rapid multiple sequence alignment based on fast Fourier transform. *Nucleic Acids Research*, 30(14), 3059–3066. https://doi.org/10.1093/NAR/GKF436

Kazamia, E., Sutak, R., Paz-Yepes, J., Dorrell, R. G., Vieira, F. R. J., Mach, J., Morrissey, J., Leon, S., Lam, F., Pelletier, E., Camadro, J. M., Bowler, C., & Lesuisse, E. (2018). Endocytosis-mediated siderophore uptake as a strategy for Fe acquisition in diatoms. *Science Advances,* 4(5), eaar4536. https://doi.org/10.1126/sciadv.aar4536

Klindworth, A., Mann, A. J., Huang, S., Wichels, A., Quast, C., Waldmann, J., Teeling, H., & Glöckner, F. O. (2014). Diversity and activity of marine bacterioplankton during a diatom bloom in the North Sea assessed by total RNA and pyrotag sequencing. *Marine Genomics,* 18(PB), 185–192. https://doi.org/10.1016/J.MARGEN.2014.08.007

KNOLL, A. H., SUMMONS, R. E., WALDBAUER, J. R., & ZUMBERGE, J. E. (2007). The Geological Succession of Primary Producers in the Oceans. In *Evolution of Primary Producers in the Sea* (pp. 133–163). Elsevier. https://doi.org/10.1016/B978-012370518-1/50009-6

Kong, X., Seewald, M., Dadi, T., Friese, K., Mi, C., Boehrer, B., Schultze, M., Rinke, K., & Shatwell, T. (2021). Unravelling winter diatom blooms in temperate lakes using high frequency data and ecological modeling. *Water Res*earch, 190, 116681. https://doi.org/10.1016/j.watres.2020.116681

Kooistra, W. H. C. F., Gersonde, R., Medlin, L. K., & Mann, D. G. (2007). The Origin and Evolution of the Diatoms: Their Adaptation to a Planktonic Existence. *Evolution of Primary Producers i*n the Sea, 207–249. https://doi.org/10.1016/B978-012370518-1/50012-6

Kooistra, W. H. C. F., & Medlin, L. K. (1996). Evolution of the Diatoms (Bacillariophyta): IV. A Reconstruction of Their Age from Small Subunit rRNA Coding Regions and the Fossil Record. *Molecular Phylogenetics and Evolut*ion, 6(3), 391–407. https://doi.org/10.1006/MPEV.1996.0088

Lane, D. J., Pace, B., Olsen, G. J., Stahl, D. A., Sogin, M. L., & Pace, N. R. (1985). Rapid determination of 16S ribosomal RNA sequences for phylogenetic analyses. *Proceedings of the National Academy of Sciences of the United States of America*, 82(20), 6955–6959. https://doi.org/10.1073/PNAS.82.20.6955

Lane DJ. (1991). *Nucleic Acid Techniques in Bacterial Systematics.* (Stackebrandt E & Goodfellow M, Eds.). Wiley & Sons.

Laundon, D., Mock, T., Wheeler, G., & Cunliffe, M. (2021). Healthy herds in the phytoplankton: the benefit of selective parasitism. *The ISME Journal,* 15(7), 2163–2166. https://doi.org/10.1038/S41396-021-00936-8

Leblanc, K., Quéguiner, B., Diaz, F., Cornet, V., Michel-Rodriguez, M., Durrieu de Madron, X., Bowler, C., Malviya, S., Thyssen, M., Grégori, G., Rembauville, M., Grosso, O., Poulain, J., de Vargas, C., Pujo-Pay, M., & Conan, P. (2018). Nanoplanktonic diatoms are globally overlooked but play a role in spring blooms and carbon export. *Nature Communi*cations, 9(1), 953. https://doi.org/10.1038/s41467-018-03376-9

Lenneman, E. M., Wang, P., & Barney, B. M. (2014). Potential application of algicidal bacteria for improved lipid recovery with specific algae. *FEMS Microbiology Letter*s, 354(2), 102–110. https://doi.org/10.1111/1574-6968.12436

Li, D., Zhang, H., Fu, L., An, X., Zhang, B., Li, Y., Chen, Z., Zheng, W., Yi, L., & Zheng, T. (2014). A Novel Algicide: Evidence of the Effect of a Fatty Acid Compound from the Marine Bacterium, Vibrio sp. BS02 on the Harmful Dinoflagellate, Alexandrium tamarense. *PLOS* ONE, 9(3), e91201. https://doi.org/10.1371/JOURNAL.PONE.0091201

Loeffler, F. (1884). *Untersuchungen über die Bedeutung der Mikroorganismen für die Entstehung der Diphtherie beim Menschen, bei der Taube und beim Kalbe.*

Lomas, M. W., & Glibert, P. M. (1999). Temperature regulation of nitrate uptake: A novel hypothesis about nitrate uptake and reduction in cool-water diatoms. *Limnology and Oceanograp*hy, 44(3), 556–572. https://doi.org/10.4319/lo.1999.44.3.0556

Lu, X., Zhou, B., Xu, L., Liu, L., Wang, G., Liu, X., & Tang, X. (2016). A marine algicidal Thalassospira and its active substance against the harmful algal bloom species Karenia mikimotoi. *Applied Microbiology and Biotechnology*, 100(11), 5131–5139. https://doi.org/10.1007/S00253-016-7352-8

Luo, H., & Moran, M. A. (2014). Evolutionary Ecology of the Marine Roseobacter Clade. *Microbiology and Molecular Biology Revie*ws, 78(4), 573–587. https://doi.org/10.1128/mmbr.00020-14

Malviya, S., Scalco, E., Audic, S., Vincent, F., Veluchamy, A., Poulain, J., Wincker, P., Iudicone, D., De Vargas, C., Bittner, L., Zingone, A., & Bowler, C. (2016). Insights into global diatom distribution and diversity in the world's ocean. *Proceedings of the National Academy of Sciences of the United States of America*, *11*3(11), E1516–E1525. https://doi.org/10.1073/pnas.1509523113

Mann, D. G., & Vanormelingen, P. (2013). *An Inordinate Fondness? The Number, Distributions, and Origins* of Diatom *Species*. https://doi.org/10.1111/jeu.12047

Marchetti, A., Parker, M. S., Moccia, L. P., Lin, E. O., Arrieta, A. L., Ribalet, F., Murphy, M. E. P., Maldonado, M. T., & Armbrust, E. V. (2008). Ferritin is used for iron storage in bloom-forming marine pennate diatoms. *Nature 2008 457:7228*, 457(7228), 467–470. https://doi.org/10.1038/nature07539

Mayali, X., & Azam, F. (2004). Algicidal bacteria in the sea and their impact on algal blooms. *Journal of Eukaryotic Microbiolo*gy, 51(2), 139–144. https://doi.org/10.1111/j.1550-7408.2004.tb00538.x

McMurdie, P. J., & Holmes, S. (2013). Phyloseq: An R Package for Reproducible Interactive Analysis and Graphics of Microbiome Census Data. *PLOS* ONE, 8(4), e61217. https://doi.org/10.1371/JOURNAL.PONE.0061217

Medlin, L., Elwood, H. J., Stickel, S., & Sogin, M. L. (1988). The characterization of enzymatically amplified eukaryotic 16S-like rRNA-coding regions. *Ge*ne, 71(2), 491–499. https://doi.org/10.1016/0378-1119(88)90066-2

Menden-Deuer, S., & Lessard, E. J. (2000). Carbon to volume relationships for dinoflagellates, diatoms, and other protist plankton. *Limnology and Oceanograp*hy, 45(3), 569–579. https://doi.org/10.4319/LO.2000.45.3.0569

Meyer, N., & Pohnert, G. (2019). Isolate-specific resistance to the algicidal bacterium Kordia algicida in the diatom Chaetoceros genus. *Botanica Mari*na, 62(6), 527–535. https://doi.org/10.1515/BOT-2019-0007/ASSET/GRAPHIC/J_BOT-2019-0007_CV_002.JPG

Meyer, N., Rettner, J., Werner, M., Werz, O., & Pohnert, G. (2018). Algal Oxylipins Mediate the Resistance of Diatoms against Algicidal Bacteria. *Marine* Drugs, 16(12), 486. https://doi.org/10.3390/md16120486

Miller, M. B., & Bassler, B. L. (2001). Quorum sensing in bacteria. *Annual Review of Microbi*ology, 55, 165–199. https://doi.org/10.1146/ANNUREV.MICRO.55.1.165

Mitsutani, A., Yamasaki, I., Kitaguchi, H., Kato, J., Ueno, S., & Ishida, Y. (2001). Analysis of algicidal proteins of a diatom-lytic marine bacterium Pseudoalteromonas sp. strain A25 by two-dimensional electrophoresis. *Phycolog*ia, 40(3), 286–291. https://doi.org/10.2216/i0031-8884-40-3-286.1

Mönnich, J., Tebben, J., Bergemann, J., Case, R., Wohlrab, S., & Harder, T. (2020). Niche-based assembly of bacterial consortia on the diatom Thalassiosira rotula is stable and reproducible. *The ISME Journal 2020 14:6,* 14(6), 1614–1625. https://doi.org/10.1038/s41396-020-0631-5

Moore, J. K., Doney, S. C., Glover, D. M., & Fung, I. Y. (2001). Iron cycling and nutrient-limitation patterns in surface waters of the World Ocean. *Deep Sea Research Part II: Topical Studies in Oceanography,* 49(1–3), 463–507. https://doi.org/10.1016/S0967-0645(01)00109-6

Moustafa, A., Beszteri, B., Maier, U. G., Bowler, C., Valentin, K., & Bhattacharya, D. (2009). Genomic footprints of a cryptic plastid endosymbiosis in diatoms. *Science*, *324*(5935), 1724–1726. https://doi.org/10.1126/SCIENCE.1172983/SUPPL_FILE/MOUSTAFA.SOM.PDF

Murchie, E.H. and Lawson, T., 2013. Chlorophyll fluorescence analysis: a guide to good practice and understanding some new applications. *Journal of experimental botany*, 64(13), pp.3983-3998. https://doi.org/10.1093/jxb/ert208

Nagasaki, K., Tomaru, Y., Katanozaka, N., Shirai, Y., Nishida, K., Itakura, S. and Yamaguchi, M., 2004. Isolation and characterization of a novel single-stranded RNA virus infecting the bloom-forming diatom Rhizosolenia setigera. *Applied and Environmental Microbiology*, 70(2), pp.704-711. https://doi.org/10.1128/AEM.70.2.704-711.2004

Nelson, D. M., Tréguer, P., Brzezinski, M. A., Leynaert, A., & Quéguiner, B. (1995). Production and dissolution of biogenic silica in the ocean: Revised global estimates, comparison with regional data and relationship to biogenic sedimentation. *Global Biogeochemical Cycles*, *9*(3), 359–372. https://doi.org/10.1029/95GB01070

Olenina, I., 2006. Biovolumes and size-classes of phytoplankton in the Baltic Sea. *Helsinki Commission Baltic Marine Environment Protection Commission*.

Parada, A.E., Needham, D.M. and Fuhrman, J.A., 2016. Every base matters: assessing small subunit rRNA primers for marine microbiomes with mock communities, time series and global field samples. *Environmental microbiology*, 18(5), pp.1403-1414. https://doi.org/10.1111/1462-2920.13023

Park, J., Yoshinaga, I., Nishikawa, T., & Imai, I. (2010). Algicidal bacteria in particle-associated form and in free-living form during a diatom bloom in the Seto Inland Sea, Japan. *Aquatic Microbial Ecology*, *60*(2), 151–161. https://doi.org/10.3354/ame01416

Parker, M. S., Mock, T., & Armbrust, E. V. (2008). Genomic Insights into Marine Microalgae. https://doi.org/10.1146/ANNUREV.GENET.42.110807.091417, *42*, 619–645.

Paul, C., & Pohnert, G. (2011). Interactions of the Algicidal Bacterium Kordia algicida with Diatoms: Regulated Protease Excretion for Specific Algal Lysis. *PloS ONE*, *6*(6), e21032. https://doi.org/10.1371/journal.pone.0021032

Paul, C., & Pohnert, G. (2013). Induction of Protease Release of the Resistant Diatom Chaetoceros didymus in Response to Lytic Enzymes from an Algicidal Bacterium. *PloS ONE*, *8*(3), e57577. https://doi.org/10.1371/journal.pone.0057577

Quast, C., Pruesse, E., Yilmaz, P., Gerken, J., Schweer, T., Yarza, P., Peplies, J., Glöckner, F. O. (2013). The SILVA ribosomal RNA gene database project: improved data processing and web-based tools. *Nucleic Acids Research*. 2013 41(Database issue). Doi: 10.1093/nar/gks1219.

Rico, M., López, A., Santana-Casiano, J. M., González, A. G., & González-Dávila, M. (2013). Variability of the phenolic profile in the diatom Phaeodactylum tricornutum growing under copper and iron stress. *Limnology and Oceanography*, *58*(1), 144–152. https://doi.org/10.4319/LO.2013.58.1.0144

Riemann, L., Steward, G. F., & Azam, F. (2000). Dynamics of Bacterial Community Composition and Activity during a Mesocosm Diatom Bloom. In *APPLIED AND ENVIRONMENTAL MICROBIOLOGY* (Vol. 66, Issue 2). http://isar.mpi-bremen.de

Risgaard-Petersen, N., Nicolaisen, M. H., Revsbech, N. P., & Lomstein, B. A. (2004). Competition between ammonia-oxidizing bacteria and benthic microalgae. *Applied and Environmental Microbiology*, *70*(9), 5528–5537. https://doi.org/10.1128/AEM.70.9.5528-5537.2004

Rothpletz, & August. (1896). Ueber die Flysch-Fucoiden und einige andere fossile Algen, sowie über liasische, Diatomeen führende Hornschwämme. *Zeitschrift Der Deutschen Geologischen Gesellschaft*, 854–914.

Round, F, E, Crawford, R, M, Mann, D, G. The Diatoms: Biology and Morphology of the Genera*, Cambridge University Press*, Cambridge, 1990.

Sabatino, V., Russo, M. T., Patil, S., d'Ippolito, G., Fontana, A., & Ferrante, M. I. (2015). Establishment of Genetic Transformation in the Sexually Reproducing Diatoms Pseudo-nitzschia multistriata and Pseudo-nitzschia arenysensis and Inheritance of the Transgene. *Marine Biotechnology*, *17*(4), 452–462. https://doi.org/10.1007/S10126-015-9633-0/FIGURES/6

Sakata, T., Yoshikawa, T., & Nishitarumizu, S. (2011). Algicidal activity and identification of an algicidal substance produced by marine Pseudomonas sp. C55a-2. *Fisheries Science*, *77*(3), 397–402. https://doi.org/10.1007/S12562-011-0345-8/TABLES/1

Sapp, M., Gerdts, G., Wellinger, M., & Wichels, A. (2008). Consuming algal products: Trophic interactions of bacteria and a diatom species determined by

RNA stable isotope probing. *Helgoland Marine Research*, *62*(3), 283–287. https://doi.org/10.1007/S10152-008-0110-2

Sapp, M., Schwaderer, A. S., Wiltshire, K. H., Hoppe, H. G., Gerdts, G., & Wichels, A. (2007). Species-specific bacterial communities in the phycosphere of microalgae? *Microbial Ecology*, *53*(4), 683–699. https://doi.org/10.1007/s00248-006-9162-5

Sayers, E. W., Bolton, E. E., Brister, J. R., Canese, K., Chan, J., Comeau, D. C., Connor, R., Funk, K., Kelly, C., Kim, S., Madej, T., Marchler-Bauer, A., Lanczycki, C., Lathrop, S., Lu, Z., Thibaud-Nissen, F., Murphy, T., Phan, L., Skripchenko, Y., … Sherry, S. T. (2022). Database resources of the national center for biotechnology information. *Nucleic Acids Research*, *50*(D1), D20–D26. https://doi.org/10.1093/NAR/GKAB1112

Schäfer, H., Abbas, B., Witte, H., & Muyzer, G. (2002). Genetic diversity of 'satellite' bacteria present in cultures of marine diatoms. *FEMS Microbiology Ecology*, *42*(1), 25–35. https://doi.org/10.1111/J.1574-6941.2002.TB00992.X

Seyedsayamdost, M. R., Case, R. J., Kolter, R., & Clardy, J. (2011). The Jekyll-and-Hyde chemistry of phaeobacter gallaeciensis (Sup). *Nature Chemistry*, *3*(4), 331–335. https://doi.org/10.1038/nchem.1002

Shibl, A. A., Isaac, A., Ochsenkühn, M. A., Cárdenas, A., Fei, C., Behringer, G., Arnoux, M., Drou, N., Santos, M. P., Gunsalus, K. C., Voolstra, C. R., & Amin, S. A. (2020). Diatom modulation of select bacteria through use of two unique secondary metabolites. *Proceedings of the National Academy of Sciences of the United States of America*, *117*(44), 27445–27455. https://doi.org/10.1073/PNAS.2012088117/SUPPL_FILE/PNAS.2012088117.SD04.TXT

Shipe, R. F., Leinweber, A., & Gruber, N. (2008). Abiotic controls of potentially harmful algal blooms in Santa Monica Bay, California. *Continental Shelf Research*, *28*(18), 2584–2593. https://doi.org/10.1016/j.csr.2008.08.003

Sison-Mangus, M. P., Jiang, S., Kudela, R. M., & Mehic, S. (2016). Phytoplankton-Associated Bacterial Community Composition and Succession during Toxic Diatom Bloom and Non-Bloom Events. *Frontiers in Microbiology*, *7*. https://doi.org/10.3389/fmicb.2016.01433

Sison-Mangus, M. P., Jiang, S., Tran, K. N., & Kudela, R. M. (2014). Host-specific adaptation governs the interaction of the marine diatom, Pseudo-nitzschia and their microbiota. *ISME Journal*, *8*(1), 63–76. https://doi.org/10.1038/ismej.2013.138

Smetacek, V. S. (1985). Role of sinking in diatom life-history cycles: ecological, evolutionary and geological significance. *Marine Biology*, *84*(3), 239–251. https://doi.org/10.1007/BF00392493

Smriga, S., Fernandez, V. I., Mitchell, J. G., & Stocker, R. (2016). Chemotaxis toward phytoplankton drives organic matter partitioning among marine bacteria.

Proceedings of the National Academy of Sciences, *113*(6), 1576–1581. https://doi.org/10.1073/pnas.1512307113

Sohn, J. H., Lee, J. H., Yi, H., Chun, J., Bae, K. S., Ahn, T. Y., & Kim, S. J. (2004). Kordia algicida gen. nov., sp. nov., an algicidal bacterium isolated from red tide. *International Journal of Systematic and Evolutionary Microbiology*, *54*(3), 675–680. https://doi.org/10.1099/ijs.0.02689-0

Sonnenschein, E. C., Syit, D. A., Grossart, H. P., & Ullrich, M. S. (2012). Chemotaxis of Marinobacter adhaerens and its impact on attachmentto the diatom Thalassiosira weissflogii. *Applied and Environmental Microbiology*, *78*(19), 6900–6907. https://doi.org/10.1128/AEM.01790-12

Sonnenschein, E., Phippen, C. B. W., Bentzon-Tilia, M., Rasmussen, S. A., Nielsen, K. F., & Gram, L. (2018). Phylogenetic distribution of roseobacticides in the Roseobacter group and their effect on microalgae. *BioRxiv*, 242842. https://doi.org/10.1101/242842

Sorhannus, U. (2007). *A nuclear-encoded small-subunit ribosomal RNA timescale for diatom evolution*. https://doi.org/10.1016/j.marmicro.2007.05.002

Stachura-Suchoples, K., & Williams, D. M. (2009) Description of Conticribra tricircularis , a new genus and species of Thalassiosirales, with a discussion on its relationship to other continuous cribra species of Thalassiosira Cleve (Bacillariophyta) and its freshwater origin. *European Journal of Phycology*, 44(4), 477-486, https://doi.org/10.1080/09670260903225431

Stock, W., Blommaert, L., De Troch, M., Mangelinckx, S., Willems, A., Vyverman, W., & Sabbe, K. (2019). Host specificity in diatom–bacteria interactions alleviates antagonistic effects. *FEMS Microbiology Ecology*, *95*(11), 171. https://doi.org/10.1093/FEMSEC/FIZ171

Su, J., Yang, X., Zhou, Y., & Zheng, T. (2011). Marine bacteria antagonistic to the harmful algal bloom species Alexandrium tamarense (Dinophyceae). *Biological Control*, *56*(2), 132–138. https://doi.org/10.1016/J.BIOCONTROL.2010.10.004

Sun, X., Li, Z., Ding, X., Ji, G., Wang, L., Gao, X., Chang, Q., & Zhu, L. (2022). Effects of Algal Blooms on Phytoplankton Composition and Hypoxia in Coastal Waters of the Northern Yellow Sea, China. *Frontiers in Marine Science*, *9*, 897418. https://doi.org/10.3389/FMARS.2022.897418/BIBTEX

Sunagawa, S., Coelho, L. P., Chaffron, S., Kultima, J. R., Labadie, K., Salazar, G., Djahanschiri, B., Zeller, G., Mende, D. R., Alberti, A., Cornejo-Castillo, F. M., Costea, P. I., Cruaud, C., d'Ovidio, F., Engelen, S., Ferrera, I., Gasol, J. M., Guidi, L., Hildebrand, F., … Velayoudon, D. (2015). Structure and function of the global ocean microbiome. *Science*, *348*(6237). https://doi.org/10.1126/science.1261359

Tamura, K., Stecher, G., & Kumar, S. (n.d.). *MEGA11: Molecular Evolutionary Genetics Analysis Version 11*. https://doi.org/10.1093/molbev/msab120

Tang, Y. Z., Koch, F., & Gobler, C. J. (2010). Most harmful algal bloom species are vitamin B1 and B 12 auxotrophs. *Proceedings of the National Academy of*

Sciences of the United States of America, *107*(48), 20756–20761. https://doi.org/10.1073/pnas.1009566107

Taylor, J. D., Cottingham, S. D., Billinge, J., & Cunliffe, M. (2014). Seasonal microbial community dynamics correlate with phytoplankton-derived polysaccharides in surface coastal waters. *The ISME Journal*, *8*(1), 245–248. https://doi.org/10.1038/ismej.2013.178

Teeling, H., Fuchs, B. M., Becher, D., Klockow, C., Gardebrecht, A., Bennke, C. M., Kassabgy, M., Huang, S., Mann, A. J., Waldmann, J., Weber, M., Klindworth, A., Otto, A., Lange, J., Bernhardt, J., Reinsch, C., Hecker, M., Peplies, J., Bockelmann, F. D., … Amann, R. (2012). Substrate-controlled succession of marine bacterioplankton populations induced by a phytoplankton bloom. *Science (New York, N.Y.)*, *336*(6081), 608–611. https://doi.org/10.1126/SCIENCE.1218344

Thingstad, T. F., Skjoldal, E. F., & Bohne, R. A. (1993). Phosphorus cycling and algal-bacterial competition in Sandsfjord, western Norway. In *MARINE ECOLOGY PROGRESS SERIES Mar. Ecol. Prog. Ser* (Vol. 99).

Tiselius, P., & Kuylenstierna, M. (1996). Growth and decline of a diatom spring bloom: phytoplankton species composition, formation of marine snow and the role of heterotrophic dinoflagellates. In *Journal of Plankton Research* (Vol. 18, Issue 2). https://academic.oup.com/plankt/article-abstract/18/2/133/1521161

Tomaru, Y., Toyoda, K., & Kimura, K. (2018). Occurrence of the planktonic bloom-forming marine diatom Chaetoceros tenuissimus Meunier and its infectious viruses in western Japan. *Hydrobiologia*, *805*(1), 221–230. https://doi.org/10.1007/S10750-017-3306-0/TABLES/3

Tréguer, P. J., & De La Rocha, C. L. (2013). The World Ocean Silica Cycle. *Annual Review of Marine Science*, *5*(1), 477–501. https://doi.org/10.1146/annurev-marine-121211-172346

Turner, S., Pryer, K. M., Miao, V. P. W., & Palmer, J. D. (1999). Investigating deep phylogenetic relationships among cyanobacteria and plastids by small subunit rRNA sequence analysis. *The Journal of Eukaryotic Microbiology*, *46*(4), 327–338. https://doi.org/10.1111/J.1550-7408.1999.TB04612.X

Underwood, G. J. C., & Paterson, D. M. (2003). The importance of extracellular carbohydrate productionby marine epipelic diatoms. *Advances in Botanical Research*, *40*, 183–240. https://doi.org/10.1016/S0065-2296(05)40005-1

Utermöhl, H. (2017). Zur Vervollkommnung der quantitativen Phytoplankton-Methodik. Https://Doi.*Org/10.1080/05384680.1958.11904091*, *9*(1), 1–38. https://doi.org/10.1080/05384680.1958.11904091

Van Der Heul, H. U., Bilyk, B. L., McDowall, K. J., Seipke, R. F., & Van Wezel, G. P. (2018). Regulation of antibiotic production in Actinobacteria: new perspectives from the post-genomic era. *Natural Product Reports*, *35*(6), 575–604. https://doi.org/10.1039/C8NP00012C

Van Tol, H. M., Amin, S. A., & Virginia Armbrust, E. (2017). Ubiquitous marine bacterium inhibits diatom cell division. *ISME Journal*, *11*(1), 31–42. https://doi.org/10.1038/ismej.2016.112

Vernette, C., Henry, N., Lecubin, J., de Vargas, C., Hingamp, P., & Lescot, M. (2021). The Ocean barcode atlas: A web service to explore the biodiversity and biogeography of marine organisms. *Molecular Ecology Resources*, *21*(4), 1347–1358. https://doi.org/10.1111/1755-0998.13322

Waksman, S. A., & Butler, M. R. (1937). Relation of Bacteria to Diatoms In Sea Water. *Journal of the Marine Biological Association of the United Kingdom*, *22*(1), 359–373. https://doi.org/10.1017/S0025315400012054

Wang, H., Butt, L., Rooks, P., Khan, F., Allen, M. J., & Ali, S. T. (2015). *Characterisation of algicidal bacterial exometabolites against the lipid-accumulating diatom Skeletonema sp*. https://doi.org/10.1016/j.algal.2015.11.012

Wang, Y., Li, S., Liu, G., Li, X., Yang, Q., Xu, Y., Hu, Z., Chen, C. Y., & Chang, J. S. (2020). Continuous production of algicidal compounds against Akashiwo sanguinea via a Vibrio sp. co-culture. *Bioresource Technology*, *295*, 122246. https://doi.org/10.1016/J.BIORTECH.2019.122246

Widdicombe, C. E., Eloire, D., Harbour, D., Harris, R. P., & Somerfield, P. J. (2010). Long-term phytoplankton community dynamics in the Western English Channel. *Journal of Plankton Research*, *32*(5), 643–655. https://doi.org/10.1093/plankt/fbp127

Wilson, W. H., Tarran, G. A., Schroeder, D., Cox, M., Oke, J., & Malin, G. (2002). Isolation of viruses responsible for the demise of an *Emiliania huxleyi* bloom in the English Channel. *Journal of the Marine Biological Association of the United Kingdom*, *82*(3), 369–377. https://doi.org/10.1017/S002531540200560X

Worden, A. Z., Lee, J. H., Mock, T., Rouzé, P., Simmons, M. P., Aerts, A. L., Allen, A. E., Cuvelier, M. L., Derelle, E., Everett, M. V., Foulon, E., Grimwood, J., Gundlach, H., Henrissat, B., Napoli, C., McDonald, S. M., Parker, M. S., Rombauts, S., Salamov, A., … Grigoriev, I. V. (2009). Green evolution and dynamic adaptations revealed by genomes of the marine picoeukaryotes micromonas. *Science*, *324*(5924), 268–272. https://doi.org/10.1126/SCIENCE.1167222

Yang, B., Wang, Y., & Qian, P. Y. (2016). Sensitivity and correlation of hypervariable regions in 16S rRNA genes in phylogenetic analysis. *BMC Bioinformatics*, *17*(1), 1–8. https://doi.org/10.1186/S12859-016-0992-Y

Yang, Q., Zhang, X., Li, L., Zhang, R., Feng, L., & Mu, J. (2018). Ponticoccus alexandrii sp. nov., a novel bacterium isolated from the marine toxigenic dinoflagellate Alexandrium minutum. *Antonie van Leeuwenhoek*, *111*(6), 995–1000. https://doi.org/10.1007/S10482-017-0996-2

Yoon, H. S., Hackett, J. D., Ciniglia, C., Pinto, G., & Bhattacharya, D. (2004). A Molecular Timeline for the Origin of Photosynthetic Eukaryotes. *Molecular*

Biology and Evolution, *21*(5), 809–818. https://doi.org/10.1093/MOLBEV/MSH075

Yoshida, K., Ota, H., Iwanaga, T., Yoshitake, A., Mine, T., Omura, M., & Kimura, K. (2023). Species-specific monitoring of Skeletonema blooms in the coastal waters of Ariake Sound, Japan. *Marine Ecology Progress Series*, *703*, 31–46. https://doi.org/10.3354/meps14200

Zheng, N., Ding, N., Gao, P., Han, M., Liu, X., Wang, J., Sun, L., Fu, B., Wang, R., & Zhou, J. (2018). Diverse algicidal bacteria associated with harmful bloom-forming Karenia mikimotoi in estuarine soil and seawater. *Science of The Total Environment*, *631–632*, 1415–1420. https://doi.org/10.1016/J.SCITOTENV.2018.03.035

Appendix

Chapter 1: Characterising the diversity and seasonal patterns of bacterial antagonists of bloom-forming diatom species in the Western English Channel

Appendix Table 1. Recipe for 1 % ½ YTSS agar for the cultivation of antagonistic bacteria obtained from soft-agar overlay assays. All ingredients dissolved in distilled water.

Ingredient	Manufacturer	Weight (g l^{-1})
Yeast extract	Sigma-Aldrich, USA	2.00
Tryptone	Oxoid, UK	1.25
Sea salts	Sigma-Aldrich, USA	20.00
Agar	Thermo Fisher, USA	10.00

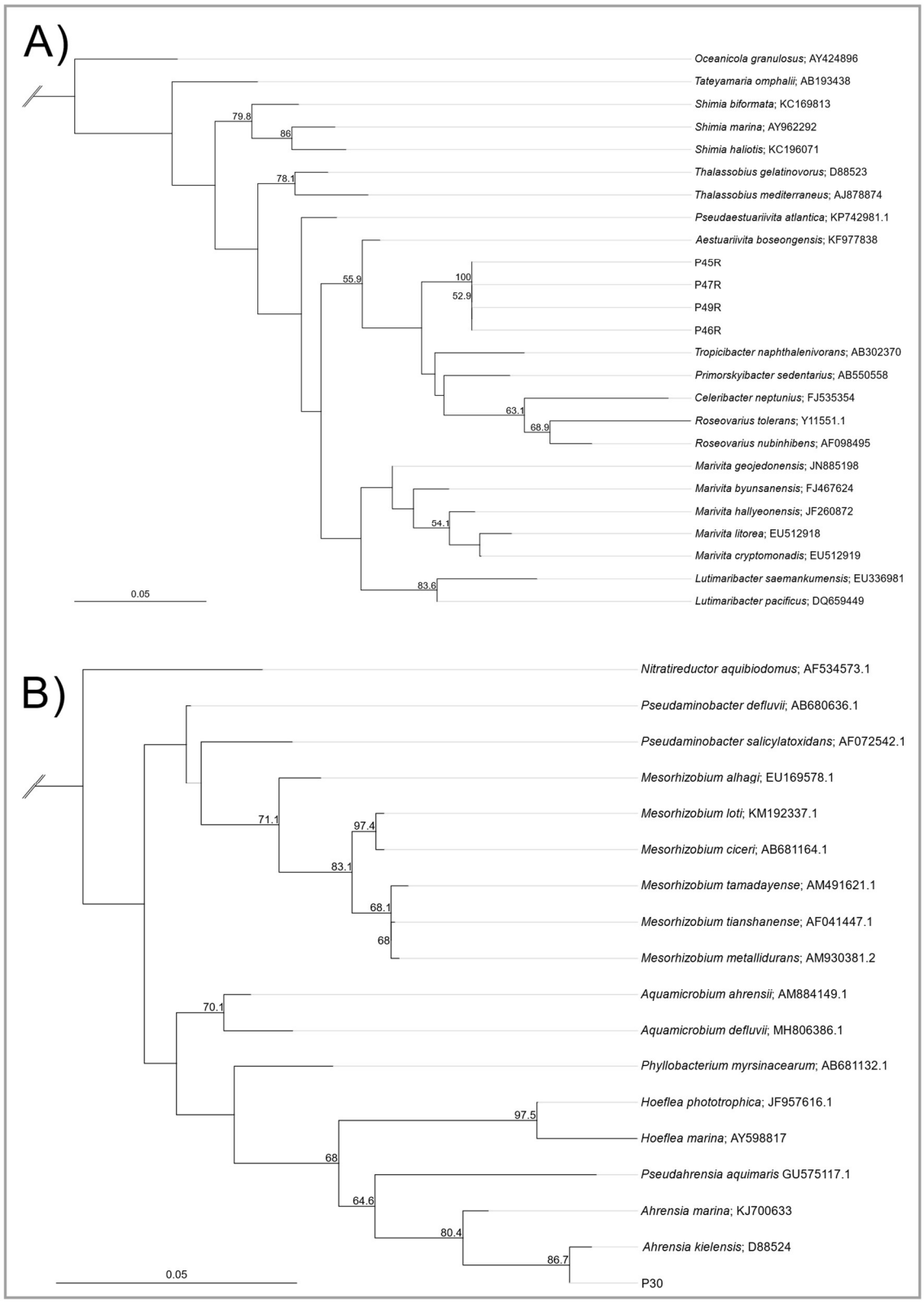

Appendix Figure 1. Maximum Likelihood trees constructed to verify the taxonomic assignment of plaque assay isolates. ML trees were constructed using full-length 16S rRNA sequences of plaque assay isolates and type strains of top NCBI BLAST hit and closely related species. Branch support values above 50 % are shown (calculated from 1000 bootstraps). **A)** ML tree of P45R, P46R, P47R, P49R, for which the top NCBI hit was *Aestuariivita* sp. *Stappia stellulata* was used as an outgroup. **B)** ML tree of P30, for which the top NCBI hit was *Ahrensia kielensis*. *Hyphomicrobium denitrificans* was used as an outgroup.

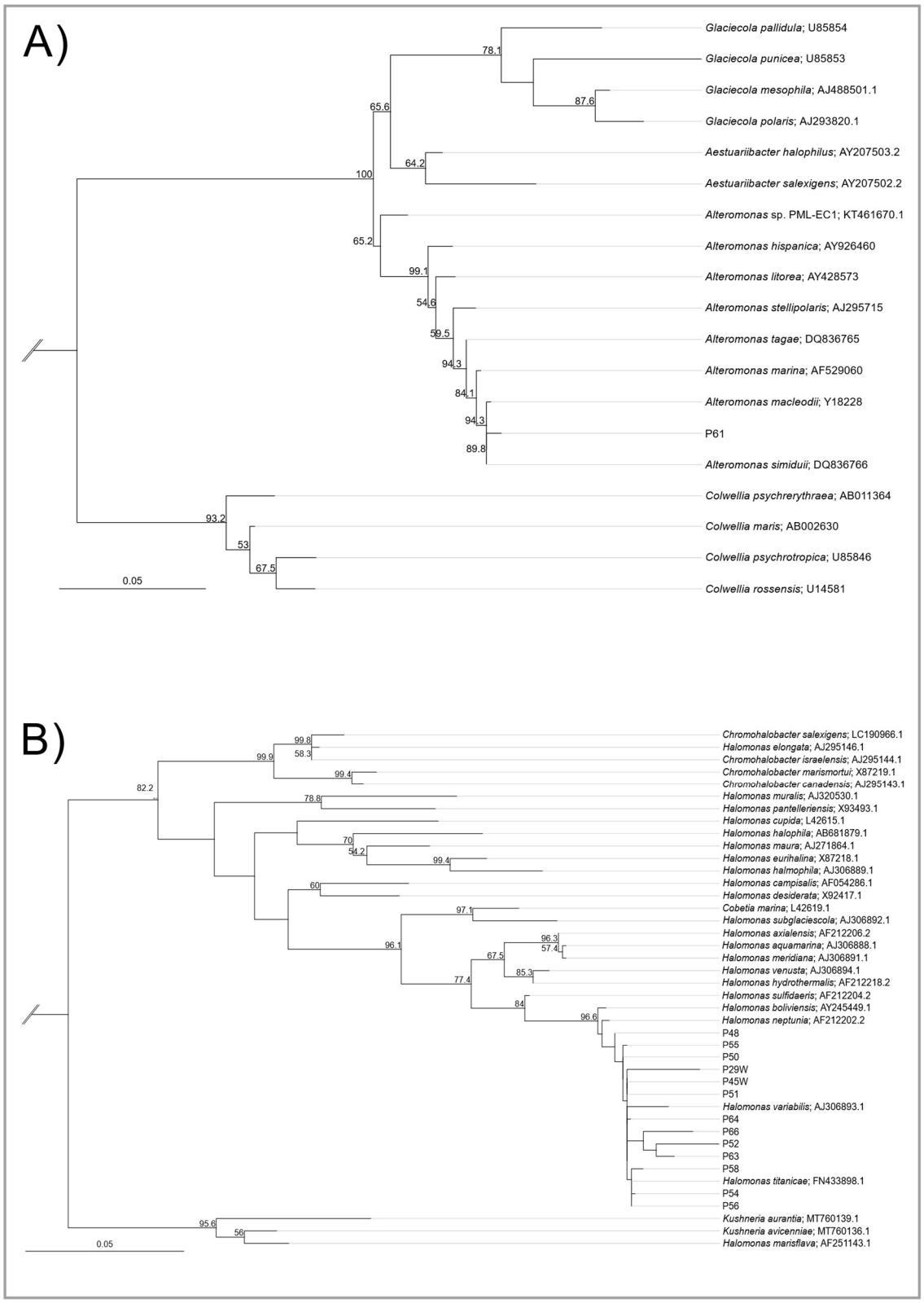

Appendix Figure 2. Maximum Likelihood trees constructed to verify the taxonomic assignment of plaque assay isolates. ML trees were constructed using full-length 16S rRNA sequences of plaque assay isolates and type strains of top NCBI BLAST hit and closely related species. Branch support values above 50 % are shown (calculated from 1000 bootstraps). **A)** ML tree of 61, for which the top NCBI hits were *Alteromonas macleodii and Alteromonas simiduii*. Also included is the diatom-antagonistic *Alteromonas* sp. strain (*Alteromonas* sp. PML-EC1) isolated from Station L4 by Wang et al., 2016. *Pseudomonas aeruginosa* was used as an outgroup. **B)** ML tree of P29W, P45W, P48, P50 – P52, P54 – P56, P58, P63 – P64 and P66, for which the top NCBI hit was *Halomonas titanicae*. *Zymobacter palmae* was used as an outgroup.

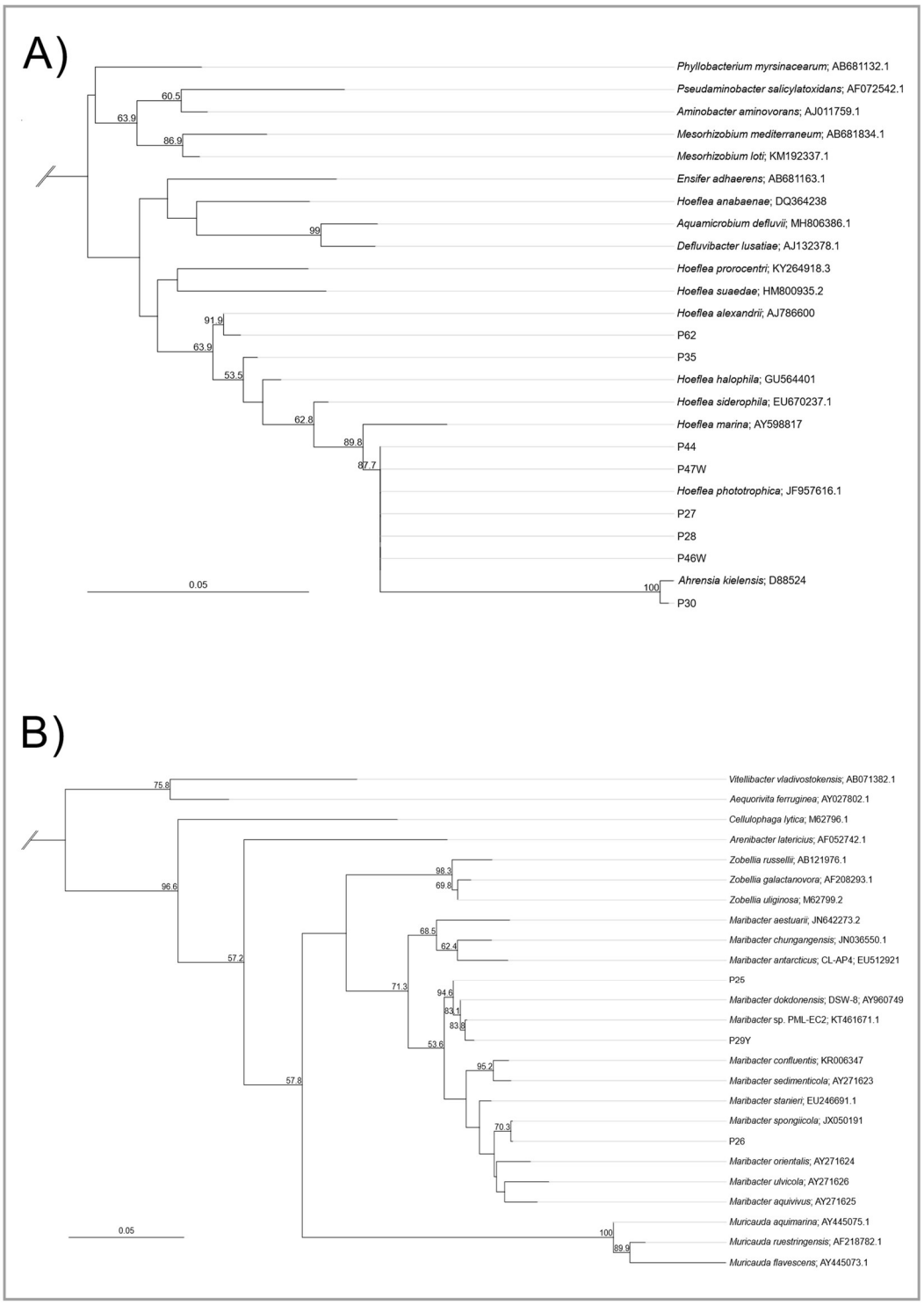

Appendix Figure 3. Maximum Likelihood trees constructed to verify the taxonomic assignment of plaque assay isolates. ML trees were constructed using full-length 16S rRNA sequences of plaque assay isolates and type strains of top NCBI BLAST hit and closely related species. Branch support values above 50 % are shown (calculated from 1000 bootstraps). **A)** ML tree of plaque assay isolates related to *Hoeflea* sp. strains. Top NCBI hits for P27 – P28, P44, P46W and P47W were *Hoeflea phototrophica and/or Hoeflea marina*, top NCBI hit for P35 was *Hoeflea halophila* and top NCBI hit for P62 was *Hoeflea alexandrii*. *Parvibaculum lavamentivorans* was used as an outgroup. **B)** ML tree of P25 and P29Y, and for P26, for which the top NCBI hit were *Maribacter dokdonensis* and *Maribacter spongiicola* respectively. Also included is the diatom-antagonistic *Maribacter* sp. strain (*Maribacter* sp. PML-EC2) isolated at Station L4 by Wang et al., 2016. *Flavobacterium aquatile* was used as an outgroup.

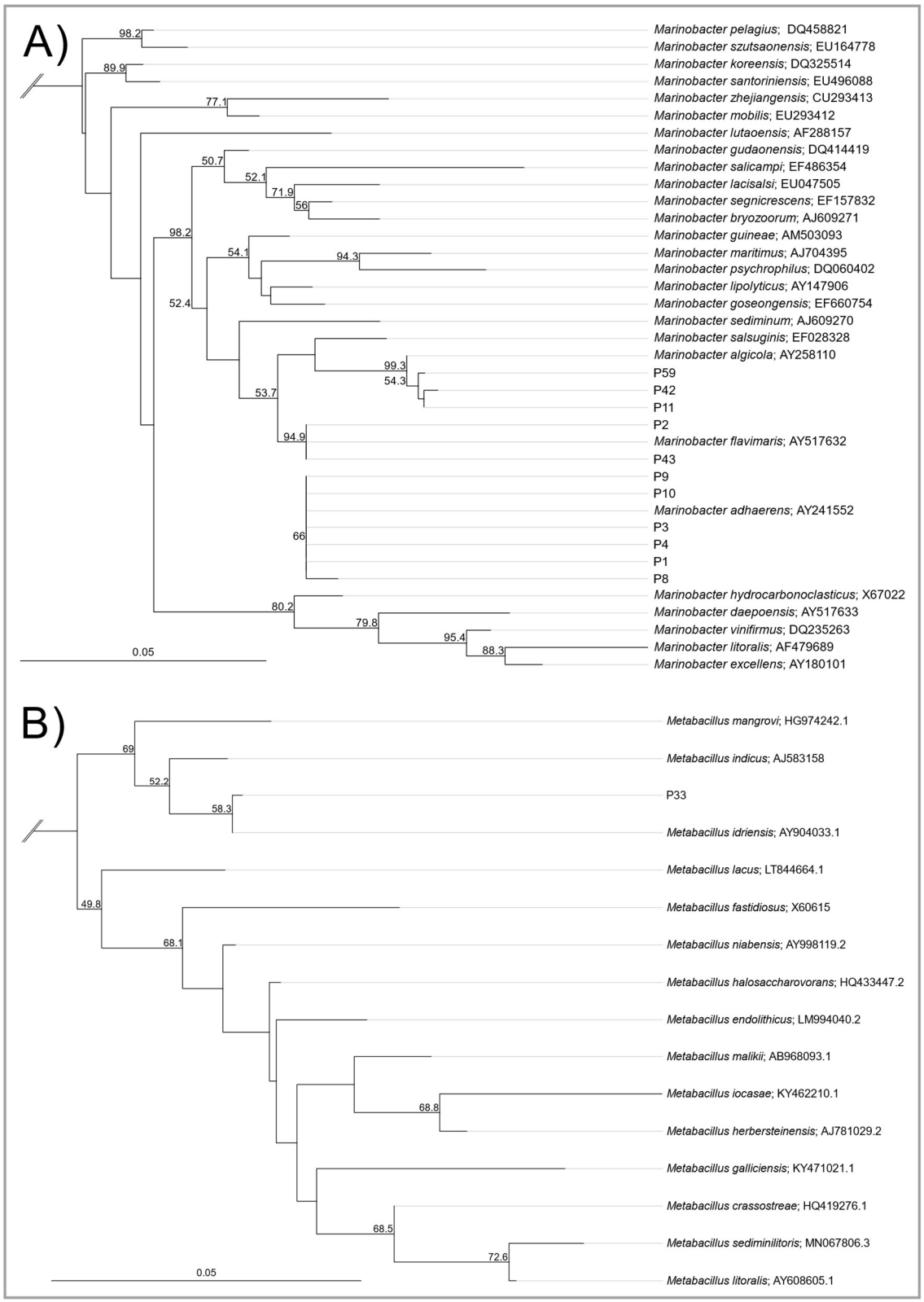

Appendix Figure 4. Maximum Likelihood trees constructed to verify the taxonomic assignment of plaque assay isolates. ML trees were constructed using full-length 16S rRNA sequences of plaque assay isolates and type strains of top NCBI BLAST hit and closely related species. Branch support values above 50 % are shown (calculated from 1000 bootstraps). **A)** ML tree of plaque assay isolates related to *Marinobacter* sp. strains. Top hit for P1 - P4, P8 – P10 and P43 was *Marinobacter adhaerens*, and top hit for P11, P42 and P59 was *Marinobacter algicola*. *Salicola marasensis* was used as an outgroup. **B)** ML tree of P33, for which the top NCBI hit was *Metabacillus idriensis*. *Lysinibacillus boronitolerans* was used as an outgroup.

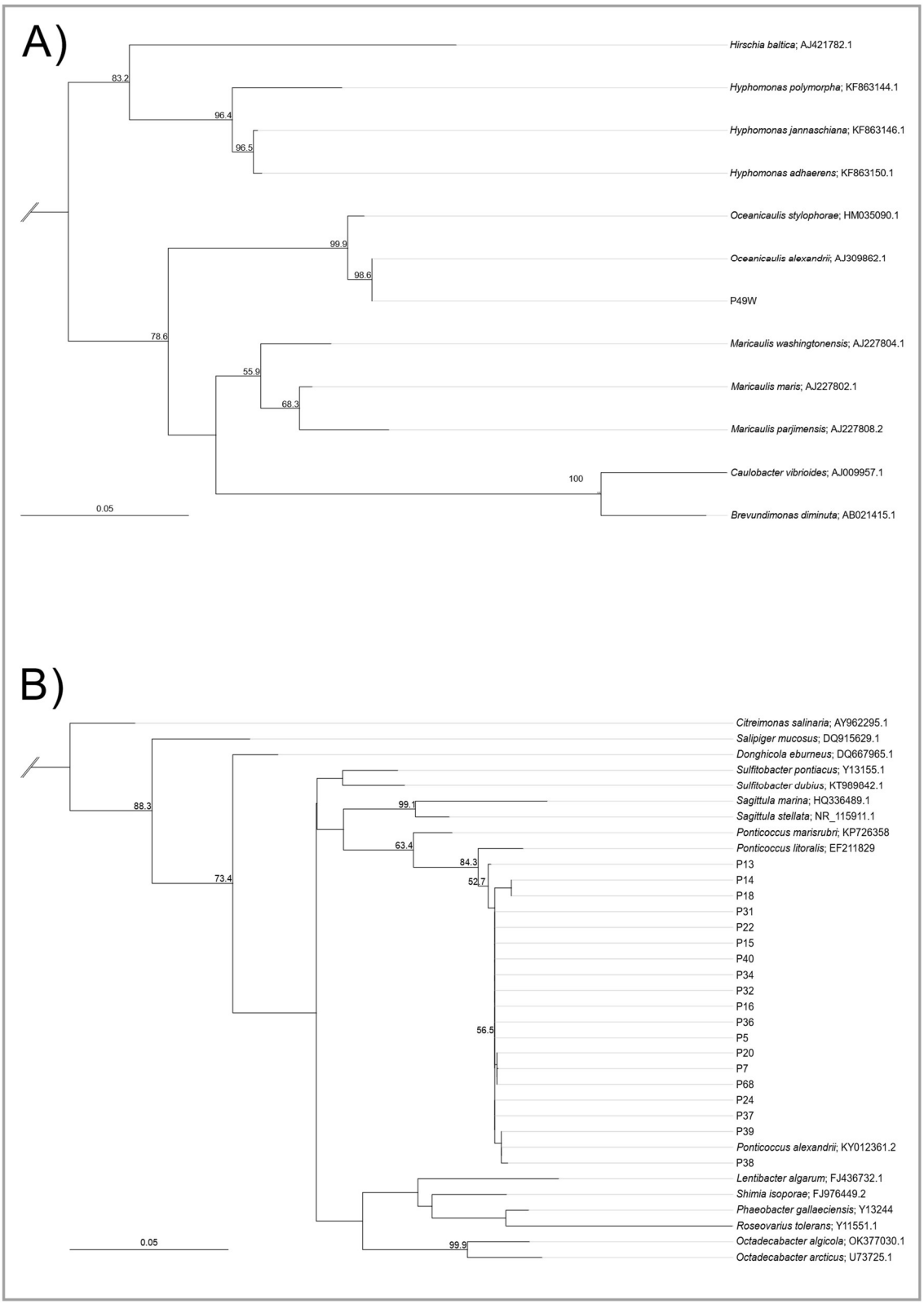

Appendix Figure 5. Maximum Likelihood trees constructed to verify the taxonomic assignment of plaque assay isolates. ML trees were constructed using full-length 16S rRNA sequences of plaque assay isolates and type strains of top NCBI BLAST hit and closely related species. Branch support values above 50 % are shown (calculated from 1000 bootstraps). **A)** ML tree of P49W, for which the top NCBI hit was *Oceanicaulis alexandrii*. *Jannaschia seosinensis* was used as an outgroup. **B)** ML tree of P5, P7, P13 – P16, P18, P20, P22, P31 – P32, P34, P35 – P40 and P64, for which the top NCBI hit was *Ponticoccus alexandrii*. *Rubellimicrobium aerolatum* was used as an outgroup.

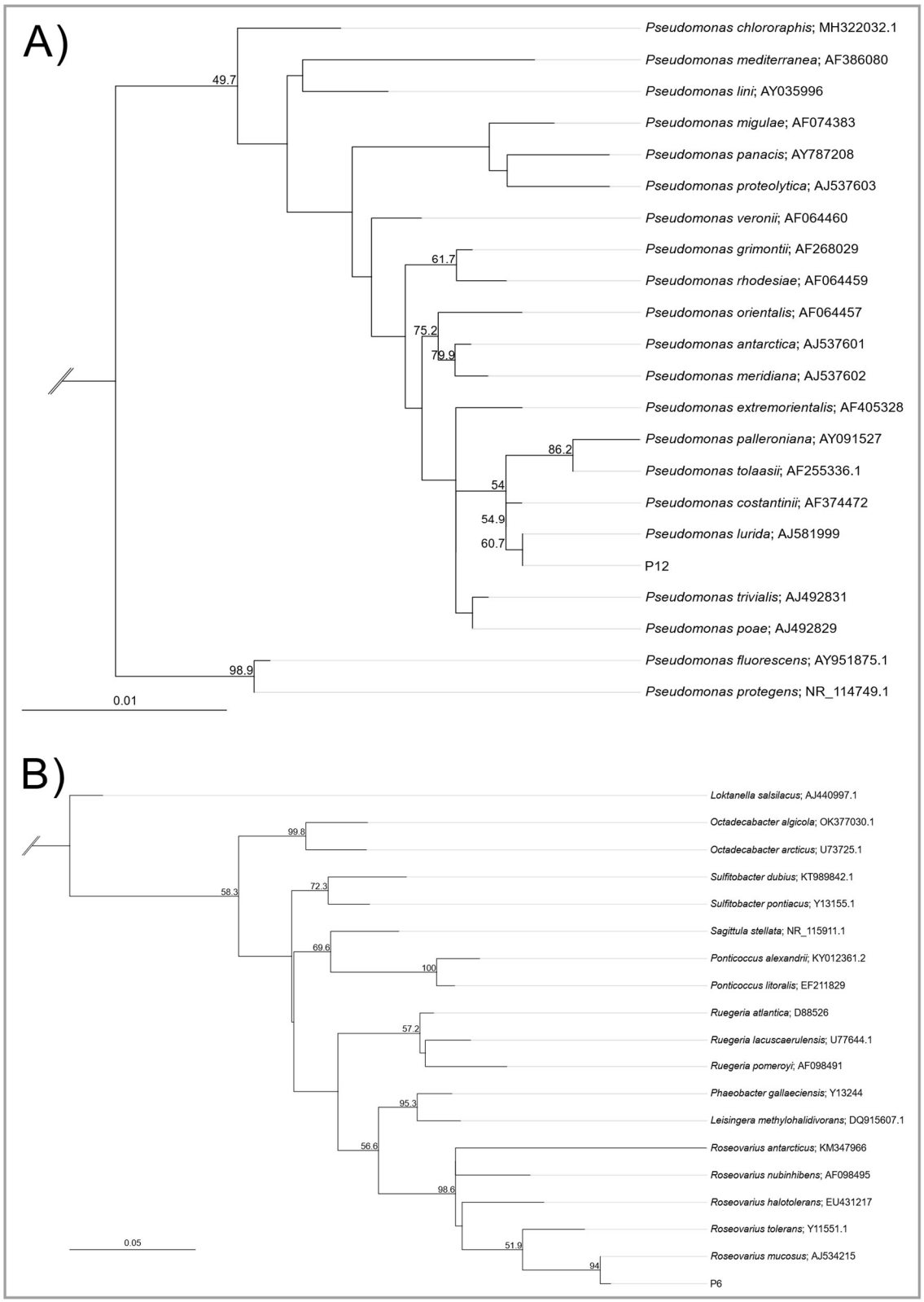

Appendix Figure 6. Maximum Likelihood trees constructed to verify the taxonomic assignment of plaque assay isolates. ML trees were constructed using full-length 16S rRNA sequences of plaque assay isolates and type strains of top NCBI BLAST hit and closely related species. Branch support values above 50 % are shown (calculated from 1000 bootstraps). **A)** ML tree of P12, for which the top NCBI hit was *Pseudomonas lurida*. *Pseudomonas aeruginosa* was used as an outgroup. **B)** ML tree of P6, for which the top NCBI hit was *Roseovarius mucosus*. *Rubellimicrobium aerolatum* was used as an outgroup.

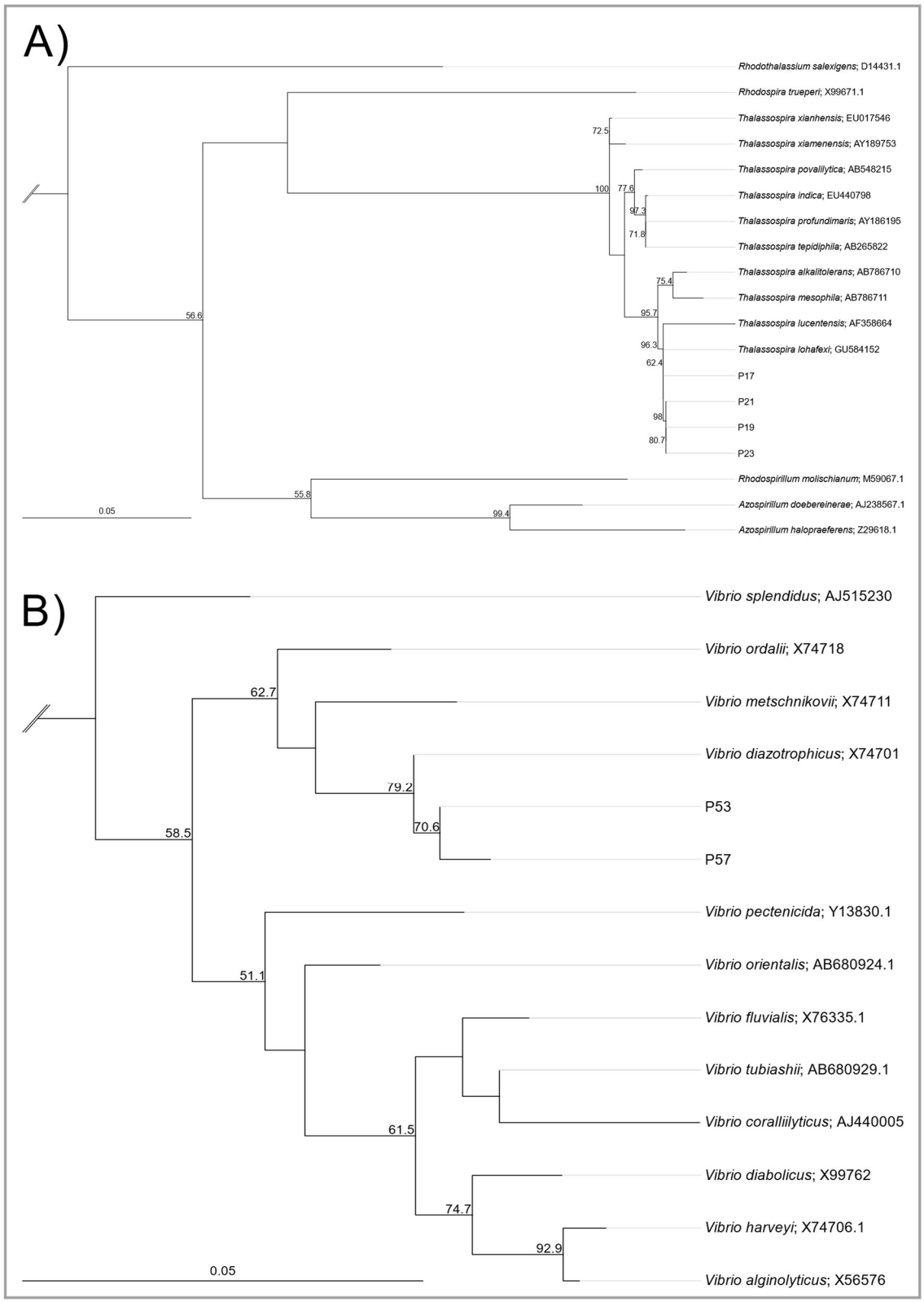

Appendix Figure 7. Maximum Likelihood trees constructed to verify the taxonomic assignment of plaque assay isolates. ML trees were constructed using full-length 16S rRNA sequences of plaque assay isolates and type strains of top NCBI BLAST hit and closely related species. Branch support values above 50 % are shown (calculated from 1000 bootstraps). **A)** ML tree of P17, P19, P21 and P23, for which the top NCBI hit was *Thalassospira lohafexi* and/or *Thalassospira lucentensis*. *Azorhizobium caulinodans* was used as an outgroup. **B)** ML tree of P53 and P57, for which the top NCBI hit was *Vibrio diazotrophicus*. *Salinivibrio costicola* was used as an outgroup.

A)  B) 

Appendix Figure 8. Images of soft-agar overlay assay using *P. tricornutum* in December 2020, which resulted in 'bubble' like plaques. **A)** Top view of assay plate, **B)** side view of assay plate showing raised, gas-filled 'bubbles'.

Appendix Table 2. Bacterial antagonists isolated from soft-agar overlay assay plaques. Nearest hit was determined via examination of 16S rRNA sequences using the NCBI BLAST database and construction of maximum likelihood phylogenetic trees using type strains of closely related species. Information on diatom host, location and date of isolation, and whether antagonistic activity has previously been reported for the species is also included.

Plaque number	Isolate number	Nearest Hit	Date isolated	Location of sample collection	Diatom Host	Bacterial class	Previously reported antagonistic activity	Previously reported diatom-antagonist?	Reference
1	P1	*Marinobacter adhaerens*	02/06/2020	Plymouth seafront	*C. simplex*	Gammaproteobacteria	Yes	Yes	10.1128/aem.01619-22
2	P2	*Marinobacter adhaerens*	02/06/2020	Plymouth seafront	*C. simplex*	Gammaproteobacteria	Yes	Yes	10.1128/aem.01619-22
3	P3	*Marinobacter adhaerens*	02/06/2020	Plymouth seafront	*C. simplex*	Gammaproteobacteria	Yes	Yes	10.1128/aem.01619-22
4	P4	*Marinobacter adhaerens*	02/06/2020	Plymouth seafront	*C. simplex*	Gammaproteobacteria	Yes	Yes	10.1128/aem.01619-22
5	P5	*Ponticoccus alexandrii*	02/06/2020	Plymouth seafront	*S. marinoi*	Alphaproteobacteria	*Ponticoccus* sp. only	No	10.1186/s13568-017-0357-6
6	P6	*Roseovarius mucosus*	16/06/2020	Plymouth seafront	*C. simplex*	Alphaproteobacteria	No	No	
7	P7	*Ponticoccus alexandrii*	16/06/2020	Plymouth seafront	*C. simplex*	Alphaproteobacteria	*Ponticoccus* sp. only	No	10.1186/s13568-017-0357-6
8	P8	*Marinobacter adhaerens*	16/06/2020	Plymouth seafront	*C. simplex*	Gammaproteobacteria	Yes	Yes	10.1128/aem.01619-22
9	P9	*Marinobacter adhaerens*	16/06/2020	Plymouth seafront	*C. simplex*	Gammaproteobacteria	Yes	Yes	10.1128/aem.01619-22
10	P10	*Marinobacter adhaerens*	16/06/2020	Plymouth seafront	*C. simplex*	Gammaproteobacteria	Yes	Yes	10.1128/aem.01619-22
11	P11	*Marinobacter algicola*	04/08/2020	Station L4	*S. marinoi*	Gammaproteobacteria	Yes	No	10.1016/j.scitotenv.2018.03.035
12	P12	*Pseudomonas lurida*	04/08/2020	Station L4	*S. marinoi*	Gammaproteobacteria	*Pseudomonas* sp. only	*Pseudomonas* sp. only	10.1007/s12562-011-0345-8
13	P13	*Ponticoccus alexandrii*	04/08/2020	Station L4	*S. marinoi*	Alphaproteobacteria	*Ponticoccus* sp. only	No	10.1186/s13568-017-0357-6
14	P14	*Ponticoccus alexandrii*	04/08/2020	Station L4	*S. marinoi*	Alphaproteobacteria	*Ponticoccus* sp. only	No	10.1186/s13568-017-0357-6
15	P15	*Ponticoccus alexandrii*	04/08/2020	Station L4	*S. marinoi*	Alphaproteobacteria	*Ponticoccus* sp. only	No	10.1186/s13568-017-0357-6
16	P16	*Ponticoccus alexandrii*	17/12/2020	Station L4	*S. marinoi*	Alphaproteobacteria	*Ponticoccus* sp. only	No	10.1186/s13568-017-0357-6
17	P17	*Thalassospira lohafexi*	17/12/2020	Station L4	*S. marinoi*	Alphaproteobacteria	*Thalassospira* sp. only	No	10.1007/s00253-016-7352-8
18	P18	*Ponticoccus alexandrii*	17/12/2020	Station L4	*S. marinoi*	Alphaproteobacteria	*Ponticoccus* sp. only	No	10.1186/s13568-017-0357-6
19	P19	*Thalassospira lohafexi*	17/12/2020	Station L4	*T. pseudonana*	Alphaproteobacteria	*Thalassospira* sp. only	No	10.1007/s00253-016-7352-8
20	P20	*Ponticoccus alexandrii*	17/12/2020	Station L4	*T. pseudonana*	Alphaproteobacteria	*Ponticoccus* sp. only	No	10.1186/s13568-017-0357-6
21	P21	*Thalassospira lohafexi*	17/12/2020	Station L4	*T. pseudonana*	Alphaproteobacteria	*Thalassospira* sp. only	No	10.1007/s00253-016-7352-8
22	P22	*Ponticoccus alexandrii*	17/12/2020	Station L4	*T. weissflogii*	Alphaproteobacteria	*Ponticoccus* sp. only	No	10.1186/s13568-017-0357-6
23	P23	*Thalassospira lohafexi*	17/12/2020	Station L4	*T. weissflogii*	Alphaproteobacteria	*Thalassospira* sp. only	No	10.1007/s00253-016-7352-8
24	P24	*Ponticoccus alexandrii*	17/12/2020	Station L4	*T. weissflogii*	Alphaproteobacteria	*Ponticoccus* sp. only	No	10.1186/s13568-017-0357-6
25	P25	*Maribacter dokdonensis*	17/12/2020	Station L4	*P. tricornutum*	Flavobacteria	Yes	Yes	10.1016/j.algal.2015.11.012
26	P26	*Maribacter spongiicola*	17/12/2020	Station L4	*P. tricornutum*	Flavobacteria	No	No	
27	P27	*Hoeflea phototrophica*	17/12/2020	Station L4	*P. tricornutum*	Alphaproteobacteria	No	No	
28	P28	*Hoeflea phototrophica*	17/12/2020	Station L4	*C. simplex*	Alphaproteobacteria	No	No	
29	P29Y	*Maribacter dokdonensis*	17/12/2020	Station L4	*C. simplex*	Flavobacteria	Yes	Yes	10.1016/j.algal.2015.11.012
	P29W	*Halomonas titanicae*	17/12/2020	Station L4	*C. simplex*	Gammaproteobacteria	*Halomonas* sp. only	No	10.1016/j.scitotenv.2018.03.035 10.1016/j.biocontrol.2010.10.004
30	P30	*Ahrensia kielensis*	17/12/2020	Station L4	*C. simplex*	Alphaproteobacteria	No	No	
31	P31	*Ponticoccus alexandrii*	12/10/2020	Station L4	*T. weissflogii*	Alphaproteobacteria	*Ponticoccus* sp. only	No	10.1186/s13568-017-0357-6
32	P32	*Ponticoccus alexandrii*	12/10/2020	Station L4	*T. weissflogii*	Alphaproteobacteria	*Ponticoccus* sp. only	No	10.1186/s13568-017-0357-6
33	P33	*Metabacillus idriensis*	04/08/2020	Station L4	*P. tricornutum*	Bacilli	No	No	

Plaque number	Isolate number	Nearest Hit	Date isolated	Location of sample collection	Diatom Host	Bacterial class	Previously reported antagonistic activity	Previously reported diatom-antagonist?	Reference
34	P34	*Ponticoccus alexandrii*	12/10/2020	Station L4	*T. pseudonana*	Alphaproteobacteria	*Ponticoccus* sp. only	No	10.1186/s13568-017-0357-6
35	P35	*Hoeflea halophila*	12/10/2020	Station L4	*S. marinoi*	Alphaproteobacteria	No	No	
36	P36	*Ponticoccus alexandrii*	12/10/2020	Station L4	*S. marinoi*	Alphaproteobacteria	*Ponticoccus* sp. only	No	10.1186/s13568-017-0357-6
37	P37	*Ponticoccus alexandrii*	01/02/2021	Station L4	*T. pseudonana*	Alphaproteobacteria	*Ponticoccus* sp. only	No	10.1186/s13568-017-0357-6
38	P38	*Ponticoccus alexandrii*	01/03/2021	Station L4	*S. marinoi*	Alphaproteobacteria	*Ponticoccus* sp. only	No	10.1186/s13568-017-0357-6
39	P39	*Ponticoccus alexandrii*	01/03/2021	Station L4	*S. marinoi*	Alphaproteobacteria	*Ponticoccus* sp. only	No	10.1186/s13568-017-0357-6
40	P40	*Ponticoccus alexandrii*	01/03/2021	Station L4	*S. marinoi*	Alphaproteobacteria	*Ponticoccus* sp. only	No	10.1186/s13568-017-0357-6
41	P41B	*Paracoccus* sp.	01/02/2021	Station L4	*C. simplex*	Alphaproteobacteria			
	P41F	Unidentified	01/02/2021	Station L4	*C. simplex*	Unidentified			
42	P42	*Marinobacter algicola*	07/09/2020	Station L4	*T. pseudonana*	Gammaproteobacteria	Yes	No	10.1016/j.scitotenv.2018.03.035
43	P43	*Marinobacter adhaerens*	01/02/2021	Station L4	*T. weissflogii*	Gammaproteobacteria	Yes	Yes	10.1128/aem.01619-22
44	P44	*Hoeflea phototrophica*	01/03/2021	Station L4	*C. simplex*	Alphaproteobacteria	No	No	
45	P45R	*Aestuariivita* sp.	01/03/2021	Station L4	*C. simplex*	Alphaproteobacteria	No	No	
45 46	P45W	*Halomonas titanicae*	01/03/2021	Station L4	*C. simplex*	Gammaproteobacteria	*Halomonas* sp. only	No	10.1016/j.scitotenv.2018.03.035 10.1016/j.biocontrol.2010.10.004
	P46R	*Aestuariivita* sp.	01/03/2021	Station L4	*C. simplex*	Alphaproteobacteria	No	No	
46	P46W	*Hoeflea phototrophica*	01/03/2021	Station L4	*C. simplex*	Alphaproteobacteria	No	No	
47	P47R	*Aestuariivita* sp.	06/04/2021	Station L4	*C. simplex*	Alphaproteobacteria	No	No	
47 48	P47W	*Hoeflea phototrophica*	06/04/2021	Station L4	*C. simplex*	Alphaproteobacteria	No	No	
	P48	*Halomonas titanicae*	01/03/2021	Station L4	*T. weissflogii*	Gammaproteobacteria	*Halomonas* sp. only	No	10.1016/j.scitotenv.2018.03.035 10.1016/j.biocontrol.2010.10.004
49	P49R	*Aestuariivita* sp.	01/03/2021	Station L4	*T. weissflogii*	Alphaproteobacteria	No	No	
49 50	P49W	*Oceanicaulis alexandrii*	01/03/2021	Station L4	*T. weissflogii*	Alphaproteobacteria	No	No	
	P50	*Halomonas titanicae*	01/03/2021	Station L4	*T. weissflogii*	Gammaproteobacteria	*Halomonas* sp. only	No	10.1016/j.scitotenv.2018.03.035 10.1016/j.biocontrol.2010.10.004
51	P51	*Halomonas titanicae*	01/03/2021	Station L4	*T. weissflogii*	Gammaproteobacteria	*Halomonas* sp. only	No	10.1016/j.scitotenv.2018.03.035 10.1016/j.biocontrol.2010.10.004
52	P52	*Halomonas titanicae*	01/03/2021	Station L4	*T. weissflogii*	Gammaproteobacteria	*Halomonas* sp. only	No	10.1016/j.scitotenv.2018.03.035 10.1016/j.biocontrol.2010.10.004
53	P53	*Vibrio diazotrophicus*	27/07/2021	Station L4	*T. pseudonana*	Gammaproteobacteria	*Vibrio* sp. only	No	10.1371/journal.pone.0091201 10.1016/j.biortech.2019.122246
54	P54	*Halomonas titanicae*	27/07/2021	Station L4	*T. pseudonana*	Gammaproteobacteria	*Halomonas* sp. only	No	10.1016/j.scitotenv.2018.03.035 10.1016/j.biocontrol.2010.10.004
55	P55	*Halomonas titanicae*	27/07/2021	Station L4	*T. pseudonana*	Gammaproteobacteria	*Halomonas* sp. only	No	10.1016/j.scitotenv.2018.03.035 10.1016/j.biocontrol.2010.10.004
56	P56	*Halomonas titanicae*	27/07/2021	Station L4	*T. pseudonana*	Gammaproteobacteria	*Halomonas* sp. only	No	10.1016/j.scitotenv.2018.03.035 10.1016/j.biocontrol.2010.10.004
57	P57	*Vibrio diazotrophicus*	27/07/2021	Station L4	*T. pseudonana*	Gammaproteobacteria	*Vibrio* sp. only	No	10.1371/journal.pone.0091201 10.1016/j.biortech.2019.122246
58	P58	*Halomonas titanicae*	27/07/2021	Station L4	*T. pseudonana*	Gammaproteobacteria	*Halomonas* sp. only	No	10.1016/j.scitotenv.2018.03.035 10.1016/j.biocontrol.2010.10.004
59	P59	*Marinobacter algicola*	27/07/2021	Station L4	*T. weissflogii*	Gammaproteobacteria	Yes	No	10.1016/j.scitotenv.2018.03.035
60	P60	Unidentified	27/07/2021	Station L4	*T. pseudonana*	Unidentified			
61	P61	*Alteromonas simiduii*	27/07/2021	Station L4	*T. pseudonana*	Gammaproteobacteria	*Alteromonas* sp. only	*Alteromonas* sp. only	10.1016/j.scitotenv.2018.03.035 10.1016/j.algal.2015.11.012
62	P62	*Hoeflea alexandrii*	20/07/2021	Station L4	*T. weissflogii*	Alphaproteobacteria	No	No	

63	P63	*Halomonas titanicae*	20/07/2021	Station L4	*T. weissflogii*	Gammaproteobacteria	*Halomonas* sp. only	No	10.1016/j.scitotenv.2018.03.035 10.1016/j.biocontrol.2010.10.004
Plaque number	**Isolate number**	**Nearest Hit**	**Date isolated**	**Location of sample collection**	**Diatom Host**	**Bacterial class**	**Previously reported antagonistic activity**	**Previously reported diatom-antagonist?**	**Reference**
64	P64	*Halomonas titanicae*	20/07/2021	Station L4	*T. weissflogii*	Gammaproteobacteria	*Halomonas* sp. only	No	10.1016/j.scitotenv.2018.03.035 10.1016/j.biocontrol.2010.10.004
65	P65	Unidentified	20/07/2021	Station L4	*T. weissflogii*	Unidentified			
66	P66	*Halomonas titanicae*	20/07/2021	Station L4	*T. weissflogii*	Gammaproteobacteria	*Halomonas* sp. only	No	10.1016/j.scitotenv.2018.03.035 10.1016/j.biocontrol.2010.10.004
67	P67	Unidentified	20/07/2021	Station L4	*T. weissflogii*	Unidentified			
68	P68	*Ponticoccus alexandrii*	20/07/2021	Station L4	*S. marinoi*	Alphaproteobacteria	*Ponticoccus* sp. only	No	10.1186/s13568-017-0357-6

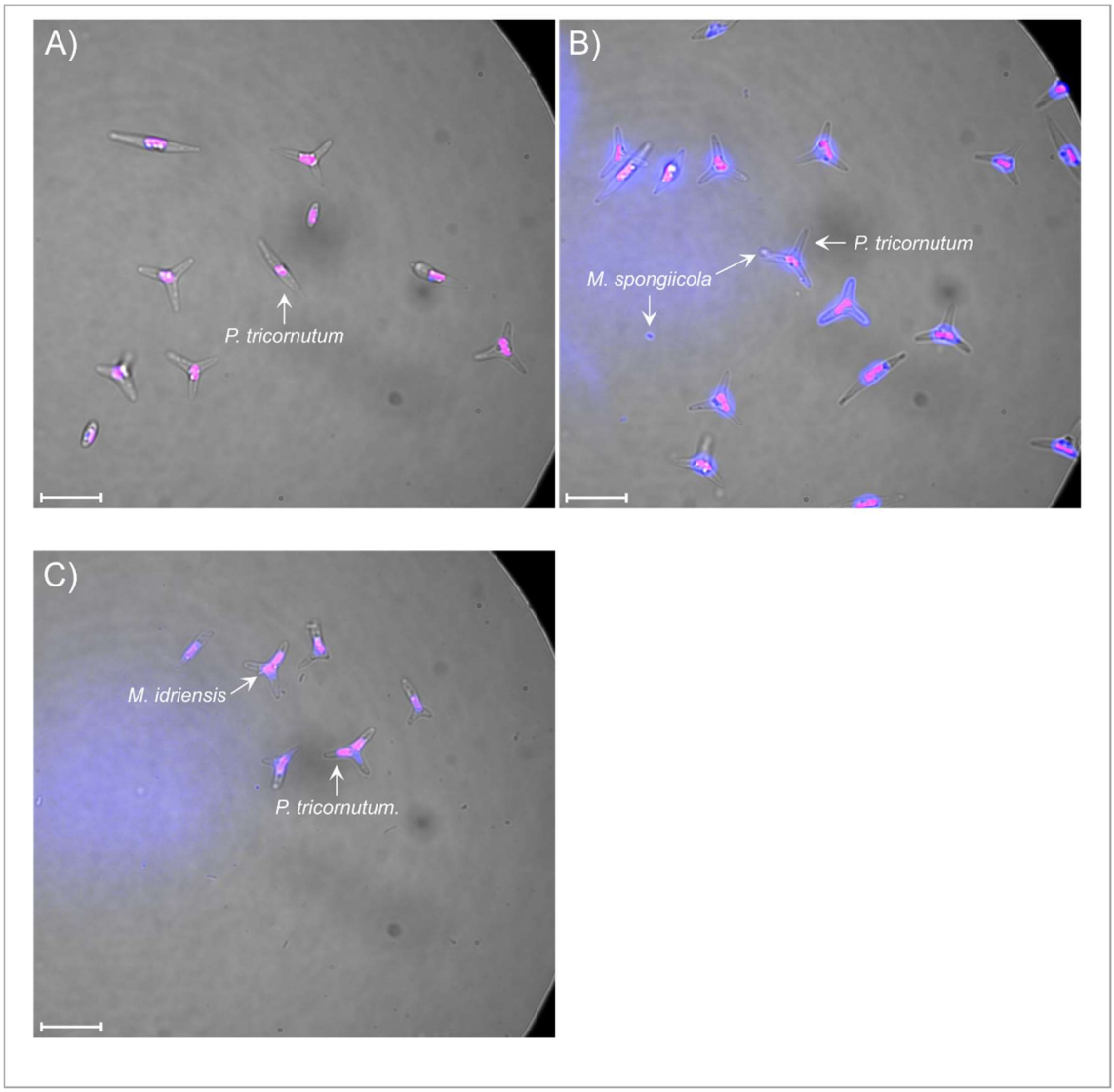

Appendix Figure 9. Epifluorescence micrographs of **A)** axenic *P. tricornutum* control culture, **B)** *P. tricornutum* co-cultured with *M. spongiicola* cultured on DDM, and **C)** *P. tricornutum* co-cultured with *M. idriensis* cultured on DDM after 4 days of co-cultivation. Subsamples of each culture were incubated with Hoechst 33342 nucleic acid and imaged using a LEICA DMi8, excited with 395 nm excitation and 460 nm emission filters, with a 63 × 1.4NA oil immersion objective. Blue fluorescence represents DNA Hoescht-stained DNA of both bacteria and diatom material and red fluorescence represents diatom chloroplast autofluorescence. *P. tricornutum*, *M. spongiicola* and *M. idriensis* cells are indicated by white arrows. Scale bars represent 15 µm.

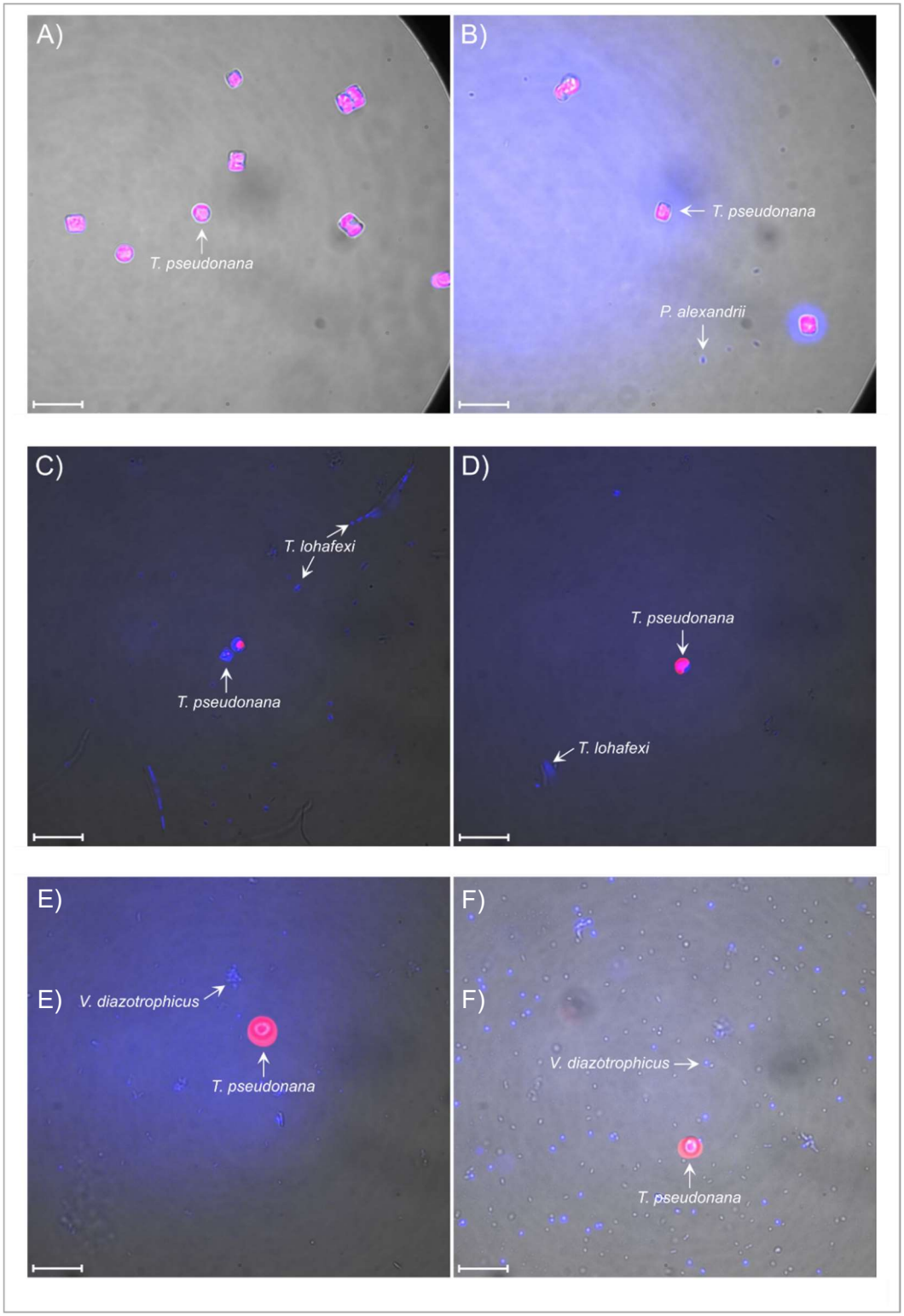

Appendix Figure 10. Epifluorescence micrographs of **A)** axenic *T. pseudonana* control culture, **B)** *T. pseudonana* co-cultured with *P. alexandrii* cultured on DDM, **C)** *T. pseudonana* co-cultured with *T. lohafexi* cultured on DDM, **D)** *T. pseudonana* co-cultured with *T. lohafexi* cultured on ½ YTSS, **E)** *T. pseudonana* co-cultured with *V. diazotrophicus* cultured on DDM, and **F)** *T. pseudonana* co-cultured with *V. diazotrophicus* cultured on ½ YTSS, after 14 days of co-cultivation. Subsamples of each culture were incubated with Hoechst 33342 nucleic acid and imaged using a LEICA DMi8, excited with 395 nm excitation and 460 nm emission filters, with a 63 × 1.4NA oil immersion objective. Blue fluorescence represents DNA Hoescht-stained DNA of both bacteria and diatom material and red fluorescence represents diatom chloroplast autofluorescence. *T. pseudonana, P. alexandrii, T. lohafexi* and *V. diazotrophicus* cells are indicated by white arrows. Scale bars represent 15 µm.

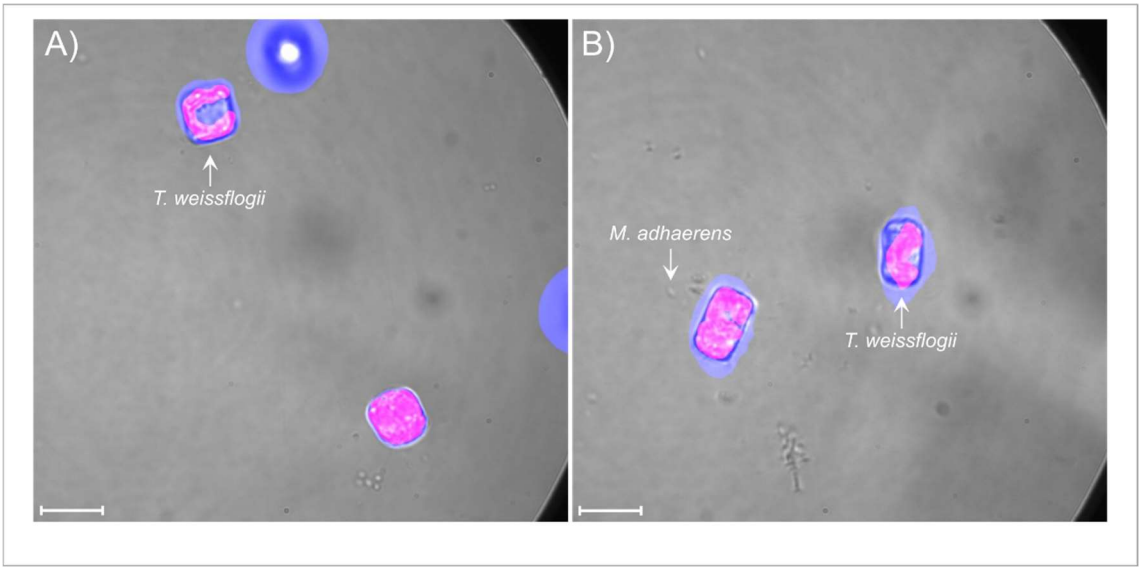

Appendix Figure 11. Epifluorescence micrographs of **A)** axenic *T. weissflogii* control culture, and **B)** *T. weissflogii* co-cultured with *M. adhaerens* cultured on DDM, after 6 days of co-cultivation. Subsamples of each culture were incubated with Hoechst 33342 nucleic acid and imaged using a LEICA DMi8, excited with 395 nm excitation and 460 nm emission filters, with a 63 × 1.4NA oil immersion objective. Blue fluorescence represents DNA Hoescht-stained DNA of both bacteria and diatom material and red fluorescence represents diatom chloroplast autofluorescence. *T. weissflogii* and *M. adhaerens* cells are indicated by white arrows. Scale bars represent 15 µm.

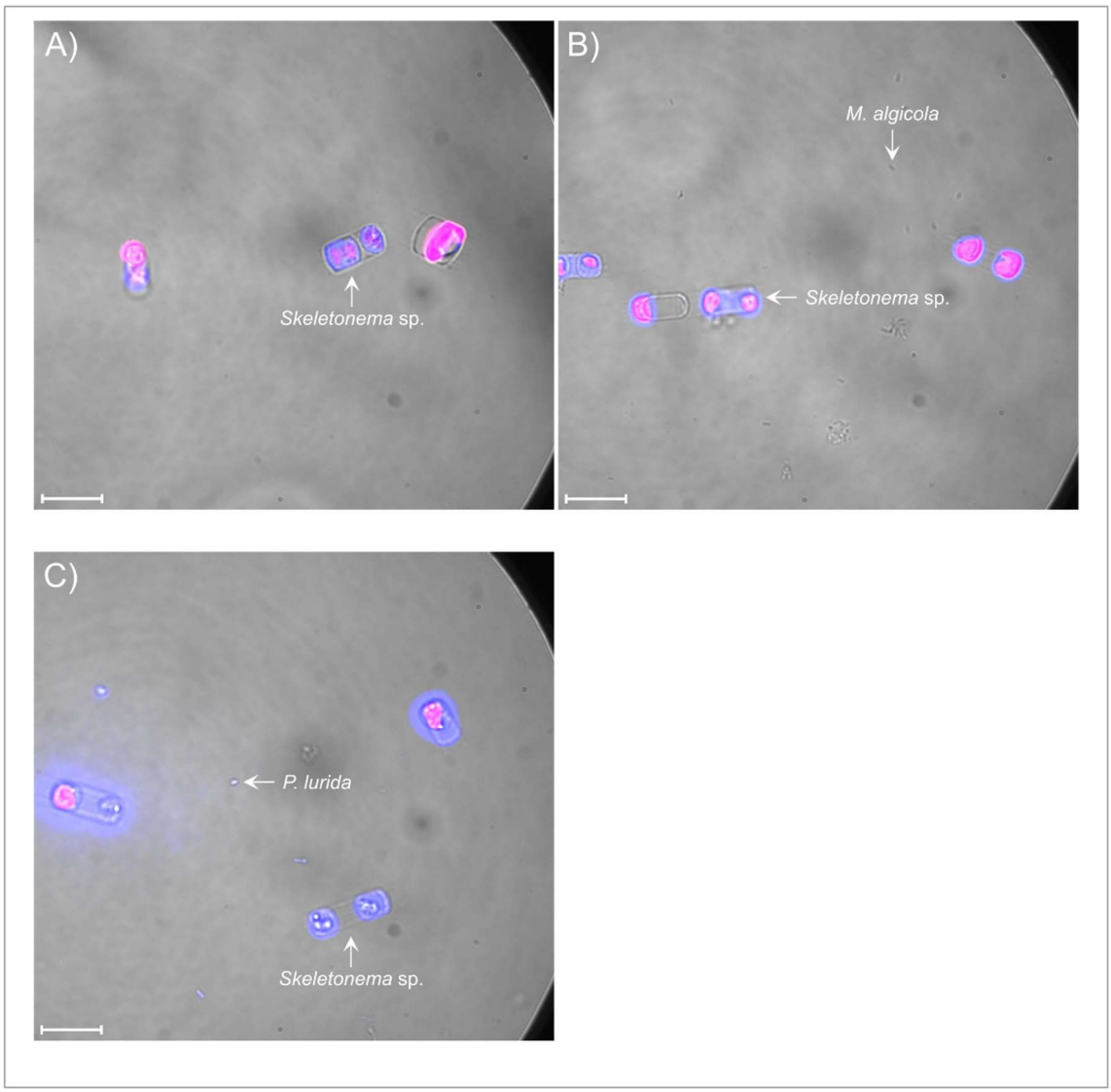

Appendix Figure 12. Epifluorescence micrographs of **A)** axenic *Skeletonema* sp. PLY627 control culture, **B)** *Skeletonema* sp. PLY627 co-cultured with *M. algicola* cultured on DDM and **C)** *Skeletonema* sp. PLY627 co-cultured with *P. lurida* cultured on DDM after 7 days of co-cultivation. Subsamples of each culture were incubated with Hoechst 33342 nucleic acid and imaged using a LEICA DMi8, excited with 395 nm excitation and 460 nm emission filters, with a 63 × 1.4NA oil immersion objective. Blue fluorescence represents DNA Hoescht-stained DNA of both bacteria and diatom material and red fluorescence represents diatom chloroplast autofluorescence. *Skeletonema* sp., *M. algicola* and *P. lurida* cells are indicated by white arrows. Scale bars represent 15 µm.

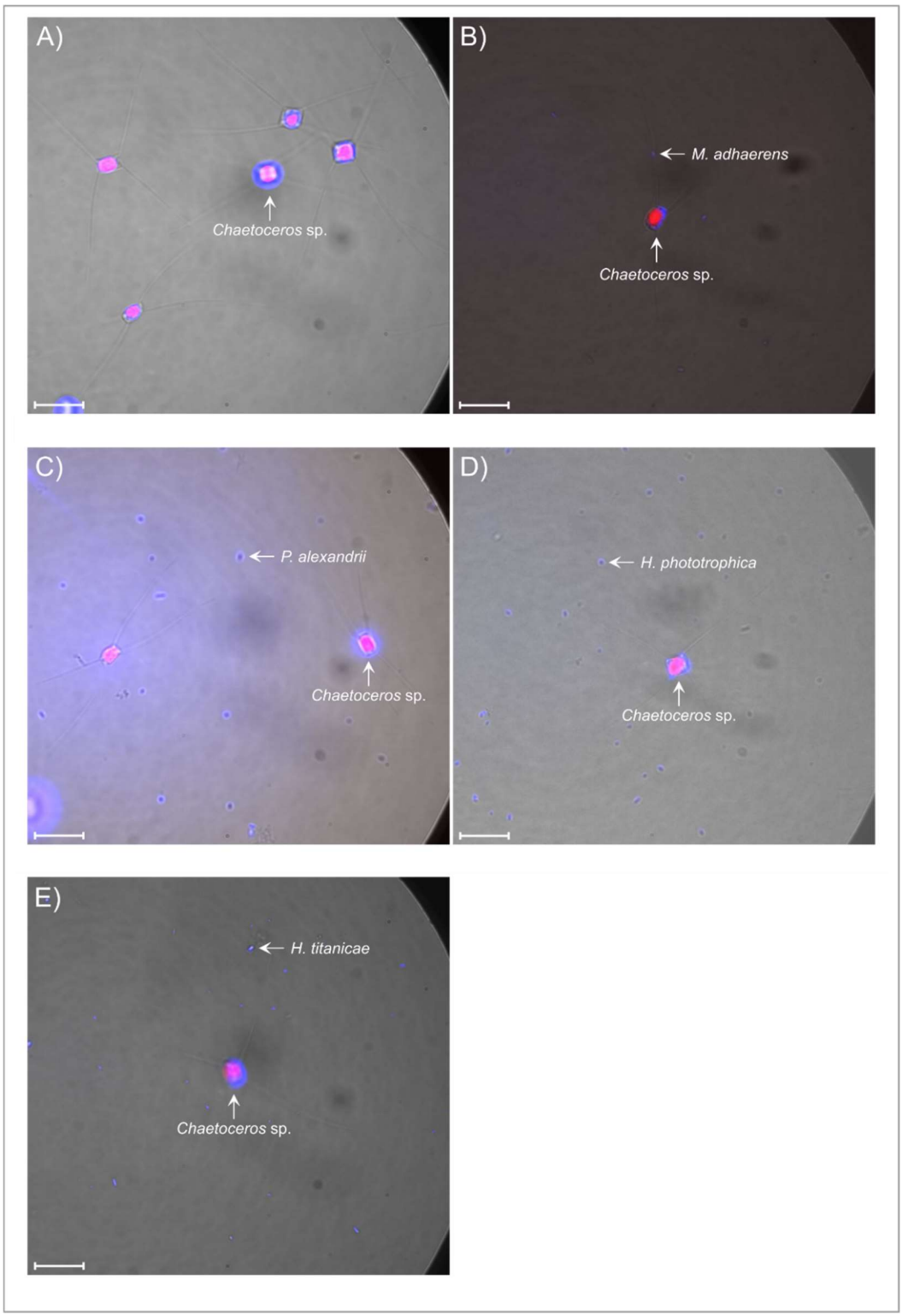

Appendix Figure 13. Epifluorescence micrographs of ***A)*** axenic *Chaetoceros* sp. PLY617 control culture, ***B)*** *Chaetoceros* sp. PLY617 co-cultured with *M. adhaerens* cultured on DDM, ***C)*** Chaetoceros sp. PLY617 co-cultured with *P. alexandrii* cultured on DDM, ***D)*** *Chaetoceros* sp. PLY617 co-cultured with *H. phototrophica* cultured on DDM, and ***E)*** *Chaetoceros* sp. PLY617 co-cultured with *H. titanicae* cultured on DDM, after 4 days of co-cultivation. Subsamples of each culture were incubated with Hoechst 33342 nucleic acid and imaged using a LEICA DMi8, excited with 395 nm excitation and 460 nm emission filters, with a 63 × 1.4NA oil immersion objective. Blue fluorescence represents DNA Hoescht-stained DNA of both bacteria and diatom material and red fluorescence represents diatom chloroplast autofluorescence. *Chaetoceros* sp., *M. adhaerens*, *P. alexandrii*, *H. phototrophica* and *H. titanicae* cells are indicated by white arrows. Scale bars represent 15 µm.

Chapter 3: Prevalence and seasonal trends of diatom-antagonistic bacteria in the Western English Channel

Appendix Table 3. Samples removed from the 16S rRNA amplicon sequence dataset due to low read depth to reduce diversity loss. Sample date, replicate number (four replicates were processed per sampling point) and read depth of each sample are given.

Sample	Sampling Date	Replicate	Sampling Location	Read depth
P1KBird41	30/03/2021	1	Station L4	8,391
P1KBird42	30/03/2021	2	Station L4	6,753
P1KBird73	28/04/2021	1	Station L4	8,966
P1KBird75	28/04/2021	3	Station L4	6,043

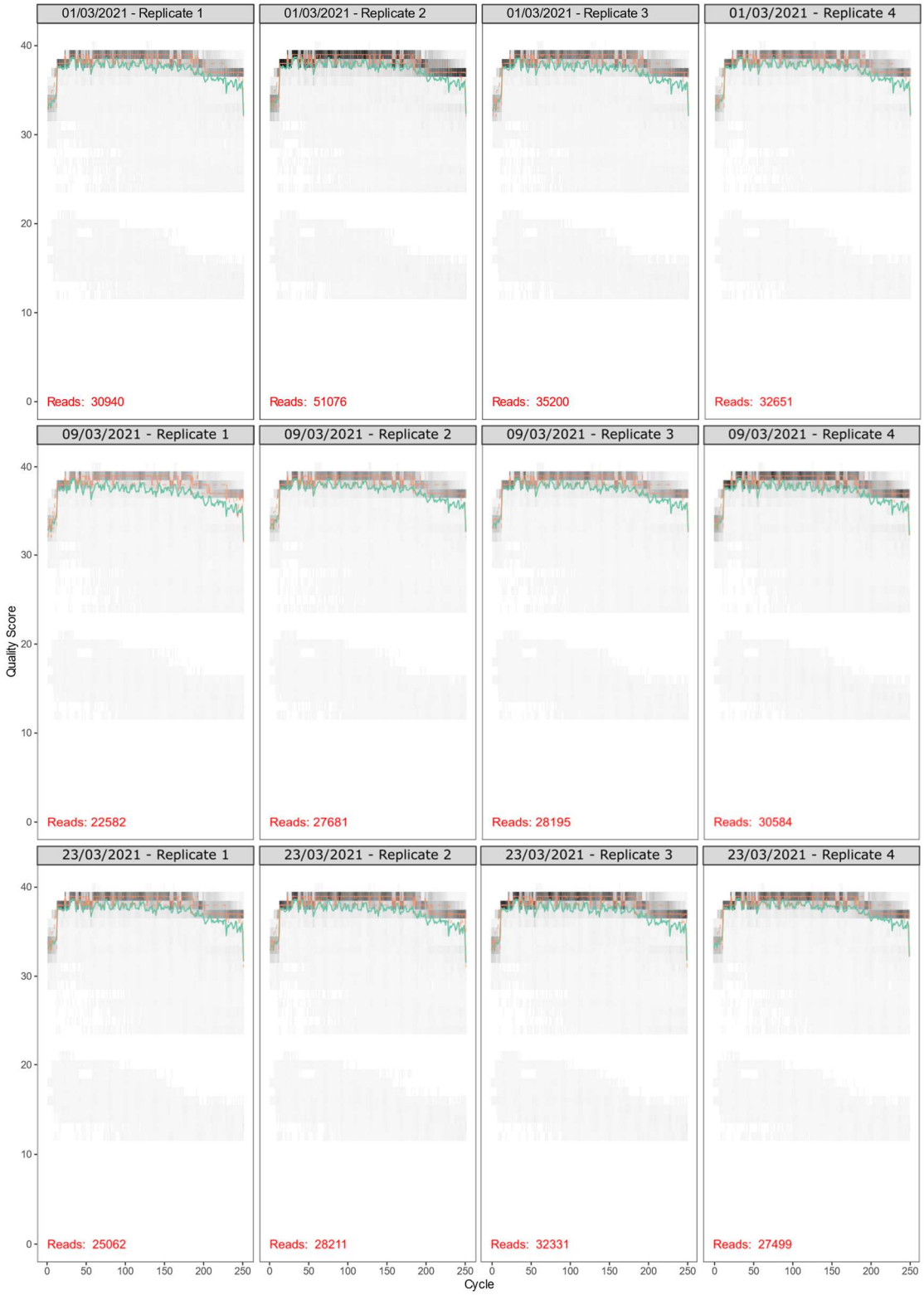

Appendix Figure 14. A-H) Quality profiles for each of the 16S rRNA samples (forward reads) produced by Illumina MiSeq sequencing. Quality profiles were produced using the DADA2 pipeline (Callahan et al., 2016) and visually inspected to ensure all samples were of sufficient quality before continuing with subsequent analysis. Each sample is labelled with the date the sample was collected and replicate number.

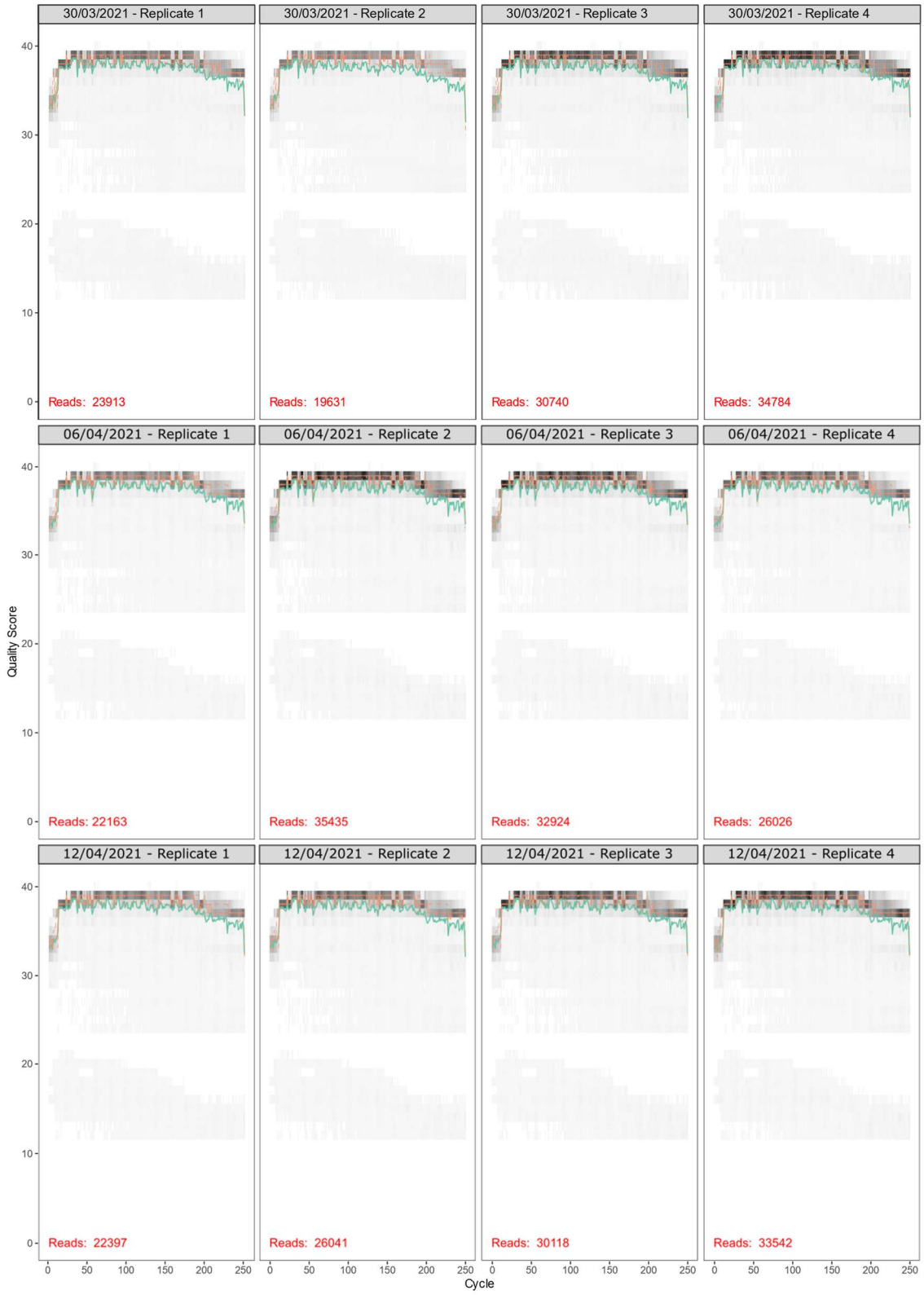

Appendix Figure 14. B) Quality profiles for each of the 16S rRNA samples (forward reads) produced by Illumina MiSeq sequencing. Quality profiles were produced using the DADA2 pipeline (Callahan et al., 2016) and visually inspected to ensure all samples were of sufficient quality before continuing with subsequent analysis. Each sample is labelled with the date the sample was collected and replicate number.

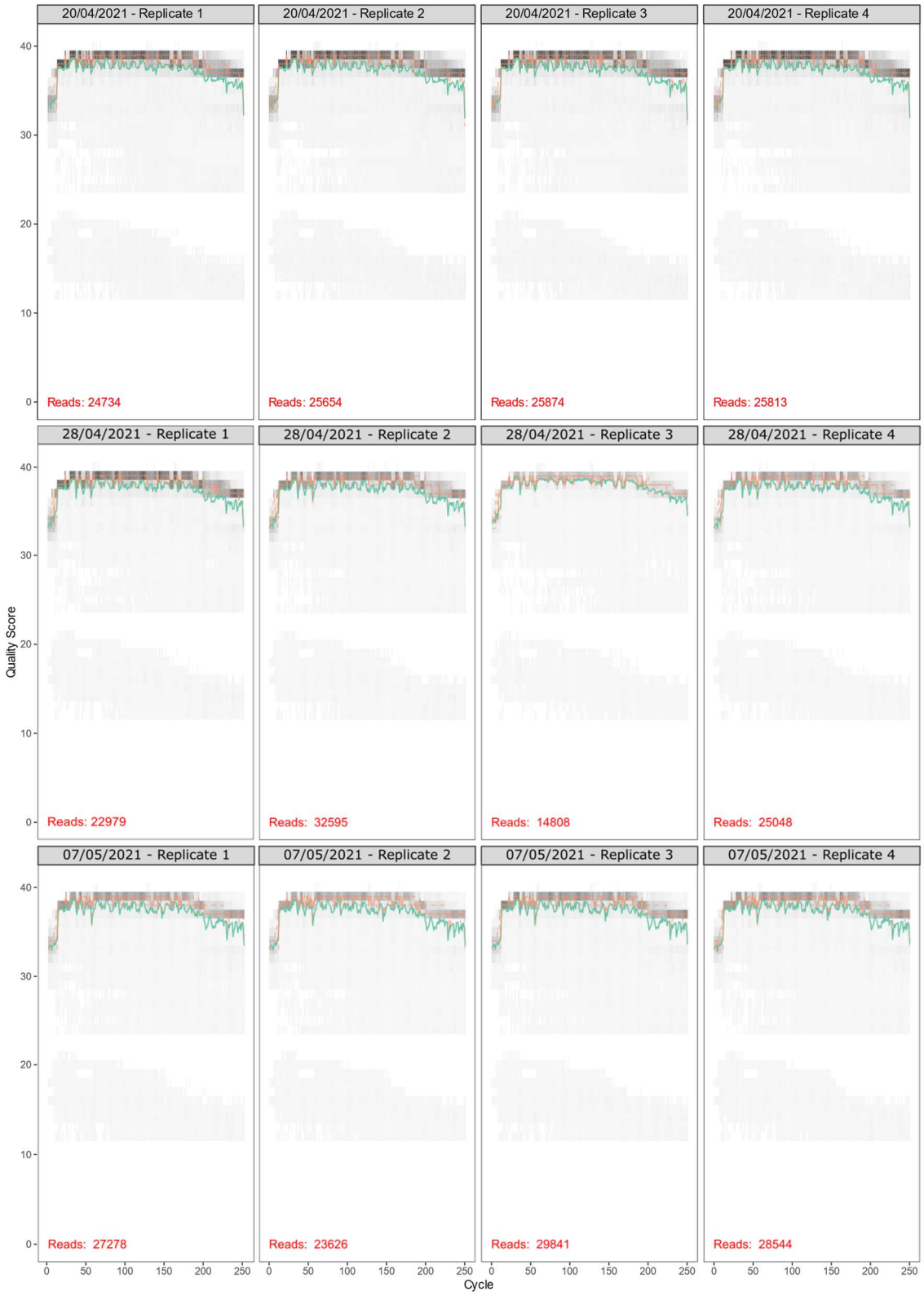

Appendix Figure 14. C) Quality profiles for each of the 16S rRNA samples (forward reads) produced by Illumina MiSeq sequencing. Quality profiles were produced using the DADA2 pipeline (Callahan et al., 2016) and visually inspected to ensure all samples were of sufficient quality before continuing with subsequent analysis. Each sample is labelled with the date the sample was collected and replicate number.

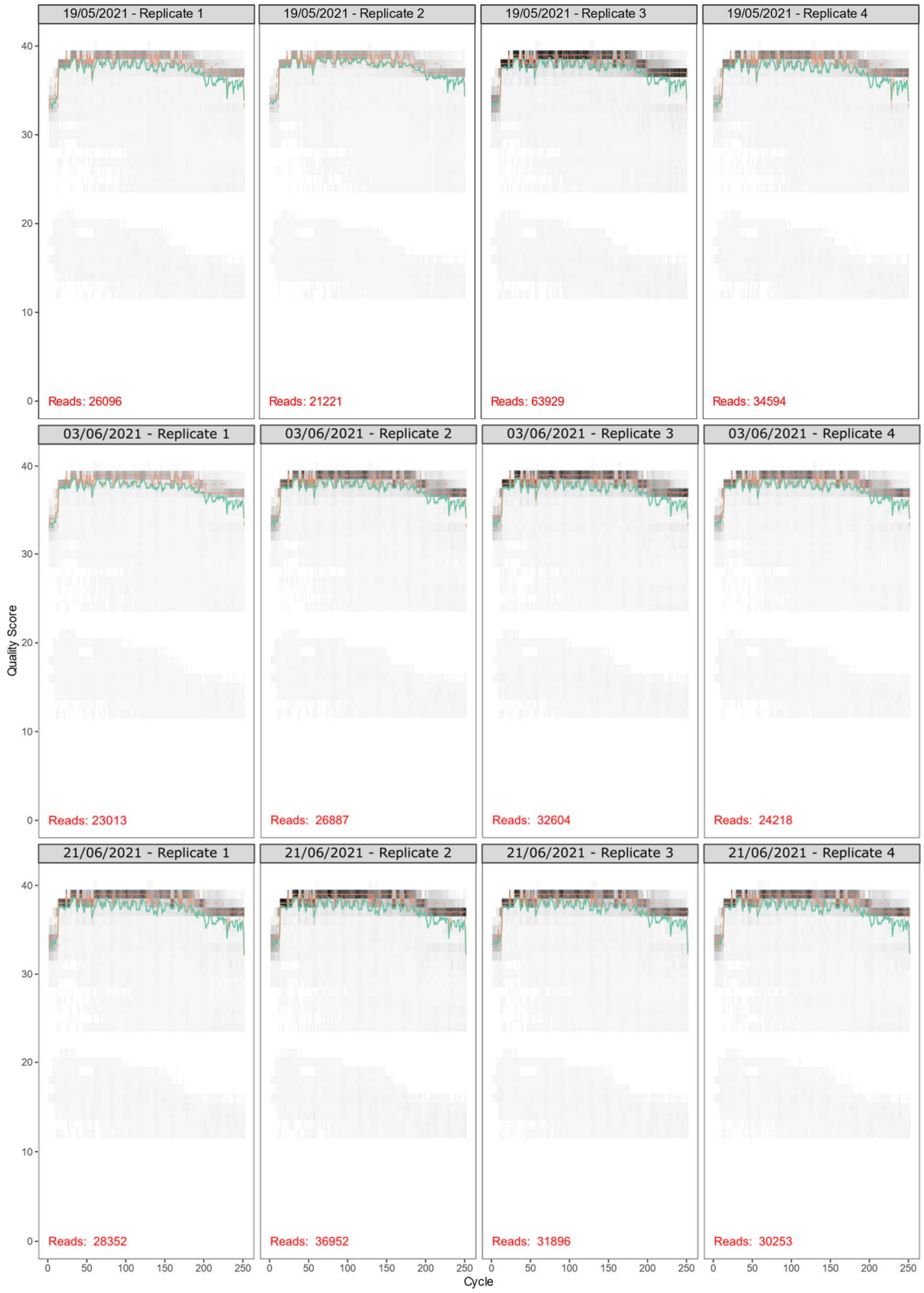

Appendix Figure 14. D) Quality profiles for each of the 16S rRNA samples (forward reads) produced by Illumina MiSeq sequencing. Quality profiles were produced using the DADA2 pipeline (Callahan et al., 2016) and visually inspected to ensure all samples were of sufficient quality before continuing with subsequent analysis. Each sample is labelled with the date the sample was collected and replicate number.

Appendix Figure 14. E) Quality profiles for each of the 16S rRNA samples (forward reads) produced by Illumina MiSeq sequencing. Quality profiles were produced using the DADA2 pipeline (Callahan et al., 2016) and visually inspected to ensure all samples were of sufficient quality before continuing with subsequent analysis. Each sample is labelled with the date the sample was collected and replicate number.

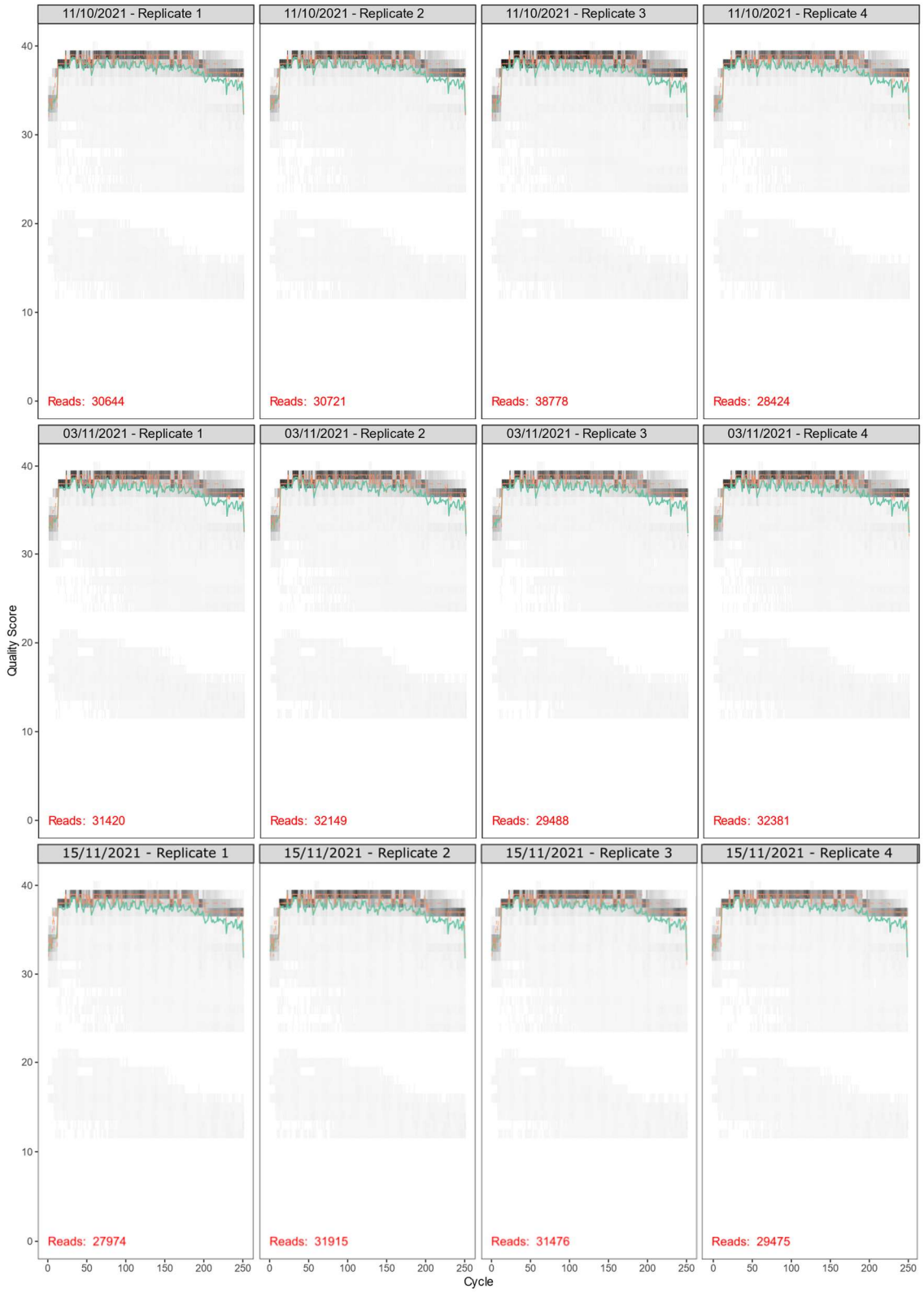

Appendix Figure 14. F) Quality profiles for each of the 16S rRNA samples (forward reads) produced by Illumina MiSeq sequencing. Quality profiles were produced using the DADA2 pipeline (Callahan et al., 2016) and visually inspected to ensure all samples were of sufficient quality before continuing with subsequent analysis. Each sample is labelled with the date the sample was collected and replicate number.

Appendix Figure 14. G) Quality profiles for each of the 16S rRNA samples (forward reads) produced by Illumina MiSeq sequencing. Quality profiles were produced using the DADA2 pipeline (Callahan et al., 2016) and visually inspected to ensure all samples were of sufficient quality before continuing with subsequent analysis. Each sample is labelled with the date the sample was collected and replicate number.

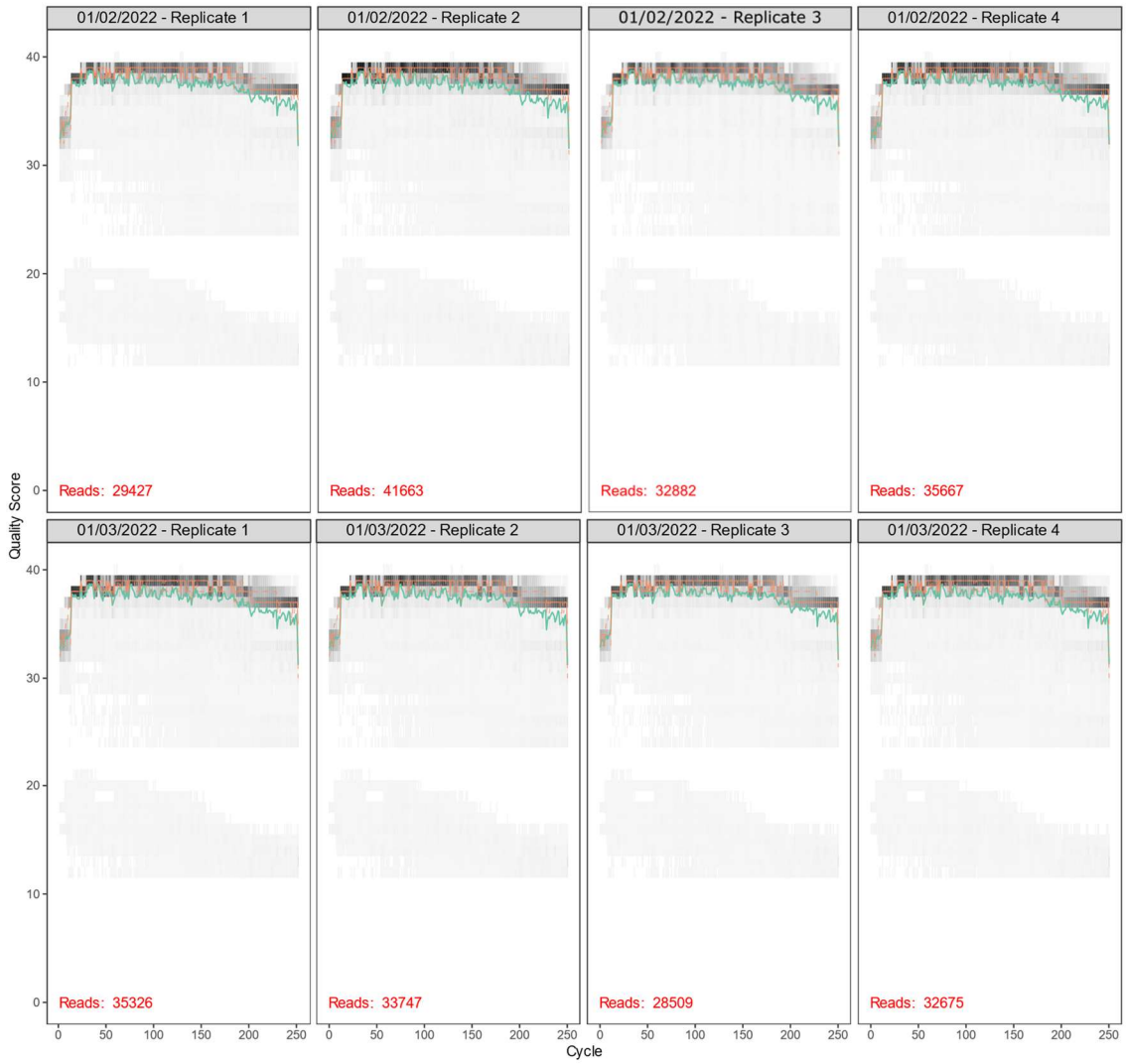

Appendix Figure 14. H) Quality profiles for each of the 16S rRNA samples (forward reads) produced by Illumina MiSeq sequencing. Quality profiles were produced using the DADA2 pipeline (Callahan et al., 2016) and visually inspected to ensure all samples were of sufficient quality before continuing with subsequent analysis. Each sample is labelled with the date the sample was collected and replicate number.

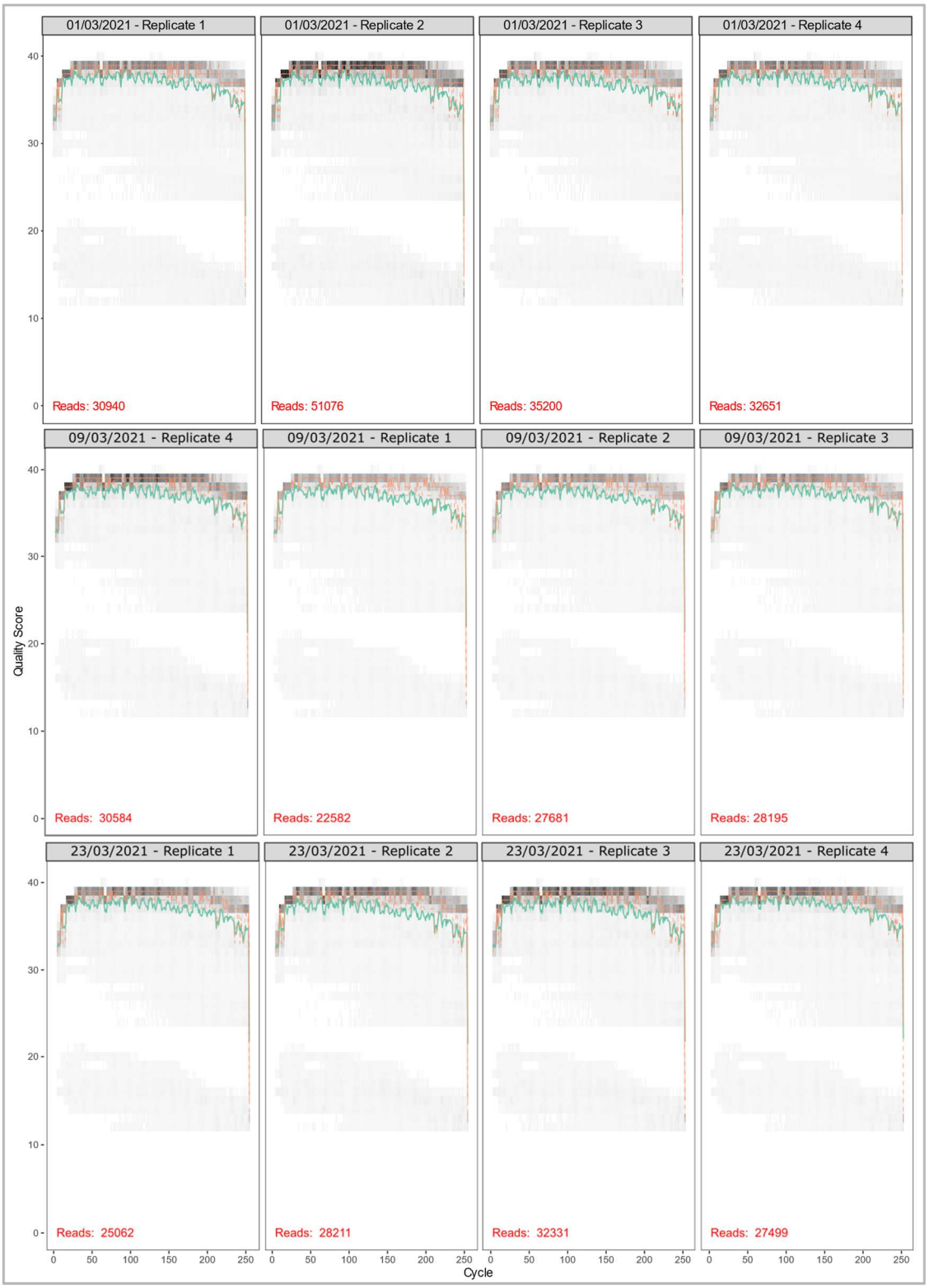

Appendix Figure 15. A) Quality profiles for each of the 16S rRNA samples (reverse reads) produced by Illumina MiSeq sequencing. Quality profiles were produced using the DADA2 pipeline (Callahan et al., 2016) and visually inspected to ensure all samples were of sufficient quality before continuing with subsequent analysis. Each sample is labelled with the date the sample was collected and replicate number.

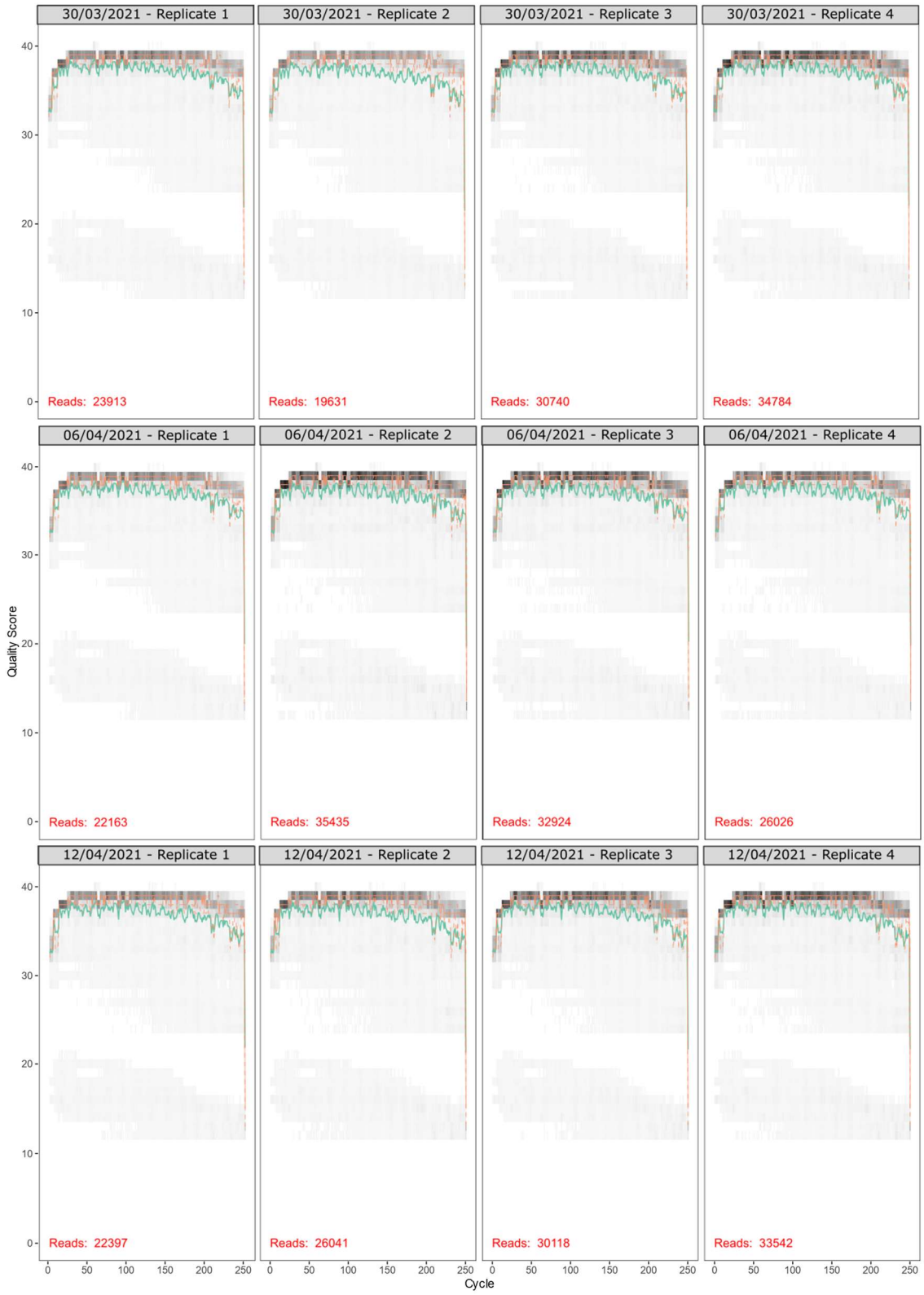

Appendix Figure 15. B) Quality profiles for each of the 16S rRNA samples (reverse reads) produced by Illumina MiSeq sequencing. Quality profiles were produced using the DADA2 pipeline (Callahan et al., 2016) and visually inspected to ensure all samples were of sufficient quality before continuing with subsequent analysis. Each sample is labelled with the date the sample was collected and replicate number.

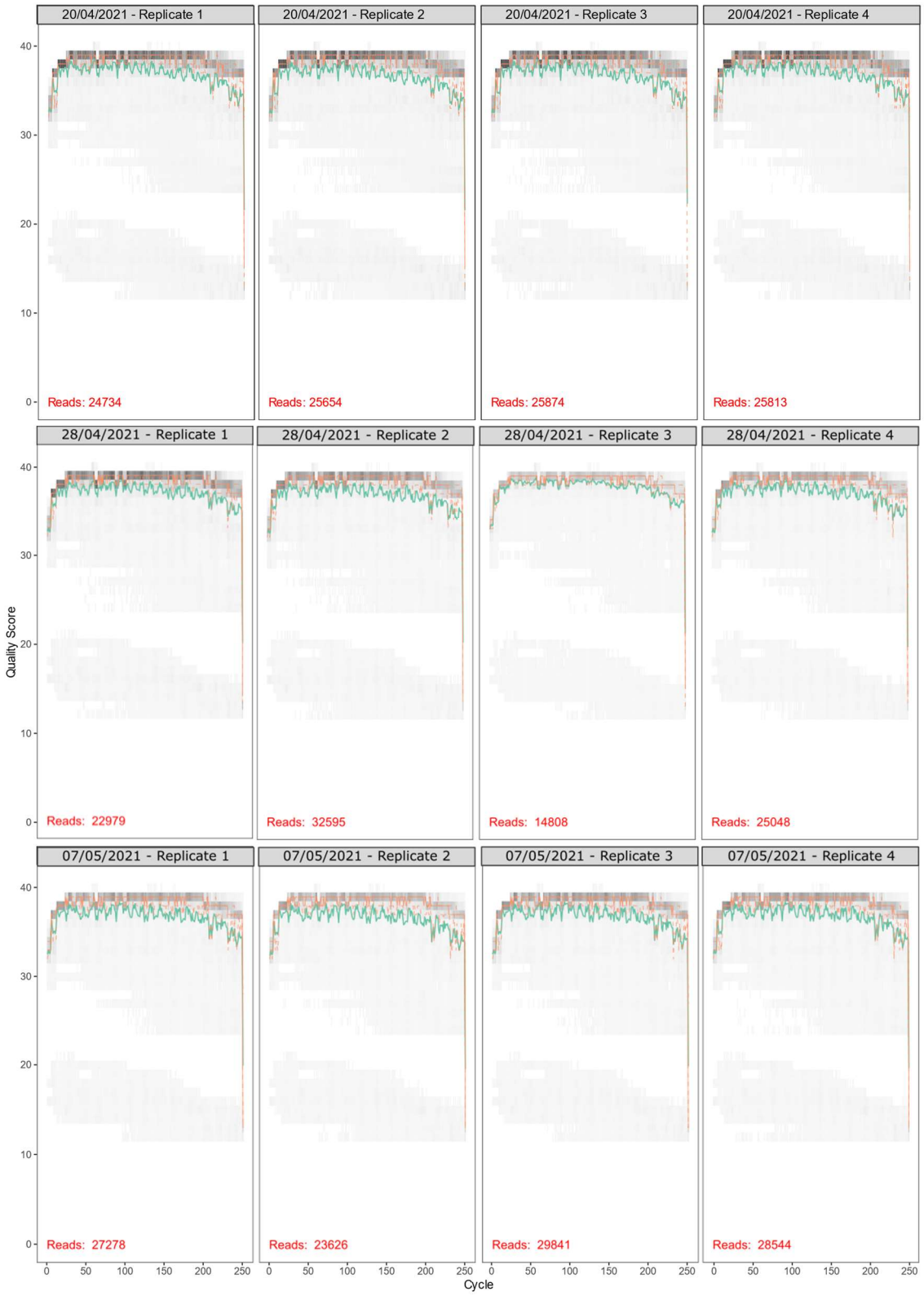

Appendix Figure 15. C) Quality profiles for each of the 16S rRNA samples (reverse reads) produced by Illumina MiSeq sequencing. Quality profiles were produced using the DADA2 pipeline (Callahan et al., 2016) and visually inspected to ensure all samples were of sufficient quality before continuing with subsequent analysis. Each sample is labelled with the date the sample was collected and replicate number.

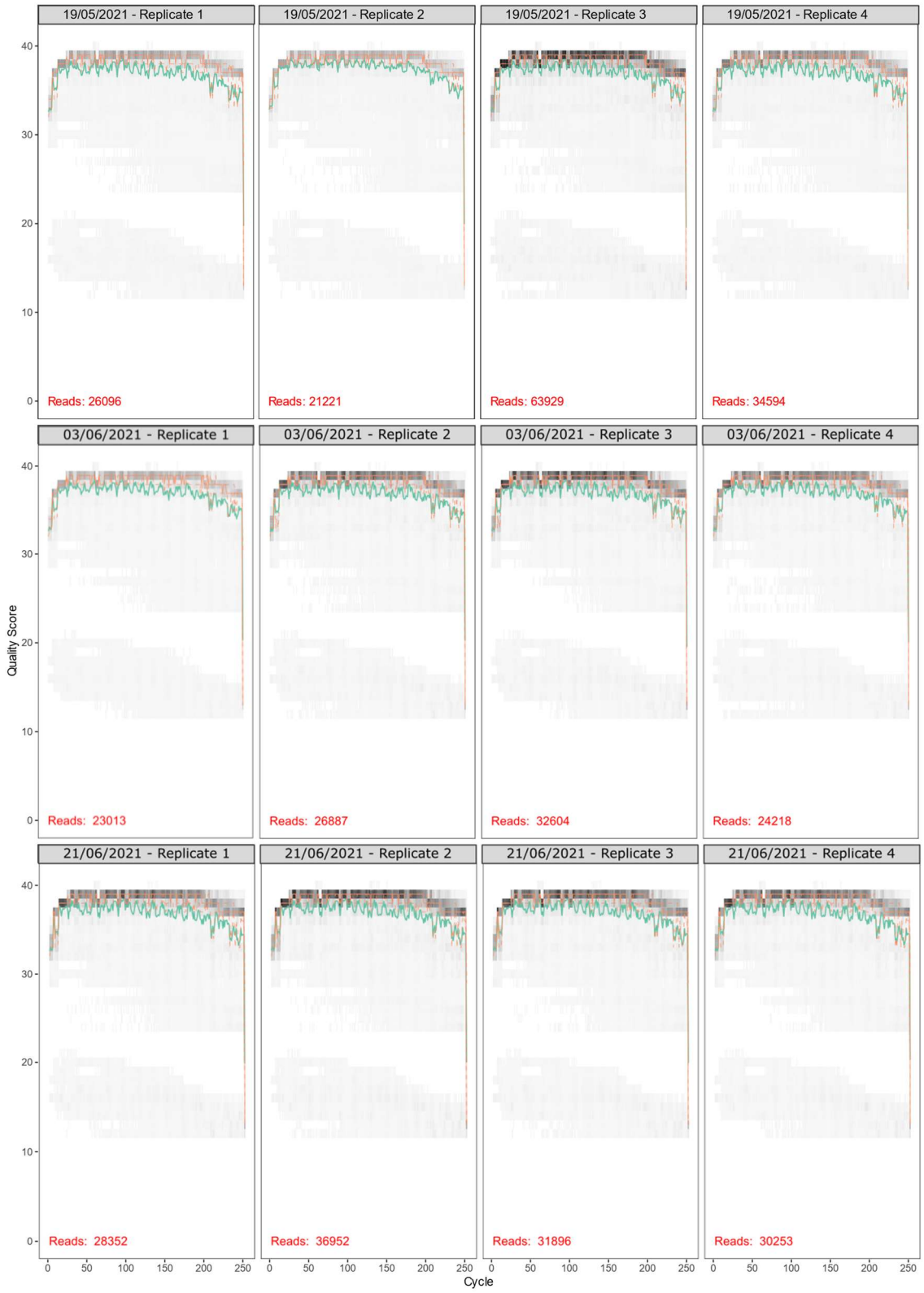

Appendix Figure 15. D) Quality profiles for each of the 16S rRNA samples (reverse reads) produced by Illumina MiSeq sequencing. Quality profiles were produced using the DADA2 pipeline (Callahan et al., 2016) and visually inspected to ensure all samples were of sufficient quality before continuing with subsequent analysis. Each sample is labelled with the date the sample was collected and replicate number.

Appendix Figure 15. E) Quality profiles for each of the 16S rRNA samples (reverse reads) produced by Illumina MiSeq sequencing. Quality profiles were produced using the DADA2 pipeline (Callahan et al., 2016) and visually inspected to ensure all samples were of sufficient quality before continuing with subsequent analysis. Each sample is labelled with the date the sample was collected and replicate number.

Appendix Figure 15. F) Quality profiles for each of the 16S rRNA samples (reverse reads) produced by Illumina MiSeq sequencing. Quality profiles were produced using the DADA2 pipeline (Callahan et al., 2016) and visually inspected to ensure all samples were of sufficient quality before continuing with subsequent analysis. Each sample is labelled with the date the sample was collected and replicate number.

Appendix Figure 15. G) Quality profiles for each of the 16S rRNA samples (reverse reads) produced by Illumina MiSeq sequencing. Quality profiles were produced using the DADA2 pipeline (Callahan et al., 2016) and visually inspected to ensure all samples were of sufficient quality before continuing with subsequent analysis. Each sample is labelled with the date the sample was collected and replicate number.

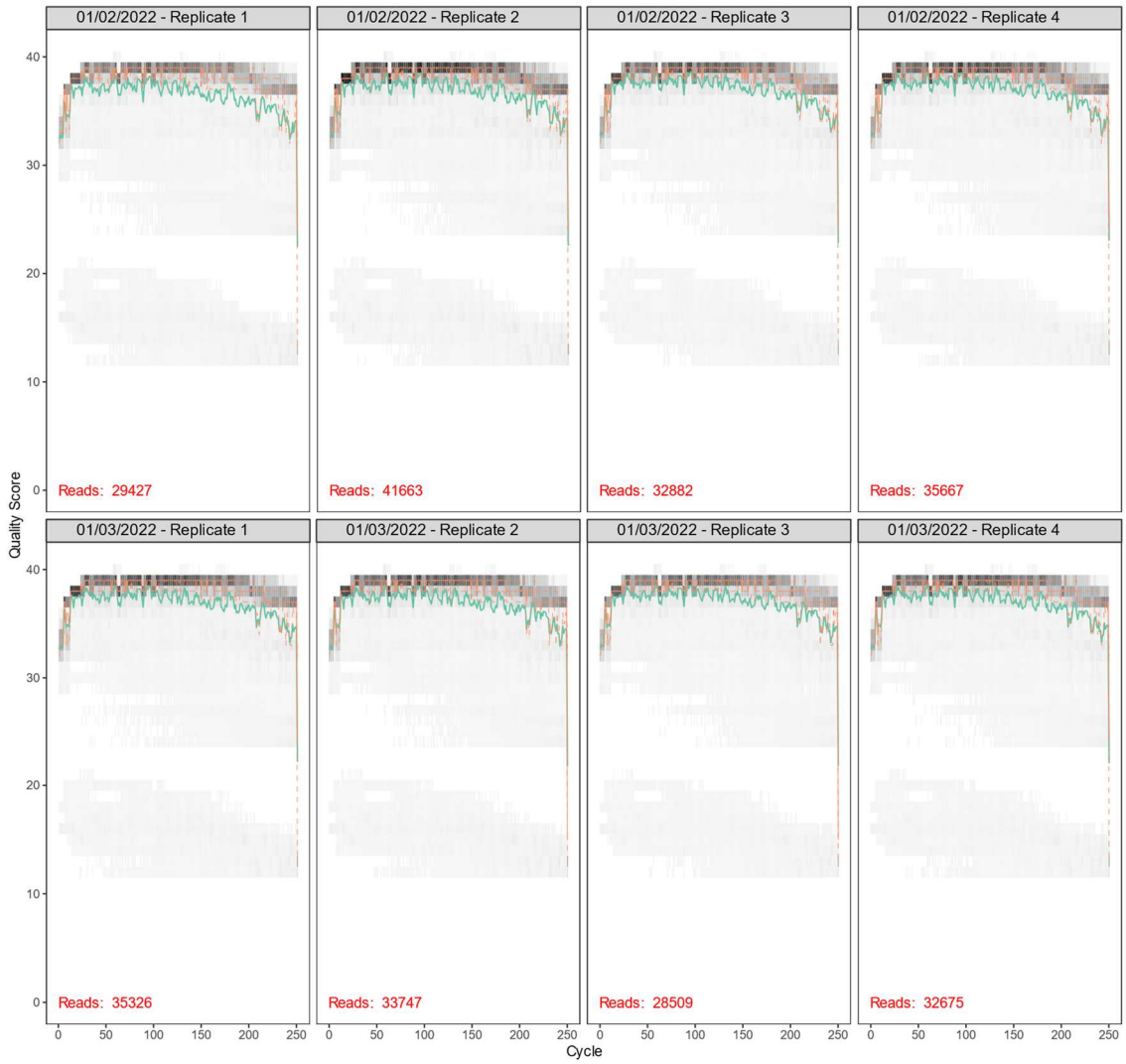

Appendix Figure 15. H) Quality profiles for each of the 16S rRNA samples (reverse reads) produced by Illumina MiSeq sequencing. Quality profiles were produced using the DADA2 pipeline (Callahan et al., 2016) and visually inspected to ensure all samples were of sufficient quality before continuing with subsequent analysis. Each sample is labelled with the date the sample was collected and replicate number.

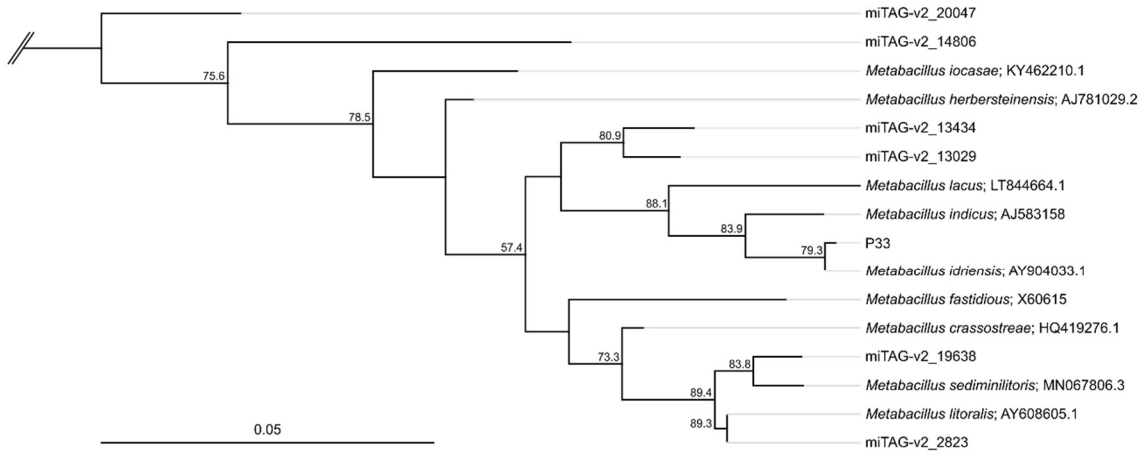

Appendix Figure 16. Maximum Likelihood tree constructed to verify the identity of miTAG hits (obtained from the Tara Ocean Barcode Atlas Portal) most closely related to *Metabacillus idriensis* (P33 query sequence) using *Lysinibacillus boronitolerans* as an outgroup. ML tree was constructed using full-length 16S rRNA sequences of miTAG hits, query bacteria (bacterium with confirmed antagonistic activity), and type strains of closely related bacterial species. Branch support values above 50 % are indicated at branch nodes (calculated from 1000 bootstrap replicates).